University of Alberta

The roles of Pbx and Meis TALE-class homeodomain transcription factors in vertebrate neural patterning.

by

Timothy Paul Erickson

A thesis submitted to the Faculty of Graduate Studies and Research
in partial fulfillment of the requirements for the degree of

Doctor of Philosophy

in

Molecular Biology and Genetics

Department of Biological Sciences

Fall 2010
Edmonton, Alberta

Examining Committee

Dr. Andrew Waskiewicz, Department of Biological Sciences

Dr. Ted Allison, Department of Biological Sciences

Dr. Roseline Godbout, Department of Oncology

Dr. Ordan Lehmann, Department of Ophthalmology

Dr. Carol Schuurmans, Department Biochemistry & Molecular Biology,
University of Calgary

Dedication

I dedicate this thesis to the memory of my grandmother, Sylvia Evelyn Howard (1919 – 2001), who introduced me to wonders of the natural world.

Abstract

One of the major goals of developmental biology is to understand how specialized groups of cells arise from an initially unspecified cell population. The vertebrate hindbrain is transiently segmented along its anterior-posterior axis into lineage-restricted compartments called rhombomeres, making it an excellent model in which to study the genetic mechanisms of axial patterning. Hox homeodomain transcription factors (TF), in close partnership with the Pbx and Meis families of TALE-class homeodomain proteins, impart unique molecular identities to the hindbrain rhombomeres, thereby specifying functionally specialized neurons within each segment. The broad goals of this thesis are to clarify the roles of Meis1 and Tshz3b TFs in Hox-dependent hindbrain patterning, and to examine the Hox-independent roles of Pbx and Meis proteins in axial patterning of the visual system.

While it is clear that Hox-Pbx-Meis complexes regulate hindbrain segmentation, the contributions of individual Meis proteins are not well understood. I have shown that Meis1-depleted embryos exhibit neuronal patterning defects, even though the hindbrain retains its segmental organization. This suggests that Meis1 is making important contributions to neuronal development downstream of rhombomeric specification.

A zinc-finger TF called Teashirt (Tsh) cooperates with Hox-Pbx-Meis complexes to establish segmental identity in *Drosophila*, but this role not been tested in vertebrates. I found that overexpression of *tshz3b* produces segmentation defects reminiscent of Hox-Pbx-Meis loss of function phenotype, likely by acting

as a transcriptional repressor. Thus, Tshz3b may be a negative regulator of Hox-dependent hindbrain patterning.

Like the hindbrain, visual system function requires that positional information be correctly specified in the retina and midbrain. I found that zebrafish Pbx and Engrailed homeodomain TFs are biochemical DNA binding partners, and that this interaction is required to maintain the midbrain as a lineage-restricted compartment. Additionally, I show that Meis1 specifies positional information in both the retina and midbrain, thereby helping to organize the axonal connections between the eye and brain.

Taken together, this thesis clarifies our understanding of Hox-dependent hindbrain patterning, and makes the claim that Pbx and Meis perform a general axial patterning function in anterior neural tissues such as the hindbrain, midbrain and retina.

Acknowledgements

A doctorate does not get done without assistance from one's colleagues. For reagents and other help of a scientific nature, I would like to thank the following people (in alphabetical order):

Ted Allison for teaching me how to make microscalpels;

Todd Evans for providing *smad5* morpholino that was used in some preliminary experiments;

Kirst King-Jones and Mattéa Bujold for supplying Drosophila RNA used to clone the *teashirt* gene;

Ordan Lehmann and Ming Ye for the human *GDF6* expression construct;

Charles Sagerström for the HA-*hoxb1b* and *pbx4*Δ*C* expression constructs;

Christine and Bernard Thisse for the *fsta* expression construct;

Michael Tsang for the *Tg[dusp6:d2eGFP]* line of fish and good advice on Fgf receptor inhibitors;

Andrew Waskiewicz for everything else. Thank you for your support over the years, both scientifically and personally.

Perhaps even more importantly, a doctorate does not get done without the support of one's friends and family. So, thank you friends, even though I've mostly ignored you over the past year or so. My family's love and support has been invaluable, and I couldn't have done this without them. Thank you so much mom, dad, and mother-in-law; you're the greatest! I especially need to acknowledge my amazing wife Christine, who was not only a constant source of love and moral support, but also assisted me in making graphics and figures. You get top prize! And best of all, I was lucky enough to have my family expand by one during the course of my graduate studies. To my sweet daughter Sadie – thank you for making my life a better one to live.

Table of Contents

List of Tables

List of Figures

Figure S6-2. Meis1-knockdown does not affect patterning of the midbrain-hindbrain boundary

Figure S6-3. *meis1* and *smad1* expression in the early optic vesicle

Figure S6-4. Morpholino-insensitive *myc-meis1* RNA can rescue the *smad1* expression defects in *meis1* morphants

Figure S6-5. *gdf6a* morphants have normal *smad1* and *fsta* expression at 13 hpf

Figure S6-6. *smad5* expression is normal in *meis1* morphants

Figure S6-7. Morpholino-insensitive *myc-meis1* RNA can rescue the *fsta* expression defects in *meis1* morphants

Figure S6-8. Interaction between Meis1-knockdown and reduced Fgf signaling using the Fgf receptor inhibitor SU5402

Figure S6-9. The RGC axon stalling phenotype in *meis1* morphants

Figure S7-1. The expression of *pax2a* at the midbrain-hindbrain boundary in wild type and *pknox1.1, 1.2, 2* triple-morphant embryos at 20 hpf

List of Symbols, Nomenclature, or Abbreviations

aa - amino acid

Abd-A - Abdominal-A (Hox 8)

Abd-B - Abdominal-B (Hox 9)

Aldh - Aldehyde dehydrogenase

Antp - Antennapedia (Hox 6)

AP - anterior-posterior

ARE – autoregulatory enhancer

BC-X - Bithorax complex

BCIP - bromo-chloro indoyl phosphate

bHLH - basic helix-loop-helix

BMP – Bone morphogenetic protein

bp - base pairs

BSA - bovine serum albumen

cb - cerebellum

CBP – CREB-binding protein

Ccnd1 - Cyclin D1

Cdx - Caudal homeobox

CMZ - ciliary marginal zone

CNS – central nervous system

CtBP – C-terminal binding protein

Cxcr4b - Chemokine (C-X-C motif), receptor 4b

Cyp26 - cytochrome P450, family 26

DEAB - diethylaminobenzaldehyde

Dfd - Deformed (Hox 4)

DIG - digoxigenin

DMB – diencephalic-mesencephalic boundary

DN - dominant negative

DNA - Deoxyribonucleic acid

dpf – days post fertilization

Dusp6 - Dual specificity phosphatase 6

DV - dorsal-ventral	HDAC – histone deacetylase
DWB - deyolking wash buffer	Hox – Homeotic complex
DYB - deyolking buffer	hpf – Hours post fertilization
En /Eng - Engrailed	hth - homothorax
EnR - Engrailed repressor domain	il17rd - interleukin 17 receptor D (sef - syn-expressed with fgfs)
Eph - Eph tyrosine receptor kinase	Irx – Iroquois homeobox
Ephrin - Eph receptor ligand	LOF - loss-of-function
Exd - Extradenticle	mafB - v-maf musculoaponeurotic fibrosarcoma oncogene homolog B
Fgf – Fibroblast Growth Factor	MB - midbrain
FMN – Facial motorneuron	Meinox - Meis / Knox
Fox - Forkhead box	Meis - Myeloid ecotropic viral integration site
Fsta - Follistatin a	MeOH - methanol
Gdf - Growth and differentiation factor	MH – Meis homology
GFP - green fluorescent protein	MHB – midbrain-hindbrain boundary
GOF - gain-of-function	MO - morpholino

mRNA - messenger ribonucleic acid	PBST - phosphate buffered saline / 0.1% Tween-20
myca / c-myc - myelocytomatosis oncogene a	PBT - phosphate buffered saline / 0.1% Triton-X
myf - myogenic factor	Pbx – Pre-B-cell leukemia homeobox
myoD - myogenic differentiation	Pdx1 - Pancreas/duodenum homeobox protein 1
myoG - myogenin	PG – paralog group
NBT - nitroblue tetrazolium	PID - PBC-interaction domain
NES - nuclear export signal	pk1b - prickle homolog 1 (Drosophila) b
NLS - nuclear localization signal	PKA – protein kinase A
NOL - non-overlapping morpholino	Pknox – Pbx/knotted homeobox
NT - nasal-temporal	PSB - pallial–subpallial boundary
ORF - open reading frame	PVDF - polyvinylidene fluoride
ov - otic vesicle	r - rhombomere
pax - paired box gene	RA – retinoic acid
Pb - proboscipedia (Hox 2)	RGC – retinal ganglion cell
PBC - PBX / ceh-20	RN – reticulospinal neuron

Shh – Sonic Hedgehog	tshz - teashirt zinc finger homeobox
TALE - three amino-acid loop extension	Ubx - Ultrabithorax (Hox7)
TBST - tris buffered saline - 0.1% Tween-20	vax2 - ventral anterior homeobox 2
tec - tectum	vhnf1 - variant hepatocyte nuclear factor 1
TF - transcription factor	VP16 - virion protein 16 activation domain
Tgfb - Transforming growth factor beta	Wnt – Wingless / Int
Tlx1 - T-cell leukemia, homeobox 1	ZIRC -Zebrafish International Resource Center
TSA - Trichostatin A	ZLI - zona limitans intrathalamica
tsh - teashirt	ZnF - zinc finger

Chapter One - Introduction

1. Introduction

1.1 Morphogen signaling and the specification of positional information in the developing embryo

One of the defining features of multicellularity is not only that an organism is composed of many cells, but also that the cells are molecularly and functionally distinct from one another (Bonner, 2002). To achieve this, mechanisms must be in place to instruct one part of the embryo to be different from another. From relatively simple multicellular organisms to the most complex, there are evolutionarily conserved mechanisms that function to specify axial position in an embryo. By subdividing the embryo, axial patterning allows genetically and functionally specialized groups of cells to emerge, thereby promoting cellular specialization, tissue development, and ultimately, the emergence of complex body plans. The vertebrate central nervous system (CNS) is an excellent illustration of the importance of axial patterning to the development of functional complexity. Although positional specification is required throughout the CNS, segmental patterning of the hindbrain, the evolutionarily oldest part of the brain, is one of the most striking and well understood examples of this phenomenon (reviewed in Moens and Prince, 2002). Overall, the study of axial patterning is of fundamental importance to the fields of evolution, developmental biology, neuroscience and medicine.

Anterior-posterior (AP) patterning of the vertebrate neural tube is an important model for studying the molecular mechanisms of cellular specification and tissue polarity. Studies in this field have highlighted the importance of morphogens and their downstream transcription factors in axial patterning of the embryo. Morphogens are defined as secreted molecules that can deliver distinct signaling messages to cells in a concentration-dependent manner. For example, a morphogen may specify one cell type at a high concentration, while instructing a different cellular identity at a lower concentration. In this way, morphogens contribute to the specification of positional information during development (Kerszberg and Wolpert, 2007; Wolpert, 1969).

There are five main classes of morphogens that are especially important for regionalization of the vertebrate embryo: the Bmp/Tgfβ (Bone Morphogenetic Protein / Transforming Growth Factor Beta) family, the Hedgehogs, the Wnt (Wingless / Int) family, Fgfs (Fibroblast Growth Factors) and RA (retinoic acid) (reviewed in Slack, 1993). Despite the different mechanisms employed by each signaling pathway employs, the end result is that morphogenic signaling leads to a change in gene transcription via the activation or repression of specific transcription factor (TF) activities in the cell that receives the signal (reviewed in Freeman and Gurdon, 2002). By signaling for a change in the transcriptional program of a cell, morphogens are able to specify positional information across the developing embryo, thereby making one part of the embryo different from another. Multiple regulatory and feedback-induced mechanisms lead to a refinement of positional identity in the embryos, and allows for the process of patterning to be a robust one (reviewed in Freeman and Gurdon, 2002). This complex interaction between the signaling pathways and their transcription factors is a common theme, and one that plays out during the axial patterning of all tissues during development.

1.2 Vertebrate neural induction and regionalization of the nervous system

Anterior-posterior patterning of neural tissue begins very early in development. In frog and chick, dorsal ectoderm with neural character is induced as early as the blastula stage (Kuroda et al., 2004; Streit et al., 2000). Experiments in frog and chick were the first to demonstrate that neural induction requires the inhibition of Bmp signaling in the presumptive neuroectoderm (reviewed in Harland, 1994; reviewed in Hemmati-Brivanlou and Melton, 1997; Hemmati-Brivanlou and Melton, 1994). Inhibition of Bmp signaling appears to occur via multiple mechanisms. First, presumptive neural tissue must be exposed to secreted Bmp antagonists such as Chordin, Noggin and Follistatin (Hemmati-Brivanlou et al., 1994; Lamb et al., 1993; Sasai et al., 1995; Wilson and Hemmati-Brivanlou, 1995). Secondly, Fgf signaling is also participating in the inhibition of Bmp signaling by promoting the degradation of the Smad transcription factors

required for the transcriptional response to Bmps (Pera et al., 2003). Taken together, the early inhibition of Bmp signaling in the presumptive neuroectoderm is required for the subsequent development of all neural tissue.

During or soon after the specification of neural tissue, the presumptive brain is patterned along its AP axis into three broad domains: the forebrain, midbrain, and hindbrain (Lumsden and Krumlauf, 1996). All neural tissue is initially fated to be anterior (forebrain), but is subdivided into forebrain, midbrain and hindbrain through the active induction of posterior fates. Wnt signaling is particularly important for AP neural patterning, as graded levels of Wnt signaling can induce caudal forebrain, midbrain and hindbrain character from cells with an initially rostral neural fate (Nordstrom et al., 2002). Fgfs again play a role in AP patterning by inducing posterior neural fates (Cox and Hemmati-Brivanlou, 1995; Lamb and Harland, 1995; Rentzsch et al., 2004; Streit et al., 2000). Retinoic acid (RA) signaling also posteriorizes neural tissue, and is particularly important for caudal hindbrain and spinal cord specification (Blumberg et al., 1997; Grandel et al., 2002; Kudoh et al., 2002). In addition to Wnt, Fgf, and RA posteriorizing signals, proper AP patterning also requires that these posteriorizing signals be actively antagonized in anterior regions of the brain. For example, secreted proteins Dickkopf-1 and Tlc in the anterior embryo inhibit the posteriorizing influence of Wnt signaling (Glinka et al., 1998; Hashimoto et al., 2000; Houart et al., 2002; Mukhopadhyay et al., 2001; Shinya et al., 2000), while cytochrome P450, family 26 (Cyp26) enzymes inactivate retinoic acid to maintain anterior character in the neuroectoderm (Hernandez et al., 2007; Sakai et al., 2001; Uehara et al., 2007; White et al., 2007). Taken together, these studies have highlighted the importance of secreted morphogens and their inhibitors in the initial specification and broad regionalization of neural tissue.

1.3 The vertebrate hindbrain as a model to understand the transcriptional regulation of neural patterning

Although essential to the entire process of AP specification, it is not the secreted morphogens themselves that actively specify AP identity in the neural

tube. Rather, it is the tissue-specific transcription factors, particularly homeodomain TFs, that function downstream of these signaling pathways that give each region of the brain its unique identity and transcriptional program. In particular, anterior-posterior patterning of the hindbrain is an excellent system in which to study the transcriptional regulation of pattern formation. During embryonic development, the vertebrate hindbrain is transiently segmented along its AP axis into seven or eight morphological and genetic compartments called rhombomeres (r1 in the anterior to r7/8 in the posterior; Figure 1-1) (Lumsden and Keynes, 1989). The strong AP polarity in the hindbrain is exemplified by the fact that each rhombomere possesses a unique transcriptional program and is molecularly distinct from one another. Among other things, the output of hindbrain segmentation is the specification and segmental organization of branchiomotor and reticulospinal neurons and their nerves, as well as patterning of the branchial arches and cranial neural crest cells that can contribute cartilage, bone and nerves in the head (reviewed in Alexander et al., 2009; reviewed in Trainor and Krumlauf, 2001). Thus, hindbrain patterning is essential for normal brain function and craniofacial development.

1.4 Hindbrain induction and regionalization by the Wnt, Fgf and RA pathways

To understand how the hindbrain is patterned along its AP axis, one must first understand the signaling pathways involved in hindbrain induction. Table 1-1 outlines some of the important milestones in hindbrain development that are relevant for this thesis. In zebrafish, cells near the germ ring and lateral to the embryonic organizer contribute to the hindbrain region (Woo and Fraser, 1995). By transplanting lateral germ ring cells to areas of the embryos that are fated to be forebrain, it was shown that hindbrain fate with AP polarity is induced. This suggests that signals originating from the non-axial lateral germ ring between 6-8.5 hours post fertilization (hpf) can induce hindbrain identity (Woo and Fraser, 1997; Woo and Fraser, 1998). Perturbing the specification of these lateral mesendodermal cells by overexpressing a Nodal-antagonist called Antivin also

leads to a loss of hindbrain fate and an expansion of the forebrain (Thisse et al., 2000). The identity of these lateral germ ring signals is probably Wnt and RA ligands (reviewed in Moens and Prince, 2002). Removing Wnt8 activity leads to an expansion of anterior neural fates at the expense of the hindbrain and spinal cord (Lekven et al., 2001; McGrew et al., 1997). This phenotype is enhanced by overexpressing Antivin (Erter et al., 2001), suggesting that, in addition to Wnt8, other signals from the lateral germ ring are involved in hindbrain induction.

Besides the possibility of other Wnt ligands, retinoic acid is likely one of these signals. The final synthesis step of biologically active RA is performed by aldehyde dehydrogenase (Aldh) enzymes. The expression of *aldh* genes is an important indicator of potential sources of RA during development. In zebrafish, chick, frogs and mice, these enzymes are present in the lateral mesoderm and somites just next to the neural tube, providing a source of RA to the presumptive hindbrain. Genetic or pharmacological perturbations in RA synthesis lead to a deletion of the caudal hindbrain (Begemann et al., 2001; Dupe and Lumsden, 2001; reviewed in Gavalas, 2002; reviewed in Gavalas and Krumlauf, 2000; Maden et al., 1996; Maves and Kimmel, 2005; Niederreither et al., 2000; Sirbu et al., 2005). Conversely, ectopic RA or a loss of Cyp26 function leads to an expansion of caudal identity at the expense of the rostral hindbrain (Abu-Abed et al., 2001; Hernandez et al., 2007; White et al., 2007). Interestingly, Wnt signaling may act upstream of RA signaling in posterior hindbrain specification in zebrafish, as overexpression of Wnt8 can increase *aldh1a2* expression in the germ ring, while blocking the Wnt pathway has the opposite effect (Weidinger et al., 2005). RA signaling also plays an important role in hindbrain segmentation through the direct regulation of *Hoxa1*, *Hoxb1*, *Hoxa4*, *Hoxb4* and *Hoxd4* gene expression (reviewed in Alexander et al., 2009).

In addition to Wnt and RA signaling, the Fgf pathway is also critical for the establishment of the rhombomeres 5 and 6 in the caudal hindbrain. RA and Fgf signaling cooperate to pattern the caudal hindbrain with RA acting first to activate transcription of a homeodomain transcription factor called *variant hepatocyte nuclear factor 1* (*vhnf1*) in the presumptive r5-6 region (Maves and

Kimmel, 2005; Pouilhe et al., 2007). Subsequently, Vhnf1 and Fgf signaling cooperate to establish the expression of a zinc finger transcription factor called *v-maf musculoaponeurotic fibrosarcoma oncogene homolog B (avian)* (*mafB* / *Kreisler* / *valentino*) in r5-6 (Aragon et al., 2005; Hernandez et al., 2004; Kim et al., 2005; Wiellette and Sive, 2003). Besides their role in establishing the caudal hindbrain, Fgfs originating both from the midbrain-hindbrain organizer and from within the hindbrain itself, may also play a part in establishing the rostral hindbrain, though the specific mechanisms have not been as well characterized (Maves et al., 2002; Roy and Sagerstrom, 2004; Walshe et al., 2002).

1.5 Early studies on the function and structure of Hox transcription factors

The Wnt, RA and Fgf pathways impart neural tissue with "hindbrain competency" and act to establish broad regional domains within the hindbrain. But how does the hindbrain take on its segmented character and how are the unique identities of each rhombomere specified? This is the job of the Homeotic complex (Hox / HOM-C) homeodomain transcription factors. The name "Homeotic complex" signifies two things about the nature of Hox proteins. The first is that gain or loss-of-function mutations in Hox genes can cause homeotic transformations, or the conversion of one body segment to the identity of another. Homeotic transformations were first described in 1894 by William Bateson, who was keenly interested by natural variations in repeated body segments (Bateson, 1894). In 1978, Edward Lewis clearly described how different mutations within the Bithorax complex (BX-C) of Hox genes caused homeotic transformations of thoracic and abdominal segments in *Drosophila melanogaster* (Lewis, 1978). Lewis also described the second important point that the "Homeotic complex" moniker suggests, that the Hox genes are arranged in a complex. Using mutant mapping data to arrive at a genomic structure of the BX-C, Lewis was able to deduce that genes at the 5' end of the complex controlled more posterior identities, while those at the 3' end specified more anterior fates. Even more striking is the observation that the genomic organization of a Hox complex is also reflected in the temporal and spatial patterns of Hox gene expression. With regard

to the vertebrate anterior-posterior body axis, Hox genes at the 3' end of the complex are expressed first and have their anterior limit of expression in the anterior hindbrain, while those at the 5' end are expressed later and have their anterior limit of expression in the posterior trunk and spinal cord (Figure 1-1). This evolutionarily conserved phenomenon is known as colinearity, and the exact mechanism of Hox gene regulation is a very active area of research. Colinearity may be an important defining component of chromatin structure that regulates Hox expression (Bickmore et al., 2004; Chambeyron and Bickmore, 2004). Additionally, post-transcription regulation of Hox function by microRNA (miRNA) genes found within Hox clusters has provided some insight into how colinearity is regulated (reviewed in Pearson et al., 2005; Yekta et al., 2004).

Although, Lewis defined two of the most important genetic characteristics of the BX-C "substances" (as Lewis called them), the molecular characteristics of Hox genes were still unknown. Clarity in this regard would have to wait until 1984 when the first Hox genes from Drosophila were cloned independently in the Gehring and Weiner labs (McGinnis et al., 1984; Scott and Weiner, 1984). At this time, it was recognized that Hox genes share high DNA sequence homology in a region called the homeobox. This 180 base pair region codes for a 60 amino acid domain called the homeodomain that was later characterized as the helix-turn-helix DNA-binding domain of the Hox transcription factors (Otting et al., 1990; Qian et al., 1989). Later in 1984, it was shown that Hox genes were present in genomes of other metazoans, including vertebrates (Carrasco et al., 1984; McGinnis et al., 1984). The homeodomain is not exclusive to Hox proteins, and since cloning the first Hox genes, numerous other homeodomain transcription factors have been characterized, many of which have been conserved throughout metazoan evolution. Subsequent research has characterized the large family of homeodomain transcription factors as essential regulators of positional information during vertebrate development (reviewed in Keynes and Krumlauf, 1994; reviewed in Krumlauf, 1994), and has highlighted the remarkable degree of molecular homology between segmentation of the fly body plan and AP patterning of the vertebrate nervous system.

1.6 Patterning functions of vertebrate Hox proteins and the "Hox code"

In vertebrates, there are between 3-8 Hox gene clusters per genome, with tetrapods possessing four, and teleost fishes having 7-8 Hox clusters (Wagner et al., 2003). All of these clusters retain collinear genomic organization, and each member of a cluster is assigned to one of thirteen Hox paralog groups (PGs). Along the AP axis of the nervous system, Hox PG genes 5-13 are expressed in the spinal cord and posterior mesoderm, while the anterior expression limits of PGs1-4 are restricted to specific rhombomeres within the hindbrain up to the r1-r2 boundary (Figure 1-1). As a result of this spatial and temporal regulation, unique combinations of Hox genes are expressed within different AP regions of the hindbrain and spinal cord. This observation lead to the idea that a "Hox code" (a region-specific signature of Hox proteins) may specify the identity of each AP region (reviewed in Hunt and Krumlauf, 1991; Hunt et al., 1991; Kessel and Gruss, 1990).

Evidence for a developmentally functional Hox code is present wherever Hox genes are expressed. The posterior Hox PGs 5-13 are involved in a wide variety of developmental processes (reviewed in Mallo et al., 2010). Some of these are homeotic in nature, such as AP patterning of the spinal cord and specification of motor neuron identity (reviewed inCarpenter, 2002; reviewed in Dasen and Jessell, 2009; Rijli et al., 1995), and axial skeleton and rib cage patterning (Horan et al., 1995; Kessel and Gruss, 1991; McIntyre et al., 2007; reviewed in Wellik, 2009). However, other functions of Hox PGs 5-13 are not homeotic, such as organogenesis (reviewed in Hombria and Lovegrove, 2003), limb development (reviewed in Zakany and Duboule, 2007), and hematopoiesis (reviewed in Argiropoulos and Humphries, 2007).

The anterior Hox PGs1-4 exhibit very clear homeotic functions in segmental hindbrain patterning (reviewed in Alexander et al., 2009). With the exception of r1, all rhombomeres express one or more Hox genes (Figure 1-1). *Hoxa2* is rather unique amongst the PG1-4 Hox genes in that it is the only one to regulate the identity of a rhombomere without being a part of a "Hox code". *Hoxa2* is the sole Hox gene to be expressed in r2, and in *Hoxa2* mutant mice, r2 is

transformed to an r1-like (Hox-free) identity (Gavalas et al., 1997). In *Hoxb1* knockout mice, r4 is transformed to an r2-like identity, while *Hoxb1* or *Hoxa1* overexpression in mice and fish has the converse effect of transforming r2 to an r4-like identity (McClintock et al., 2001; Vlachakis et al., 2001; Zhang et al., 1994). *Hoxa1* / *Hoxb1* double null embryos have a more severe cranial nerve and neural crest patterning defect than either of the single mutants, suggesting that the two PG1 genes have some redundant functions in hindbrain patterning (Carpenter et al., 1993; Gavalas et al., 1998). Similar redundancy is observed with regard to the Hox PG3 genes, where the deletion of three Hox PG3 genes in mice causes an r6-to-r4-like transformation (Gaufo et al., 2003). Lastly, a triple knockdown of PG1 genes in Xenopus leads to a complete loss of hindbrain segmentation altogether (McNulty et al., 2005). Together, these studies highlight two important points. Firstly, Hox genes are essential regulators of segmental identity in the hindbrain. Other factors may regulate Hox gene expression, but only changes in Hox gene function can re-specify one segmental identity to another. Secondly, the fact that compound Hox mutants must typically be generated in order to observe homeotic transformations suggests that there is a high degree of redundancy and robustness built into the Hox code.

1.7 Hox target genes – *eph* and *ephrin* genes mediate boundary formation in the hindbrain

The observation that Hox transcription factors can generate very specific cellular and regional identities begs the obvious question of how this occurs. The answer can be addressed in two parts: [1] what are the downstream targets of Hox genes, and [2] how do Hox proteins recognize and regulate these specific target genes? Although it is clear that the Hox-dependent regulation of segmental identity is not a simple process, significant progress has been made towards answering the first question through the use of high-throughput genomics and microarray analysis in *Drosophila* (reviewed in Hueber and Lohmann, 2008). Several studies have found that Hox proteins regulate genes involved with cell polarity, the cytoskeleton, and cell adhesion (Chen and Ruley, 1998; Hueber et al.,

2007; Jones et al., 1992; Lovegrove et al., 2006; reviewed in Pearson et al., 2005; Rohrschneider et al., 2007; reviewed in Svingen and Tonissen, 2006). This was a satisfying finding since differential cell adhesion must necessarily be involved in creating borders between neighbouring segments.

The segments of the hindbrain are lineage-restricted compartments, meaning that cells from one rhombomere cannot cross a boundary and enter a neighbouring rhombomere (Fraser et al., 1990). This differential cell adhesion is present in a two-rhombomere periodicity. Cells from even numbered rhombomeres (r2, r4, and r6) can mix with other even numbered rhombomeres, and the same rules apply to the odd numbered segments (Guthrie and Lumsden, 1991). At least part of the molecular basis for this lineage restriction and two-rhombomere periodicity is the rhombomere-specific expression of Eph receptor tyrosine kinases in odd rhombomeres and membrane-bound Ephrin ligands in the even segments. Eph and Ephrin interactions can result in repulsive responses between two cells, and thus lead to cell sorting in the hindbrain (Cooke et al., 2001; Cooke et al., 2005; reviewed in Cooke and Moens, 2002; Mellitzer et al., 1999; Xu et al., 1999; reviewed in Xu et al., 2000). Boundary formation, over and above merely preventing cell mixing, may also be important to establish and regulate local signaling centers in the hindbrain, such as the Fgf signaling center in r4, and Wnt signaling at rhombomere boundaries (Amoyel et al., 2005; Maves et al., 2002; Riley et al., 2004; Sela-Donenfeld et al., 2009; Walshe et al., 2002).

Eph and Ephrin proteins serve multiple functions during development where trans-interactions between adjacent cells are required (reviewed in Frisen et al., 1999). In addition to the cell sorting and tissue morphogenesis functions mentioned above (reviewed in Poliakov et al., 2004), Eph and Ephrin interactions also play important roles in cell migration, vasculogenesis, and synapse formation (reviewed in Kullander and Klein, 2002). This latter role is well characterized with regard to the topographical mapping of retinal ganglion cells in the optic tectum / superior colliculus (reviewed in Scicolone et al., 2009), which will be discussed in more detail in Chapter 6 of this thesis.

The reason why Eph and Ephrin signaling is limited to adjacent cells is because both the Eph receptor tyrosine kinase (RTK) and the Ephrin ligand are membrane bound (Figure 1-2). Based on their sequence similarity and ligand-binding preferences, the Eph RTKs are categorized as belonging to either the EphA or EphB sub-class. Although some receptor-ligand promiscuity has been observed, it is generally true that EphA RTKs bind to EphrinA ligands, while EphB RTKs bind to EphrinB ligands. The ligand sub-classes themselves are designated on the basis of whether they are tethered to the membrane by a glycosylphosphatidylinositol (GPI) anchor (EphrinAs), or a single transmembrane domain with a short cytoplasmic tail (EphrinBs). Thus, Eph and Ephrin signaling is generally limited to a very short range, except during synapse formation, where axon-dendrite interactions can occur over long distances.

A unique feature of the Eph-Ephrin system is that, because both the receptor and ligand are associated with plasma membranes, both the "sending" and "receiving" cell can respond to the signal. This phenomenon is called bi-directional signaling (Figure 1-2). Upon binding to membrane-clustered Ephrin ligands, the kinase activity of the dimerized Eph RTK becomes activated, leading to autophosphorylation of several cytoplasmic tyrosine residues. This creates a molecular beacon for the recruitment of larger protein complexes that are involved in modulating cytoskeletal dynamics and cell-cell adhesion in the *Eph*-expressing cell (reviewed in Arvanitis and Davy, 2008). This process is referred to as "forward signaling".

In contrast, "reverse signaling" occurs when, upon binding to their cognate Eph receptor, Ephrin ligands can transduce a signal into their host cell (Figure 1-2) (reviewed in Cowan and Henkemeyer, 2002). How this occurs depends on the sub-class of Ephrin ligand. Reverse signaling was first described for EphrinB proteins when it was observed that their short cytoplasmic tail was phosphorylated upon interacting with EphB RTKs (Bruckner et al., 1997). Similar to what occurs downstream of Eph RTK activation, the phosphorylated tail of EphrinB proteins recruit cytoplasmic protein complexes that can modulate cytoskeletal dynamics. Interestingly, reverse signaling also occurs through the GPI-anchored EphrinA

ligands, which can direct changes in cell adhesion through the Fyn protein tyrosine kinase pathway (Davy et al., 1999). Thus, the bi-directional nature of Eph and Ephrin signaling can lead to cytoskeletal and cell adhesion changes in both cells, and blurs the traditional distinction between receptor and ligand.

Although it is well established that rhombomere lineage restriction requires Eph and Ephrin function, the roles Ephs and Ephrins in establishing other tissues has not been as well studied. As mentioned previously, Ephs and Ephrins play a central role in visual system development by regulating retinotectal map formation (reviewed in McLaughlin and O'Leary, 2005). Additionally, they may also function to establish lineage-restricted compartments along the nasal-temporal and dorsal-ventral axes of the retina (Peters and Cepko, 2002; Picker et al., 2009). Chapter 6 of this thesis will explore the Hox-independent roles of the TALE-class homeodomain transcription factor Meis1 in regulating the domains of *eph* and *ephrin* expression in the zebrafish visual system.

1.8 Hox target genes – Hox proteins regulate their own mRNA expression and the expression of other *hox* genes

Another major category of Hox regulated genes is other transcription factors, including the Hox genes themselves. In *Drosophila*, in which there are only eight Hox genes, extensive Hox-dependent transcriptional networks have been worked out, especially for the posterior Hox genes such as Abd-B (reviewed in Hueber and Lohmann, 2008; Lovegrove et al., 2006; Zhai et al., 2010). In vertebrates, where mice and zebrafish have 39 and 48 Hox genes respectively, gene redundancy has made the picture less clear. What is clear, in the hindbrain at least, is that Hox gene expression is highly auto- and cross-regulatory, both through direct and indirect mechanisms. There is evidence through expression and enhancer analysis in mice that the Hox PG1-4 genes directly auto- and cross-regulate each other's rhombomere-specific expression. For example, *Hoxb2* knockout mice exhibit severe facial paralysis and sternal defects that can, in part, be attributed to decreased *Hoxb1* and *Hoxb4* expression (Barrow and Capecchi, 1996). *Hoxb3* and *Hoxb4* share an evolutionarily conserved autoregulatory

enhancer that directs r7-specific expression of these genes (Gould et al., 1997) while *Hoxb3* lacks an autoregulatory enhancer that maintains *Hoxa3* expression in r5-6 (Manzanares et al., 2001). The regulatory landscape of *Hoxb1* is well characterized, both with regard to its own enhancer and its effect on other *Hox* gene expression. *Hoxa1* and *Hoxb1* are each required in the initiation and maintenance, respectively, of *Hoxb1* expression in r4 (Gavalas et al., 2003; Popperl et al., 1995; Studer et al., 1998). *Hoxb1* also directly activates the r4 expression of *Hoxb2* (Maconochie et al., 1997) and *Hoxa2* (Lampe et al., 2008; Tumpel et al., 2007). Furthermore, *Hoxa2* regulates its own expression in r2 (Lampe et al., 2004). Together, these studies demonstrate that the Hox genes themselves comprise a major category of Hox targets.

There are other indirect mechanisms of Hox auto/cross regulation at work as well. The best example of this comes from an analysis of *Krox20* regulation in the hindbrain. *Krox20* (also known as *Early growth response 2* / *egr2*) is a zinc-finger transcription factor whose expression is restricted to r3 and r5 where it plays an evolutionarily conserved role in establishing the identity of these two rhombomeres (Schneider-Maunoury et al., 1997; Schneider-Maunoury et al., 1993; Seitanidou et al., 1997; Wilkinson et al., 1989). Besides regulating its own expression (Chomette et al., 2006), Krox20 also directly regulates the r3 and r5 expression of *Hoxa2* and *Hoxb2* (Maconochie et al., 2001; Manzanares et al., 2002; Nonchev et al., 1996a; Nonchev et al., 1996b; Vesque et al., 1996). In turn, Hoxb1 positively regulates *Krox20* expression, which is required for the maintenance of *Hox* expression (Wassef et al., 2008). This is but one example of how Hox proteins participate in indirect auto/crossregulatory loops to maintain their own expression. Other examples in the hindbrain include the interactions between Hox proteins and the Fgf and RA signaling pathways.

Taken together, this limited list of vertebrate Hox target genes in the hindbrain only serves to reinforce the idea that Hox proteins specify rhombomere identity by making the segments different from one another with respect to their cell-cell adhesion and Hox code. Clearly, more work needs to be done in order to

satisfactorily determine how neighbouring segments that start out being "not the same" come to take on a specific identity.

1.9 The "Hox paradox" and the TALE-class homeodomain transcription factors Pbx and Meis

Soon after the initial discovery of the Hox genes, a significant research effort was put towards the characterization of Hox proteins and the DNA binding characteristics of their homeodomains. The homeodomain (HD) is a DNA-binding motif found not just in Hox proteins, but also in a wide variety of other transcription factors that play essential roles in pattern formation and embryonic development. Structurally, the HD falls within the helix-turn-helix class of motifs that are found in DNA binding proteins present in both prokaryotes and eukaryotes. The HD itself is a tri-alpha-helical structure composed of, at minimum, 60 amino acids. Homeodomain-DNA contacts are made by helix 3 contacting the major groove, while a series of amino acids N-terminal to Helix 1 (the N-terminal arm) contact bases in the minor groove. Through a combination of sequence comparisons, DNA footprinting, NMR and X-ray crystallography studies, it was determined that the Hox homeodomain was highly conserved at both the sequence and structural levels, and that all Hox proteins bound to a 5'-TAAT-3' core motif with similar affinities *in vitro* (Desplan et al., 1988; Hoey and Levine, 1988). These early findings have since been confirmed using high throughput methodologies (reviewed in Affolter et al., 2008; Berger et al., 2008; Noyes et al., 2008). These findings presented a problem (called the Hox paradox) of how the Hox code can generate specific axial identities when the paralogues do not exhibit unique and discriminant DNA-binding properties.

The solution to this paradox came with the discovery that, *in vivo*, Hox DNA-binding specificity was modulated through direct interactions with other transcription factors from the TALE-superclass of homeodomain proteins. These are a group of atypical homeodomain proteins that are characterized by a Three Amino-acid Loop Extension (TALE) between alpha-helices 1 and 2 of their homeodomains (Burglin, 1997). The TALE motif is evolutionarily wide spread,

with genes coding for TALE-superclass proteins present in yeast (M-ATYP and Cup genes), plants (Knox and Bel genes), and animals, where there are four distinct families of TALE-superclass genes. The Meinox (Meis / Knox) class is considered to be the ancestral TALE group from which the other families were derived (Burglin, 1998). Clear Meinox homologues are found in plants and animals, and it is hypothesized that the yeast Mating Type genes (M-ATYP) may also be distant Meinox relatives (Burglin, 1998). In vertebrates, the Meinox class is split into two subclasses, the Meis and Pknox (Prep) genes. This Meinox classification is based on a conserved N-terminal Meis homology (MH) domain that is important for direct binding to the PBC TALE family. The PBC (PBX and ceh-20) class is closely related to the Meinox genes and distinguished by the conserved N-terminal PBC domain that mediates direct binding to Meinox proteins. The PBC class includes the *Drosophila* Extradenticle, *C.elegans ceh-20* and vertebrate *Pbx* genes (Burglin and Ruvkun, 1992). Together, the PBC and Meinox classes of TALE proteins turned out to be the solution to the "Hox paradox" via their heterodimeric and –trimeric binding to Hox proteins (reviewed in Moens and Selleri, 2006). The other two vertebrate TALE-superclass groups, Iroquois (Iro / Irx) and TG-Interacting Factor (Tgif) are more diverged from the ancestral Meinox group, and have lost the Meinox-PBC protein-protein interaction domain. Interestingly, although Iro and Tgif proteins do not directly interact with Hox proteins, these two classes of TALE homeodomain transcription factors also play roles in hindbrain development (reviewed in Gomez-Skarmeta and Modolell, 2002; Gongal and Waskiewicz, 2008; reviewed in Moens and Selleri, 2006; Stedman et al., 2009).

1.10 The interaction between Hox and PBC proteins

As with the characterization of Hox proteins, research in Drosophila has been central to understanding the function of PBC and Meinox proteins. The protein encoded by Drosophila gene *extradenticle* (*exd*) was the first characterized Hox cofactor. Originally found in an EMS-induced mutagenesis screen for defects in larval cuticle formation (Wieschaus et al., 1984), *exd* was subsequently found

to alter the activity of Hox proteins without altering their expression (Peifer and Wieschaus, 1990). At approximately the same time, it was recognized that some human pre-B cell acute lymphoblastic leukemias were caused by a t(1:19) chromosomal translocation that resulted in a chimeric protein containing the N-terminus activation domain of the E2A transcription factor gene and the DNA-binding homeodomain of pre-B-cell leukemia homeobox 1 (PBX1) (Kamps et al., 1990; Nourse et al., 1990). Thus, the discovery of PBC genes in vertebrates was due to their role in blood development, not segmental patterning. Once the sequence homology between *exd* and *PBX1* was established (Rauskolb et al., 1993), it was quickly realized that Pbx/Exd might act as *in vivo* DNA-binding partners for Hox proteins. *In vitro* evidence demonstrated that both Pbx and Exd were able to cooperatively bind DNA with Hox proteins (Chan et al., 1994; van Dijk and Murre, 1994; van Dijk et al., 1995), while *in vivo* studies showed that Exd is required for Hox target gene regulation in multiple tissues (Rauskolb et al., 1995; Rauskolb and Wieschaus, 1994). Together, these studies helped to resolve the Hox paradox, and highlighted the importance of Pbx / Exd in mediating Hox-dependent embryonic patterning events.

The physical interaction between Pbx / Exd and Hox proteins was subsequently shown to require the TALE-motif in Pbx and what is known as the Pbx-interaction domain (PID; a.k.a. hexapeptide or pentapeptide) in Hox PGs 1-10 (Chang et al., 1995; Knoepfler and Kamps, 1995; reviewed in Mann, 1995; reviewed in Mann and Chan, 1996; Neuteboom et al., 1995; Peltenburg and Murre, 1996; Phelan et al., 1995). A simplified schematic of the Hox-Pbx interaction is shown in Figure 1-3. The PID is minimally composed of a core tryptophan residue separated from a basic arginine or lysine located between +2 to +5 amino acids away, and is connected to the N-terminal end of the homeodomain by a linker region (In der Rieden et al., 2004). The residues surrounding the core tryptophan are highly conserved amongst members of a particular Hox paralogue group (Shanmugam et al., 1997), and together with the distance between the PID and the HD, may confer some binding specificity between Pbx proteins and the different Hox paralogues (In der Rieden et al., 2004). The TALE-motif between

alpha-helices 1 and 2 of the Pbx homeodomain are essential for forming a hydrophobic pocket that accepts the PID tryptophan residue (Lu and Kamps, 1996; Peltenburg and Murre, 1996). In addition to the TALE-motif, PBC proteins also contain a conserved region C-terminal to the HD that increases the affinity of PBC proteins for binding both Hox and DNA (Green et al., 1998; Lu and Kamps, 1996; Piper et al., 1999; Sprules et al., 2003). In fact, some PBC proteins are unable to bind DNA in the absence of a Hox binding partner (Neuteboom and Murre, 1997). Not only does the interaction increase the affinity of PBC proteins for DNA, both the DNA-binding specificity and affinity of Hox proteins are increased as well. Some of this extra specificity / affinity is simply due to the fact that a PBC-Hox binding sequence has a greater complexity than that of a Hox monomer. However, Hox proteins also undergo a conformational change upon binding to a PBC protein that modifies the *in vitro* preference for the 5'-TAAT-3' recognition sequence and reveals a new DNA-binding specificity that differs from Hox paralogue to paralogue (Chan et al., 1994; Chan and Mann, 1996; Chan et al., 1996; Chan et al., 1997; Lu and Kamps, 1996; reviewed in Mann and Chan, 1996; reviewed in Mann et al., 2009; Neuteboom and Murre, 1997; Passner et al., 1999; Sanchez et al., 1997). The N-terminal arm of the Hox homeodomain, which contacts the minor groove of the DNA helix, is an especially important determinant of Hox DNA-binding specificity that can be modulated by PBC proteins (Chang et al., 1996; Joshi et al., 2007; Phelan and Featherstone, 1997; Piper et al., 1999). Taken together, all Hox proteins from PG 1-10 can cooperatively bind DNA with PBC proteins, and a PBC-Hox dimer generally exhibits a much greater DNA-binding specificity and affinity than either monomer alone.

Interestingly, not all Hox functions are performed in partnership with PBC proteins, and the requirement and benefits of cooperative binding differs between the Hox paralogue groups (reviewed in Mann et al., 2009). For example, Ubx regulates haltere development in an Exd-independent fashion, and may bind DNA as a monomer to repress target gene expression (Azpiazu and Morata, 1998; Galant et al., 2002). *In vivo* mutation of the mouse *Hoxb8* PID ($Hoxb8^{hp}$) causes

an axial patterning phenotype that resembles a loss of multiple *HoxB* genes, suggesting that the PID mutation causes a gain of function phenotype through inappropriate binding of *Hoxb8*^{hp} to other Hoxb sites (Medina-Martinez and Ramirez-Solis, 2003). Perhaps related to this finding, it was found that interactions between Pbx and Hoxc6, Hoxb7 or Hoxb8 raised the DNA binding specificity of these Hox proteins, but did not alter their target site selection (Neuteboom and Murre, 1997), suggesting that Hox PG6-8 will bind the same DNA sequence with or without Pbx. Likewise, a Pbx1-HoxA9 complex will bind DNA with high specificity, but the partnership with Pbx1 does not appear to increase the affinity of HoxA9 for DNA (LaRonde-LeBlanc and Wolberger, 2003). Conversely, anterior Hox proteins appear to rely on an interaction with PBC proteins for all transcriptional activity (Uhl et al., 2010), as mutations in the PID of *Hoxa1* produce only loss of function phenotypes (Remacle et al., 2004; Remacle et al., 2002). Thus, there is a differential requirement for the PBC-Hox interaction amongst the various Hox paralogues, and this requirement may also be sensitive to the genetic context.

1.11 Non-TALE-class Hox partners

Additionally, many non-TALE-class transcription factors can interact directly with Hox proteins to regulate gene transcription. However, there is currently no evidence to suggest that these non-TALE-class cofactors globally modulate Hox DNA binding specificity in the same way that the PBC and Meinox interactions do. Nonetheless, these other partners include the homeodomain protein Engrailed (Gebelein et al., 2004), the zinc finger protein Teashirt (Tsh) (Taghli-Lamallem et al., 2007), amongst a growing list of other potential collaborators (reviewed in Mann et al., 2009). In particular, Tsh plays a prominent role in AP patterning during fly development by establishing a trunk groundstate that posterior Hox proteins then impose segmental identity upon (Fasano et al., 1991; Roder et al., 1992). Flies have a second *tsh*-like gene called *tiptop* (*tio*) that is functionally equivalent to *tsh* in some aspects of trunk patterning, eye formation and imaginal disc development (Bessa et al., 2009; Datta et al., 2009; Laugier et

al., 2005). Vertebrates also possess three (or four in zebrafish) *teashirt* / *tiptop* homologues whose role in modulating Hox function has not been examined. Chapter 4 of this thesis will discuss the function of one of these genes, *teashirt zinc finger homeobox 3b* (*tshz3b*), in regulating Hox-dependent hindbrain segmentation.

1.12 Structure and function of Meinox proteins

As with the discovery of human PBX1, the TALE-superclass gene *Myeloid ecotropic viral integration site 1* (*Meis1*) was also initially characterized as a proto-oncogene involved in retroviral-induced myeloid leukemias in mice (Moskow et al., 1995). The first genetic evidence that Meis might also cooperate with Hox came through the demonstration that *Hoxa7*, *Hoxa9* and *Meis1* expression are co-activated in myeloid leukemias (Nakamura et al., 1996). Subsequently, it was found that Pbx and Meinox (Meis / Pknox) proteins are *in vivo* DNA-binding partners, that they can interact in the absence of DNA, and that their binding is disrupted in the E2A-PBX1 chimeric protein due to the loss of the N-terminal PBC domain required to bind Meinox proteins (Berthelsen et al., 1998b; Chang et al., 1997; Knoepfler et al., 1997). Additionally, because Meinox and Hox proteins do not utilize the same binding sites on Pbx proteins, Meinox-Pbx-Hox trimeric complexes can cooperatively bind DNA and regulate the expression of target genes (Berthelsen et al., 1998a; Ferretti et al., 2000; Jacobs et al., 1999; reviewed in Mann and Affolter, 1998; Ryoo et al., 1999; Shanmugam et al., 1999; Shen et al., 1999). A simplified schematic of the Hox-Pbx-Meinox trimeric complex is shown in Figure 1-3. Some targets include the Hox genes themselves, thus, Pbx and Meinox proteins are essential components of the auto- and cross-regulatory loops that maintain and refine Hox expression domains along the anterior-posterior axis.

Interestingly, both *in vivo* and *in vitro* evidence suggests that a C-terminal domain in Meis (but not Pknox) proteins is sufficient for a direct interaction with Hox PG 9-13 proteins, including members of the Hox PGs 11-13 that do not contain a PID and do not interact with Pbx (Shen et al., 1997; Williams et al.,

2005). These Meis-Hox interactions can occur both in the presence or absence of DNA. It should be pointed out, however, that the two studies that examined these Meis-Hox interactions disagreed on whether Meis1 could interact with anterior Hox proteins. The study by Shen et al. used a strictly *in vitro* EMSA approach and could not detect an interaction between Meis1 and Hox PG4, 6, 7, or 8. However, the yeast-2-hybrid method used by Williams et al. detected a wider range of Meis-Hox interactions that included Hox PGs 9-13, as well as more anterior Hox proteins from PGs 2, 4, 5 and 8. The interaction with anterior Hox proteins required the Meis1 C-terminal Hox interaction domain with an additional contribution from N-terminal residues. While a direct interaction between Meis1 and the posterior Hox proteins makes biological sense given their genetic cooperativity in leukemogenesis, the biological significance of an interaction with anterior Hox proteins has not been demonstrated. Nonetheless, Meinox proteins represent an additional layer of Hox regulation via their ability to further modulate the DNA-binding specificity of Hox proteins, whether directly with Hox or as part of a complex with Pbx.

1.13 PBC and Meinox proteins regulate each other's protein stability and subcellular localization

Pbx and Meinox proteins have a much more intimate biochemical relationship over and above their mutual roles in regulating Hox function. Although not unique to flies, this relationship has been most extensively characterized in *Drosophila* where it was first noticed that, even though *exd* mRNA is uniformly present throughout the fly embryo, the nuclear localization of Exd protein is temporally and spatially regulated (Aspland and White, 1997; Mann and Abu-Shaar, 1996). The first study that identified Homothorax (Hth), the Drosophila orthologue of vertebrate Meis, recognized that the nuclear localization of Exd depended upon Hth (Rieckhof et al., 1997). The segmental identity defects in *hth* mutants are similar to a loss of *exd* function, perhaps due to the cytoplasmic localization of Exd protein. Ectopic Hth acts post-translationally to promote the nuclear accumulation of Exd (Casares and Mann, 1998; Pai et al.,

1998). Furthermore, the ectopic expression of either Hth, mouse Meis1 or human Pknox1 (Prep1) in flies is able to induce the nuclear translocation of Exd (Jaw et al., 2000; Rieckhof et al., 1997), demonstrating that Exd localization is an evolutionarily conserved function of Meinox proteins. This activity of Hth / Meis1 does not require a functional DNA-binding domain, suggesting that the Exd and Meinox proteins interact in the cytoplasm and then translocate as a pair to the nucleus (Abu-Shaar et al., 1999). The relationship works both ways, as the stability and nuclear accumulation of Hth protein likewise depends on the presence of Exd (Abu-Shaar and Mann, 1998; Kurant et al., 1998). Detailed studies have revealed that Exd contains two nuclear localization signals (NLS) and single nuclear export signal (NES), while Hth contains a single putative NLS that is dispensable for nuclear localization of the Exd-Hth complex (Abu-Shaar et al., 1999; Stevens and Mann, 2007). When not complexed with Hth, Exd is in a conformation where NLS activity is inhibited by an NLS mask, and the NES activity predominates leading to cytoplasmic localization of Exd. Conversely, Hth binding to Exd inhibits both the NLS mask and the NES, thereby shifting the balance from nuclear export to nuclear import.

A similar relationship exists in vertebrates, though analysis is complicated by the existence of multiple Pbx and Meinox genes. As with fly Exd, vertebrate Pbx protein levels and localization are regulated post-translationally (Gonzalez-Crespo et al., 1998; Popperl et al., 2000). High levels of endogenous nuclear Pbx correlate with regions that express high levels of *Meis* mRNA, ectopic Meinox proteins promote the stability of Pbx, and a loss of Meinox proteins cause a decrease in Pbx protein levels (Deflorian et al., 2004; Ferretti et al., 2006; Gonzalez-Crespo et al., 1998; Longobardi and Blasi, 2003; Mercader et al., 1999; reviewed in Moens and Prince, 2002; Saleh et al., 2000a; Waskiewicz et al., 2001). However, the modulation of NLS and NES activity by Meinox proteins may not be the only mechanism that governs Pbx localization. In a mechanism that is conserved between flies and vertebrates, there is evidence that nonmuscle myosin II heavy chain B (NMHCB) can compete with Meinox proteins for binding to Pbx and promote the cytoplasmic retention of Pbx (Huang et al., 2003).

Additionally, the nuclear export of PBX1 is negatively regulated by Protein Kinase A-mediated phosphorylation on the PBC-B domain (Kilstrup-Nielsen et al., 2003), a mechanism that may not exist in flies (Stevens and Mann, 2007). Pbx has also been shown to interact directly with two non-homeodomain proteins, Hematopoietic Pbx1 Interacting Protein (HPIP) (Abramovich et al., 2002; Abramovich et al., 2000) and Zinc Finger Pbx1 Interacting Protein (ZFPIP) (Laurent et al., 2007). Besides inhibiting the ability of Pbx to cooperatively bind DNA with Hox proteins, both HPIP and ZFPIP contain nuclear localization signals that may affect Pbx subcellular localization. All together, it is clear that the subcellular localization of Pbx is a highly regulated process that potentially involves many different partners.

With regard to Meinox proteins, it has been clearly demonstrated that an interaction with Pbx proteins is required for Meis / Pknox stability as well as their ability to enter the nucleus (Berthelsen et al., 1999; Choe et al., 2002; Longobardi and Blasi, 2003; Maeda et al., 2002; Pillay et al., 2010; Vlachakis et al., 2001; Waskiewicz et al., 2001). Furthermore, the two NLS motifs located in the homeodomain of Pbx proteins are required for Meinox nuclear localization, as ectopic Pbx4ΔC protein (lacking the HD) retains Meinox proteins in the cytoplasm (Choe et al., 2002). Additionally, Meinox protein localization may be an active process mediated by nuclear export machinery and cytoskeletal-dependent cytoplasmic retention (Diaz et al., 2007; Haller et al., 2004). Interestingly, a recent report also suggests that the MH domain of Meis2 can inhibit the transactivating properties of its C-terminal domain, and that Pbx binding partially relieves this inhibition (Hyman-Walsh et al., 2010). Taken together, these studies in flies and vertebrates suggest that PBC and Meinox proteins regulate one another's stability and access to the nucleus in a temporal and tissue-specific manner. As well, this intimate relationship between PBC and Meinox proteins regulates not only their own function, but also represents another level at which TALE-class proteins can regulate Hox activity.

This co-dependent biochemical relationship between PBC and Meinox proteins presents a unique challenge when it comes to assigning individual

transcriptional functions to these factors. This difficulty has been previously demonstrated with regard to Pknox loss-of-function models, where a loss of Pknox1 protein leads to a reduction in Pbx and Meis protein levels (Deflorian et al., 2004; Ferretti et al., 2006). Similarly, Pbx2/4-knockdown in zebrafish causes a destabilization and mislocalization of Meis1 protein (Pillay et al., 2010). As discussed previously, the reduction in protein levels may be due to bidirection protein stabilization, but might also reflect positive input from TALE-class proteins into their own gene transcription (Erickson and Waskiewicz, unpublished results; French et al., 2007). The lessons learned from these specific examples can be generalized to any PBC and Meinox loss-of-function study. While in no way invalidating the results gathered from such studies, it should simply be noted that any PBC or Meinox loss-of-function model might also include complete or partial deficiencies in the corresponding partner proteins. Therefore, the results of such studies must be interpreted from the point of view that the knockdown phenotype of any single Pbx or Meinox protein is the sum of its biochemical and transcriptional activities.

1.14 The roles of Pbx and Meinox proteins in regulating Hox function

It is apparent that, when required, PBC and Meinox proteins aid Hox-dependent gene regulation by generally increasing the DNA-binding specificity and affinity of Hox proteins for a given regulatory DNA element. But how do PBC and Meinox proteins influence these Hox-dependent transcriptional events? Do these Hox complexes activate or repress transcription? The answer is that, depending on a variety of factors, Hox complexes can either activate or repress transcription. Hox complexes tend to activate transcription more often than repress, and this is especially true for those containing TALE-class partners (reviewed in Mann et al., 2009). Whether Hox complexes will activate or repress transcription is, in part, determined by the identity of the Hox protein itself, as numerous Hox paralogue-specific activator or repressor domains have been identified (Rambaldi et al., 1994; Tour et al., 2005; Vigano et al., 1998; Zhao et al., 1996). Similarly, the regulatory DNA sequence of the target gene itself may

select for regulation by one Hox paralogue over another. In *Drosophila*, there is an example of this where Ubx / Exd / Hth cooperatively bind a repressor element in the Distalless promoter to shut off expression in the abdomen, but Antp / Exd / Hth complexes in the thorax do not use this element (Gebelein et al., 2002). An alternate splice isoform of Ubx is also a factor in Distalless repression. Thus, the Hox code for a given axial position may be executed in part by the unique combination of activating and repressing Hox complexes acting in a promoter-specific fashion. Lastly, the availability of TALE-class partners and other Hox collaborators will also influence transcriptional output of a Hox complex. Thus, the type of Hox complex that can form at a given enhancer is regulated at many levels that can differ from cell type to cell type, and change over developmental time.

In order for Hox complexes to regulate transcription, they must associate with transcriptional machinery that either activate or repress transcription. Much of the work in this regard has focused on the functional and biochemical association between Hox complexes and chromatin-modifying complexes containing either histone acetyltransferases or histone deacetylases. Histone acetyltransferases (HAT) are chromatin-remodeling factors that stimulate transcription by the addition of acetyl groups to specific lysine residues on histone tails, thereby creating a looser DNA-histone association and making the DNA more accessible to other regulatory proteins (Bannister and Kouzarides, 1996; Ogryzko et al., 1996). The histone deacetylases (HDAC) have the opposite activity; they remove acetyl groups from histones, thereby promoting transcriptional repression (reviewed in Sterner and Berger, 2000).

Interestingly, while it has been shown that HoxB proteins can bind to the histone acetyltransferases CBP and p300, reports differ on how this interaction affects transcription. Consistent with the idea that an interaction with CBP would promote transcription, one study found that the presence of CBP enhanced HoxB7 transcriptional activity in MDA-MB231 breast cancer cells, suggesting that histone acetylation is an important factor in Hox-mediated transactivation (Chariot et al., 1999). However, another group used *in vitro* assays to show that

HoxB proteins may promote transcriptional repression via their ability to inhibit CBP / p300 transactivating function (Shen et al., 2001). They also observed an antagonistic interaction between HoxB6 and CBP in K562 leukemia cells that resulted in repression of globin gene expression in a Pbx-independent fashion (Shen et al., 2004). These seemingly incongruous results may be explained by differences between the cell cultures with regard to their adhesive and molecular properties. Consistent with the idea that the cellular context plays an instructive role in Hox-TALE-class function, it has been shown in HEK293 cells that HOXB1-PBX complexes associate with a large multi-protein transcriptional repressor complex. However, upon activating protein kinase A (PKA) signaling, or inducing cell aggregation, HOXB1-PBX complexes can switch from repressors to activators, perhaps by recruiting HATs instead of HDACs (Saleh et al., 2000b). Taken together, these studies highlight the importance of the cellular, molecular, and genetic context on determining whether Hox proteins can activate or repress target gene transcription.

Pbx proteins have a very important role in determining the transcriptional activity of a Hox complex. Overexpression and reporter gene assays have confirmed that HoxB1-Pbx complexes repress transcription in a dose-dependent fashion, and that this repression is alleviated by TSA treatment (Trichostatin A; an HDAC inhibitor) (Choe et al., 2009; Saleh et al., 2000b). Biochemical evidence suggests that the N-terminus of Pbx can interact directly with HDACs, while the C-terminus of the PBX1a isoform can directly bind to the corepressors Silencing Mediator of Retinoid and Thyroid hormone receptors (SMRT) and Nuclear Receptor Co-Repressor (NCoR) (Asahara et al., 1999; Saleh et al., 2000b). Additionally, it has also been shown that the association between Pbx1 and HDACs can inhibit osteoblast differentiation by antagonizing HoxA10-mediated transactivation of osteoblast-specific genes (Gordon et al., 2010). Thus, it appears that Pbx proteins act as transcriptional repressors when complexed with Hox partners.

If Hox-PBC complexes recruit chromatin-inactivating proteins, how is it then that these complexes are often associated with transcriptional activation? The

answer may lie with the Meinox family of proteins, which possess the ability to convert Hox-Pbx complexes from transcriptional repressors to activators. They perform this task via two non-exclusive mechanisms. The first characterized of these was the role of the Meis1 C-terminus in mediating transcriptional activation by Hox-Pbx complexes in response to TSA treatment (Huang et al., 2005). In a HoxB1-ARE (autoregulatory enhancer) reporter assay, the different C-termini found in two Meis1 isoforms both activated transcription in response to TSA and protein kinase A treatment. This effect is specific for Meis proteins, as the Pknox C-terminus did not produce a change in the reporter gene assay. Meis C-termini interact directly with CREB regulated transcription coactivator (CRTC / TORC) proteins, which are required for Meis to respond to PKA signaling (Goh et al., 2009). Thus, the PKA-regulated switch in the transcriptional activity of Hox-Pbx complexes may be mediated by an interaction between Meis and CRTC. Recently, a second mechanism was proposed to explain how Meis proteins act as transcriptional activators (Choe et al., 2009). Both Meis and HDAC bind to the Pbx N-terminal domain in a mutually exclusive fashion. Thus, in addition to its C-terminal activation domain, Meis proteins may promote transcription at Hox-regulated promoters simply by preventing the association between Pbx and HDAC.

It is likely that Hox PG1-4 proteins, which depend heavily on PBC and Meinox proteins for their transcriptional activity (reviewed in Mann et al., 2009; Uhl et al., 2010), invariably act as transcriptional activators. The known auto- and cross-regulatory loops that initiate and maintain *Hox* expression in the hindbrain all involve direct, positive input from TALE-class proteins (Di Rocco et al., 2001; Ferretti et al., 2005; Ferretti et al., 2000; Gould et al., 1997; Lampe et al., 2004; Lampe et al., 2008; Maconochie et al., 1997; Manzanares et al., 2001; Nakano et al., 2005; Popperl et al., 1995; Tumpel et al., 2007). This is also true with regard to other known Hox PG1-4-dependent targets such as *Collagen, type V, alpha 2* (*COL5A2)*, *Eph Receptor A2* (*Epha2*), *Krox20*, *Motor neuron and pancreas homeobox 1* (*Mnx1* / *Hb9*), *Paired-like homeobox 2b* (*Phox2b*) and *Retinoic acid receptor, beta* (*Rarb*) (Chen and Ruley, 1998; Penkov et al., 2000; Samad et al.,

2004; Serpente et al., 2005; Wassef et al., 2008). Thus, these examples of direct gene regulation by Hox complexes in the hindbrain support the idea that Hox-PBC-Meinox heterotrimers activate transcription.

1.15 Hindbrain patterning functions of PBC proteins

The importance of PBC and Meinox proteins in positively regulating hindbrain segmentation is most clearly illustrated in studies from frog and zebrafish. There are two broadly expressed *pbx* genes (*pbx2* and *pbx4*) that function during the early segmentation stages of zebrafish hindbrain development. The *lazarus* mutant (*pbx4*$^{-/-}$) was found in an N-ethyl-N-nitrosourea (ENU) mutagenesis screen for genes that governed *egr2b* (*krox20*) expression in rhombomeres 3 and 5 (Moens et al., 1996; Popperl et al., 2000). Embryos lacking zygotic *pbx4* function display severe anterior hindbrain patterning defects, including a substantial loss of r3 *krox20* expression. Pbx4 is able for form trimeric complexes with Meis and Hox proteins (Vlachakis et al., 2000), and the ability of overexpressed *hoxb2* to drive *krox20* expression in the zebrafish retina is attenuated in *lazarus* mutants, suggesting that Hox proteins functionally require Pbx4 (Popperl et al., 2000). The partial segmentation defects in the *lazarus* mutants is due to the presence of maternally-contributed *pbx4* transcripts as well as partial redundancy with *pbx2*. The most striking example of the role for Pbx proteins in hindbrain segmentation comes from maternal/zygotic *pbx4* mutants injected with *pbx2* morpholino (Waskiewicz et al., 2002). These "Pbx-less" embryos lack all segmental character in the hindbrain. Furthermore, the hindbrain adopts the ground-state identity of rhombomere 1, which is the only rhombomere whose identity is not specified by Hox proteins. Interestingly, *hoxb1b* expression is initiated normally in Pbx-less embryos, and *fgf8a* is still expressed in the presumptive hindbrain region, but in the absence of Pbx proteins, these factors are unable to impart segmental identity to the hindbrain. These studies are complemented by those done in *Xenopus*, where ectopic expression of *Xpbx1* and *Xmeis1* in animal cap assays activate hindbrain markers, while overexpression of *Xpbx1* fused to an Engrailed repressor domain blocks this activity (Maeda et al.,

2002; Maeda et al., 2001). Thus, while Pbx proteins are not required to specify the hindbrain region, by acting together with Hox proteins, they are critically required for hindbrain patterning.

1.16 Hindbrain patterning functions of Meinox proteins

Similar defects in zebrafish hindbrain patterning are observed by manipulating Meis protein function. During hindbrain segmentation, there are three *pknox* genes (*pknox1.1*, *pknox1.2*, and *pknox2*), and four *meis* genes (*meis1*, *meis2.1*, *meis2.2*, and *meis3*) expressed in the hindbrain. The *pknox* genes are broadly expressed, while the *meis* genes display more rhombomere-restricted expression patterns in the hindbrain (Thisse and Thisse, 2004; Waskiewicz et al., 2001). The large number of Meinox genes expressed in the hindbrain makes it difficult to model a complete loss of Meinox function by conventional antisense knockdown or mutagenesis strategies. However, two dominant negative (DN) constructs have been effectively used to globally block Meinox function. The first takes advantage of the requirement for Meinox proteins to participate as DNA-binding partners with Hox and Pbx proteins. Overexpressing either a homeodomain-less (ΔHD) Meis1, or a version of Meis1 with a single amino acid mutation in a critical DNA-binding residue within its homeodomain (N323D), blocks all Meinox (Meis and Pknox) protein function that requires a partnership with Pbx proteins. These MeinoxDN proteins are not able to bind DNA, but can outcompete endogenous Meinox proteins for binding to their Pbx partners. It this way, endogenous Meinox proteins may not be able to gain access to the nucleus. Additionally, the Hox-Pbx-MeisDN complexes are unable to correctly recognize their DNA target sequences, presumably due to the lack of DNA-binding input from the mutant Meinox partner. Overexpression of these constructs produces hindbrain segmentation defects that are similar to, but not as severe as, those observed in Pbx-less embryos (Waskiewicz et al., 2001).

Interestingly, there are endogenous splice isoforms of *hth* and *Meis* proteins that retain the PBC-interaction domain, but lack the homeodomain. These HD-less versions can still promote the nuclear localization of PBC proteins, but

cannot bind DNA. In flies, the HD-less version of *hth* can perform most of the activities of the full-length protein, including almost all Hox-related functions (Noro et al., 2006). Similarly, alleles of *hth* with mutations in the homeodomain cause less severe phenotypes than mutations that abolish the *hth-exd* interaction (Kurant et al., 2001). Intriguingly, although little work has been done to characterize them, vertebrates also express multiple splice isoforms of Meis genes, one of which lacks the homeodomain (reviewed in Geerts et al., 2005). The dominant negative activity of Meis1ΔC and Meis1N323D in the hindbrain suggests that the role of Meis proteins in this tissue requires DNA binding, and is not merely to block the association between Pbx and HDAC proteins, or to translocate Pbx to the nucleus.

The second Meinox dominant negative construct exploits the need for Meinox proteins to utilize the Pbx nuclear localization signals (NLS) for translocation to the nucleus. A Pbx4ΔC construct lacks the NLS sequences in the homeodomain, but retains the ability to bind Meinox proteins. Overexpression of Pbx4ΔC retains endogenous Meinox proteins in the cytoplasm, while still allowing the endogenous Pbx proteins to go to the nucleus, and produces hindbrain segmentation defects similar to those seen for the other MeisDN constructs (Choe et al., 2002). That these MeisDN proteins all perturb hindbrain segmentation while allowing Pbx to localize to the nucleus normally suggests that Meinox proteins are a critical component of the Hox complexes that transcriptionally regulate hindbrain segmentation.

Although these dominant negative studies suggest an important role for Meis and Pknox proteins in hindbrain patterning, there are no known Meinox mutants in zebrafish, and very few studies have been performed where individual Meinox genes have been targeted by antisense morpholinos. The reason why no Meinox genes have been recovered in mutagenesis screens could be due to the fact that there are multiple Meinox genes expressed in the hindbrain and this, combined with maternally contributed transcript, could mask any hindbrain phenotypes in the F1 generation. There are no published studies that have focused on the hindbrain patterning roles of individual Meis genes in zebrafish, and only

one that has examined the role of *pknox1.1* (*prep1*). This study confirmed that Pbx is important for the nuclear translocation of Meinox proteins, and suggested that morpholino-knockdown of Pknox1.1 causes a decrease in Pbx protein levels and severe hindbrain segmentation defects (Deflorian et al., 2004). While this phenotype is consistent with the previous described roles for Meinox proteins, there are several problems with this study that limit its usefulness. First and foremost, the phenotypes reported by these authors could not be replicated in an independent study performed in our lab, despite the fact that we used the same *pknox1.*1 morpholino and also included morpholinos against other possibly redundant *pknox* genes. Secondly, the specification of the reticulospinal and branchiomotor neurons was relatively normal in *pknox1.1* morphants, despite the rather severe defects in hindbrain segmentation and loss of Hox gene expression. These shortcomings, combined with a lack of protein loading controls for the Western analysis demonstrating a decrease in Pbx protein levels, make this study of *pknox1.1* function less than convincing. In Chapter 3 of this thesis, I will describe the hindbrain phenotype of Meis1-depleted zebrafish embryos, thereby contributing to the scant literature on the individual functions of Meinox genes in neural patterning.

Meinox overexpression studies in zebrafish also confirm that Meinox proteins act as partners with Hox and Pbx proteins to activate hindbrain marker genes. Co-expressing *hoxb1b* with *pbx4* and *meis3* activates *hoxb1a*, *hoxb2*, *krox20* and *mafB* / *valentino* expression to a much greater extent than overexpressing any of those genes alone or in pairs, and is able to transform anterior neural tissues to a hindbrain identity (Vlachakis et al., 2001). Interestingly, the overexpression phenotypes of *hoxb1a* and *hoxb1b* differ in their requirement for Meinox proteins (Choe and Sagerstrom, 2005). Hoxb1b shows a greater reliance on Meinox proteins, and this requirement can be mapped to the N-terminus of the protein. Thus, Meinox proteins synergize with Hox and Pbx to activate hindbrain genes, but not all Hox proteins require Meinox proteins to the same extent.

Unlike zebrafish, where individual Meinox gene function has remained relatively unexamined, there are a number of studies in Xenopus that have focused on the role of *Xmeis3*. *Xmeis3* plays an important role downstream of Wnt signaling to activate hindbrain markers either directly or through its genetic interactions with RA and Fgfs (Aamar and Frank, 2004; Dibner et al., 2001; Dibner et al., 2004; Elkouby et al., 2010; Gutkovich et al., 2010; Salzberg et al., 1999). Overexpression of wild type *Xmeis3* activates hindbrain marker expression and, consistent with the MeisDN phenotype in zebrafish, Xmeis3 fused to a transcriptional repressor blocks hindbrain gene expression. This provides further evidence that Meis proteins act as transcriptional activators in hindbrain patterning. Strikingly, antisense morpholino knockdown of Xmeis3 protein produces severe hindbrain segmentation defects very similar to that observed in MeisDN or Pbx-less zebrafish embryos. This suggests that Hox-Pbx complexes in *Xenopus* rely solely on *Xmeis3* function, or that *Xmeis3* functions upstream of all other Meinox genes in the hindbrain.

1.17 Non-neural patterning roles of PBC and Meinox proteins

Besides playing a critical role as Hox partners in hindbrain patterning, TALE-class proteins also cooperate with Hox proteins in non-neural developmental processes. One of the best studied of these is blood development and leukemogenesis, where the vertebrate TALE-class genes were first characterized. The posterior Hox genes have been extensively studied with regard to their role in leukemia and hematopoietic stem cell renewal (reviewed in Argiropoulos and Humphries, 2007). Similarly, increased *Pbx* and *Meis* expression and / or protein function is often observed in many types of leukemias. This correlation has been confirmed experimentally in mice and zebrafish, with Pbx and Meinox loss and gain of function models displaying defects in blood development (Azcoitia et al., 2005; Di Rosa et al., 2007; DiMartino et al., 2001; Ferretti et al., 2006; Hisa et al., 2004; Penkov et al., 2005; Penkov et al., 2008; Pillay et al., 2010; Wang et al., 2005; Wang et al., 2006; Wong et al., 2007).

Hox and TALE-class proteins also play a non-neural patterning role in establishing axial position in the vertebrate skeleton and limb. The essential role of Hox proteins in these processes has been shown in mice, where deletions in individual posterior Hox genes, or compound deletions of the entire Hox clusters, cause severe forelimb trunctions and mispatterning of the axial skeleton (reviewed in Wellik, 2007; reviewed in Zakany and Duboule, 2007). The role of Pbx proteins in skeletal and limb patterning has also been explored in mice where *Pbx1*$^{-/-}$ embryos display proximal limb defects, as well as rib and vertebral malformations (Selleri et al., 2001). Consistent with the functional redundancy between *pbx2* and *pbx4* in zebrafish hindbrain patterning (Waskiewicz et al., 2002), studies using *Pbx1*$^{-/-}$ / *Pbx2*$^{-/-}$ compound mutants have revealed that these mice display more severe limb and vertebral defects than the single mutants, and that Pbx1 and Pbx2 function redundantly to regulate the spatial distribution of Hox gene expression in these tissues (Capellini et al., 2006; Capellini et al., 2008).

Meinox genes also play an important role in proximal-distal patterning of the limb. In mice, chick and zebrafish, *Meis* gene expression is restricted to the proximal part of the developing limb (Capdevila et al., 1999; Mercader et al., 2009; Waskiewicz et al., 2001). In chick, this proximally-restricted Meis expression correlates with nuclear localized Pbx proteins in the proximal limb only (Mercader et al., 1999). Interestingly, *Pknox* / *Prep2* is expressed throughout the developing chick limb bud (Coy and Borycki, 2010), suggesting that in this context, Prep2 is unable to promote the nuclear localization of Pbx proteins. Overexpression of *Meis1/2* in chick and mouse limbs causes a distal-to-proximal transformation and alters the spatial arrangement of *Hox* gene expression, perhaps by antagonizing distal Bmp expression required for distal limb outgrowth (Capdevila et al., 1999; Mercader et al., 1999; Mercader et al., 2009). Meis also functions downstream of RA signaling in Axolotl to promote proximalization of the limb during regeneration (Mercader et al., 2005). In a striking example of evolutionary conservation, *Drosophila* Exd and Hth also promote proximal leg identity by antagonizing distal Dpp / Bmp signaling and activating the expression

of proximal factors like the zinc-finger transcription factor Teashirt (Azpiazu and Morata, 2002; Wu and Cohen, 2000). Meinox genes may also play a role in skeletal patterning, as mouse Meis1, Meis2 and Pknox proteins all colocalize with Pbx1 and Pbx2 in the developing notochord, although their function has not yet been analyzed (Capellini et al., 2008). Taken together, it is clear that Hox-Pbx-Meinox interactions perform numerous roles during vertebrate development, from neural patterning, to blood development, to limb and axial skeleton patterning.

1.18 Hox-independent functions of invertebrate PBC and Meinox proteins

One aspect of TALE-class function that has not been as extensively studied is the Hox-independent roles of PBC and Meinox proteins. These genes are broadly expressed during both vertebrate and invertebrate development, and display robust expression patterns in numerous tissues that do not express *Hox* genes. In *Drosophila*, both *exd* and *hth* perform Hox-independent pattern roles. *hth* is particularly important in deciding between antennal vs. leg fate (Casares and Mann, 1998; Casares and Mann, 2001). Ectopic *hth* can transform legs into antennae, and conversely, ectopic Antp (Hox) expression can transform antennae into legs. The major role of *Antp* is to repress *hth* expression in the distal leg of the second thoracic segment. Thus, far from acting as partners, *hth* and *Antp* antagonize each other in this context. *hth* also plays an important Hox-independent role in Drosophila eye development by maintaining a proliferating pool of eye progenitors (Lopes and Casares, 2010). The downregulation of *hth* expression by Bmp / *decapentaplegic* (*dpp*) signaling promotes the differentiation of these immature progenitors, while ectopic full-length *hth* (not the HD-less version) reduces eye size by preventing progenitors from adopting an eye fate (Bessa et al., 2002; Noro et al., 2006). *exd* can also function without a Hox partner, and has been shown to independently repress *dpp* expression in the anterior visceral mesoderm anterior to parasegment 7 (Rauskolb and Wieschaus, 1994). As well, Exd and Hth can activate the expression of the Fibroblast growth factor-like gene *branchless* in the mesodermal bridge cells of the tracheal system, and they do so without any genetic contribution from Hox genes (Merabet et al.,

2005). Thus, Exd and Hth regulate some aspects of fly development independently of Hox proteins.

The nematode *Caenorhabditis elegans* also possesses six Hox, three PBC and two Meinox homologues, and although not as well conserved at the sequence level, they maintain the same functional interactions as their fly and vertebrate counterparts (Arata et al., 2006; Hunter and Kenyon, 1995; Van Auken et al., 2002; Van Auken et al., 2000). In addition to their cooperative interactions with Hox proteins, the *C. elegans* PBC (*ceh-20*) and Meinox (*unc-62*) homologues also perform Hox-independent functions during mesoderm and vulva development, as well as cell migration (Jiang et al., 2009; Yang et al., 2005).

TALE-class and Hox-related genes are evolutionarily ancient and found throughout the animal kingdom, although true Hox genes are unique to eumetazoans (reviewed in Larroux et al., 2007; Martindale, 2005; Ryan et al., 2006). In spite of this, their interactions and functions have not been as well studied in other invertebrates and basal chordates. It is possible that both Hox-dependent and Hox-independent functions for TALE-class proteins will be uncovered in these other organisms. Nonetheless, *Drosophila* and *C. elegans* PBC and Meinox proteins perform Hox-independent functions.

1.19 Hox-independent functions of vertebrate PBC and Meinox proteins: the interaction with other PID-containing transcription factors

Examples of Hox-independent PBC and Meinox function have also been described in vertebrates (reviewed in Laurent et al., 2008; reviewed in Moens and Selleri, 2006). The tryptophan-containing PBC-interaction domain (PID) that Hox proteins use to bind to Pbx is also found in a wide range of other transcription factors (Figure 1-3) (In der Rieden et al., 2004), many of which are part of the extended Hox family of homeodomain proteins (Banerjee-Basu and Baxevanis, 2001; Brooke et al., 1998). Some of these are called orphan Hox genes, since they are believed to have arisen from ancient duplications of clustered Hox genes. Pancreas/duodenum homeobox protein 1 (Pdx1) is one of these orphan Hox family members, and was the first non-Hox protein for which a PID-mediated

biochemical interaction with Pbx was described (Peers et al., 1995). *Pbx1*$^{-/-}$ mice exhibit pancreatic defects that are very similar to those found in *Pdx1* mutants, and these two genes show a genetic interaction, as double heterozygotes have phenotypes present in neither of the single heterozygotes (Kim et al., 2002). Trimeric complexes of Pdx1, Pbx1 and Meinox proteins are responsible for directly regulating *somatostatin* and *elastase 1* expression in the pancreas (Andersen et al., 1999; Goudet et al., 1999; Swift et al., 1998). Pbx and Meis proteins also regulate *Pax6* expression in the pancreas, and play a role in patterning the endoderm to restrict insulin expression, but whether this requires input from Pdx1 is not clear (diIorio et al., 2007; Zhang et al., 2006). Interestingly, a direct interaction between Meis1 and the C-terminus of Pdx1 has also been reported, and that a trimeric complex of Pdx1, Pbx1 and Meis1 regulates transcription at the keratin 19 promoter (Deramaudt et al., 2006).

T-cell leukemia, homeobox 1 (Tlx1 / Hox11) is another orphan Hox protein that interacts with Pbx. Like Pbx1, Tlx1 was first characterized as a proto-oncogene involved in leukemia, specifically T-cell acute lymphoblastic leukemia caused by a t(10;14) (q24;q11) chromosomal translocation (Dear et al., 1993; Hatano et al., 1991). The biochemical interaction between Pbx1 and Tlx1 is required for murine spleen development. Analogous to what was found for Pdx1, *Pbx1*-null mice have defects in spleen development that phenocopy those observed in *Tlx1*-deficient mice, and *Pbx1*$^{+/-}$; *Tlx1*$^{+/-}$ double heterozygotes reveal a genetic interaction between the two genes (Allen et al., 2000; Brendolan et al., 2005). The similarities with Pdx1 continue, as a recent report has also demonstrated a direct binding between Tlx1 and Meis (but not Pknox) proteins (Milech et al., 2010). Respiratory neuron homeobox (Rnx / Hox11-like2 / Tlx3), an orphan Hox protein closely related to Tlx1, can also bind directly to Pbx3, and trimeric complexes of Rnx, Pbx3 and Meis1 are thought to regulate the development of neurons in the ventral medullary respiratory center that are responsible for breathing behaviour (Rhee et al., 2004). No direct interaction between Meis and Rnx as been reported as of yet. Tlx2 (Enx2 / Hox11-like1) is another related orphan Hox protein in which a putative PID has been identified (In

der Rieden et al., 2004). While no direct interaction between Pbx and Tlx2 has been demonstrated yet, there is evidence to suggest that Pbx is a direct regulator of *Tlx2* expression (Borghini et al., 2009). In summary, the TALE-PID interaction between Pbx and Hox proteins is also observed for orphan Hox family members, and these interactions are important for organogenesis and neuronal function.

The Caudal homeobox (Cdx) genes are another example of an orphan Hox family that contains a tryptophan PID. In zebrafish, Cdx1/4-depleted embryos exhibit a loss of posterior Hox gene expression, accompanied by severe defects in blood development (Davidson et al., 2003; Davidson and Zon, 2006; Serpente et al., 2005), and a transformation of spinal cord identity to a duplicated hindbrain (Shimizu et al., 2006; Skromne et al., 2007). Given that Pbx and Meinox genes also play a role in blood hematopoiesis, a functional interaction between Cdx and Pbx might be expected. In support of this idea, our lab has demonstrated PID-dependent binding between Cdx4 and Pbx4 *in vitro* (Pillay and Waskiewicz, unpublished results). However, a Cdx-Pbx interaction may not be required *in vivo*, as overexpression of a PID-mutant version of Cdx4 (W154A) in bone marrow cells causes an acute myeloid leukemia (AML)-like phenotype indistinguishable from the wild type protein (Bansal et al., 2006). Similarly, neither the phenotype nor the latency of AML were affected in mice that received bone marrow cells engineered to overexpress a PID-deficient Cdx2 (W167A) (Rawat et al., 2008). It should be noted, however, that the authors of these two studies did not perform any experiments to show that Cdx4-W154A or Cdx2-W167A failed to interact with Pbx. Conversely, a study by Liu et al. also established a biochemical interaction between Cdx2 and Pbx1 that was functionally required to activate proglucagon expression (Herzig et al., 2000; Liu et al., 2006). Interestingly though, while mutating the tryptophan residue of the PID attenuates proglucagon expression, it does not abolish the biochemical interaction between the two proteins *in vivo*. This suggests that Cdx-Pbx binding involves additional interactions, and may also explain why Cdx4-W154A and Cdx2-W167A still have AML-inducing activity. Thus, Pbx and Cdx can bind to one another and regulate

gene expression, but the details and functional significance of this interaction are still not clear.

Engrailed is not considered to be an orphan Hox, but is part of the extended Hox family. The Drosophila Engrailed locus was first identified in 1929 (Eker, 1929), and investigations into its function has produced a vast body of literature. In the first report describing Extradenticle function, it was noted that zygotic *exd* mutants had phenotypes resembling that of *engrailed* (*en*) mutant flies and that *en* expression was not maintained, providing the first hint that these two genes interact genetically (Peifer and Wieschaus, 1990). Subsequent biochemical evidence supported that idea that Exd and En are direct binding partners, and that Engrailed's divergent PID, which contains two tryptophan residues, is required for cooperative DNA binding with PBC proteins *in vitro* and *in vivo* (Peltenburg and Murre, 1996; Peltenburg and Murre, 1997; Serrano and Maschat, 1998; van Dijk and Murre, 1994; van Dijk et al., 1995). Engrailed proteins contain a strong repressor domain that, when fused to other transcription factors, is sufficient to repress target gene expression (Jaynes and O'Farrell, 1991). In spite of this, Hth-Exd-En trimeric complexes in *Drosophila* are required for both transcriptional activation and repression, and function to maintain segmental polarity during embryonic development (Alexandre and Vincent, 2003; Kobayashi et al., 2003). Vertebrates also express *Engrailed* homologues during embryonic development, most notably at the midbrain-hindbrain boundary and in the somatic muscle pioneer cells (Davidson et al., 1988; Ekker et al., 1992; Gardner et al., 1988). An *in vivo* role for the Pbx-Eng interaction had not been previously shown in vertebrates, and Chapter 5 of this thesis will describe how Pbx and Engrailed cooperate to compartmentalize the midbrain region in zebrafish.

All of the non-Hox proteins described above that bind to Pbx via a TALE-PID interaction have contained homeodomains, perhaps giving the impression that the mechanism is exclusive to this class of transcription factor. However, it also extends to members of the basic helix-loop-helix (bHLH) class of transcription factors as well (Knoepfler et al., 1999). Myogenic bHLH transcription factors such as myogenic differentiation (MyoD), myogenin (Myog),

myogenic factor 5 (Myf5), and myogenic factor 6 (Myf6 / Mrf4) all contain a conserved tryptophan-containing C-L-X-W motif N-terminal to their DNA-binding bHLH domains. *In vitro* studies show that this divergent PID is required for these bHLH factors to cooperatively bind DNA with a Pbx-Meinox dimer. Thus far, only the Pbx-MyoD interaction has been shown to function *in vivo*, such that MyoD requires Pbx and Meis partners to activate transcription at the myogenin promoter (Berkes et al., 2004; Maves et al., 2007). By performing a time course assay for Pbx-Meis occupancy on the myogenin promoter in differentiating myoblasts, Berkes et al. showed that Pbx-Meis proteins were constitutively bound to this regulatory region, even before initiation of the myogenic program. Conversely, MyoD, possibly in a complex with chromatin remodeling proteins, is recruited to the myogenin promoter only after differentiation has begun (Bergstrom et al., 2002; de la Serna et al., 2005). This suggests that Pbx and Meis promote muscle differentiation by acting as "molecular beacons" that recruit MyoD to the myogenin promoter. While it has not yet been described in other contexts, this pioneering role for Pbx and Meis could be a widespread phenomenon and represent an important mechanism by which they contribute to the transcriptional regulation of embryonic development (reviewed in Sagerstrom, 2004).

Perhaps related to their role in muscle differentiation, Pbx and Meinox proteins also play a role in heart development. Human genetic studies have found an association between heart disease and mutations in *MEIS2* (Crowley et al., 2010; Stankunas et al., 2008), although causation has not been established. By way of a possible explanation, a recent study in zebrafish has found that Pbx-depleted embryos have defects in heart morphology and myocardial differentiation (Maves et al., 2009). Microarray analysis found that a number of genes required for proper heart development are misregulated in Pbx-depleted embryos, including *myl7*, a gene encoding a cardiac myosin light peptide. An *in vitro* EMSA assay confirmed that Pbx and Meinox proteins can bind directly to the *myl7* promoter, thereby providing some insight into how Pbx and Meinox proteins may regulate heart development. Whether Pbx and Meis act as part of a

larger complex to regulate transcription in heart cells is not known at this time, though the promoter sequence bound by Pbx and Meis also contains a nearby canonical E-box that could be bound by an as-of-yet unidentified bHLH Pbx-binding partner.

1.20 Hox-independent functions of vertebrate PBC and Meinox proteins: the interaction with non-PID-containing transcription factors

Numerous other transcription factors have been shown to interact directly with Pbx proteins, possibly in a PID-independent fashion (reviewed in Laurent et al., 2008). These include the fork head transcription factor FoxC1 (Berry et al., 2005), and the nuclear receptors Triiodothyronine (T3) receptor-alpha (TRα) (Wang et al., 2001) and glucocorticoid receptor (GR) (Subramaniam et al., 2003). These last two studies suggest a novel role for Pbx proteins as metabolic regulators. Perhaps most interesting of all is the physical interaction demonstrated between Pbx1 and Smad proteins (Bailey et al., 2004). Smad proteins are central transcriptional regulators of the TGFβ / Bmp signaling pathways that play numerous pattern roles during embryonic development (reviewed in Massague et al., 2005). Although no structure-function assays were performed, Bailey et al. found a biochemical interaction between Pbx1 and Smads 2, 3, and 4. Furthermore, they provide evidence that a trimeric Smad4-Pbx1-Pknox1 complex regulates responsiveness of the follicle-stimulating hormone beta (FSHβ) promoter to activin (TGFβ) signaling. Although there is currently no evidence that TALE-class proteins are global regulators of TGFβ / Bmp signaling, it would be of interest to examine this interaction further in tissues where Pbx, Meinox, and Smad genes are co-expressed, such as the optic vesicle and hindbrain.

1.21 Hox-independent functions of vertebrate PBC and Meinox proteins in visual system development

From the previous examples, it is clear that both Hox and non-Hox proteins can participate in trimeric complexes with Pbx and Meis. However, Pbx and Meis genes are also expressed in tissues where no Hox genes are expressed,

and no other Pbx or Meis binding partner has yet been described. The most obvious of these is the visual system, which is comprised of the neural retina and visual processing centres in the midbrain. In particular, zebrafish, frog, chick and mouse all express Meis1 and Meis2 in these regions, suggesting that Meis genes play a role in vertebrate visual system development (Biemar et al., 2001; Cecconi et al., 1997; Coy and Borycki, 2010; Hisa et al., 2004; Oulad-Abdelghani et al., 1997; Waskiewicz et al., 2001; Zerucha and Prince, 2001). Consistent with this hypothesis, both *Meis1*-deficient mice and *Pknox* hypomorphs have microphthalmia and defects in retinal morphogenesis (Ferretti et al., 2006; Hisa et al., 2004). In Drosophila, Homothorax plays an important role in eye development by keeping eye progenitor cells in a proliferative, multipotent state. The downregulation of *hth* expression by Bmp and Hedgehog signaling marks the transition from proliferation to differentiation. Remarkably, this Hox-independent role for Meis proteins is conserved in vertebrates. In zebrafish, morpholino knockdown of Meis1 protein causes microphthalmia. This Meis1-knockdown phenotype is caused by a decrease in *cyclin D1* (*ccnd1*) and *myelocytomatosis oncogene a* (*myca* / *c-myc*) expression in retinal progenitor cells leading to a stall in the G1-S transition of the cell cycle (Bessa et al., 2008). In chick, a similar role was described for Meis2 through the overexpression of a MeisEnR antimorphic construct (Heine et al., 2008). Furthermore, Meis2 expression in differentiating retinal cells is downregulated by Shh signaling (Heine et al., 2009), similar to what is observed in flies. Thus, Meis genes play an evolutionarily conserved role in regulating retinal progenitor cell proliferation and differentiation.

As mentioned earlier, the hindbrain is an excellent system in which to examine the transcriptional regulation of axial patterning due to its clear AP polarity and reiterated segmental units. However, the establishment of positional information is an essential step in the development of all tissues, and the visual system is no different. In order for us to process and act upon a visual stimulus, it is essential that this information be correctly communicated to the brain. To do this, retinal ganglion cells (RGCs) send their axons out of the eye to innervate visual processing centers in the midbrain. In fish, frogs and chick, this region is

called the optic tectum, while the homologous structure in mammals is called the superior colliculus. The orderly process by which RGCs precisely innervate the tectum is called retinotectal mapping, and its fidelity requires that axial information be established in both the retina and the tectum (reviewed in Lemke and Reber, 2005). Although Meis genes are required for hindbrain patterning, their role in patterning the retina and tectum have not been investigated. Chapter 6 of this thesis will describe the roles of Meis1 in establishing positional information in the zebrafish visual system.

1.22 Summary

Overall, this thesis will cover two broad themes related to the roles of Pbx and Meinox genes during embryonic zebrafish development. The first will be hindbrain patterning. While the field of Hox-dependent hindbrain patterning is a well-studied one, there are still many unanswered questions. Chapter 3 will assess the contribution of Meis1 to the establishment of rhombomere identity and neuronal specification in the hindbrain. I will show that Meis1 is critically required only to specify rhombomere 2 identity. However, even though rhombomeres 3-7 retain their segmental identities, the reticulospinal and branchiomotor neurons in r4 are affected by a loss of Meis1. This suggests that Meis1 is making specific transcriptional contributions to neuronal development downstream of r4 specification. The second outstanding problem in hindbrain development that I will address is the role of zebrafish *teashirt* genes regulating Hox function. In Chapter 4, I will detail the expression of *teashirt zinc finger homeobox 3b* (*tshz3b*) during hindbrain development, and show through overexpression and structure-function assays that *tshz3b* is a negative regulator of Hox-dependent hindbrain segmentation.

The second theme that this thesis will cover is the role of Pbx2/4 and Meis1 in patterning the zebrafish visual system. The midbrain is enclosed by two lineage-restricted boundaries, the midbrain-hindbrain boundary (MHB) at its posterior, and the diencephalic-mesencephalic boundary (DMB) anteriorly. The maintenance of these two boundaries is required for midbrain development, and

ultimately, the formation of the optic tectum. Chapter 5 will show that zebrafish Pbx and Engrailed proteins are biochemical binding partners, and that this interaction is required to maintain both the MHB and DMB. Lastly, Chapter 6 will highlight the involvement of Meis1 in patterning the visual system and organizing the retinotectal map. An analysis of retinal patterning reveals that Meis1 is required to correctly specify both dorsal-ventral and nasal-temporal identity in the zebrafish retina. Meis1-knockdown results in a loss of *smad1* expression and an upregulation in *follistatin* expression, thereby causing lower levels of Bmp signaling and a partial ventralization of the retina. Additionally, Meis1-deficient embryos exhibit ectopic Fgf signaling in the developing retina and a corresponding loss of temporal identity. Meis1 also positively regulates *ephrin* gene expression in the tectum, but is not involved in maintaining MHB or DMB integrity. Consistent with these patterning phenotypes, Meis1 knockdown ultimately results in disorganization of the retinotectal map. Taken together, this thesis will clarify our understanding of Hox-dependent hindbrain patterning, and demonstrate that Pbx and Meis perform a general axial patterning function in anterior neural tissues such as the hindbrain, midbrain and retina.

1.23 Tables

Hpf	Stage	Developmental milestones
6	shield stage	Hindbrain-fated neuroectoderm already specified by signals from the lateral germ ring[1,2].
7.5	70% epiboly	*hoxb1b* expressed in the presumptive hindbrain[3]; Mauthner neuron born[4].
9-10	90% epiboly - tailbud	Regionalized *hox* gene expression established[5]; *egr2b / krox20* expressed in presumptive r3[6].
10-12	1 - 6 somites	Refinement of *hox* gene expression and rhombomere boundaries[5].
14	10 somites	Endogenous *isl1* expression in postmitotic BMNs[7].
16	14 somites	In the *Tg[isl1:GFP]* transgenic line of fish, trigeminal (r2) and FMNs (r4) start to express GFP under the control of the *isl1* promoter[8].
21	24 somites	FMNs have started their tangential migration from their birthplace in r4 to r6/7[9].
36	prim-25	FMNs have largely completed their migration[8,9].

Table 1-1. Milestones of zebrafish hindbrain development. The developmental stage is given in both hours post-fertilization (hpf) and by its common name, as previously described (Kimmel et al., 1995). Abbreviations: BMN – branchiomotor neurons; FMN – facial motor neurons; Hpf – hours post-fertilization; prim – lateral line primordium; r – rhombomere. References: [1](Woo et al., 1995); [2](Woo and Fraser, 1997); [3](Waskiewicz et al., 2002); [4](Mendelson, 1986); [5](Prince et al., 1998); [6](Oxtoby and Jowett, 1993); [7](Thisse and Thisse, 2005); [8](Cooper et al., 2003); [9](Higashijima et al., 2000).

1.24 Figures

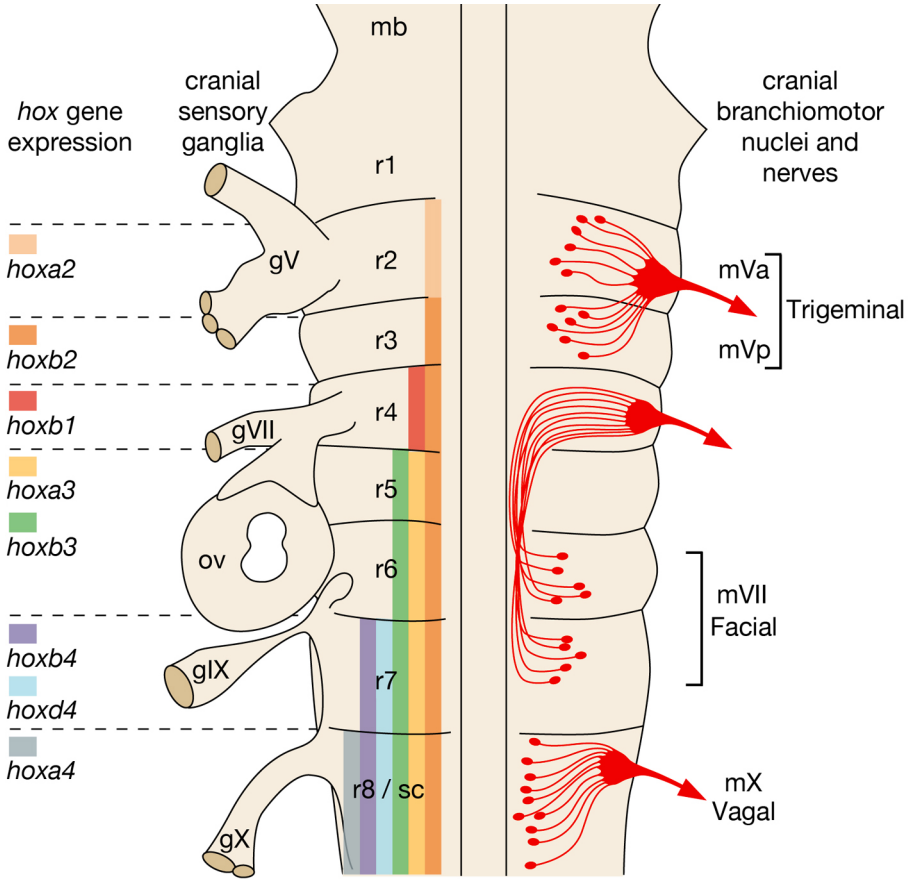

Figure 1-1. Schematic of *hox* gene expression and cranial nerve position in the zebrafish hindbrain. In this schematic, the neural tube is shown in dorsal view with anterior at the top. For clarity, certain features of the hindbrain are shown on one side only. The rhombomere-restricted patterns of *hox* gene expression (reviewed in Moens and Prince, 2002; Prince et al., 1998) are shown on the left, along with the positions of the cranial sensory ganglia. The positions of the cranial branchiomotor nuclei and their nerve exit points are shown on the right (reviewed in Chandrasekhar, 2004). Abbreviations: g – ganglion; mb – midbrain; m – motor; ov – otic vesicle; r – rhombomere; sc – spinal cord. This figure was modified after Kiecker and Lumsden (2005).

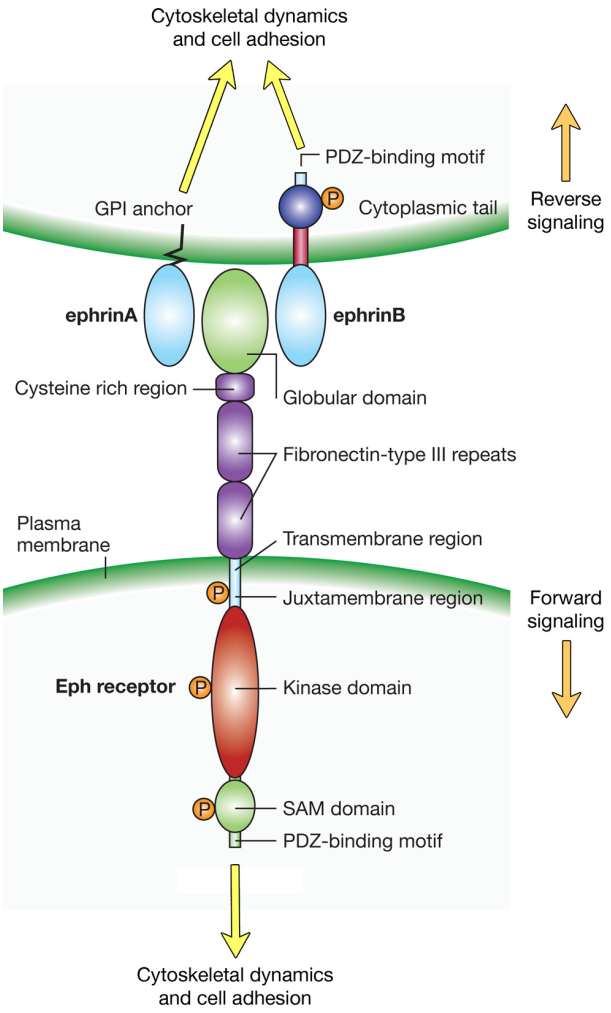

Figure 1-2. Schematic of the interaction between Eph receptor tyrosine kinases (RTK) and their Ephrin ligands. Eph RTKs are transmembrane proteins with extracellular Fibronectin-type III repeats and a globular domain that interacts with Ephrin ligands. Intracellularly, Eph RTKs contain a kinase domain that autophosphorylates the receptor. Once phosphorylated, the protein-protein interaction domains (PDZ and SAM) at the C-terminus promote the assembly of complexes that modulate cytoskeletal dynamics and cell-cell adhesion in what is called "forward signaling". The transduction of a signal into the *ephrin*-expressing cell is called "reverse signaling". The exact mechanism of how this occurs depends on whether the Ephrin is a GPI-anchored Type A ligand, or a transmembrane Type B ligand. Regardless of the type of Ephrin ligand, the downstream effects of reverse signaling also involve changes to the cytoskeletaon and cel adhesion. In this way, Eph and Ephrin interactions can promote cell sorting (e.g. hindbrain rhombomeres), and regulate axon guidance and synpase formation (retinotectal mapping). This figure was modified after Kullander and Klein (2002).

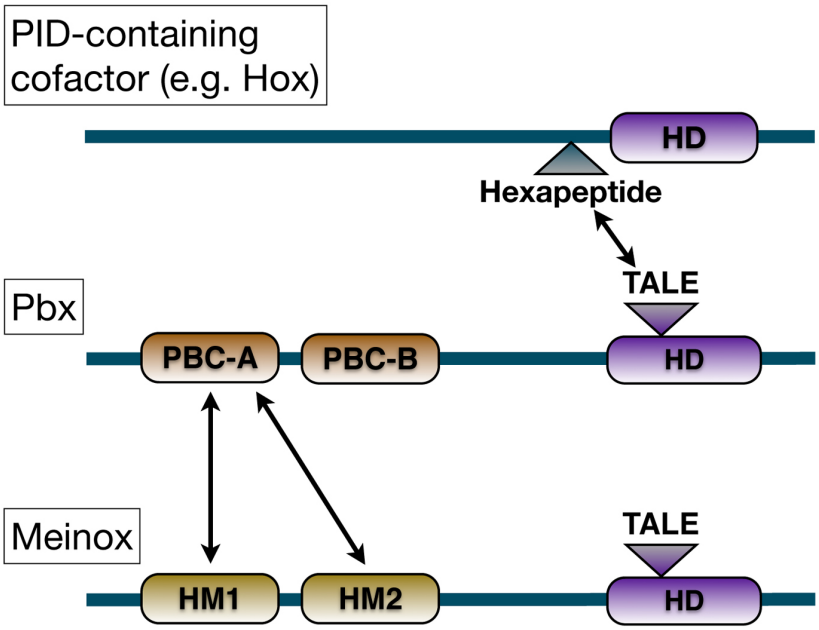

Figure 1-3. Schematic of the domains required for the biochemical interactions between Pbx, Meinox, and PID-containing transcription factors such as Hox PG 1-10 proteins. The PID (PBC-interaction domain; a.k.a. hexapeptide or pentapeptide) invariably contains a tryptophan residue that can insert into the hydrophobic pocket formed by the Pbx TALE-motif. Although first described in Hox PG 1-10, PIDs are also found in other members of the extended Hox class, such as the Tlx, Pdx, Cdx, and Eng families of homeodomain proteins, as well as in bHLH transcription factors such as MyoD. Although Meinox proteins also contain a TALE-motif, it has not been shown to directly interact with Hox proteins. The Pbx-Meinox interaction is mediated by the PBC-A domain in Pbx proteins and the Hth-Meis (HM) 1 and 2 domains in Meinox proteins, all located near the N-termini of their respective proteins.

1.25 References

Aamar, E., Frank, D., 2004. Xenopus Meis3 protein forms a hindbrain-inducing center by activating FGF/MAP kinase and PCP pathways. Development. 131**,** 153-63.

Abramovich, C., Chavez, E. A., Lansdorp, P. M., Humphries, R. K., 2002. Functional characterization of multiple domains involved in the subcellular localization of the hematopoietic Pbx interacting protein (HPIP). Oncogene. 21**,** 6766-71.

Abramovich, C., Shen, W. F., Pineault, N., Imren, S., Montpetit, B., Largman, C., Humphries, R. K., 2000. Functional cloning and characterization of a novel nonhomeodomain protein that inhibits the binding of PBX1-HOX complexes to DNA. J Biol Chem. 275**,** 26172-7.

Abu-Abed, S., Dolle, P., Metzger, D., Beckett, B., Chambon, P., Petkovich, M., 2001. The retinoic acid-metabolizing enzyme, CYP26A1, is essential for normal hindbrain patterning, vertebral identity, and development of posterior structures. Genes Dev. 15**,** 226-40.

Abu-Shaar, M., Mann, R. S., 1998. Generation of multiple antagonistic domains along the proximodistal axis during Drosophila leg development. Development. 125**,** 3821-30.

Abu-Shaar, M., Ryoo, H. D., Mann, R. S., 1999. Control of the nuclear localization of Extradenticle by competing nuclear import and export signals. Genes Dev. 13**,** 935-45.

Affolter, M., Slattery, M., Mann, R. S., 2008. A lexicon for homeodomain-DNA recognition. Cell. 133**,** 1133-5.

Alexander, T., Nolte, C., Krumlauf, R., 2009. Hox genes and segmentation of the hindbrain and axial skeleton. Annu Rev Cell Dev Biol. 25**,** 431-56.

Alexandre, C., Vincent, J. P., 2003. Requirements for transcriptional repression and activation by Engrailed in Drosophila embryos. Development. 130**,** 729-39.

Allen, T. D., Zhu, Y. X., Hawley, T. S., Hawley, R. G., 2000. TALE homeoproteins as HOX11-interacting partners in T-cell leukemia. Leuk Lymphoma. 39**,** 241-56.

Amoyel, M., Cheng, Y. C., Jiang, Y. J., Wilkinson, D. G., 2005. Wnt1 regulates neurogenesis and mediates lateral inhibition of boundary cell specification in the zebrafish hindbrain. Development. 132**,** 775-85.

Andersen, F. G., Jensen, J., Heller, R. S., Petersen, H. V., Larsson, L. I., Madsen, O. D., Serup, P., 1999. Pax6 and Pdx1 form a functional complex on the rat somatostatin gene upstream enhancer. FEBS Lett. 445**,** 315-20.

Aragon, F., Vazquez-Echeverria, C., Ulloa, E., Reber, M., Cereghini, S., Alsina, B., Giraldez, F., Pujades, C., 2005. vHnf1 regulates specification of caudal rhombomere identity in the chick hindbrain. Dev Dyn. 234**,** 567-76.

Arata, Y., Kouike, H., Zhang, Y., Herman, M. A., Okano, H., Sawa, H., 2006. Wnt signaling and a Hox protein cooperatively regulate psa-3/Meis to determine daughter cell fate after asymmetric cell division in C. elegans. Dev Cell. 11**,** 105-15.

Argiropoulos, B., Humphries, R. K., 2007. Hox genes in hematopoiesis and leukemogenesis. Oncogene. 26**,** 6766-76.

Arvanitis, D., Davy, A., 2008. Eph/ephrin signaling: networks. Genes Dev. 22**,** 416-29.

Asahara, H., Dutta, S., Kao, H. Y., Evans, R. M., Montminy, M., 1999. Pbx-Hox heterodimers recruit coactivator-corepressor complexes in an isoform-specific manner. Mol Cell Biol. 19**,** 8219-25.

Aspland, S. E., White, R. A., 1997. Nucleocytoplasmic localisation of extradenticle protein is spatially regulated throughout development in Drosophila. Development. 124**,** 741-7.

Azcoitia, V., Aracil, M., Martinez, A. C., Torres, M., 2005. The homeodomain protein Meis1 is essential for definitive hematopoiesis and vascular patterning in the mouse embryo. Dev Biol. 280**,** 307-20.

Azpiazu, N., Morata, G., 1998. Functional and regulatory interactions between Hox and extradenticle genes. Genes Dev. 12**,** 261-73.

Azpiazu, N., Morata, G., 2002. Distinct functions of homothorax in leg development in Drosophila. Mech Dev. 119**,** 55-67.

Bailey, J. S., Rave-Harel, N., McGillivray, S. M., Coss, D., Mellon, P. L., 2004. Activin regulation of the follicle-stimulating hormone beta-subunit gene involves Smads and the TALE homeodomain proteins Pbx1 and Prep1. Mol Endocrinol. 18**,** 1158-70.

Banerjee-Basu, S., Baxevanis, A. D., 2001. Molecular evolution of the homeodomain family of transcription factors. Nucleic Acids Res. 29**,** 3258-69.

Bannister, A. J., Kouzarides, T., 1996. The CBP co-activator is a histone acetyltransferase. Nature. 384**,** 641-3.

Bansal, D., Scholl, C., Frohling, S., McDowell, E., Lee, B. H., Dohner, K., Ernst, P., Davidson, A. J., Daley, G. Q., Zon, L. I., Gilliland, D. G., Huntly, B. J., 2006. Cdx4 dysregulates Hox gene expression and generates acute myeloid leukemia alone and in cooperation with Meis1a in a murine model. Proc Natl Acad Sci U S A. 103**,** 16924-9.

Barrow, J. R., Capecchi, M. R., 1996. Targeted disruption of the Hoxb-2 locus in mice interferes with expression of Hoxb-1 and Hoxb-4. Development. 122**,** 3817-28.

Bateson, W., 1894. Materials for the study of variation: treated with special regard to discontinuity in the origin of species. Macmillan and Co., New York.

Begemann, G., Schilling, T. F., Rauch, G. J., Geisler, R., Ingham, P. W., 2001. The zebrafish neckless mutation reveals a requirement for raldh2 in mesodermal signals that pattern the hindbrain. Development. 128**,** 3081-94.

Berger, M. F., Badis, G., Gehrke, A. R., Talukder, S., Philippakis, A. A., Pena-Castillo, L., Alleyne, T. M., Mnaimneh, S., Botvinnik, O. B., Chan, E. T., Khalid, F., Zhang, W., Newburger, D., Jaeger, S. A., Morris, Q. D., Bulyk, M. L., Hughes, T. R., 2008. Variation in homeodomain DNA binding revealed by high-resolution analysis of sequence preferences. Cell. 133**,** 1266-76.

Bergstrom, D. A., Penn, B. H., Strand, A., Perry, R. L., Rudnicki, M. A., Tapscott, S. J., 2002. Promoter-specific regulation of MyoD binding and signal transduction cooperate to pattern gene expression. Mol Cell. 9**,** 587-600.

Berkes, C. A., Bergstrom, D. A., Penn, B. H., Seaver, K. J., Knoepfler, P. S., Tapscott, S. J., 2004. Pbx marks genes for activation by MyoD indicating a role for a homeodomain protein in establishing myogenic potential. Mol Cell. 14**,** 465-77.

Berry, F. B., O'Neill, M. A., Coca-Prados, M., Walter, M. A., 2005. FOXC1 transcriptional regulatory activity is impaired by PBX1 in a filamin A-mediated manner. Mol Cell Biol. 25**,** 1415-24.

Berthelsen, J., Kilstrup-Nielsen, C., Blasi, F., Mavilio, F., Zappavigna, V., 1999. The subcellular localization of PBX1 and EXD proteins depends on nuclear import and export signals and is modulated by association with PREP1 and HTH. Genes Dev. 13**,** 946-53.

Berthelsen, J., Zappavigna, V., Ferretti, E., Mavilio, F., Blasi, F., 1998a. The novel homeoprotein Prep1 modulates Pbx-Hox protein cooperativity. EMBO J. 17**,** 1434-45.

Berthelsen, J., Zappavigna, V., Mavilio, F., Blasi, F., 1998b. Prep1, a novel functional partner of Pbx proteins. EMBO J. 17**,** 1423-33.

Bessa, J., Carmona, L., Casares, F., 2009. Zinc-finger paralogues tsh and tio are functionally equivalent during imaginal development in Drosophila and maintain their expression levels through auto- and cross-negative feedback loops. Dev Dyn. 238**,** 19-28.

Bessa, J., Gebelein, B., Pichaud, F., Casares, F., Mann, R. S., 2002. Combinatorial control of Drosophila eye development by eyeless, homothorax, and teashirt. Genes Dev. 16**,** 2415-27.

Bessa, J., Tavares, M. J., Santos, J., Kikuta, H., Laplante, M., Becker, T. S., Gomez-Skarmeta, J. L., Casares, F., 2008. meis1 regulates cyclin D1 and c-myc expression, and controls the proliferation of the multipotent cells in the early developing zebrafish eye. Development. 135**,** 799-803.

Bickmore, W. A., Mahy, N. L., Chambeyron, S., 2004. Do higher-order chromatin structure and nuclear reorganization play a role in regulating Hox gene expression during development? Cold Spring Harb Symp Quant Biol. 69**,** 251-7.

Biemar, F., Devos, N., Martial, J. A., Driever, W., Peers, B., 2001. Cloning and expression of the TALE superclass homeobox Meis2 gene during zebrafish embryonic development. Mech Dev. 109**,** 427-31.

Blumberg, B., Bolado, J., Jr., Moreno, T. A., Kintner, C., Evans, R. M., Papalopulu, N., 1997. An essential role for retinoid signaling in anteroposterior neural patterning. Development. 124**,** 373-9.

Bonner, J. T., 2002. First Signals: The Evolution of Multicellular Development. Princeton University Press, Princeton.

Borghini, S., Bachetti, T., Fava, M., Duca, M. D., Ravazzolo, R., Ceccherini, I., 2009. Functional characterization of a minimal sequence essential for the expression of human TLX2 gene. BMB Rep. 42**,** 788-93.

Brendolan, A., Ferretti, E., Salsi, V., Moses, K., Quaggin, S., Blasi, F., Cleary, M. L., Selleri, L., 2005. A Pbx1-dependent genetic and transcriptional network regulates spleen ontogeny. Development. 132**,** 3113-26.

Brooke, N. M., Garcia-Fernandez, J., Holland, P. W., 1998. The ParaHox gene cluster is an evolutionary sister of the Hox gene cluster. Nature. 392**,** 920-2.

Bruckner, K., Pasquale, E. B., Klein, R., 1997. Tyrosine phosphorylation of transmembrane ligands for Eph receptors. Science. 275**,** 1640-3.

Burglin, T. R., 1997. Analysis of TALE superclass homeobox genes (MEIS, PBC, KNOX, Iroquois, TGIF) reveals a novel domain conserved between plants and animals. Nucleic Acids Res. 25**,** 4173-80.

Burglin, T. R., 1998. The PBC domain contains a MEINOX domain: coevolution of Hox and TALE homeobox genes? Dev Genes Evol. 208**,** 113-6.

Burglin, T. R., Ruvkun, G., 1992. New motif in PBX genes. Nat Genet. 1**,** 319-20.

Capdevila, J., Tsukui, T., Rodriquez Esteban, C., Zappavigna, V., Izpisua Belmonte, J. C., 1999. Control of vertebrate limb outgrowth by the

proximal factor Meis2 and distal antagonism of BMPs by Gremlin. Mol Cell. 4**,** 839-49.

Capellini, T. D., Di Giacomo, G., Salsi, V., Brendolan, A., Ferretti, E., Srivastava, D., Zappavigna, V., Selleri, L., 2006. Pbx1/Pbx2 requirement for distal limb patterning is mediated by the hierarchical control of Hox gene spatial distribution and Shh expression. Development. 133**,** 2263-73.

Capellini, T. D., Zewdu, R., Di Giacomo, G., Asciutti, S., Kugler, J. E., Di Gregorio, A., Selleri, L., 2008. Pbx1/Pbx2 govern axial skeletal development by controlling Polycomb and Hox in mesoderm and Pax1/Pax9 in sclerotome. Dev Biol. 321**,** 500-14.

Carpenter, E. M., 2002. Hox genes and spinal cord development. Dev Neurosci. 24**,** 24-34.

Carpenter, E. M., Goddard, J. M., Chisaka, O., Manley, N. R., Capecchi, M. R., 1993. Loss of Hox-A1 (Hox-1.6) function results in the reorganization of the murine hindbrain. Development. 118**,** 1063-75.

Carrasco, A. E., McGinnis, W., Gehring, W. J., De Robertis, E. M., 1984. Cloning of an X. laevis gene expressed during early embryogenesis coding for a peptide region homologous to Drosophila homeotic genes. Cell. 37**,** 409-14.

Casares, F., Mann, R. S., 1998. Control of antennal versus leg development in Drosophila. Nature. 392**,** 723-6.

Casares, F., Mann, R. S., 2001. The ground state of the ventral appendage in Drosophila. Science. 293**,** 1477-80.

Cecconi, F., Proetzel, G., Alvarez-Bolado, G., Jay, D., Gruss, P., 1997. Expression of Meis2, a Knotted-related murine homeobox gene, indicates a role in the differentiation of the forebrain and the somitic mesoderm. Dev Dyn. 210**,** 184-90.

Chambeyron, S., Bickmore, W. A., 2004. Chromatin decondensation and nuclear reorganization of the HoxB locus upon induction of transcription. Genes Dev. 18**,** 1119-30.

Chan, S. K., Jaffe, L., Capovilla, M., Botas, J., Mann, R. S., 1994. The DNA binding specificity of Ultrabithorax is modulated by cooperative interactions with extradenticle, another homeoprotein. Cell. 78**,** 603-15.

Chan, S. K., Mann, R. S., 1996. A structural model for a homeotic protein-extradenticle-DNA complex accounts for the choice of HOX protein in the heterodimer. Proc Natl Acad Sci U S A. 93**,** 5223-8.

Chan, S. K., Popperl, H., Krumlauf, R., Mann, R. S., 1996. An extradenticle-induced conformational change in a HOX protein overcomes an inhibitory function of the conserved hexapeptide motif. EMBO J. 15**,** 2476-87.

Chan, S. K., Ryoo, H. D., Gould, A., Krumlauf, R., Mann, R. S., 1997. Switching the in vivo specificity of a minimal Hox-responsive element. Development. 124**,** 2007-14.

Chandrasekhar, A., 2004. Turning heads: development of vertebrate branchiomotor neurons. Dev Dyn. 229**,** 143-61.

Chang, C. P., Brocchieri, L., Shen, W. F., Largman, C., Cleary, M. L., 1996. Pbx modulation of Hox homeodomain amino-terminal arms establishes different DNA-binding specificities across the Hox locus. Mol Cell Biol. 16**,** 1734-45.

Chang, C. P., Jacobs, Y., Nakamura, T., Jenkins, N. A., Copeland, N. G., Cleary, M. L., 1997. Meis proteins are major in vivo DNA binding partners for wild-type but not chimeric Pbx proteins. Mol Cell Biol. 17**,** 5679-87.

Chang, C. P., Shen, W. F., Rozenfeld, S., Lawrence, H. J., Largman, C., Cleary, M. L., 1995. Pbx proteins display hexapeptide-dependent cooperative DNA binding with a subset of Hox proteins. Genes Dev. 9**,** 663-74.

Chariot, A., van Lint, C., Chapelier, M., Gielen, J., Merville, M. P., Bours, V., 1999. CBP and histone deacetylase inhibition enhance the transactivation potential of the HOXB7 homeodomain-containing protein. Oncogene. 18**,** 4007-14.

Chen, J., Ruley, H. E., 1998. An enhancer element in the EphA2 (Eck) gene sufficient for rhombomere-specific expression is activated by HOXA1 and HOXB1 homeobox proteins. J Biol Chem. 273**,** 24670-5.

Choe, S. K., Lu, P., Nakamura, M., Lee, J., Sagerstrom, C. G., 2009. Meis cofactors control HDAC and CBP accessibility at Hox-regulated promoters during zebrafish embryogenesis. Dev Cell. 17**,** 561-7.

Choe, S. K., Sagerstrom, C. G., 2005. Variable Meis-dependence among paralog group-1 Hox proteins. Biochem Biophys Res Commun. 331**,** 1384-91.

Choe, S. K., Vlachakis, N., Sagerstrom, C. G., 2002. Meis family proteins are required for hindbrain development in the zebrafish. Development. 129**,** 585-95.

Chomette, D., Frain, M., Cereghini, S., Charnay, P., Ghislain, J., 2006. Krox20 hindbrain cis-regulatory landscape: interplay between multiple long-range initiation and autoregulatory elements. Development. 133**,** 1253-62.

Cooke, J., Moens, C., Roth, L., Durbin, L., Shiomi, K., Brennan, C., Kimmel, C., Wilson, S., Holder, N., 2001. Eph signalling functions downstream of Val to regulate cell sorting and boundary formation in the caudal hindbrain. Development. 128**,** 571-80.

Cooke, J. E., Kemp, H. A., Moens, C. B., 2005. EphA4 is required for cell adhesion and rhombomere-boundary formation in the zebrafish. Curr Biol. 15**,** 536-42.

Cooke, J. E., Moens, C. B., 2002. Boundary formation in the hindbrain: Eph only it were simple. Trends Neurosci. 25**,** 260-7.

Cooper, K. L., Leisenring, W. M., Moens, C. B., 2003. Autonomous and nonautonomous functions for Hox/Pbx in branchiomotor neuron development. Dev Biol. 253**,** 200-13.

Cowan, C. A., Henkemeyer, M., 2002. Ephrins in reverse, park and drive. Trends Cell Biol. 12**,** 339-46.

Cox, W. G., Hemmati-Brivanlou, A., 1995. Caudalization of neural fate by tissue recombination and bFGF. Development. 121**,** 4349-58.

Coy, S. E., Borycki, A. G., 2010. Expression analysis of TALE family transcription factors during avian development. Dev Dyn. 239**,** 1234-45.

Crowley, M. A., Conlin, L. K., Zackai, E. H., Deardorff, M. A., Thiel, B. D., Spinner, N. B., 2010. Further evidence for the possible role of MEIS2 in

the development of cleft palate and cardiac septum. Am J Med Genet A. 152A**,** 1326-7.

Dasen, J. S., Jessell, T. M., 2009. Hox networks and the origins of motor neuron diversity. Curr Top Dev Biol. 88**,** 169-200.

Datta, R. R., Lurye, J. M., Kumar, J. P., 2009. Restriction of ectopic eye formation by Drosophila teashirt and tiptop to the developing antenna. Dev Dyn. 238**,** 2202-10.

Davidson, A. J., Ernst, P., Wang, Y., Dekens, M. P., Kingsley, P. D., Palis, J., Korsmeyer, S. J., Daley, G. Q., Zon, L. I., 2003. cdx4 mutants fail to specify blood progenitors and can be rescued by multiple hox genes. Nature. 425**,** 300-6.

Davidson, A. J., Zon, L. I., 2006. The caudal-related homeobox genes cdx1a and cdx4 act redundantly to regulate hox gene expression and the formation of putative hematopoietic stem cells during zebrafish embryogenesis. Dev Biol. 292**,** 506-18.

Davidson, D., Graham, E., Sime, C., Hill, R., 1988. A gene with sequence similarity to Drosophila engrailed is expressed during the development of the neural tube and vertebrae in the mouse. Development. 104**,** 305-16.

Davy, A., Gale, N. W., Murray, E. W., Klinghoffer, R. A., Soriano, P., Feuerstein, C., Robbins, S. M., 1999. Compartmentalized signaling by GPI-anchored ephrin-A5 requires the Fyn tyrosine kinase to regulate cellular adhesion. Genes Dev. 13**,** 3125-35.

de la Serna, I. L., Ohkawa, Y., Berkes, C. A., Bergstrom, D. A., Dacwag, C. S., Tapscott, S. J., Imbalzano, A. N., 2005. MyoD targets chromatin remodeling complexes to the myogenin locus prior to forming a stable DNA-bound complex. Mol Cell Biol. 25**,** 3997-4009.

Dear, T. N., Sanchez-Garcia, I., Rabbitts, T. H., 1993. The HOX11 gene encodes a DNA-binding nuclear transcription factor belonging to a distinct family of homeobox genes. Proc Natl Acad Sci U S A. 90**,** 4431-5.

Deflorian, G., Tiso, N., Ferretti, E., Meyer, D., Blasi, F., Bortolussi, M., Argenton, F., 2004. Prep1.1 has essential genetic functions in hindbrain

development and cranial neural crest cell differentiation. Development. 131**,** 613-27.

Deramaudt, T. B., Sachdeva, M. M., Wescott, M. P., Chen, Y., Stoffers, D. A., Rustgi, A. K., 2006. The PDX1 homeodomain transcription factor negatively regulates the pancreatic ductal cell-specific keratin 19 promoter. J Biol Chem. 281**,** 38385-95.

Desplan, C., Theis, J., O'Farrell, P. H., 1988. The sequence specificity of homeodomain-DNA interaction. Cell. 54**,** 1081-90.

Di Rocco, G., Gavalas, A., Popperl, H., Krumlauf, R., Mavilio, F., Zappavigna, V., 2001. The recruitment of SOX/OCT complexes and the differential activity of HOXA1 and HOXB1 modulate the Hoxb1 auto-regulatory enhancer function. J Biol Chem. 276**,** 20506-15.

Di Rosa, P., Villaescusa, J. C., Longobardi, E., Iotti, G., Ferretti, E., Diaz, V. M., Miccio, A., Ferrari, G., Blasi, F., 2007. The homeodomain transcription factor Prep1 (pKnox1) is required for hematopoietic stem and progenitor cell activity. Dev Biol. 311**,** 324-34.

Diaz, V. M., Bachi, A., Blasi, F., 2007. Purification of the Prep1 interactome identifies novel pathways regulated by Prep1. Proteomics. 7**,** 2617-23.

Dibner, C., Elias, S., Frank, D., 2001. XMeis3 protein activity is required for proper hindbrain patterning in Xenopus laevis embryos. Development. 128**,** 3415-26.

Dibner, C., Elias, S., Ofir, R., Souopgui, J., Kolm, P. J., Sive, H., Pieler, T., Frank, D., 2004. The Meis3 protein and retinoid signaling interact to pattern the Xenopus hindbrain. Dev Biol. 271**,** 75-86.

diIorio, P., Alexa, K., Choe, S. K., Etheridge, L., Sagerstrom, C. G., 2007. TALE-family homeodomain proteins regulate endodermal sonic hedgehog expression and pattern the anterior endoderm. Dev Biol. 304**,** 221-31.

DiMartino, J. F., Selleri, L., Traver, D., Firpo, M. T., Rhee, J., Warnke, R., O'Gorman, S., Weissman, I. L., Cleary, M. L., 2001. The Hox cofactor and proto-oncogene Pbx1 is required for maintenance of definitive hematopoiesis in the fetal liver. Blood. 98**,** 618-26.

Dupe, V., Lumsden, A., 2001. Hindbrain patterning involves graded responses to retinoic acid signalling. Development. 128**,** 2199-208.

Eker, R., 1929. The recessive mutant engrailed in Drosophila melanogaster. Hereditas. 12**,** 217-222.

Ekker, M., Wegner, J., Akimenko, M. A., Westerfield, M., 1992. Coordinate embryonic expression of three zebrafish engrailed genes. Development. 116**,** 1001-10.

Elkouby, Y. M., Elias, S., Casey, E. S., Blythe, S. A., Tsabar, N., Klein, P. S., Root, H., Liu, K. J., Frank, D., 2010. Mesodermal Wnt signaling organizes the neural plate via Meis3. Development. 137**,** 1531-41.

Erter, C. E., Wilm, T. P., Basler, N., Wright, C. V., Solnica-Krezel, L., 2001. Wnt8 is required in lateral mesendodermal precursors for neural posteriorization in vivo. Development. 128**,** 3571-83.

Fasano, L., Roder, L., Core, N., Alexandre, E., Vola, C., Jacq, B., Kerridge, S., 1991. The gene teashirt is required for the development of Drosophila embryonic trunk segments and encodes a protein with widely spaced zinc finger motifs. Cell. 64**,** 63-79.

Ferretti, E., Cambronero, F., Tumpel, S., Longobardi, E., Wiedemann, L. M., Blasi, F., Krumlauf, R., 2005. Hoxb1 enhancer and control of rhombomere 4 expression: complex interplay between PREP1-PBX1-HOXB1 binding sites. Mol Cell Biol. 25**,** 8541-52.

Ferretti, E., Marshall, H., Popperl, H., Maconochie, M., Krumlauf, R., Blasi, F., 2000. Segmental expression of Hoxb2 in r4 requires two separate sites that integrate cooperative interactions between Prep1, Pbx and Hox proteins. Development. 127**,** 155-66.

Ferretti, E., Villaescusa, J. C., Di Rosa, P., Fernandez-Diaz, L. C., Longobardi, E., Mazzieri, R., Miccio, A., Micali, N., Selleri, L., Ferrari, G., Blasi, F., 2006. Hypomorphic mutation of the TALE gene Prep1 (pKnox1) causes a major reduction of Pbx and Meis proteins and a pleiotropic embryonic phenotype. Mol Cell Biol. 26**,** 5650-62.

Fraser, S., Keynes, R., Lumsden, A., 1990. Segmentation in the chick embryo hindbrain is defined by cell lineage restrictions. Nature. 344**,** 431-5.

Freeman, M., Gurdon, J. B., 2002. Regulatory principles of developmental signaling. Annu Rev Cell Dev Biol. 18**,** 515-39.

French, C. R., Erickson, T., Callander, D., Berry, K. M., Koss, R., Hagey, D. W., Stout, J., Wuennenberg-Stapleton, K., Ngai, J., Moens, C. B., Waskiewicz, A. J., 2007. Pbx homeodomain proteins pattern both the zebrafish retina and tectum. BMC Dev Biol. 7**,** 85.

Frisen, J., Holmberg, J., Barbacid, M., 1999. Ephrins and their Eph receptors: multitalented directors of embryonic development. EMBO J. 18**,** 5159-65.

Galant, R., Walsh, C. M., Carroll, S. B., 2002. Hox repression of a target gene: extradenticle-independent, additive action through multiple monomer binding sites. Development. 129**,** 3115-26.

Gardner, C. A., Darnell, D. K., Poole, S. J., Ordahl, C. P., Barald, K. F., 1988. Expression of an engrailed-like gene during development of the early embryonic chick nervous system. J Neurosci Res. 21**,** 426-37.

Gaufo, G. O., Thomas, K. R., Capecchi, M. R., 2003. Hox3 genes coordinate mechanisms of genetic suppression and activation in the generation of branchial and somatic motoneurons. Development. 130**,** 5191-201.

Gavalas, A., 2002. ArRAnging the hindbrain. Trends Neurosci. 25**,** 61-4.

Gavalas, A., Davenne, M., Lumsden, A., Chambon, P., Rijli, F. M., 1997. Role of Hoxa-2 in axon pathfinding and rostral hindbrain patterning. Development. 124**,** 3693-702.

Gavalas, A., Krumlauf, R., 2000. Retinoid signalling and hindbrain patterning. Curr Opin Genet Dev. 10**,** 380-6.

Gavalas, A., Ruhrberg, C., Livet, J., Henderson, C. E., Krumlauf, R., 2003. Neuronal defects in the hindbrain of Hoxa1, Hoxb1 and Hoxb2 mutants reflect regulatory interactions among these Hox genes. Development. 130**,** 5663-79.

Gavalas, A., Studer, M., Lumsden, A., Rijli, F. M., Krumlauf, R., Chambon, P., 1998. Hoxa1 and Hoxb1 synergize in patterning the hindbrain, cranial nerves and second pharyngeal arch. Development. 125**,** 1123-36.

Gebelein, B., Culi, J., Ryoo, H. D., Zhang, W., Mann, R. S., 2002. Specificity of Distalless repression and limb primordia development by abdominal Hox proteins. Dev Cell. 3**,** 487-98.

Gebelein, B., McKay, D. J., Mann, R. S., 2004. Direct integration of Hox and segmentation gene inputs during Drosophila development. Nature. 431**,** 653-9.

Geerts, D., Revet, I., Jorritsma, G., Schilderink, N., Versteeg, R., 2005. MEIS homeobox genes in neuroblastoma. Cancer Lett. 228**,** 43-50.

Glinka, A., Wu, W., Delius, H., Monaghan, A. P., Blumenstock, C., Niehrs, C., 1998. Dickkopf-1 is a member of a new family of secreted proteins and functions in head induction. Nature. 391**,** 357-62.

Goh, S. L., Looi, Y., Shen, H., Fang, J., Bodner, C., Houle, M., Ng, A. C., Screaton, R. A., Featherstone, M., 2009. Transcriptional activation by MEIS1A in response to protein kinase A signaling requires the transducers of regulated CREB family of CREB co-activators. J Biol Chem. 284**,** 18904-12.

Gomez-Skarmeta, J. L., Modolell, J., 2002. Iroquois genes: genomic organization and function in vertebrate neural development. Curr Opin Genet Dev. 12**,** 403-8.

Gongal, P. A., Waskiewicz, A. J., 2008. Zebrafish model of holoprosencephaly demonstrates a key role for TGIF in regulating retinoic acid metabolism. Hum Mol Genet. 17**,** 525-38.

Gonzalez-Crespo, S., Abu-Shaar, M., Torres, M., Martinez, A. C., Mann, R. S., Morata, G., 1998. Antagonism between extradenticle function and Hedgehog signalling in the developing limb. Nature. 394**,** 196-200.

Gordon, J. A., Hassan, M. Q., Saini, S., Montecino, M., van Wijnen, A. J., Stein, G. S., Stein, J. L., Lian, J. B., 2010. Pbx1 represses osteoblastogenesis by

blocking Hoxa10-mediated recruitment of chromatin remodeling factors. Mol Cell Biol.

Goudet, G., Delhalle, S., Biemar, F., Martial, J. A., Peers, B., 1999. Functional and cooperative interactions between the homeodomain PDX1, Pbx, and Prep1 factors on the somatostatin promoter. J Biol Chem. 274**,** 4067-73.

Gould, A., Morrison, A., Sproat, G., White, R. A., Krumlauf, R., 1997. Positive cross-regulation and enhancer sharing: two mechanisms for specifying overlapping Hox expression patterns. Genes Dev. 11**,** 900-13.

Grandel, H., Lun, K., Rauch, G. J., Rhinn, M., Piotrowski, T., Houart, C., Sordino, P., Kuchler, A. M., Schulte-Merker, S., Geisler, R., Holder, N., Wilson, S. W., Brand, M., 2002. Retinoic acid signalling in the zebrafish embryo is necessary during pre-segmentation stages to pattern the anterior-posterior axis of the CNS and to induce a pectoral fin bud. Development. 129**,** 2851-65.

Green, N. C., Rambaldi, I., Teakles, J., Featherstone, M. S., 1998. A conserved C-terminal domain in PBX increases DNA binding by the PBX homeodomain and is not a primary site of contact for the YPWM motif of HOXA1. J Biol Chem. 273**,** 13273-9.

Guthrie, S., Lumsden, A., 1991. Formation and regeneration of rhombomere boundaries in the developing chick hindbrain. Development. 112**,** 221-9.

Gutkovich, Y. E., Ofir, R., Elkouby, Y. M., Dibner, C., Gefen, A., Elias, S., Frank, D., 2010. Xenopus Meis3 protein lies at a nexus downstream to Zic1 and Pax3 proteins, regulating multiple cell-fates during early nervous system development. Dev Biol. 338**,** 50-62.

Haller, K., Rambaldi, I., Daniels, E., Featherstone, M., 2004. Subcellular localization of multiple PREP2 isoforms is regulated by actin, tubulin, and nuclear export. J Biol Chem. 279**,** 49384-94.

Harland, R. M., 1994. Neural induction in Xenopus. Curr Opin Genet Dev. 4**,** 543-9.

Hashimoto, H., Itoh, M., Yamanaka, Y., Yamashita, S., Shimizu, T., Solnica-Krezel, L., Hibi, M., Hirano, T., 2000. Zebrafish Dkk1 functions in

forebrain specification and axial mesendoderm formation. Dev Biol. 217**,** 138-52.

Hatano, M., Roberts, C. W., Minden, M., Crist, W. M., Korsmeyer, S. J., 1991. Deregulation of a homeobox gene, HOX11, by the t(10;14) in T cell leukemia. Science. 253**,** 79-82.

Heine, P., Dohle, E., Bumsted-O'Brien, K., Engelkamp, D., Schulte, D., 2008. Evidence for an evolutionary conserved role of homothorax/Meis1/2 during vertebrate retina development. Development. 135**,** 805-11.

Heine, P., Dohle, E., Schulte, D., 2009. Sonic hedgehog signaling in the chick retina accelerates Meis2 downregulation simultaneously with retinal ganglion cell genesis. Neuroreport. 20**,** 279-84.

Hemmati-Brivanlou, A., Kelly, O. G., Melton, D. A., 1994. Follistatin, an antagonist of activin, is expressed in the Spemann organizer and displays direct neuralizing activity. Cell. 77**,** 283-95.

Hemmati-Brivanlou, A., Melton, D., 1997. Vertebrate neural induction. Annu Rev Neurosci. 20**,** 43-60.

Hemmati-Brivanlou, A., Melton, D. A., 1994. Inhibition of activin receptor signaling promotes neuralization in Xenopus. Cell. 77**,** 273-81.

Hernandez, R. E., Putzke, A. P., Myers, J. P., Margaretha, L., Moens, C. B., 2007. Cyp26 enzymes generate the retinoic acid response pattern necessary for hindbrain development. Development. 134**,** 177-87.

Hernandez, R. E., Rikhof, H. A., Bachmann, R., Moens, C. B., 2004. vhnf1 integrates global RA patterning and local FGF signals to direct posterior hindbrain development in zebrafish. Development. 131**,** 4511-20.

Herzig, S., Fuzesi, L., Knepel, W., 2000. Heterodimeric Pbx-Prep1 homeodomain protein binding to the glucagon gene restricting transcription in a cell type-dependent manner. J Biol Chem. 275**,** 27989-99.

Higashijima, S., Hotta, Y., Okamoto, H., 2000. Visualization of cranial motor neurons in live transgenic zebrafish expressing green fluorescent protein under the control of the islet-1 promoter/enhancer. J Neurosci. 20**,** 206-18.

Hisa, T., Spence, S. E., Rachel, R. A., Fujita, M., Nakamura, T., Ward, J. M., Devor-Henneman, D. E., Saiki, Y., Kutsuna, H., Tessarollo, L., Jenkins, N. A., Copeland, N. G., 2004. Hematopoietic, angiogenic and eye defects in Meis1 mutant animals. EMBO J. 23**,** 450-9.

Hoey, T., Levine, M., 1988. Divergent homeo box proteins recognize similar DNA sequences in Drosophila. Nature. 332**,** 858-61.

Hombria, J. C., Lovegrove, B., 2003. Beyond homeosis--HOX function in morphogenesis and organogenesis. Differentiation. 71**,** 461-76.

Horan, G. S., Kovacs, E. N., Behringer, R. R., Featherstone, M. S., 1995. Mutations in paralogous Hox genes result in overlapping homeotic transformations of the axial skeleton: evidence for unique and redundant function. Dev Biol. 169**,** 359-72.

Houart, C., Caneparo, L., Heisenberg, C., Barth, K., Take-Uchi, M., Wilson, S., 2002. Establishment of the telencephalon during gastrulation by local antagonism of Wnt signaling. Neuron. 35**,** 255-65.

Huang, H., Paliouras, M., Rambaldi, I., Lasko, P., Featherstone, M., 2003. Nonmuscle myosin promotes cytoplasmic localization of PBX. Mol Cell Biol. 23**,** 3636-45.

Huang, H., Rastegar, M., Bodner, C., Goh, S. L., Rambaldi, I., Featherstone, M., 2005. MEIS C termini harbor transcriptional activation domains that respond to cell signaling. J Biol Chem. 280**,** 10119-27.

Hueber, S. D., Bezdan, D., Henz, S. R., Blank, M., Wu, H., Lohmann, I., 2007. Comparative analysis of Hox downstream genes in Drosophila. Development. 134**,** 381-92.

Hueber, S. D., Lohmann, I., 2008. Shaping segments: Hox gene function in the genomic age. Bioessays. 30**,** 965-79.

Hunt, P., Krumlauf, R., 1991. Deciphering the Hox code: clues to patterning branchial regions of the head. Cell. 66**,** 1075-8.

Hunt, P., Whiting, J., Nonchev, S., Sham, M. H., Marshall, H., Graham, A., Cook, M., Allemann, R., Rigby, P. W., Gulisano, M., et al., 1991. The branchial

Hox code and its implications for gene regulation, patterning of the nervous system and head evolution. Development. Suppl 2**,** 63-77.

Hunter, C. P., Kenyon, C., 1995. Specification of anteroposterior cell fates in Caenorhabditis elegans by Drosophila Hox proteins. Nature. 377**,** 229-32.

Hyman-Walsh, C., Bjerke, G. A., Wotton, D., 2010. An autoinhibitory effect of the homothorax domain of Meis2. FEBS J.

In der Rieden, P. M., Mainguy, G., Woltering, J. M., Durston, A. J., 2004. Homeodomain to hexapeptide or PBC-interaction-domain distance: size apparently matters. Trends Genet. 20**,** 76-9.

Jacobs, Y., Schnabel, C. A., Cleary, M. L., 1999. Trimeric association of Hox and TALE homeodomain proteins mediates Hoxb2 hindbrain enhancer activity. Mol Cell Biol. 19**,** 5134-42.

Jaw, T. J., You, L. R., Knoepfler, P. S., Yao, L. C., Pai, C. Y., Tang, C. Y., Chang, L. P., Berthelsen, J., Blasi, F., Kamps, M. P., Sun, Y. H., 2000. Direct interaction of two homeoproteins, homothorax and extradenticle, is essential for EXD nuclear localization and function. Mech Dev. 91**,** 279-91.

Jaynes, J. B., O'Farrell, P. H., 1991. Active repression of transcription by the engrailed homeodomain protein. EMBO J. 10**,** 1427-33.

Jiang, Y., Shi, H., Liu, J., 2009. Two Hox cofactors, the Meis/Hth homolog UNC-62 and the Pbx/Exd homolog CEH-20, function together during C. elegans postembryonic mesodermal development. Dev Biol. 334**,** 535-46.

Jones, F. S., Prediger, E. A., Bittner, D. A., De Robertis, E. M., Edelman, G. M., 1992. Cell adhesion molecules as targets for Hox genes: neural cell adhesion molecule promoter activity is modulated by cotransfection with Hox-2.5 and -2.4. Proc Natl Acad Sci U S A. 89**,** 2086-90.

Joshi, R., Passner, J. M., Rohs, R., Jain, R., Sosinsky, A., Crickmore, M. A., Jacob, V., Aggarwal, A. K., Honig, B., Mann, R. S., 2007. Functional specificity of a Hox protein mediated by the recognition of minor groove structure. Cell. 131**,** 530-43.

Kamps, M. P., Murre, C., Sun, X. H., Baltimore, D., 1990. A new homeobox gene contributes the DNA binding domain of the t(1;19) translocation protein in pre-B ALL. Cell. 60**,** 547-55.

Kerszberg, M., Wolpert, L., 2007. Specifying positional information in the embryo: looking beyond morphogens. Cell. 130**,** 205-9.

Kessel, M., Gruss, P., 1990. Murine developmental control genes. Science. 249**,** 374-9.

Kessel, M., Gruss, P., 1991. Homeotic transformations of murine vertebrae and concomitant alteration of Hox codes induced by retinoic acid. Cell. 67**,** 89-104.

Keynes, R., Krumlauf, R., 1994. Hox genes and regionalization of the nervous system. Annu Rev Neurosci. 17**,** 109-32.

Kilstrup-Nielsen, C., Alessio, M., Zappavigna, V., 2003. PBX1 nuclear export is regulated independently of PBX-MEINOX interaction by PKA phosphorylation of the PBC-B domain. EMBO J. 22**,** 89-99.

Kim, F. A., Sing l, A., Kaneko, T., Bieman, M., Stallwood, N., Sadl, V. S., Cordes, S. P., 2005. The vHNF1 homeodomain protein establishes early rhombomere identity by direct regulation of Kreisler expression. Mech Dev. 122**,** 1300-9.

Kim, S. K., Selleri, L., Lee, J. S., Zhang, A. Y., Gu, X., Jacobs, Y., Cleary, M. L., 2002. Pbx1 inactivation disrupts pancreas development and in Ipf1-deficient mice promotes diabetes mellitus. Nat Genet. 30**,** 430-5.

Kimmel, C. B., Ballard, W. W., Kimmel, S. R., Ullmann, B., Schilling, T. F., 1995. Stages of embryonic development of the zebrafish. Dev Dyn. 203**,** 253-310.

Knoepfler, P. S., Bergstrom, D. A., Uetsuki, T., Dac-Korytko, I., Sun, Y. H., Wright, W. E., Tapscott, S. J., Kamps, M. P., 1999. A conserved motif N-terminal to the DNA-binding domains of myogenic bHLH transcription factors mediates cooperative DNA binding with pbx-Meis1/Prep1. Nucleic Acids Res. 27**,** 3752-61.

Knoepfler, P. S., Calvo, K. R., Chen, H., Antonarakis, S. E., Kamps, M. P., 1997. Meis1 and pKnox1 bind DNA cooperatively with Pbx1 utilizing an interaction surface disrupted in oncoprotein E2a-Pbx1. Proc Natl Acad Sci U S A. 94**,** 14553-8.

Knoepfler, P. S., Kamps, M. P., 1995. The pentapeptide motif of Hox proteins is required for cooperative DNA binding with Pbx1, physically contacts Pbx1, and enhances DNA binding by Pbx1. Mol Cell Biol. 15**,** 5811-9.

Kobayashi, M., Fujioka, M., Tolkunova, E. N., Deka, D., Abu-Shaar, M., Mann, R. S., Jaynes, J. B., 2003. Engrailed cooperates with extradenticle and homothorax to repress target genes in Drosophila. Development. 130**,** 741-51.

Krumlauf, R., 1994. Hox genes in vertebrate development. Cell. 78**,** 191-201.

Kudoh, T., Wilson, S. W., Dawid, I. B., 2002. Distinct roles for Fgf, Wnt and retinoic acid in posteriorizing the neural ectoderm. Development. 129**,** 4335-46.

Kullander, K., Klein, R., 2002. Mechanisms and functions of Eph and ephrin signalling. Nat Rev Mol Cell Biol. 3**,** 475-86.

Kurant, E., Eytan, D., Salzberg, A., 2001. Mutational analysis of the Drosophila homothorax gene. Genetics. 157**,** 689-98.

Kurant, E., Pai, C. Y., Sharf, R., Halachmi, N., Sun, Y. H., Salzberg, A., 1998. Dorsotonals/homothorax, the Drosophila homologue of meis1, interacts with extradenticle in patterning of the embryonic PNS. Development. 125**,** 1037-48.

Kuroda, H., Wessely, O., De Robertis, E. M., 2004. Neural induction in Xenopus: requirement for ectodermal and endomesodermal signals via Chordin, Noggin, beta-Catenin, and Cerberus. PLoS Biol. 2**,** E92.

Lamb, T. M., Harland, R. M., 1995. Fibroblast growth factor is a direct neural inducer, which combined with noggin generates anterior-posterior neural pattern. Development. 121**,** 3627-36.

Lamb, T. M., Knecht, A. K., Smith, W. C., Stachel, S. E., Economides, A. N., Stahl, N., Yancopolous, G. D., Harland, R. M., 1993. Neural induction by the secreted polypeptide noggin. Science. 262**,** 713-8.

Lampe, X., Picard, J. J., Rezsohazy, R., 2004. The Hoxa2 enhancer 2 contains a critical Hoxa2 responsive regulatory element. Biochem Biophys Res Commun. 316**,** 898-902.

Lampe, X., Samad, O. A., Guiguen, A., Matis, C., Remacle, S., Picard, J. J., Rijli, F. M., Rezsohazy, R., 2008. An ultraconserved Hox-Pbx responsive element resides in the coding sequence of Hoxa2 and is active in rhombomere 4. Nucleic Acids Res. 36**,** 3214-25.

LaRonde-LeBlanc, N. A., Wolberger, C., 2003. Structure of HoxA9 and Pbx1 bound to DNA: Hox hexapeptide and DNA recognition anterior to posterior. Genes Dev. 17**,** 2060-72.

Larroux, C., Fahey, B., Degnan, S. M., Adamski, M., Rokhsar, D. S., Degnan, B. M., 2007. The NK homeobox gene cluster predates the origin of Hox genes. Curr Biol. 17**,** 706-10.

Laugier, E., Yang, Z., Fasano, L., Kerridge, S., Vola, C., 2005. A critical role of teashirt for patterning the ventral epidermis is masked by ectopic expression of tiptop, a paralog of teashirt in Drosophila. Dev Biol. 283**,** 446-58.

Laurent, A., Bihan, R., Deschamps, S., Guerrier, D., Dupe, V., Omilli, F., Burel, A., Pellerin, I., 2007. Identification of a new type of PBX1 partner that contains zinc finger motifs and inhibits the binding of HOXA9-PBX1 to DNA. Mech Dev. 124**,** 364-76.

Laurent, A., Bihan, R., Omilli, F., Deschamps, S., Pellerin, I., 2008. PBX proteins: much more than Hox cofactors. Int J Dev Biol. 52**,** 9-20.

Lekven, A. C., Thorpe, C. J., Waxman, J. S., Moon, R. T., 2001. Zebrafish wnt8 encodes two wnt8 proteins on a bicistronic transcript and is required for mesoderm and neurectoderm patterning. Dev Cell. 1**,** 103-14.

Lemke, G., Reber, M., 2005. Retinotectal Mapping: New Insights from Molecular Genetics. Annual Review of Cell and Developmental Biology. 21**,** 551-580.

Lewis, E. B., 1978. A gene complex controlling segmentation in Drosophila. Nature. 276**,** 565-70.

Liu, T., Branch, D. R., Jin, T., 2006. Pbx1 is a co-factor for Cdx-2 in regulating proglucagon gene expression in pancreatic A cells. Mol Cell Endocrinol. 249**,** 140-9.

Longobardi, E., Blasi, F., 2003. Overexpression of PREP-1 in F9 teratocarcinoma cells leads to a functionally relevant increase of PBX-2 by preventing its degradation. J Biol Chem. 278**,** 39235-41.

Lopes, C. S., Casares, F., 2010. hth maintains the pool of eye progenitors and its downregulation by Dpp and Hh couples retinal fate acquisition with cell cycle exit. Dev Biol. 339**,** 78-88.

Lovegrove, B., Simoes, S., Rivas, M. L., Sotillos, S., Johnson, K., Knust, E., Jacinto, A., Hombria, J. C., 2006. Coordinated control of cell adhesion, polarity, and cytoskeleton underlies Hox-induced organogenesis in Drosophila. Curr Biol. 16**,** 2206-16.

Lu, Q., Kamps, M. P., 1996. Structural determinants within Pbx1 that mediate cooperative DNA binding with pentapeptide-containing Hox proteins: proposal for a model of a Pbx1-Hox-DNA complex. Mol Cell Biol. 16**,** 1632-40.

Lumsden, A., Keynes, R., 1989. Segmental patterns of neuronal development in the chick hindbrain. Nature. 337**,** 424-8.

Lumsden, A., Krumlauf, R., 1996. Patterning the vertebrate neuraxis. Science. 274**,** 1109-15.

Maconochie, M. K., Nonchev, S., Manzanares, M., Marshall, H., Krumlauf, R., 2001. Differences in Krox20-dependent regulation of Hoxa2 and Hoxb2 during hindbrain development. Dev Biol. 233**,** 468-81.

Maconochie, M. K., Nonchev, S., Studer, M., Chan, S. K., Popperl, H., Sham, M. H., Mann, R. S., Krumlauf, R., 1997. Cross-regulation in the mouse HoxB

complex: the expression of Hoxb2 in rhombomere 4 is regulated by Hoxb1. Genes Dev. 11**,** 1885-95.

Maden, M., Gale, E., Kostetskii, I., Zile, M., 1996. Vitamin A-deficient quail embryos have half a hindbrain and other neural defects. Curr Biol. 6**,** 417-26.

Maeda, R., Ishimura, A., Mood, K., Park, E. K., Buchberg, A. M., Daar, I. O., 2002. Xpbx1b and Xmeis1b play a collaborative role in hindbrain and neural crest gene expression in Xenopus embryos. Proc Natl Acad Sci U S A. 99**,** 5448-53.

Maeda, R., Mood, K., Jones, T. L., Aruga, J., Buchberg, A. M., Daar, I. O., 2001. Xmeis1, a protooncogene involved in specifying neural crest cell fate in Xenopus embryos. Oncogene. 20**,** 1329-42.

Mallo, M., Wellik, D. M., Deschamps, J., 2010. Hox genes and regional patterning of the vertebrate body plan. Dev Biol. 344**,** 7-15.

Mann, R. S., 1995. The specificity of homeotic gene function. Bioessays. 17**,** 855-63.

Mann, R. S., Abu-Shaar, M., 1996. Nuclear import of the homeodomain protein extradenticle in response to Wg and Dpp signalling. Nature. 383**,** 630-3.

Mann, R. S., Affolter, M., 1998. Hox proteins meet more partners. Curr Opin Genet Dev. 8**,** 423-9.

Mann, R. S., Chan, S. K., 1996. Extra specificity from extradenticle: the partnership between HOX and PBX/EXD homeodomain proteins. Trends Genet. 12**,** 258-62.

Mann, R. S., Lelli, K. M., Joshi, R., 2009. Hox specificity unique roles for cofactors and collaborators. Curr Top Dev Biol. 88**,** 63-101.

Manzanares, M., Bel-Vialar, S., Ariza-McNaughton, L., Ferretti, E., Marshall, H., Maconochie, M. M., Blasi, F., Krumlauf, R., 2001. Independent regulation of initiation and maintenance phases of Hoxa3 expression in the vertebrate hindbrain involve auto- and cross-regulatory mechanisms. Development. 128**,** 3595-607.

Manzanares, M., Nardelli, J., Gilardi-Hebenstreit, P., Marshall, H., Giudicelli, F., Martinez-Pastor, M. T., Krumlauf, R., Charnay, P., 2002. Krox20 and kreisler co-operate in the transcriptional control of segmental expression of Hoxb3 in the developing hindbrain. EMBO J. 21**,** 365-76.

Martindale, M. Q., 2005. The evolution of metazoan axial properties. Nat Rev Genet. 6**,** 917-27.

Massague, J., Seoane, J., Wotton, D., 2005. Smad transcription factors. Genes Dev. 19**,** 2783-810.

Maves, L., Jackman, W., Kimmel, C. B., 2002. FGF3 and FGF8 mediate a rhombomere 4 signaling activity in the zebrafish hindbrain. Development. 129**,** 3825-37.

Maves, L., Kimmel, C. B., 2005. Dynamic and sequential patterning of the zebrafish posterior hindbrain by retinoic acid. Dev Biol. 285**,** 593-605.

Maves, L., Tyler, A., Moens, C. B., Tapscott, S. J., 2009. Pbx acts with Hand2 in early myocardial differentiation. Dev Biol. 333**,** 409-18.

Maves, L., Waskiewicz, A. J., Paul, B., Cao, Y., Tyler, A., Moens, C. B., Tapscott, S. J., 2007. Pbx homeodomain proteins direct Myod activity to promote fast-muscle differentiation. Development. 134**,** 3371-82.

McClintock, J. M., Carlson, R., Mann, D. M., Prince, V. E., 2001. Consequences of Hox gene duplication in the vertebrates: an investigation of the zebrafish Hox paralogue group 1 genes. Development. 128**,** 2471-84.

McGinnis, W., Levine, M. S., Hafen, E., Kuroiwa, A., Gehring, W. J., 1984. A conserved DNA sequence in homoeotic genes of the Drosophila Antennapedia and bithorax complexes. Nature. 308**,** 428-33.

McGrew, L. L., Hoppler, S., Moon, R. T., 1997. Wnt and FGF pathways cooperatively pattern anteroposterior neural ectoderm in Xenopus. Mech Dev. 69**,** 105-14.

McIntyre, D. C., Rakshit, S., Yallowitz, A. R., Loken, L., Jeannotte, L., Capecchi, M. R., Wellik, D. M., 2007. Hox patterning of the vertebrate rib cage. Development. 134**,** 2981-9.

McLaughlin, T., O'Leary, D. D., 2005. Molecular gradients and development of retinotopic maps. Annu Rev Neurosci. 28**,** 327-55.

McNulty, C. L., Peres, J. N., Bardine, N., van den Akker, W. M., Durston, A. J., 2005. Knockdown of the complete Hox paralogous group 1 leads to dramatic hindbrain and neural crest defects. Development. 132**,** 2861-71.

Medina-Martinez, O., Ramirez-Solis, R., 2003. In vivo mutagenesis of the Hoxb8 hexapeptide domain leads to dominant homeotic transformations that mimic the loss-of-function mutations in genes of the Hoxb cluster. Dev Biol. 264**,** 77-90.

Mellitzer, G., Xu, Q., Wilkinson, D. G., 1999. Eph receptors and ephrins restrict cell intermingling and communication. Nature. 400**,** 77-81.

Mendelson, B., 1986. Development of reticulospinal neurons of the zebrafish. I. Time of origin. J Comp Neurol. 251**,** 160-71.

Merabet, S., Ebner, A., Affolter, M., 2005. The Drosophila Extradenticle and Homothorax selector proteins control branchless/FGF expression in mesodermal bridge-cells. EMBO Rep. 6**,** 762-8.

Mercader, N., Leonardo, E., Azpiazu, N., Serrano, A., Morata, G., Martinez, C., Torres, M., 1999. Conserved regulation of proximodistal limb axis development by Meis1/Hth. Nature. 402**,** 425-9.

Mercader, N., Selleri, L., Criado, L. M., Pallares, P., Parras, C., Cleary, M. L., Torres, M., 2009. Ectopic Meis1 expression in the mouse limb bud alters P-D patterning in a Pbx1-independent manner. Int J Dev Biol. 53**,** 1483-94.

Mercader, N., Tanaka, E. M., Torres, M., 2005. Proximodistal identity during vertebrate limb regeneration is regulated by Meis homeodomain proteins. Development. 132**,** 4131-42.

Milech, N., Gottardo, N. G., Ford, J., D'Souza, D., Greene, W. K., Kees, U. R., Watt, P. M., 2010. MEIS proteins as partners of the TLX1/HOX11 oncoprotein. Leuk Res. 34**,** 358-63.

Moens, C. B., Prince, V. E., 2002. Constructing the hindbrain: insights from the zebrafish. Dev Dyn. 224**,** 1-17.

Moens, C. B., Selleri, L., 2006. Hox cofactors in vertebrate development. Dev Biol. 291**,** 193-206.

Moens, C. B., Yan, Y. L., Appel, B., Force, A. G., Kimmel, C. B., 1996. valentino: a zebrafish gene required for normal hindbrain segmentation. Development. 122**,** 3981-90.

Moskow, J. J., Bullrich, F., Huebner, K., Daar, I. O., Buchberg, A. M., 1995. Meis1, a PBX1-related homeobox gene involved in myeloid leukemia in BXH-2 mice. Mol Cell Biol. 15**,** 5434-43.

Mukhopadhyay, M., Shtrom, S., Rodriguez-Esteban, C., Chen, L., Tsukui, T., Gomer, L., Dorward, D. W., Glinka, A., Grinberg, A., Huang, S. P., Niehrs, C., Izpisua Belmonte, J. C., Westphal, H., 2001. Dickkopf1 is required for embryonic head induction and limb morphogenesis in the mouse. Dev Cell. 1**,** 423-34.

Nakamura, T., Largaespada, D. A., Shaughnessy, J. D., Jr., Jenkins, N. A., Copeland, N. G., 1996. Cooperative activation of Hoxa and Pbx1-related genes in murine myeloid leukaemias. Nat Genet. 12**,** 149-53.

Nakano, T., Windrem, M., Zappavigna, V., Goldman, S. A., 2005. Identification of a conserved 125 base-pair Hb9 enhancer that specifies gene expression to spinal motor neurons. Dev Biol. 283**,** 474-85.

Neuteboom, S. T., Murre, C., 1997. Pbx raises the DNA binding specificity but not the selectivity of antennapedia Hox proteins. Mol Cell Biol. 17**,** 4696-706.

Neuteboom, S. T., Peltenburg, L. T., van Dijk, M. A., Murre, C., 1995. The hexapeptide LFPWMR in Hoxb-8 is required for cooperative DNA binding with Pbx1 and Pbx2 proteins. Proc Natl Acad Sci U S A. 92**,** 9166-70.

Niederreither, K., Vermot, J., Schuhbaur, B., Chambon, P., Dolle, P., 2000. Retinoic acid synthesis and hindbrain patterning in the mouse embryo. Development. 127**,** 75-85.

Nonchev, S., Maconochie, M., Vesque, C., Aparicio, S., Ariza-McNaughton, L., Manzanares, M., Maruthainar, K., Kuroiwa, A., Brenner, S., Charnay, P.,

Krumlauf, R., 1996a. The conserved role of Krox-20 in directing Hox gene expression during vertebrate hindbrain segmentation. Proc Natl Acad Sci U S A. 93**,** 9339-45.

Nonchev, S., Vesque, C., Maconochie, M., Seitanidou, T., Ariza-McNaughton, L., Frain, M., Marshall, H., Sham, M. H., Krumlauf, R., Charnay, P., 1996b. Segmental expression of Hoxa-2 in the hindbrain is directly regulated by Krox-20. Development. 122**,** 543-54.

Nordstrom, U., Jessell, T. M., Edlund, T., 2002. Progressive induction of caudal neural character by graded Wnt signaling. Nat Neurosci. 5**,** 525-32.

Noro, B., Culi, J., McKay, D. J., Zhang, W., Mann, R. S., 2006. Distinct functions of homeodomain-containing and homeodomain-less isoforms encoded by homothorax. Genes Dev. 20**,** 1636-50.

Nourse, J., Mellentin, J. D., Galili, N., Wilkinson, J., Stanbridge, E., Smith, S. D., Cleary, M. L., 1990. Chromosomal translocation t(1;19) results in synthesis of a homeobox fusion mRNA that codes for a potential chimeric transcription factor. Cell. 60**,** 535-45.

Noyes, M. B., Christensen, R. G., Wakabayashi, A., Stormo, G. D., Brodsky, M. H., Wolfe, S. A., 2008. Analysis of homeodomain specificities allows the family-wide prediction of preferred recognition sites. Cell. 133**,** 1277-89.

Ogryzko, V. V., Schiltz, R. L., Russanova, V., Howard, B. H., Nakatani, Y., 1996. The transcriptional coactivators p300 and CBP are histone acetyltransferases. Cell. 87**,** 953-9.

Otting, G., Qian, Y. Q., Billeter, M., Muller, M., Affolter, M., Gehring, W. J., Wuthrich, K., 1990. Protein--DNA contacts in the structure of a homeodomain--DNA complex determined by nuclear magnetic resonance spectroscopy in solution. EMBO J. 9**,** 3085-92.

Oulad-Abdelghani, M., Chazaud, C., Bouillet, P., Sapin, V., Chambon, P., Dolle, P., 1997. Meis2, a novel mouse Pbx-related homeobox gene induced by retinoic acid during differentiation of P19 embryonal carcinoma cells. Dev Dyn. 210**,** 173-83.

Oxtoby, E., Jowett, T., 1993. Cloning of the zebrafish krox-20 gene (krx-20) and its expression during hindbrain development. Nucleic Acids Res. 21**,** 1087-95.

Pai, C. Y., Kuo, T. S., Jaw, T. J., Kurant, E., Chen, C. T., Bessarab, D. A., Salzberg, A., Sun, Y. H., 1998. The Homothorax homeoprotein activates the nuclear localization of another homeoprotein, extradenticle, and suppresses eye development in Drosophila. Genes Dev. 12**,** 435-46.

Passner, J. M., Ryoo, H. D., Shen, L., Mann, R. S., Aggarwal, A. K., 1999. Structure of a DNA-bound Ultrabithorax-Extradenticle homeodomain complex. Nature. 397**,** 714-9.

Pearson, J. C., Lemons, D., McGinnis, W., 2005. Modulating Hox gene functions during animal body patterning. Nat Rev Genet. 6**,** 893-904.

Peers, B., Sharma, S., Johnson, T., Kamps, M., Montminy, M., 1995. The pancreatic islet factor STF-1 binds cooperatively with Pbx to a regulatory element in the somatostatin promoter: importance of the FPWMK motif and of the homeodomain. Mol Cell Biol. 15**,** 7091-7.

Peifer, M., Wieschaus, E., 1990. Mutations in the Drosophila gene extradenticle affect the way specific homeo domain proteins regulate segmental identity. Genes Dev. 4**,** 1209-23.

Peltenburg, L. T., Murre, C., 1996. Engrailed and Hox homeodomain proteins contain a related Pbx interaction motif that recognizes a common structure present in Pbx. EMBO J. 15**,** 3385-93.

Peltenburg, L. T., Murre, C., 1997. Specific residues in the Pbx homeodomain differentially modulate the DNA-binding activity of Hox and Engrailed proteins. Development. 124**,** 1089-98.

Penkov, D., Di Rosa, P., Fernandez Diaz, L., Basso, V., Ferretti, E., Grassi, F., Mondino, A., Blasi, F., 2005. Involvement of Prep1 in the alphabeta T-cell receptor T-lymphocytic potential of hematopoietic precursors. Mol Cell Biol. 25**,** 10768-81.

Penkov, D., Palazzolo, M., Mondino, A., Blasi, F., 2008. Cytosolic sequestration of Prep1 influences early stages of T cell development. PLoS One. 3**,** e2424.

Penkov, D., Tanaka, S., Di Rocco, G., Berthelsen, J., Blasi, F., Ramirez, F., 2000. Cooperative interactions between PBX, PREP, and HOX proteins modulate the activity of the alpha 2(V) collagen (COL5A2) promoter. J Biol Chem. 275**,** 16681-9.

Pera, E. M., Ikeda, A., Eivers, E., De Robertis, E. M., 2003. Integration of IGF, FGF, and anti-BMP signals via Smad1 phosphorylation in neural induction. Genes Dev. 17**,** 3023-8.

Peters, M. A., Cepko, C. L., 2002. The dorsal-ventral axis of the neural retina is divided into multiple domains of restricted gene expression which exhibit features of lineage compartments. Dev Biol. 251**,** 59-73.

Phelan, M. L., Featherstone, M. S., 1997. Distinct HOX N-terminal arm residues are responsible for specificity of DNA recognition by HOX monomers and HOX.PBX heterodimers. J Biol Chem. 272**,** 8635-43.

Phelan, M. L., Rambaldi, I., Featherstone, M. S., 1995. Cooperative interactions between HOX and PBX proteins mediated by a conserved peptide motif. Mol Cell Biol. 15**,** 3989-97.

Picker, A., Cavodeassi, F., Machate, A., Bernauer, S., Hans, S., Abe, G., Kawakami, K., Wilson, S. W., Brand, M., 2009. Dynamic coupling of pattern formation and morphogenesis in the developing vertebrate retina. PLoS Biol. 7**,** e1000214.

Pillay, L. M., Forrester, A. M., Erickson, T., Berman, J. N., Waskiewicz, A. J., 2010. The Hox cofactors Meis1 and Pbx act upstream of gata1 to regulate primitive hematopoiesis. Dev Biol. 340**,** 306-17.

Piper, D. E., Batchelor, A. H., Chang, C. P., Cleary, M. L., Wolberger, C., 1999. Structure of a HoxB1-Pbx1 heterodimer bound to DNA: role of the hexapeptide and a fourth homeodomain helix in complex formation. Cell. 96**,** 587-97.

Poliakov, A., Cotrina, M., Wilkinson, D. G., 2004. Diverse roles of eph receptors and ephrins in the regulation of cell migration and tissue assembly. Dev Cell. 7**,** 465-80.

Popperl, H., Bienz, M., Studer, M., Chan, S. K., Aparicio, S., Brenner, S., Mann, R. S., Krumlauf, R., 1995. Segmental expression of Hoxb-1 is controlled by a highly conserved autoregulatory loop dependent upon exd/pbx. Cell. 81**,** 1031-42.

Popperl, H., Rikhof, H., Chang, H., Haffter, P., Kimmel, C. B., Moens, C. B., 2000. lazarus is a novel pbx gene that globally mediates hox gene function in zebrafish. Mol Cell. 6**,** 255-67.

Pouilhe, M., Gilardi-Hebenstreit, P., Desmarquet-Trin Dinh, C., Charnay, P., 2007. Direct regulation of vHnf1 by retinoic acid signaling and MAF-related factors in the neural tube. Dev Biol. 309**,** 344-57.

Prince, V. E., Moens, C. B., Kimmel, C. B., Ho, R. K., 1998. Zebrafish hox genes: expression in the hindbrain region of wild-type and mutants of the segmentation gene, valentino. Development. 125**,** 393-406.

Qian, Y. Q., Billeter, M., Otting, G., Muller, M., Gehring, W. J., Wuthrich, K., 1989. The structure of the Antennapedia homeodomain determined by NMR spectroscopy in solution: comparison with prokaryotic repressors. Cell. 59**,** 573-80.

Rambaldi, I., Kovacs, E. N., Featherstone, M. S., 1994. A proline-rich transcriptional activation domain in murine HOXD-4 (HOX-4.2). Nucleic Acids Res. 22**,** 376-82.

Rauskolb, C., Peifer, M., Wieschaus, E., 1993. extradenticle, a regulator of homeotic gene activity, is a homolog of the homeobox-containing human proto-oncogene pbx1. Cell. 74**,** 1101-12.

Rauskolb, C., Smith, K. M., Peifer, M., Wieschaus, E., 1995. extradenticle determines segmental identities throughout Drosophila development. Development. 121**,** 3663-73.

Rauskolb, C., Wieschaus, E., 1994. Coordinate regulation of downstream genes by extradenticle and the homeotic selector proteins. EMBO J. 13**,** 3561-9.

Rawat, V. P., Thoene, S., Naidu, V. M., Arseni, N., Heilmeier, B., Metzeler, K., Petropoulos, K., Deshpande, A., Quintanilla-Martinez, L., Bohlander, S. K., Spiekermann, K., Hiddemann, W., Feuring-Buske, M., Buske, C., 2008. Overexpression of CDX2 perturbs HOX gene expression in murine progenitors depending on its N-terminal domain and is closely correlated with deregulated HOX gene expression in human acute myeloid leukemia. Blood. 111**,** 309-19.

Remacle, S., Abbas, L., De Backer, O., Pacico, N., Gavalas, A., Gofflot, F., Picard, J. J., Rezsohazy, R., 2004. Loss of function but no gain of function caused by amino acid substitutions in the hexapeptide of Hoxa1 in vivo. Mol Cell Biol. 24**,** 8567-75.

Remacle, S., Shaw-Jackson, C., Matis, C., Lampe, X., Picard, J., Rezsohazy, R., 2002. Changing homeodomain residues 2 and 3 of Hoxa1 alters its activity in a cell-type and enhancer dependent manner. Nucleic Acids Res. 30**,** 2663-8.

Rentzsch, F., Bakkers, J., Kramer, C., Hammerschmidt, M., 2004. Fgf signaling induces posterior neuroectoderm independently of Bmp signaling inhibition. Dev Dyn. 231**,** 750-7.

Rhee, J. W., Arata, A., Selleri, L., Jacobs, Y., Arata, S., Onimaru, H., Cleary, M. L., 2004. Pbx3 deficiency results in central hypoventilation. Am J Pathol. 165**,** 1343-50.

Rieckhof, G. E., Casares, F., Ryoo, H. D., Abu-Shaar, M., Mann, R. S., 1997. Nuclear translocation of extradenticle requires homothorax, which encodes an extradenticle-related homeodomain protein. Cell. 91**,** 171-83.

Rijli, F. M., Matyas, R., Pellegrini, M., Dierich, A., Gruss, P., Dolle, P., Chambon, P., 1995. Cryptorchidism and homeotic transformations of spinal nerves and vertebrae in Hoxa-10 mutant mice. Proc Natl Acad Sci U S A. 92**,** 8185-9.

Riley, B. B., Chiang, M. Y., Storch, E. M., Heck, R., Buckles, G. R., Lekven, A. C., 2004. Rhombomere boundaries are Wnt signaling centers that regulate metameric patterning in the zebrafish hindbrain. Dev Dyn. 231**,** 278-91.

Roder, L., Vola, C., Kerridge, S., 1992. The role of the teashirt gene in trunk segmental identity in Drosophila. Development. 115**,** 1017-33.

Rohrschneider, M. R., Elsen, G. E., Prince, V. E., 2007. Zebrafish Hoxb1a regulates multiple downstream genes including prickle1b. Dev Biol. 309**,** 358-72.

Roy, N. M., Sagerstrom, C. G., 2004. An early Fgf signal required for gene expression in the zebrafish hindbrain primordium. Brain Res Dev Brain Res. 148**,** 27-42.

Ryan, J. F., Burton, P. M., Mazza, M. E., Kwong, G. K., Mullikin, J. C., Finnerty, J. R., 2006. The cnidarian-bilaterian ancestor possessed at least 56 homeoboxes: evidence from the starlet sea anemone, Nematostella vectensis. Genome Biol. 7**,** R64.

Ryoo, H. D., Marty, T., Casares, F., Affolter, M., Mann, R. S., 1999. Regulation of Hox target genes by a DNA bound Homothorax/Hox/Extradenticle complex. Development. 126**,** 5137-48.

Sagerstrom, C. G., 2004. PbX marks the spot. Dev Cell. 6**,** 737-8.

Sakai, Y., Meno, C., Fujii, H., Nishino, J., Shiratori, H., Saijoh, Y., Rossant, J., Hamada, H., 2001. The retinoic acid-inactivating enzyme CYP26 is essential for establishing an uneven distribution of retinoic acid along the anterio-posterior axis within the mouse embryo. Genes Dev. 15**,** 213-25.

Saleh, M., Huang, H., Green, N. C., Featherstone, M. S., 2000a. A conformational change in PBX1A is necessary for its nuclear localization. Exp Cell Res. 260**,** 105-15.

Saleh, M., Rambaldi, I., Yang, X. J., Featherstone, M. S., 2000b. Cell signaling switches HOX-PBX complexes from repressors to activators of transcription mediated by histone deacetylases and histone acetyltransferases. Mol Cell Biol. 20**,** 8623-33.

Salzberg, A., Elias, S., Nachaliel, N., Bonstein, L., Henig, C., Frank, D., 1999. A Meis family protein caudalizes neural cell fates in Xenopus. Mech Dev. 80**,** 3-13.

Samad, O. A., Geisen, M. J., Caronia, G., Varlet, I., Zappavigna, V., Ericson, J., Goridis, C., Rijli, F. M., 2004. Integration of anteroposterior and dorsoventral regulation of Phox2b transcription in cranial motoneuron progenitors by homeodomain proteins. Development. 131**,** 4071-83.

Sanchez, M., Jennings, P. A., Murre, C., 1997. Conformational changes induced in Hoxb-8/Pbx-1 heterodimers in solution and upon interaction with specific DNA. Mol Cell Biol. 17**,** 5369-76.

Sasai, Y., Lu, B., Steinbeisser, H., De Robertis, E. M., 1995. Regulation of neural induction by the Chd and Bmp-4 antagonistic patterning signals in Xenopus. Nature. 377**,** 757.

Schneider-Maunoury, S., Seitanidou, T., Charnay, P., Lumsden, A., 1997. Segmental and neuronal architecture of the hindbrain of Krox-20 mouse mutants. Development. 124**,** 1215-26.

Schneider-Maunoury, S., Topilko, P., Seitandou, T., Levi, G., Cohen-Tannoudji, M., Pournin, S., Babinet, C., Charnay, P., 1993. Disruption of Krox-20 results in alteration of rhombomeres 3 and 5 in the developing hindbrain. Cell. 75**,** 1199-214.

Scicolone, G., Ortalli, A. L., Carri, N. G., 2009. Key roles of Ephs and ephrins in retinotectal topographic map formation. Brain Res Bull. 79**,** 227-47.

Scott, M. P., Weiner, A. J., 1984. Structural relationships among genes that control development: sequence homology between the Antennapedia, Ultrabithorax, and fushi tarazu loci of Drosophila. Proc Natl Acad Sci U S A. 81**,** 4115-9.

Seitanidou, T., Schneider-Maunoury, S., Desmarquet, C., Wilkinson, D. G., Charnay, P., 1997. Krox-20 is a key regulator of rhombomere-specific gene expression in the developing hindbrain. Mech Dev. 65**,** 31-42.

Sela-Donenfeld, D., Kayam, G., Wilkinson, D. G., 2009. Boundary cells regulate a switch in the expression of FGF3 in hindbrain rhombomeres. BMC Dev Biol. 9**,** 16.

Selleri, L., Depew, M. J., Jacobs, Y., Chanda, S. K., Tsang, K. Y., Cheah, K. S., Rubenstein, J. L., O'Gorman, S., Cleary, M. L., 2001. Requirement for

Pbx1 in skeletal patterning and programming chondrocyte proliferation and differentiation. Development. 128**,** 3543-57.

Serpente, P., Tumpel, S., Ghyselinck, N. B., Niederreither, K., Wiedemann, L. M., Dolle, P., Chambon, P., Krumlauf, R., Gould, A. P., 2005. Direct crossregulation between retinoic acid receptor {beta} and Hox genes during hindbrain segmentation. Development. 132**,** 503-13.

Serrano, N., Maschat, F., 1998. Molecular mechanism of polyhomeotic activation by Engrailed. EMBO J. 17**,** 3704-13.

Shanmugam, K., Featherstone, M. S., Saragovi, H. U., 1997. Residues flanking the HOX YPWM motif contribute to cooperative interactions with PBX. J Biol Chem. 272**,** 19081-7.

Shanmugam, K., Green, N. C., Rambaldi, I., Saragovi, H. U., Featherstone, M. S., 1999. PBX and MEIS as non-DNA-binding partners in trimeric complexes with HOX proteins. Mol Cell Biol. 19**,** 7577-88.

Shen, W., Chrobak, D., Krishnan, K., Lawrence, H. J., Largman, C., 2004. HOXB6 protein is bound to CREB-binding protein and represses globin expression in a DNA binding-dependent, PBX interaction-independent process. J Biol Chem. 279**,** 39895-904.

Shen, W. F., Krishnan, K., Lawrence, H. J., Largman, C., 2001. The HOX homeodomain proteins block CBP histone acetyltransferase activity. Mol Cell Biol. 21**,** 7509-22.

Shen, W. F., Montgomery, J. C., Rozenfeld, S., Moskow, J. J., Lawrence, H. J., Buchberg, A. M., Largman, C., 1997. AbdB-like Hox proteins stabilize DNA binding by the Meis1 homeodomain proteins. Mol Cell Biol. 17**,** 6448-58.

Shen, W. F., Rozenfeld, S., Kwong, A., Kom ves, L. G., Lawrence, H. J., Largman, C., 1999. HOXA9 forms triple complexes with PBX2 and MEIS1 in myeloid cells. Mol Cell Biol. 19**,** 3051-61.

Shimizu, T., Bae, Y. K., Hibi, M., 2006. Cdx-Hox code controls competence for responding to Fgfs and retinoic acid in zebrafish neural tissue. Development. 133**,** 4709-19.

Shinya, M., Eschbach, C., Clark, M., Lehrach, H., Furutani-Seiki, M., 2000. Zebrafish Dkk1, induced by the pre-MBT Wnt signaling, is secreted from the prechordal plate and patterns the anterior neural plate. Mech Dev. 98**,** 3-17.

Sirbu, I. O., Gresh, L., Barra, J., Duester, G., 2005. Shifting boundaries of retinoic acid activity control hindbrain segmental gene expression. Development. 132**,** 2611-22.

Skromne, I., Thorsen, D., Hale, M., Prince, V. E., Ho, R. K., 2007. Repression of the hindbrain developmental program by Cdx factors is required for the specification of the vertebrate spinal cord. Development. 134**,** 2147-58.

Slack, J. M., 1993. Embryonic induction. Mech Dev. 41**,** 91-107.

Sprules, T., Green, N., Featherstone, M., Gehring, K., 2003. Lock and key binding of the HOX YPWM peptide to the PBX homeodomain. J Biol Chem. 278**,** 1053-8.

Stankunas, K., Shang, C., Twu, K. Y., Kao, S. C., Jenkins, N. A., Copeland, N. G., Sanyal, M., Selleri, L., Cleary, M. L., Chang, C. P., 2008. Pbx/Meis deficiencies demonstrate multigenetic origins of congenital heart disease. Circ Res. 103**,** 702-9.

Stedman, A., Lecaudey, V., Havis, E., Anselme, I., Wassef, M., Gilardi-Hebenstreit, P., Schneider-Maunoury, S., 2009. A functional interaction between Irx and Meis patterns the anterior hindbrain and activates krox20 expression in rhombomere 3. Dev Biol. 327**,** 566-77.

Sterner, D. E., Berger, S. L., 2000. Acetylation of histones and transcription-related factors. Microbiol Mol Biol Rev. 64**,** 435-59.

Stevens, K. E., Mann, R. S., 2007. A balance between two nuclear localization sequences and a nuclear export sequence governs extradenticle subcellular localization. Genetics. 175**,** 1625-36.

Streit, A., Berliner, A. J., Papanayotou, C., Sirulnik, A., Stern, C. D., 2000. Initiation of neural induction by FGF signalling before gastrulation. Nature. 406**,** 74-8.

Studer, M., Gavalas, A., Marshall, H., Ariza-McNaughton, L., Rijli, F. M., Chambon, P., Krumlauf, R., 1998. Genetic interactions between Hoxa1 and Hoxb1 reveal new roles in regulation of early hindbrain patterning. Development. 125**,** 1025-36.

Subramaniam, N., Campion, J., Rafter, I., Okret, S., 2003. Cross-talk between glucocorticoid and retinoic acid signals involving glucocorticoid receptor interaction with the homoeodomain protein Pbx1. Biochem J. 370**,** 1087-95.

Svingen, T., Tonissen, K. F., 2006. Hox transcription factors and their elusive mammalian gene targets. Heredity. 97**,** 88-96.

Swift, G. H., Liu, Y., Rose, S. D., Bischof, L. J., Steelman, S., Buchberg, A. M., Wright, C. V., MacDonald, R. J., 1998. An endocrine-exocrine switch in the activity of the pancreatic homeodomain protein PDX1 through formation of a trimeric complex with PBX1b and MRG1 (MEIS2). Mol Cell Biol. 18**,** 5109-20.

Taghli-Lamallem, O., Gallet, A., Leroy, F., Malapert, P., Vola, C., Kerridge, S., Fasano, L., 2007. Direct interaction between Teashirt and Sex combs reduced proteins, via Tsh's acidic domain, is essential for specifying the identity of the prothorax in Drosophila. Dev Biol. 307**,** 142-51.

Thisse, B., Thisse, C., 2004. Fast Release Clones: A High Throughput Expression Analysis. . ZFIN Direct Data Submission.

Thisse, B., Thisse, C., 2005. High Throughput Expression Analysis of ZF-Models Consortium Clones. ZFIN Direct Data Submission.

Thisse, B., Wright, C. V., Thisse, C., 2000. Activin- and Nodal-related factors control antero-posterior patterning of the zebrafish embryo. Nature. 403**,** 425-8.

Tour, E., Hittinger, C. T., McGinnis, W., 2005. Evolutionarily conserved domains required for activation and repression functions of the Drosophila Hox protein Ultrabithorax. Development. 132**,** 5271-81.

Trainor, P. A., Krumlauf, R., 2001. Hox genes, neural crest cells and branchial arch patterning. Curr Opin Cell Biol. 13**,** 698-705.

Tumpel, S., Cambronero, F., Ferretti, E., Blasi, F., Wiedemann, L. M., Krumlauf, R., 2007. Expression of Hoxa2 in rhombomere 4 is regulated by a conserved cross-regulatory mechanism dependent upon Hoxb1. Dev Biol. 302**,** 646-60.

Uehara, M., Yashiro, K., Mamiya, S., Nishino, J., Chambon, P., Dolle, P., Sakai, Y., 2007. CYP26A1 and CYP26C1 cooperatively regulate anterior-posterior patterning of the developing brain and the production of migratory cranial neural crest cells in the mouse. Dev Biol. 302**,** 399-411.

Uhl, J. D., Cook, T. A., Gebelein, B., 2010. Comparing anterior and posterior Hox complex formation reveals guidelines for predicting cis-regulatory elements. Dev Biol. 343**,** 154-66.

Van Auken, K., Weaver, D., Robertson, B., Sundaram, M., Saldi, T., Edgar, L., Elling, U., Lee, M., Boese, Q., Wood, W. B., 2002. Roles of the Homothorax/Meis/Prep homolog UNC-62 and the Exd/Pbx homologs CEH-20 and CEH-40 in C. elegans embryogenesis. Development. 129**,** 5255-68.

Van Auken, K., Weaver, D. C., Edgar, L. G., Wood, W. B., 2000. Caenorhabditis elegans embryonic axial patterning requires two recently discovered posterior-group Hox genes. Proc Natl Acad Sci U S A. 97**,** 4499-503.

van Dijk, M. A., Murre, C., 1994. extradenticle raises the DNA binding specificity of homeotic selector gene products. Cell. 78**,** 617-24.

van Dijk, M. A., Peltenburg, L. T., Murre, C., 1995. Hox gene products modulate the DNA binding activity of Pbx1 and Pbx2. Mech Dev. 52**,** 99-108.

Vesque, C., Maconochie, M., Nonchev, S., Ariza-McNaughton, L., Kuroiwa, A., Charnay, P., Krumlauf, R., 1996. Hoxb-2 transcriptional activation in rhombomeres 3 and 5 requires an evolutionarily conserved cis-acting element in addition to the Krox-20 binding site. EMBO J. 15**,** 5383-96.

Vigano, M. A., Di Rocco, G., Zappavigna, V., Mavilio, F., 1998. Definition of the transcriptional activation domains of three human HOX proteins depends on the DNA-binding context. Mol Cell Biol. 18**,** 6201-12.

Vlachakis, N., Choe, S. K., Sagerstrom, C. G., 2001. Meis3 synergizes with Pbx4 and Hoxb1b in promoting hindbrain fates in the zebrafish. Development. 128**,** 1299-312.

Vlachakis, N., Ellstrom, D. R., Sagerstrom, C. G., 2000. A novel pbx family member expressed during early zebrafish embryogenesis forms trimeric complexes with Meis3 and Hoxb1b. Dev Dyn. 217**,** 109-19.

Wagner, G. P., Amemiya, C., Ruddle, F., 2003. Hox cluster duplications and the opportunity for evolutionary novelties. Proc Natl Acad Sci U S A. 100**,** 14603-6.

Walshe, J., Maroon, H., McGonnell, I. M., Dickson, C., Mason, I., 2002. Establishment of hindbrain segmental identity requires signaling by FGF3 and FGF8. Curr Biol. 12**,** 1117-23.

Wang, G. G., Pasillas, M. P., Kamps, M. P., 2005. Meis1 programs transcription of FLT3 and cancer stem cell character, using a mechanism that requires interaction with Pbx and a novel function of the Meis1 C-terminus. Blood. 106**,** 254-64.

Wang, G. G., Pasillas, M. P., Kamps, M. P., 2006. Persistent transactivation by meis1 replaces hox function in myeloid leukemogenesis models: evidence for co-occupancy of meis1-pbx and hox-pbx complexes on promoters of leukemia-associated genes. Mol Cell Biol. 26**,** 3902-16.

Wang, Y., Yin, L., Hillgartner, F. B., 2001. The homeodomain proteins PBX and MEIS1 are accessory factors that enhance thyroid hormone regulation of the malic enzyme gene in hepatocytes. J Biol Chem. 276**,** 23838-48.

Waskiewicz, A. J., Rikhof, H. A., Hernandez, R. E., Moens, C. B., 2001. Zebrafish Meis functions to stabilize Pbx proteins and regulate hindbrain patterning. Development. 128**,** 4139-51.

Waskiewicz, A. J., Rikhof, H. A., Moens, C. B., 2002. Eliminating zebrafish pbx proteins reveals a hindbrain ground state. Dev Cell. 3**,** 723-33.

Wassef, M. A., Chomette, D., Pouilhe, M., Stedman, A., Havis, E., Desmarquet-Trin Dinh, C., Schneider-Maunoury, S., Gilardi-Hebenstreit, P., Charnay, P., Ghislain, J., 2008. Rostral hindbrain patterning involves the direct

activation of a Krox20 transcriptional enhancer by Hox/Pbx and Meis factors. Development. 135**,** 3369-78.

Weidinger, G., Thorpe, C. J., Wuennenberg-Stapleton, K., Ngai, J., Moon, R. T., 2005. The Sp1-related transcription factors sp5 and sp5-like act downstream of Wnt/beta-catenin signaling in mesoderm and neuroectoderm patterning. Curr Biol. 15**,** 489-500.

Wellik, D. M., 2007. Hox patterning of the vertebrate axial skeleton. Dev Dyn. 236**,** 2454-63.

Wellik, D. M., 2009. Hox genes and vertebrate axial pattern. Curr Top Dev Biol. 88**,** 257-78.

White, R. J., Nie, Q., Lander, A. D., Schilling, T. F., 2007. Complex regulation of cyp26a1 creates a robust retinoic acid gradient in the zebrafish embryo. PLoS Biol. 5**,** e304.

Wiellette, E. L., Sive, H., 2003. vhnf1 and Fgf signals synergize to specify rhombomere identity in the zebrafish hindbrain. Development. 130**,** 3821-9.

Wieschaus, E., Nüsslein-Volhard, C., Jürgens, G., 1984. Mutations affecting the pattern of the larval cuticle in Drosophila melanogaster. Development Genes and Evolution. 193**,** 296-307.

Wilkinson, D. G., Bhatt, S., Chavrier, P., Bravo, R., Charnay, P., 1989. Segment-specific expression of a zinc-finger gene in the developing nervous system of the mouse. Nature. 337**,** 461-4.

Williams, T. M., Williams, M. E., Innis, J. W., 2005. Range of HOX/TALE superclass associations and protein domain requirements for HOXA13:MEIS interaction. Dev Biol. 277**,** 457-71.

Wilson, P. A., Hemmati-Brivanlou, A., 1995. Induction of epidermis and inhibition of neural fate by Bmp-4. Nature. 376**,** 331-3.

Wolpert, L., 1969. Positional information and the spatial pattern of cellular differentiation. J Theor Biol. 25**,** 1-47.

Wong, P., Iwasaki, M., Somervaille, T. C., So, C. W., Cleary, M. L., 2007. Meis1 is an essential and rate-limiting regulator of MLL leukemia stem cell potential. Genes Dev. 21**,** 2762-74.

Woo, K., Fraser, S. E., 1995. Order and coherence in the fate map of the zebrafish nervous system. Development. 121**,** 2595-609.

Woo, K., Fraser, S. E., 1997. Specification of the zebrafish nervous system by nonaxial signals. Science. 277**,** 254-7.

Woo, K., Fraser, S. E., 1998. Specification of the hindbrain fate in the zebrafish. Dev Biol. 197**,** 283-96.

Woo, K., Shih, J., Fraser, S. E., 1995. Fate maps of the zebrafish embryo. Curr Opin Genet Dev. 5**,** 439-43.

Wu, J., Cohen, S. M., 2000. Proximal distal axis formation in the Drosophila leg: distinct functions of teashirt and homothorax in the proximal leg. Mech Dev. 94**,** 47-56.

Xu, Q., Mellitzer, G., Robinson, V., Wilkinson, D. G., 1999. In vivo cell sorting in complementary segmental domains mediated by Eph receptors and ephrins. Nature. 399**,** 267-71.

Xu, Q., Mellitzer, G., Wilkinson, D. G., 2000. Roles of Eph receptors and ephrins in segmental patterning. Philos Trans R Soc Lond B Biol Sci. 355**,** 993-1002.

Yang, L., Sym, M., Kenyon, C., 2005. The roles of two C. elegans HOX co-factor orthologs in cell migration and vulva development. Development. 132**,** 1413-28.

Yekta, S., Shih, I. H., Bartel, D. P., 2004. MicroRNA-directed cleavage of HOXB8 mRNA. Science. 304**,** 594-6.

Zakany, J., Duboule, D., 2007. The role of Hox genes during vertebrate limb development. Curr Opin Genet Dev. 17**,** 359-66.

Zerucha, T., Prince, V. E., 2001. Cloning and developmental expression of a zebrafish meis2 homeobox gene. Mech Dev. 102**,** 247-50.

Zhai, Z., Fuchs, A. L., Lohmann, I., 2010. Cellular analysis of newly identified Hox downstream genes in Drosophila. Eur J Cell Biol. 89**,** 273-8.

Zhang, M., Kim, H. J., Marshall, H., Gendron-Maguire, M., Lucas, D. A., Baron, A., Gudas, L. J., Gridley, T., Krumlauf, R., Grippo, J. F., 1994. Ectopic Hoxa-1 induces rhombomere transformation in mouse hindbrain. Development. 120**,** 2431-42.

Zhang, X., Rowan, S., Yue, Y., Heaney, S., Pan, Y., Brendolan, A., Selleri, L., Maas, R. L., 2006. Pax6 is regulated by Meis and Pbx homeoproteins during pancreatic development. Dev Biol. 300**,** 748-57.

Zhao, J. J., Lazzarini, R. A., Pick, L., 1996. Functional dissection of the mouse Hox-a5 gene. EMBO J. 15**,** 1313-22.

Chapter Two - Methods and Materials

2. Methods

2.1 Animal care, fish lines and general procedures

Embryonic and adult fish were cared for according to standard protocols (Westerfield, 2000). Embryos were grown at either 25.5°C, 28.5°C, or 33°C in embryo media (EM) and staged according to standardized morphological milestones (Kimmel et al., 1995). The AB strain of wild type fish was used for all experiments except where noted. Other fish lines used in various experiments were the wild type Tübingen (TU) strain, the mutant strains *no isthmus* (*noi* / *pax2a*$^{b593/b593}$) (ZIRC) and *lazarus* (*lzr* / *pbx4*$^{b557/b557}$) (Popperl et al., 2000), and the transgenic lines *Tg[isl1:GFP]* on an AB / Wik background (Higashijima et al., 2000), *Tg[hsp70l:fgf8a]b1193* (Hans et al., 2007), and *Tg[dusp6:d2EGFP]* (Molina et al., 2007).

Embryos were dechorionated either manually using Dumont No. 5 forceps, or enzymatically. For enzymatic dechorionation, embryos were incubated with periodic swirling at room temperature in a 1 mg/ml solution of Pronase E (Sigma) until the chorions started to fall apart as observed through a stereo microscope. Pronase E was removed by three successive washes in EM.

Embryos that were analyzed past the stage of 24 hpf were grown in embryo media supplemented with 0.003% 1-phenyl 2-thiourea (PTU) (Sigma) to prevent pigment formation. When required, fish were anesthetized in a 4% dilution of a 0.4% tricaine stock solution. For mRNA in situ and immunohistochemical analyses, embryos were fixed in 4% paraformaldehyde in 1X PBS, except where noted. PFA fixation was performed for 4-5 hours on a rotating platform at room temperature, or overnight on at 4ºC.

2.2 Morpholinos

Morpholino (MO) antisense oligonucleotides (GeneTools) were used to make targeted protein knockdowns. The sequences for all MOs used in this thesis are listed in Table 2-1. MO stocks were made in water at a concentration of 10 or 20 mg/ml, diluted to the appropriate working concentration in Danieau solution.

Stock solutions were stored at -20ºC while working stocks were stored at 4ºC. Working stocks heated to 65ºC for 10 minutes and cooled on ice prior to injection. Injections were done into either the cell or yolk at the one-cell stage.

2.3 Total RNA extraction and end point RT-PCR

Total RNA was isolated from appropriately staged zebrafish embryos by TRIzol (Invitrogen) extraction by the following procedure. After removing the extra EM, 200 µl of TRIzol was added to 50 dechorionated embryos. The embryos were homogenized using a combination of vortexing and microfuge tube pestles until no visible chunks remained. After adding 300 µl more TRIzol, the samples were vortexed at maximum for 30 seconds. Next, 125 µl of chloroform ($CHCl_3$) was added and each sample was vortexed for 30 seconds followed by a spin at 14000 RPM for 20 minutes at 4ºC. The clear supernatant was transferred to a new microfuge tube where 350 µl of $CHCl_3$ was added. The tubes were vortexed for 30 seconds and spun at 14000 RPM for 20 minutes at 4 ºC. The supernatant was transferred to a new microfuge tube, at which time 20 µg (1 µl of 20 mg/ml) RNase-free glycogen (Roche) was added to each sample to act as a carrier for the RNA during precipitation. The samples were vortexed briefly and stored at -20ºC for at least one hour. To pellet the precipitated RNA, the samples were spun at 14000 RPM for 20 minutes at 4ºC. Following the spin, the supernatant was discarded and the pellet washed with 70% RNase-free ethanol (EtOH) followed by another 14000 RPM spin at 4ºC. The supernatant was removed and the pellet was allowed to air dry for 2 minutes before resuspending the pellet in 90 µl RNase-free water. To remove residual DNA, 10 µl 10X DNase buffer + 1 µl RQ1 RNase-free DNase (Promega) was added and the samples were incubated at 37ºC for 15 minutes. The RNA cleanup protocol from the Qiagen RNeasy kit was used to remove the DNase and buffer from the RNA prep.

To generate PCR product from total zebrafish RNA for either subcloning or direct use in a riboprobe synthesis reaction, the SuperScript® III One-Step RT-PCR System with Platinum® Taq DNA Polymerase kit (Invitrogen) was used following the manufacturer's recommended protocol. To make mRNA expression

constructs, cDNA was synthesized by a two-step procedure, first using the SuperScriptIII First-Strand Synthesis System for RT-PCR (Invitrogen) to make cDNA, followed by a PCR reaction using Phusion (NEB) polymerase. Both steps were performed according to the manufacturer's suggested protocols. The primers used to create inserts for the mRNA expression constructs are listed Table 2-2.

2.4 In vitro mRNA synthesis

In vitro synthesis of capped mRNA from linearized plasmid templates (Table 2-3) was performed using the SP6 mMessage Machine kit (Ambion) according to the manufacturer's suggested protocol. mRNA synthesis reactions were purified by three successive washes using Microcon YM-50 columns (Millipore).

2.5 mRNA in situ hybridization

2.5.1 Riboprobe template cloning and riboprobe synthesis

Antisense digoxigenin (DIG) or fluorescein-labelled riboprobes were prepared either from a PCR product generated using gene specific primers containing either a T3 or T7 RNA polymerase site on the 5' end of the reverse primer (Table 2-4) (Thisse and Thisse, 2008), or from a linearized plasmid template containing a gene-specific insert (Table 2-5). In either case, each 20 µl riboprobe probe synthesis reaction included 200-400 ng of template, 2 µl of 10X transcription buffer (Roche), 2 µl 10X DIG RNA labelling mix or 10X Fluorescein RNA Labeling Mix (Roche), 20 units (0.5 µl) RNAsein (Promega), 20 units (1 µl) of either T3 or T7 RNA polymerase (Roche), and RNase-free water up to 20 µl. Reactions were performed for 2 hours at 37°C, with another 20 units of the appropriate RNA polymerase added midway through the incubation. Following a 10-minute DNase treatment at 37°C, reactions were purified using SigmaSpin Post-Reaction Clean-Up Columns (Sigma) following the manufacturer's protocol. 10 µl of RNAlater (Sigma) was added to the collected flowthrough and a portion of the probe synthesis reaction was diluted 1:300 in hybridization solution and stored at -20°C. The reminder of the synthesis reaction was stored at -80ºC.

2.5.2 mRNA in situ hybridization and detection

All steps of the protocol involving embryos were performed in 1.7 ml microfuge tubes. Embryos were fixed in 4 % PFA and washed in PBST 4 times for 5 minutes. Embryos were then generally dehydrated in 100% methanol (MeOH) and stored at -20ºC for up to several months. Prior to resuming the in situ protocol, embryos were rehydrated through a 75%MeOH / 25% PBST, 50% MeOH / 50% PBST, 25% MeOH / 75% PBST series before two 5 minute PBST washes. A 10 µg/ml proteinase K in PBST solution was used to permeabilize the embryos. The length of the permeabilization step depends on the stage of development: 0-10 hpf: no proteinase K; 10-12 hpf – 1 minute; 13-16 hpf – 3 minutes; 16-21 hpf – 5 minutes; 22-28 hpf – 7 minutes; 29-36 hpf – 10 minutes; 48 hpf – 15 minutes; 4 dpf – 45 minutes; 5 dpf – 60 minutes. After proteinase K treatment, embryos were re-fixed in 4% PFA for 20 minutes and then washed four times for 5 minutes in PBST.

Pre-hybridization, hybridization, and wash steps were carried out in a 65°C waterbath. Embryos were incubated in hybridization buffer + tRNA for at least 1hour. The 65°C washes were done as follows: once for 5 minutes in each of these three solutions: [1] 66% hybridization buffer (HB) / 33% 2X SSC; [2] 33% HB / 66% 2X SSC: and [3] 100% 2X SSC / 0.1% Tween-20. High stringency washes were done one time for 20 minutes in 0.2X SSC / 0.1% Tween-20 and two times for 20 minutes in 0.1X SSC / 0.1% Tween-20. At room temperature, successive 5 minute washes were done with the following solutions: [1] 66% 0.2X SSC / 33% PBST; [2] 33% 0.2x SSC / 66% PBST; and [3] 100% PBST.

To detect DIG-labeled riboprobes, embryos were incubated for at least 2 hours in blocking solution and then incubated overnight at 4°C in a 1:5000 dilution of sheep anti-DIG-AP FAB fragments (Roche) in blocking solution. Embryos were washed 5 times for 15 minutes in PBST at room temperature to remove the antibody. The colouration reaction was performed using either the standard nitroblue tetrazolium (NBT) / bromo-chloro indoyl phosphate (BCIP) reagents dissolved in Alkaline Tris colouration buffer, or with BM Purple

(Roche). For BM Purple colouration, embryos were rinsed twice briefly with water + 0.1% Tween-20 following the PBST washes to remove salt before the addition of 500 µl of BM Purple colouration solution. The embryos were protected from light exposure during colouration and the reaction was monitored periodically through a stereomicroscope. The reaction was terminated by removing the colouration solution, rinsing the embryos twice in distilled water (0.1% Tween-20) followed by a 10 minute incubation in stop solution and two 5 minute PBST washes. Following colouration, the embryos were stored for up to a week PBST at 4ºC before mounting and photographing.

For two-color in situs, embryos were incubated in a DIG / fluorescein riboprobe mixture as described above. The detect the fluorescein-labeled riboprobe, embryos were incubated in 1M glycine pH 2.2 for 10 minutes following the termination of the DIG colouration reaction. After four 5 minute PBST washes, embryos were incubated in blocking solution for at least 1 hour followed by an overnight incubation at 4ºC in a 1:10,000 dilution of anti-fluorescein-AP FAB fragments (Roche). The antibody was removed by five 15 minute PBST washes and the colouration reaction was performed in Alkaline-Tris colouration buffer using either Fast-Red (Sigma) or Iodonitrotetrazolium-violet (Sigma) as described above for DIG-labeled probes.

To photograph the embryos, the yolk was manually removed and the embryos were equilibrated in 50% and 70% glycerol solutions before being mounted. Embryos were photographed on a Zeiss AxioImager.Z1 scope with an Axiocam HRm camera with RGB filters. Embryos still on the yolk were photographed using a Olympus SZX12 or Zeiss Discovery.V8 stereoscope fitted with a QImaging micropublisher camera. All figures were assembled in Photoshop.

2.6 Electrophoretic mobility shift assays

Electrophoretic mobility shift assays were performed using the EMSA core kit (Promega) and precast EMSA gels (Invitrogen) according to manufacturers recommendations. *eng2a* and *pbx4* open reading frames were

subcloned into pCS3MT and pCS2MT, respectively and their sequences confirmed. Protein was synthesized using a coupled in vitro transcription and translation system (SP6 Wheat germ lysate TnT, Promega). Point mutations in Eng2a were created using the Quickchange site directed mutagenesis procedure according to manufacture's recommendations (Stratagene). For the Eng-Pbx cooperative binding experiments, the following oligonucleotide was synthesized and labeled using T4 polynucleotide kinase and ^{32}[P]-ATP: 5'-GTCAATTAAATGATCAATCAATTTCG-3'.

2.7 Western analysis

2.7.1 Zebrafish cell lysate and yolk removal

The protocol to remove the embryonic yolk proteins and make cell lysates suitable for Western analysis is based on a protocol previously described (Link et al., 2006). The embryos were dechorionated either manually or enzymatically. If pronase E was used, the embryos were washed five times in EM to remove residual protease and prevent degradation of protein samples. The deyolking buffer (DYB) and deyolking wash buffer (DWB) were chilled on ice prior to use. After removing all extra EM from the embryos in microfuge tubes, 1 ml of cold DYB (plus Roche Complete Mini, EDTA-free protease inhibitor cocktail) was added and the embryos were pipetted repeatedly with a 1 ml pipette just enough to disrupt the yolk. The samples were then vortexed on low for 30 seconds to dissolve the yolk. The cells were pelleted by centrifugation at 2,000 RPM for 30 seconds at 4ºC. The supernatant containing the yolk proteins was removed and 1 ml of cold DWB was added. The tubes were again vortexed and spun as above. The DWB step was repeated. To lyse the cells, the supernatant was removed and 1x sample loading buffer (Invitrogen) with 2.5% beta-mercaptoethanol was each to each sample at a volume of 3 µl per starting embryo.

2.7.2 Western blot analysis

The protein samples were prepared by repeat pipetting to shear the DNA followed by boiling for 15 minutes at 96ºC. Western gels were run using precast

NuPAGE Novex Bis-Tris 4-12% gradient gels (Invitrogen) in a XCell SureLock Mini-Cell electrophoresis system (Invitrogen) following the manufacture's suggested protocols. Western transfer was also done in the XCell SureLock Mini-Cell electrophoresis system following the manufacture's protocol in 0.02% SDS and 5% methanol transfer buffer onto either nitrocellulose or polyvinylidene fluoride (PVDF) membranes. When using PVDF, the membrane was presoaked in 100% methanol before setting up the transfer. Following the transfer, PVDF membranes were briefly soaked in 100% methanol and rinsed twice in water. Successful protein transfer was confirmed by Ponceau S staining of the membrane.

Western blots were blocked for one hour at room temperature or overnight at 4ºC on a rotating shaker in 3% bovine serum albumen (BSA), or 1% BSA / 1% ovalbumen supplemented with 1% serum from the animal the secondary antibody was raised in, or in 5% nonfat skim milk powder without serum in Tris-buffered saline plus 0.1% Tween-20 (TBST). The primary antibody (Table 2-6) was diluted to an appropriate concentration in blocking solution and incubated with the membrane overnight at 4ºC on a rotating shaker. The primary antibody was decanted off the membrane, and the blot was washed 4 times for 5 minutes in TBST. The secondary antibody (sheep anti-mouse HPR or donkey anti-rabbit HRP FAB fragments from Amersham) was diluted 1:7,500-10,000 in blocking solution or in TBST alone and incubated with the membrane at room temperature for one hour on a rotating table. After 4 successive 5 minute washes in TBST, the membrane was incubated for 5 minutes in a 1:1 mixture of Pierce SuperSignal West Pico Chemiluminescent Substrate according to the manufacture's protocol. Kodak film was exposed to the membrane and developed in a Kodak X-OMAT 2000 Processor.

2.8 Whole mount immunohistochemistry

With the exceptions of rmo44 anti-160 kD Neurofilament Medium monoclonal and 6-11B-1 anti-acetylated tubulin monoclonal antibodies, all whole mount immunohistochemical stains were performed by the following protocol.

Embryos of the appropriate stages were fixed in 4% PFA and permeabilized with Proteinase K in the same way as for mRNA in situ hybridizations. Following the post-permeabilization incubation in 4% PFA, the embryos were washed out of fix 4 times for 5 minutes with PBT (phosphate buffered saline with 0.1% Triton-X detergent). All subsequent steps were performed on a Nutator rotating platform. The blocking step was done in PBT / 1% BSA / 10 % goat serum for at least one hour at room temperature, or overnight at 4ºC. The primary antibody (Table 2-7) was diluted to the appropriate concentration in blocking solution and incubated with the embryos overnight at 4ºC. Embryos were washed in PBT five times for 15 minutes before being reblocked for one hour in block solution. The appropriate secondary antibody (Alexa Fluor 488 or 568; goat anti-mouse IgG or goat anti-rabbit IgG from Invitrogen / Molecular Probes) was diluted 1:1,000 in blocking solution and incubated with the embryos overnight at 4ºC. To mark nuclei, Hoechst 33258 (Invitrogen) at a concentration of 10 µg/ml was included in the overnight secondary antibody incubation step. The secondary antibody was removed by 5 successive 15 minute PBT washes. Embryos were deyolked, equilibrated in 50% glycerol, mounted and imaged by either a Leica TCS-SP2 or a Zeiss LSM 510 confocal microscope. Z-projections were made in ImageJ and figures assembled in Photoshop.

The anti-acetylated tubulin antibody stain was performed as above, with the following modifications based on a previously described protocol (Kramer-Zucker et al., 2005). Dechorionated embryos were fixed overnight at 4°C in Dent's fixative (80% MeOH / 20% DMSO), gradually rehydrated, washed three times for 5 minutes in 1X PBS / 0.5% Tween-20, and blocked for at least one hour in 1X PBS / 0.5% Tween-20 / 1% DMSO / 1% BSA / 10% goat serum. The anti-acetylated tubulin primary antibody was diluted 1:500 in blocking solution and incubated with the embryos overnight at 4ºC. Primary antibody was removed by five successive 15 minute washes in 1X PBS / 0.5% Tween-20 / 1% DMSO. The remainder of the protocol follows the standard immunostain protocol.

To perform the rmo44 anti-160 kD Neurofilament immunostain, dechorionated embryos were fixed in 2% trichloroacetic acid (TCA) in 1X PBS

for 3 hours at room temperature or overnight at 4ºC. TCA fix was washed away by three successive 5 minute PBT (0.1%) washes followed by a permeabilization step involving three 5 minute PBT (0.5%) washes. Embryos were blocked in PBT (0.1%) / 1% BSA / 10% goat serum for at least one hour at room temperature, or overnight at 4ºC. The rmo44 antibody (Sigma) was diluted 1:250 in block solution and incubated with the embryos overnight at 4ºC. Primary antibody was removed by five successive 15 minute washes in PBT (0.1%). The remainder of the protocol follows the standard immunostain protocol.

2.9 Tshz3b antibody production

We used the Immunological Services of Covance Research Products Inc. (Denver, PA) to raise a polyclonal antibody against zebrafish Tshz3b. Two Tshz3b peptides were synthesized by Covance based on their high potential antigenicity: Peptide 1 - Acetyl-CSSDAGESARGESPKERR-amide representing amino acids 682-699; Peptide 2 - [C]-SKTHGKSPEDHLMYVSELEKP-acid representing amino acids 1127-1147. The peptides were conjugated to Keyhole Limpet Hemocyanin (KLH) to improve antigenicity. Both peptides were injected simultaneously into two NZW rabbits (UA004 and UA005) using Freund's Complete Adjuvant for the first injection, and Freund's Incomplete Adjuvant for subsequent boosts. A pre-immune bleed (PIB), test bleed (TB), three production bleeds (PB1-3), and an exsanguination bleed (EB) were produced from each rabbit. The third production bleeds pooled with the terminal bleeds were used as starting material for affinity purification of antibodies specific for each peptide. The ability of the unpurified and affinity purified (AP) antibodies to recognize Tshz3b protein was confirmed by injecting one cell zebrafish embryos with *tshz3b* mRNA, and then following the standard cell lysate and Western blotting protocol. All TB, PB, EB, and AP antibodies were able to detect overexpressed Tshz3b, while pre-immune serum was negative for a specific Tshz3b signal.

2.10 Pharmacological treatments

All chemicals were dissolved in DMSO and diluted to their appropriate concentrations in EM, with equivalent dilutions of DMSO alone used as solvent controls. Embryos were protected from light during the period of drug exposure and grown at either 25.5ºC or 28.5 ºC. Inhibition of Fgf signaling was done using the pharmcological Fgf receptor inhibitors PD173074 (Stemgent) or SU5402 (Calbiochem). For experiments using PD173074, wild type and *meis1* morphant embryos were incubated in a 50 μM solution of PD173074 or 0.5% DMSO control between the stages of 90% epiboly and seven somites. The embryos were removed from the treatment dishes, washed three times in embryo media, and grown at 28.5ºC until fixation at the 28 hpf stage. For experiments using SU5402, a 30 μM solution of SU5402 or 0.3% DMSO control was applied to dechorionated embryos at 9 hpf and removed upon PFA fixation at 28 hpf. To antagonize retinoic acid signaling, diethylaminobenzaldehyde (DEAB) (Sigma) was used to inhibit the retinaldehyde dehydrogenase enzymes required in the final biosynthesis step of retinoic acid. A 10-12 μM solution of DEAB was applied to embryos in their chorions at 4 hpf and removed upon fixation at 16 hpf. The retinoic acid signaling pathway was activated by the application of exogenous all-trans-retinoic acid (RA) (Sigma) at a concentration 10^{-7} – 10^{-8} M. RA was applied to embryos in their chorions at 4 hpf and removed upon fixation at 16 hpf.

2.11 Rapid amplification of cDNA ends (RACE)

To determine the full ORF for the zebrafish *tshz3b* gene, we performed 5' RACE using the BD SMART RACE kit (BD Biosciences) from total RNA isolated from 18 hpf zebrafish embryos according to the manufacture's suggested protocol. The first reaction was performed using a 5'-CTGGATTCACTCAGGTGGGACTCGCTGTC-3' *tshz3b*-specific reverse primer, while the nested PCR reaction was done using a 5'-GGCAGGTTCCTCCTCCAAAGCAGAATCC-3' *tshz3b* reverse primer.

2.12 Gene expression profiling and quantification of tectal neurolpil and otic vesicle size

The profiling of retinal mRNA in situ hybridizations was based on a previously described method (Picker and Brand, 2005) with the following modifications. The mRNA in situ hybridization data used for quantification were all from a single round of morpholino injections and / or pharmaceutical treatments in order to control for variability in experiment-to-experiment differences in mRNA in situ staining intensity. Inverted grayscale images of dissected, flat-mounted retinas were prepared and oriented in Photoshop. The images were imported to ImageJ for pixel intensity analysis using the Oval profile plugin. Using the "Along Oval" analysis mode, the pixel intensity was determined for 360 points around the circumference of the eye and these values were exported to Microsoft Excel for analysis and graphing. Two series of measurements were made per eye: one proximal to the lens, and the other more distal. These two series were averaged to arrive at a single 360°series of pixel intensities per eye. Using these averaged values, the nasal (n) and temporal (t) positions (in degrees) where pixel intensity fell to the halfway point between its minimum and maximum values (nmax/2° and tmax/2°) were determined for each eye. For the *vax2* and *ephb2* probes, the ventro-nasal and ventro-temporal regions (separated by the choroid fissure) were treated as separate domains, each with their own maximum pixel intensity value. For each in situ probe, the means of the wild type nmax/2° and/or tmax/2° were compared to the corresponding means for the *meis1* morphant eyes using an unpaired, two-tailed t-test using a P-value of 0.01 as the cutoff for significance. The resulting mean nmax/2° and tmax/2° values were graphed using the Doughnut chart in Excel. The number of eyes used for each analysis along with the mean nmax/2° and/or tmax/2° values (plus or minus one standard deviation) are provided in the tables accompanying the graphs.

To quantify tectal neuropil area in wild type and *meis1* morphant embryos, images of Hoechst 33258 stained 5 dpf embryos were analyzed in ImageJ. The nuclei-free area of the neuropil were selected freehand and the pixel area was calculated using the Measure function. To quantify otic vesicle size in wild type

and *meis1* morphant embryos, images were analyzed in Photoshop CS4. The Ellipical Marquee tool was used to select a best-fit oval around the otic vesicle. The Measurement Scale was calibrated using a stage micrometer. Otic vesicle area and circularity was measured using the Analyze>Record Measurements function. All measurements were compiled and graphed in Excel and the mean area values for wild type and *meis1* morphant embryos were compared using an unpaired, two-tailed t-test.

2.13 Retinal ganglion cell labeling

To analyze retinal ganglion cell (RGC) axon mapping, axons were labelled with two lipophilic dyes (DiI -1,1',di-octadecyl-3,3,3'3'-tetramethylindocarbocyanine perchlorate; DiO - 3,3'-dioladecyloxacarbocyanine perchlorate) and their termination zones (TZ) visualized using a Leica TCS-SP2 Confocal microscope. DiI was dissolved in dimethylformamide at a concentration of 25 mg/ml, while DiO was dissolved in chloroform at a concentration of 25 mg/ml. For visualization of nuclei, embryos were incubated in Hoechst 33258 stain (Invitrogen) at 2.5 µg/ml in PBS/0.0005% Tween-20) overnight at 28.5°C. Efforts were made to inject a lower volume of dye into *meis1* morphants to account for their reduced eye size. To ensure that any overlap in the RGC TZ's we observed was not due to dye-bleeding in the retina, labeled eyes were imaged to confirm the accuracy of the injections, and any embryos that did not have distinct red and green RGC axon tracts leaving the retina were excluded from further analysis.

2.14 Tables

Morpholino name	Sequence 5' - 3'
*eng2a*MO	CGCTCTGCTCATTCTCATCCATGCT
*eng2b*MO	CTATGATCATTTTCTTCCATAGTGA
*hoxb1a*MO	TCTGGAACTGTCCATACGCAATTAA
*hoxb1b*MO	TGATTAAGCAGGGTCAATATGAGCT
*meis1*MO	GTATATCTTCGTACCTCTGCGCCAT
*meis1*NOL	CCCTCCACACTCCCTCGTCTTCCTT
*meis2.2*MO	CCAGCTCATCGTACCTTTGCGCCAT
*pbx2*MO1	CCGTTGCCTGTGATGGGCTGCTGCG
*pbx2*MO2	GCTGCAACATCCTGAGCACTACATT
*pbx4*MO2	AATACTTTTGAGCCGAATCTCTCCG
*pbx4*MO2	CGCCGCAAACCAATGAAAGCGTGTT
*pknox1.1*MO1	CACAGACTGGGCAGCCATCATATTC
*pknox1.1*MO2	ACTGCCAACACTGGGACATTATATG
*pknox1.1*MO	TGGACACAGACTGGGCAGCCATCAT
*pknox1.2*MO1	GGGATGTCATCATAGTTACTGTTGC
*pknox1.2*MO2	GCATTCTATAAAGCTGATCTTCAGC
*pknox2*MO1	GGACACATGTTGCATCATGGGATAG
*pknox2*MO2	CTTCACATGGAGACCAGTTTGCTTG
*smad5*MO	ACATGGAGGTCATAGTGCTGGGCTG
*tshz3b*MO	CGCGGCATGTTTCTCTTTCAGGGTT
*tshz3b*SB	AAGAAGAAGAGCCGTACCTGCCGAG

Table 2-1. List of Morpholinos.

Construct	Primer sequence 5'-3'
tshz3b	F:CACA(GAATTC)CACCATGCCGCGGAGGAAACAG
	R:CACA(CTCGAG)CTAAGGTTTCTCAAGTTCACTAAC
	R2:CACA(CTCGAG)GAGGTTTCTCAAGTTCACTAAC
tshz3bZnF1-3	R:CACA(CTCGAG)TCATTTGCCTTTCTTGATGGCAGAG
tshz3bΔHD	R:CACA(CTCGAG)TCAAGCAGGAGAGATCTCCTCTGATT
tshz3bΔZnF4, 5	R:CACA(CTCGAG)TCAAGGGTGGCCAGAGTCTAGATTTTTC
tshz3bΔZnF5	R:CACA(CTCGAG)TCACTGATATGAGGTGCCATTTGCC
tshz3bΔZnF1-3	F:CACA(GAATTC)CACCATGGAGTCAATGTCCACAAC
*tshz3b*T7TS	F:CACA(GCGGCCGC)CACCATGCCGCGGAGGAAACAG
	R:CACA(ACTAGT)ATCGCTAAGGTTTCTCAAGTTCACTAAC
tsh-RA	F:CACA(AGATCT)ACATGTTACACGAGGCTCTGATGCTCGAAATCTACAG
	R:CACA(CTCGAG)AGGCGGTCTTCTCCTTCTTCACGC

Table 2-2. Primers used to create the *tshz3b* and *tsh* mRNA expression constructs. The zebrafish *tshz3b* forward primer was used to generate inserts for all pCS2+, pCS3+MT, and pCS3+FLAG expression constructs, except for *tshz3bΔZnF1-3*, which required a unique forward primer. The *tshz3b* Rev2 primer lacks a stop codon and was used to create EnR and VP16 fusions. Primer sequences annotation: CACA – leader sequence; brackets indicate a restriction enzyme site incorporated into the primer for cloning purposes; gene-specific sequence is underlined. Abbreviations: ZnF – zinc-finger; Fwd – forward primer; Rev: reverse primer.

Gene	Vector	Linearize	RNA pol	Made by TE
eng2a W1K	pCS3+MT	NotI	SP6	no
eng2a W1KW4K	pCS3+MT	NotI	SP6	no
eng2a W4K	pCS3+MT	NotI	SP6	no
eng2a W4S	pCS3+MT	NotI	SP6	no
eng2a WT	pCS3+MT	NotI	SP6	no
fst1 (fsta)	pCS2+	NotI	SP6	no
GDF6	pCS2+	NotI	SP6	no
HA-hoxb1b	pCS2+	NotI	SP6	no
meis1	pCS3+MT	NotI	SP6	no
pbx4	pCS2+	NotI	SP6	no
tshz3b	pCS2+	NotI	SP6	yes
tshz3b-EnR	pCS3-flag	NotI	SP6	yes
tshz3b-VP16	pCS3-flag	NotI	SP6	yes
tshz3bΔHD	pCS2+	NotI	SP6	yes
tshz3bΔHD	pCS3+MT	NotI	SP6	yes
tshz3bΔHD-EnR	pCS3-flag	NotI	SP6	yes
tshz3bΔHD-VP16	pCS3-flag	NotI	SP6	yes
tshz3bΔZnF1-3	pCS2+	NotI	SP6	yes
tshz3bΔZnF1-3-EnR	pCS3-flag	NotI	SP6	yes
tshz3bΔZnF1-3-VP16	pCS3-flag	NotI	SP6	yes
tshz3bΔZnF4, 5	pCS2+	NotI	SP6	yes
tshz3bΔZnF4, 5	pCS3+MT	NotI	SP6	yes
tshz3bΔZnF4, 5-EnR	pCS3-flag	NotI	SP6	yes
tshz3bΔZnF4,5-VP16	pCS3-flag	NotI	SP6	yes
tshz3bΔZnF5	pCS2+	NotI	SP6	yes
tshz3bΔZnF5	pCS3+MT	NotI	SP6	yes
tshz3bΔZnF5-EnR	pCS3-flag	NotI	SP6	yes
tshz3bΔZnF5-VP16	pCS3-flag	NotI	SP6	yes
tshz3bZnF1-3	pCS2+	NotI	SP6	yes
tshz3bZnF1-3-EnR	pCS3-flag	NotI	SP6	yes
tshz3bZnF1-3-VP16	pCS3-flag	NotI	SP6	yes

Table 2-3. List of mRNA expression constructs.

Gene	RNA pol	Primer Sequence 5'-3'
cxcr4b	T3	**Fwd:** GAC CGC TAT CTT GCA GTA GTA CGT GC **Rev:** CAT TAA CCC TCA CTA AAG GGA AGC ACA CAT ACA CAC ATT CAC AAT GGC
dusp6	T3	**Fwd:** ACG GTT CGT CAA GCA GCA GTT C **Rev:** CAT TAA CCC TCA CTA AAG GGA AAC CAG CCC CAA TAA ATC GGA TG
efna3b	T3	**Fwd:** TGC CTG AGA TTA AGA GTG TAC GTC TGC **Rev:** CAT TAA CCC TCA CTA AAG GGA ATT GAG ACA TCC CTA CCC CTT CAC G
efna5a	T7	**Fwd:** TTT TAC CTG GTT CCT GGA TTC AGA CTC **Rev:** TAA TAC GAC TCA CTA TAG GGC TAT AAG GAT GAG AGA GAG GCA AGA AGC AC
efnb3	T3	**Fwd:** TGC CTG AGA TTA AGA GTG TAC GTC TGC **Rev:** CAT TAA CCC TCA CTA AAG GGA ATT GAG ACA TCC CTA CCC CTT CAC G
epha7	T7	**Fwd:** GCT TGG ATG AAA ACT ACA CAC CCA TTC G **Rev:** TAA TAC GAC TCA CTA TAG GGT GCG ATG CTG ACG GCT GCA AAT AG
ephb4a	T7	**Fwd:** TTT CAG GCT CAG GGC GCG TG **Rev:** TAA TAC GAC TCA CTA TAG GGG TGG CCC TTC GCA AGT CGC T
fgf3	T3	**Fwd:** CTG CTC TTG TTG TTA CTG AGC TTC TTG **Rev:** CAT TAA CCC TCA CTA AAG GGA ATA AAT GTC AGC CCT TCT GTT GTG G
fgf19	T7	**Fwd:** TGT CAC TGT TTG TGG AAG TAT CGG C **Rev:** TAA TAC GAC TCA CTA TAG GGG TTG AAG CTG GGA CTC TGG ATC AC
fgf24	T3	**Fwd:** AGT TTT CCT CTT GAA CAG CGG GC **Rev:** CAT TAA CCC TCA CTA AAG GGA AAG GTC CTC TTT TCC TTT GGG TTG G
foxd1	T3	**Fwd:** AGG CAA CTA CTG GAC GCT AGA CCC TG **Rev:** CAT TAA CCC TCA CTA AAG GGA ACA GAC CGT GTA AAA ATA TCA CAC TCC GAG

foxg1a	T3	**Fwd:** AAA TGG CTT GAG TGT TGA CAG ACT CG **Rev:** CAT TAA CCC TCA CTA AAG GGA AGA ATG TGA CCT GCA TGG TGG TGA C
hoxb1a	T3	**Fwd:** TTT CCA CAC TGG ACA CGC TAG TGA C **Rev:** CAT TAA CCC TCA CTA AAG GGA ACC CAA AGT TAT TGT GCT CGG TTA GG
met	T3	**Fwd:** AGC TCC AAA CTC GAC CTC TCA GTG AC **Rev:** CAT TAA CCC TCA CTA AAG GGA ACG GGT TGG TGC TTG TAA CTT CTA GC
prickle1b	T7	**Fwd:** CGC AGG AGG ACC TTT CAC ATA GAG **Rev:** TAA TAC GAC TCA CTA TAG GGA ATA ACA TAA CGA GGG CAT CAC GC
sef / il17rd	T3	**Fwd:** AAA CCC AGA GCG GAA ACA ATG C **Rev:** CAT TAA CCC TCA CTA AAG GGA AAT CGA GCG AAT AGT TGC GGC AG
smad1	T3	**Fwd:** TTT GTT AGG GTG GGG GTC ATC G **Rev:** CAT TAA CCC TCA CTA AAG GGA ACA CGA AAA AAA AGG GAC AGA GAC GAG
smad5	T3	**Fwd:** ATG TGC AGC CAG TGG AGT ATC AGG AG **Rev:** CAT TAA CCC TCA CTA AAG GGA AGC CTT GCG AAT AAC AGG ATT AGA CAA CAT AG
sprouty4	T7	**Fwd:** TGA GAA ACC ACC CAT TCA GAA GCG **Rev:** TAA TAC GAC TCA CTA TAG GGG ACT ATT TAC CCG TAC CTG CAT AGG TCA AC
tbx5	T7	**Fwd:** AAA GAG GGA AGT TCG CTA TCA ACC G **Rev:** TAA TAC GAC TCA CTA TAG GGA GTG GTA GTC CTG TGT GTG TTC GTG G
tshz2	T3	**Fwd:** TCC AGG GAC ATC ACA ATT CGG AC **Rev:** CAT TAA CCC TCA CTA AAG GGA AGA TCG TGA GCA CCT TTG AAA GTT CG
tshz3b	T3	**Fwd:** ACC CCA GTG TCC ACC TTA TGT AGC **Rev:** CAT TAA CCC TCA CTA AAG GGA AGT GCC ATT TGC CTC CTC ATC TG

Table 2-4. PCR-based antisense riboprobe primers.

Gene	Vector	Antibiotic	Linearize	RNA pol	Made by TE
bambi	pCR4-TOPO	amp	NotI	T3	yes
efna2	pSPORT	amp	EcoRI	SP6	no
efnb2a			NotI	T3	no
egr2b			PstI	T3	no
eng2a	TOPO	amp	NotI	T3	no
epha3			NotI	T3	no
epha4a		amp	EcoRI	T3	no
epha4b			NotI	T3	no
fgf8a	pBS-SK-	amp	NotI	T7	no
fsta	pCR4-TOPO	amp	NotI	T3	yes
gbx2			BamH1	T7	no
hoxa2		amp	Asp718	T3	no
hoxb4		amp	Kpn1	T3	no
meis1	pSPORT1	amp	EcoRI	SP6	no
meis2.1	pCR4-TOPO	amp	PmeI	T7	yes
myoD		amp	XbaI	T7	no
otx2		amp	NotI	T7	no
pax2a		amp	BamH1	T7	no
pax6a			EcoRI	SP6	no
pou5f1(spg)			NotI	T7	no
smad1	pCR4-TOPO	amp	PmeI	T7	yes
spry4	pCR4-TOPO	amp	NotI	T3	yes
tbx5			NotI	T3	no
tshz1	pCR4-TOPO	amp	PmeI	T7	yes
tshz3a	pCR4-TOPO	amp	NotI	T3	yes
tshz3b	pCR4-TOPO	amp	PmeI	T7	yes
unc45b		amp	BamH1	T7	no
vax2	pCR4-TOPO	amp	NotI	T3	yes
wnt1	pCR4-TOPO	amp	NotI	T3	yes

Table 2-5. Antisense riboprobe plasmids.

Primary antibody	Host Organism	Immunogen organism	Dilution	Company
9E10 anti-c-myc MC	Mouse	Human	1:2500	Abcam
P2A6 anti-Meis1 MC	Mouse	Zebrafish	1:10	FHCRC
anti-Tsh3a UA004 PIB	Rabbit	Zebrafish	1:1000	Covance
anti-Tsh3a UA005 PIB	Rabbit	Zebrafish	1:1000	Covance
anti-Tsh3a UA004 TB PC	Rabbit	Zebrafish	1:1000	Covance
anti-Tsh3a UA005 TB PC	Rabbit	Zebrafish	1:1000	Covance
anti-Tsh3a UA004 PB1 PC	Rabbit	Zebrafish	1:1000	Covance
anti-Tsh3a UA005 PB1 PC	Rabbit	Zebrafish	1:1000	Covance
anti-Tsh3a UA004 PB2 PC	Rabbit	Zebrafish	1:1000	Covance
anti-Tsh3a UA005 PB2 PC	Rabbit	Zebrafish	1:1000	Covance
anti-Tsh3a UA004 PB3 PC	Rabbit	Zebrafish	1:1000	Covance
anti-Tsh3a UA005 PB3 PC	Rabbit	Zebrafish	1:1000	Covance
anti-Tsh3a UA004 EB PC	Rabbit	Zebrafish	1:1000	Covance
anti-Tsh3a UA005 EB PC	Rabbit	Zebrafish	1:1000	Covance
anti-Tsh3a AP peptide 1 PC	Rabbit	Zebrafish	1:500	Covance
anti-Tsh3a AP peptide 2 PC	Rabbit	Zebrafish	1:500	Covance

Table 2-6. Primary antibodies used for Western analysis. Abbreviations: AP – affinity purified; EB – exanguination bleed; MC – monoclonal; PB – production bleed; PC - polyclonal; PIB – pre-immune bleed; TB – test bleed

Primary antibody	Host Organism	Immunogen organism	Dilution	Company
9E10 anti-c-myc MC	Mouse	Human	1:250	Abcam
4D9 anti-Engrailed / Invected MC	Mouse	Drosophila	1:10	Santa Cruz
zn5/zn8 anti-alcam MC	Mouse	Zebrafish	1:250/1:10	ZIRC
rmo44 anti-160 kD NF-M MC	Mouse	Rat	1:250	Sigma
anti-phospho-Smad1/5/8 PC	Rabbit	Human	1:200	Cell Signaling
P2A6 anti-Meis1 MC	Mouse	Zebrafish	1:5	FHCRC
anti-Tsh3a AP peptide 1 MC	Rabbit	Zebrafish	1:200	Covance
6-11B-1 anti-acetylated tubulin MC	Mouse	Chlamydomonas	1:500	Sigma
anti-Pbx1/2/3/4 H-260 PC	Rabbit	Human	1:50	Santa Cruz

Table 2-7. Primary antibodies used for whole mount immunohistochemistry. Abbreviations: AP – affinity purified; MC – monoclonal; PC – polyclonal

2.15 References

Hans, S., Christison, J., Liu, D., Westerfield, M., 2007. Fgf-dependent otic induction requires competence provided by Foxi1 and Dlx3b. BMC Dev Biol. 7**,** 5.

Higashijima, S., Hotta, Y., Okamoto, H., 2000. Visualization of cranial motor neurons in live transgenic zebrafish expressing green fluorescent protein under the control of the islet-1 promoter/enhancer. J Neurosci. 20**,** 206-18.

Kimmel, C. B., Ballard, W. W., Kimmel, S. R., Ullmann, B., Schilling, T. F., 1995. Stages of embryonic development of the zebrafish. Dev Dyn. 203**,** 253-310.

Kramer-Zucker, A. G., Olale, F., Haycraft, C. J., Yoder, B. K., Schier, A. F., Drummond, I. A., 2005. Cilia-driven fluid flow in the zebrafish pronephros, brain and Kupffer's vesicle is required for normal organogenesis. Development. 132**,** 1907-21.

Link, V., Shevchenko, A., Heisenberg, C. P., 2006. Proteomics of early zebrafish embryos. BMC Dev Biol. 6**,** 1.

Molina, G. A., Watkins, S. C., Tsang, M., 2007. Generation of FGF reporter transgenic zebrafish and their utility in chemical screens. BMC Dev Biol. 7**,** 62.

Picker, A., Brand, M., 2005. Fgf signals from a novel signaling center determine axial patterning of the prospective neural retina. Development. 132**,** 4951-62.

Popperl, H., Rikhof, H., Chang, H., Haffter, P., Kimmel, C. B., Moens, C. B., 2000. lazarus is a novel pbx gene that globally mediates hox gene function in zebrafish. Mol Cell. 6**,** 255-67.

Thisse, C., Thisse, B., 2008. High-resolution in situ hybridization to whole-mount zebrafish embryos. Nat Protoc. 3**,** 59-69.

Westerfield, M., 2000. The zebrafish book. A guide for the laboratory use of zebrafish (Danio rerio). Univ. of Oregon Press., Eugene, OR.

Chapter Three - The role of Meis1 in regulating hindbrain patterning and neuronal identity

3.1 Introduction

During embryonic development, the vertebrate hindbrain is segmented along its anterior-posterior axis into seven lineage-restricted compartments called rhombomeres (r). Each segment is morphologically and molecularly distinct due to rhombomere-specific transcriptional programs executed by trimeric complexes of Hox, Pbx, and Meinox (Meis / Pknox) homeodomain transcription factors. An important output of hindbrain segmentation is the specification of unique neuronal identities within each rhombomere. The best studied of these hindbrain neurons are the cranial motor and the reticulospinal neurons. Neurons from both of these groups are organized in a segmental array that respect rhombomere boundaries and reflect the segmented nature of the hindbrain (reviewed in Moens and Prince, 2002).

Of the twelve (I-XII) bilateral pairs of cranial nerves, the motor neuron cell bodies of the V-X nerves are located within the hindbrain (Figure 1-1). The V, VII, IX, and X nerves are known as the branchiomotor cranial nerves since they are associated with the branchial / pharyngeal arches that lie adjacent to the hindbrain (reviewed in Guthrie, 2007). The branchiomotor neurons serve both sensory (afferent) and motor (efferent) functions in the craniofacial region. The trigeminal neurons in rhombomeres 2 and 3 form the V nerve and are responsible for facial sensation, jaw movement, and swallowing. The facial motor neurons (FMNs) of the VII nerve innervate the muscles that control facial expressions, while the sensory component of the VII nerve receive taste information from the tongue. In zebrafish and mouse, the FMNs are specified in r4, and then migrate caudually to r6 and r7 (reviewed in Chandrasekhar, 2004; Chandrasekhar et al., 1997). Even though this tangential migration does not occur in chick, the facial neurons undergo a lateral migration in all of these vertebrate species. The sensory neurons of the IX (glossopharyngeal) nerve specialize in taste and pharyngeal sensation, and may also undergo a tangential migration from r6 to r7 in zebrafish. The vagal neurons of the X nerve in r7 and r8 collect and relay information from the body's organs to the brain. In particular, the X nerve sensory neurons regulate

heart rate, blood pressure, respiration, and gastrointestinal function during periods of stress. Together, the branchiomotor cranial nerves perform many important motor and sensory functions, and their specification relies on proper hindbrain patterning.

The reticulospinal neurons (RNs) represent another neuronal class arranged in accordance with the metameric organization of the hindbrain (Metcalfe et al., 1986). These neurons receive auditory and visual input and relay this information to motor- and interneurons in the spinal cord, thereby performing a command function in the neural circuitry of the teleost embryonic escape response (Eaton et al., 2001). One of the most famous neurons in all of neurobiology, the Mauthner cell, is a reticulospinal neuron. The Mauthners are a bilateral pair of neurons found in r4 of fish, amphibians and birds. They are characterized by their large size (visible by light microscopy), and their contralaterally projecting axons. The fact that these cells are so large, easily identifiable and part of a relatively simple behavioural circuit has made the Mauthners a favourite of electrophysiologists and neuroethologists (reviewed in Korn and Faber, 2005). The RNs, and the Mauthners in particular, are also excellent readouts of hindbrain patterning, as their segment organization and specification are downstream of Hox function (reviewed in Moens and Prince, 2002).

There are multiple Hox, Pbx and Meinox family members expressed within the hindbrain during segmentation. It is thought that the unique combinations of these proteins within each rhombomere can transcriptionally define the identities of each segment. Evidence for this model comes from loss or gain of function of specific Hox genes, which can result in homeotic transformations of one rhombomere identity to another (reviewed in Alexander et al., 2009). Likewise, a loss of Pbx protein function in zebrafish results in the transformation of the entire hindbrain to a Hox-independent r1-like ground state identity (Waskiewicz et al., 2002). Pbx and Meinox proteins are biochemical binding partners, an interaction that regulates each protein's subcellular localization and transcriptional activity (Choe et al., 2002; Jaw et al., 2000;

Rieckhof et al., 1997; Waskiewicz et al., 2001). As such, Meinox proteins have also been implicated in hindbrain segmentation, mostly through the use of Meinox dominant-negative constructs that are designed to interfere with the ability of all Meinox proteins to either access the nucleus (Choe et al., 2002), bind DNA (Waskiewicz et al., 2001), or activate transcription (Dibner et al., 2001). However, very few studies have concentrated on the functions of individual Meinox proteins.

In this study, I have used an antisense morpholino knockdown approach to analyze the hindbrain patterning role of Meis1. Knockdown of Meis1 perturbs rhombomere 2 identity, as shown by the reduction of *hoxa2b*, and the posterior expansion of r1 identity. Additionally, there is a genetic interaction between *meis1* and *pbx* genes, where reduction of Meis1 function in *pbx4* mutants makes the hindbrain patterning defects more severe than either genetic manipulation alone. Although r3-7 appear to be segmented normally in Meis1-depleted embryos, specification of the branchiomotor and reticulospinal neurons in these segments is abnormal. This is most clearly illustrated for r4, where the facial and Mauthner neurons are specified. Although *hoxb1a*, which is required for neuronal specification in r4, is expressed normally in Meis1-depleted embryos, morphant embryos often lack Mauthner neurons, and the FMNs fail to undergo their tangential migration from r4 to r6/7. These data indicate that Meis1 is required to specify neuronal identity and behaviour in r4, although it is not required to establish r4 itself.

3.2 Results

3.2.1 *meis1* mRNA and protein expression in wild type and Pbx-depleted embryos

To determine spatial and temporal *meis1* expression during segmentation of the hindbrain, I performed whole mount mRNA in situ hybridization assays on embryos ranging from 10 – 19 hours post-fertilization (hpf). *meis1* mRNA is expressed up to the r2/3 boundary at 10 and 11.5 hpf, as determined by double staining with the r3 and r5 marker gene *egr2b* / *krox20* (Figure 3-1A, B). The

presence of nuclear Meis1 protein in the hindbrain was confirmed using the P2A6 α-Meis1 monoclonal antibody on 11.5 hpf embryos co-stained with a nuclear dye (Figure 3-1C). By 13 hpf, *meis1* expression has initiated in r2 (Figure 3-1D), and by 16.5 hpf, *meis1* expression is firmly established up to the r1/2 boundary (Figure 3-1E). Interestingly, while *meis1* continues to be strongly expressed up to the r1/2 boundary, by 19 hpf, a low level of expression is also observed in r1 and the cerebellum, between the midbrain-hindbrain boundary (MHB) and r2 (Figure 3-1F). *meis1* is also expressed in the eye field and midbrain throughout all of the developmental stages examined here. Chapter 6 of this thesis will discuss the Hox-independent functions of *meis1* in these tissues. With regard to Hox-dependent hindbrain patterning, *meis1* is expressed in the right place at the right time to be involved in this process. Furthermore, *meis1* expression is dynamic, both spatially and in terms of its expression levels. *meis1* is first expressed up to the r2/3 boundary, with expression being initiated later in r2, and then subsequently in r1 and the cerebellum. Additionally, the early uniform level of expression is refined as hindbrain development proceeds, with higher levels of *meis1* present in the anterior hindbrain (r2-4), and slightly lower levels in the caudal hindbrain and spinal cord.

The expression of *meis1* suggests that it is regulated by the same Hox-Pbx-Meinox transcriptional complexes that specify segmental identity in the hindbrain. To determine if *meis1* was regulated by Hox function, I used a combination of the *pbx4* mutant (*lazarus*) together with *pbx2* and *pbx4* morpholinos to create a stepwise decrease in hindbrain Hox function leading to a loss of r2-6 identity (Waskiewicz et al., 2002). Compared to wild type, 12 hpf *pbx4*$^{-/-}$ embryos have decreased r3 and r5 expression of *egr2b*, but normal *meis1* expression (Figure 3-2A, B). Even in *pbx4*$^{-/-}$ embryos where *pbx* function has been reduced even further through the use of *pbx2* and *pbx4* morpholinos, *egr2b* expression is eliminated, but *meis1* expression is still normal (Figure 3-2C). This indicates that Pbx-Hox function is not required for the initiation of *meis1* expression in the neural tube. However, if similarly treated embryos are examined at 19 hpf, I observe strong Pbx-Hox-dependent changes in *meis1* expression.

Compared to wild type, *pbx4*$^{-/-}$ embryos exhibit a reduction in *meis1* expression throughout r2-6, especially in rhombomeres 2-4 where *meis1* expression is strongest in wild type embryos (brackets in Figure 3-2D, E). However, *meis1* expression is still normal in the eyes, midbrain, cerebellum/r1, and spinal cord of *pbx4*$^{-/-}$ embryos, and is still excluded from the MHB. The decrease in *meis1* expression is even more obvious in *pbx4*$^{-/-}$; *pbx2,4*MO (Pbx-depleted) embryos (Figure 3-2F). Even though the retinal expression is relatively normal, *meis1* expression is reduced in the midbrain, no longer excluded from the MHB, and is present in the hindbrain at a level similar to that observed in the cerebellum/r1 region of wild type embryos. Taken together, these data suggest that Pbx-Hox function is not required to initiate *meis1* expression, but is required for the spatial refinement and the upregulation of *meis1* expression in the anterior hindbrain between 12 and 19 hpf.

It is known that Pbx proteins promote the stability and nuclear localization of Meinox proteins. To see if this is was also true of Meis1, I examined the localization of both endogenous and overexpressed Meis1 in wild type, *pbx4*$^{-/-}$, and Pbx-depleted embryos at 12 hpf. In contrast to the unaltered expression of *meis1* mRNA (Figure 3-2A-C), decreasing Pbx function leads to lower levels of endogenous Meis1 protein as well as a more diffuse subcellular localization, as shown by the lack of punctate nuclear staining in Pbx-depleted embryos (Figure 3-2G-I). I confirmed this result by injecting mRNA coding for Meis1 fused to an N-terminal Myc-epitope (Waskiewicz et al., 2001) into one cell of two-cell stage embryos (to produce more mosaic expression), and then examining the localization of myc-Meis1 using the α-Myc 9E10 monoclonal antibody. Similar to the endogenous Meis1 protein, ectopic myc-Meis1 is distinctly nuclear in wild type embryos (Figure 3-2J). However, in *pbx4-/-* embryos, myc-Meis1 staining is more diffuse, suggesting both nuclear and cytoplasmic localization (Figure 3-2K). In Pbx-depleted embryos, myc-Meis1 is present at lower levels, and is largely cytoplasmic. Together with the expression data in Figure 3-2A-C, these results suggest that although the initiation of *meis1* mRNA expression does not require

Pbx, Meis1 protein levels and nuclear localization are both compromised in Pbx-depleted embryos at 12 hpf.

3.2.2 *meis1* mRNA overexpression perturbs midbrain development

As a starting point for examining *meis1* function in hindbrain patterning, I first analyzed the phenotype of myc-Meis1 overexpression. Injecting mRNA encoding myc-Meis1 into one-cell stage embryos produces nearly ubiquitous, nuclear-localized myc-Meis1 protein, as determined by whole mount immunostaining using the P2A6 α-Meis1 monoclonal antibody (Figure 3-3A, B). To confirm the specificity of the α-Meis1 antibody, I also analyzed myc-Meis1 protein by Western blotting. Both the α-Myc 9E10 and P2A6 α-Meis1 antibodies specifically recognize a band at 80 kDa in lysates made from *myc-meis1* injected embryos (Figure 3-3C). However, although the P2A6 α-Meis1 antibody is able to detect endogenous Meis1 protein in whole mount immunostains, this antibody is not able to detect endogenous Meis1 by standard Western analysis. Taken together with other studies (Pillay et al., 2010; Waskiewicz et al., 2001), these data indicate that *myc-meis1* mRNA produces protein that is nuclear localized throughout the embryo.

To analyze the effect of myc-Meis1 on neural patterning, I performed mRNA in situ hybridization for *pax6a* (eye, forebrain, hindbrain), *eng2a* (midbrain) and *egr2b* (r3 and r5 in the hindbrain) on wild type and *myc-meis1* injected embryos. Compared to wild type, *myc-meis1* injected embryos have relatively normal hindbrain segmentation, although the size of r3 is slightly expanded (compare r3 in Figure 3-4A, E with B, F). This result is consistent with previous studies in zebrafish that have found little effect on hindbrain patterning by overexpressing Meis3 alone (Vlachakis et al., 2001). Although hindbrain patterning is not affected, the most striking phenotype of *myc-meis1* overexpression is the specific deletion of the midbrain region of the neural tube. In wild type embryos, the homeodomain transcription factor *eng2a* is expressed in the posterior midbrain, the MHB, and the anterior cerebellum (red stain in between the arrows in Figure 3-4A). In 15 hpf *myc-meis1* overexpressing

embryos, *eng2a* expression is lost, and the forebrain and hindbrain domains of *pax6a* are nearly fused (Figure 3-4B). Similar results are observed using *wnt1* expression as a MHB marker. Compared to 20 hpf wild type embryos, *myc-meis1* overexpressing embryos exhibit a specific loss of MHB wnt1 expression (Figure 3-4C, D). This is shown again using the expression of *epha4b*, which is excluded from the posterior midbrain and cerebellum, but is expressed in the anterior midbrain and in the hindbrain up to r1 (Figure 3-4E). In *myc-meis1* injected embryos, the anterior midbrain and hindbrain domains are fused (Figure 3-4F), confirming that ectopic Meis1 leads to a deletion of the MHB and cerebellum.

As will be expanded upon in Chapter 5 of this thesis, midbrain development can be divided into two broad phases: initiation and maintenance. The initiation phase occurs during gastrulation when the neural tube is initially subdivided into fore-, mid-, and hindbrain fates (Rhinn et al., 2005). While it is clear from Figure 3-4 that *myc-meis1* overexpressing embryos fail to maintain midbrain identity, we wanted to determine if this was due to a failure to properly initiate midbrain identity. To do this I examined the expression of the secreted morphogen *fgf8a*, and the transcription factors *pax2a* and *pou5f1* in wild type and *myc-meis1* injected embryos during the midbrain initiation phase between 9-11 hpf. *myc-meis1* overexpression decreases the level of *pax2a* expression in the midbrain region (black arrows) without affecting hindbrain patterning (*egr2b*) or *pax2a* expression in the otic placode or pronephric mesoderm (open arrows) (*n*=10/13; Figure 3-5A, B). Fgf8a signals originating from the MHB are required for both midbrain and cerebellar development. Similar to the *pax2a* results, *fgf8a* expression in the hindbrain and somites (open arrows) is not strongly affected by *myc-meis1* overexpression, whereas the midbrain expression domain is downregulated (*n*=6/6; Figure 3-5C, D). Unlike *pax2a* and *fgf8a*, which are expressed and required throughout the course of MHB development, the POU-class transcription factor *pou5f1* is expressed in the midbrain only for a short period of time during midbrain initiation. During that time, it confers Fgf-responsiveness to midbrain cells, thereby allowing midbrain development to proceed and maintain itself (Reim and Brand, 2002). In *myc-meis1* injected

embryos, the midbrain domain of *pou5f1* is disorganized, and there are ectopic *pou5f1*-expressing cells along the lateral edges of the neural tube (*n*=6/6; Figure 3-5E, F). The failure of *myc-meis1* overexpressing embryos to properly initiate MHB development, as well as the fusion of forebrain and hindbrain domains, is similar to that observed for *pou5f1* (*spiel-ohne-grenzen*) mutants (Reim and Brand, 2002), suggesting that ectopic Meis1 exerts a negative effect on MHB development by perturbing *pou5f1* expression in the midbrain. *pou5f1* is also expressed in the hindbrain where it is required for proper hindbrain segmentation (Hauptmann et al., 2002), but an antagonistic interaction between *meis1* and *pou5f1* has not been examined in this tissue. However, given that *pou5f1* mutants and *myc-meis1* overexpressing embryos display opposite hindbrain patterning phenotypes, it is unlikely that Meis1 antagonizes *pou5f1* in this tissue. In summary, ectopic Meis1 has little effect on overall AP hindbrain patterning, but does produce a detrimental outcome for midbrain development, possibly by perturbing *pou5f1* expression in this tissue.

3.2.3 *meis1* mRNA overexpression perturbs jaw development

In vertebrates, many elements of the craniofacial skeleton are derived from neural crest cells that originate at the interface between the ectoderm and neural tube. A subset of these cells migrates through the branchial arches to the head where they differentiate into cartilage and bone (reviewed in Knight and Schilling, 2006). Hox and Pbx proteins are required to pattern these cranial neural crest cell populations such that they form the correct bone and cartilage elements (Popperl et al., 2000; reviewed in Trainor and Krumlauf, 2001). Recently, it has been demonstrated that Cyp26b1, a retinoic acid (RA) metabolizing enzyme, is required to spatially and temporally modulate RA signaling in post migratory cranial neural crest cells (Laue et al., 2008). *cyp26b1* mutants have a characteristic jaw morphogenesis defect where the shape of the ethmoid plate is abnormally pointed and contains a reduced number of chondrocytes (Piotrowski et al., 1996). Compared to 6 dpf wild type embryos, *myc-meis1* injected embryos have a pointed, protruding lower jaw and narrowed distance between the eyes (*n*=6/12;

Figure 3-6A-B'). Although a detailed analysis of the jaw cartilage patterning was not performed on *myc-meis1* overexpressing embryos, their jaw and craniofacial phenotype is superficially similar to that observed for *cyp26b1* mutants. Thus, ectopic Meis1 may cause jaw defects via ectopic activation of retinoic acid signaling, or possibly by mispatterning the hindbrain-derived cranial neural crest cells.

3.2.4 The role of *meis1* in specifying segmental identity in the hindbrain

To create a loss of function model for *meis1* in hindbrain patterning, Meis1 protein production was blocked using an antisense Morpholino (Nasevicius and Ekker, 2000; Summerton, 1999) oligomer targeted to the *meis1* mRNA translation start site, thereby creating *meis1* "morphants". To establish that the *meis1* morpholino (MO) effectively knocks down Meis1 protein, α-Meis1 whole mount immunostains were done on 16 hpf wild type and *meis1* morphant embryos. Compared to wild type embryos, *meis1* morphants have nearly undetectable fluorescent signal, indicating that the morpholino effectively blocks Meis1 protein production (Figure 3-7A-F). A similar knockdown of Meis1 protein is observed using a second translation-blocking MO that does not overlap in sequence with the first MO (Figure S6-1C,D). As such, the morpholino-based approach is an effective method to knockdown Meis1 protein.

Morphologically, 19 hpf *meis1* morphants appear similar to their wild type counterparts (Figure 3-8A, B). Morphological segmentation of the hindbrain is still visible in morphant embryos (black arrows). However, the otic vesicle (white brackets), which depends on hindbrain-derived Fgf signals for induction, is smaller in Meis1-depleted embryos. This small ear phenotype is similar to that observed in Pbx-depleted embryos (Figure 3-8C). However, Pbx-depleted embryos have a much more severe hindbrain segmentation defect, as evidenced by the lack of visible rhombomere segments. These data suggest that, unlike Pbx proteins, *meis1* is playing specific, rather than global, roles in hindbrain patterning.

To determine the role of Meis1 in hindbrain segmentation, I analyzed the expression of various *eph* and *ephrin* (*efn*) genes. Rhombomere-restricted expression of *ephs* and *ephrins* is particularly important for hindbrain segmentation as the interaction between Eph receptor tyrosine kinases and their Ephrin ligands regulate differential cell-cell adhesion, thereby refining and maintaining rhombomere boundaries (Cooke et al., 2005). *ephb4a* is expressed in the cerebellum, r4 and the anterior spinal cord in wild type embryos, and this basic expression pattern is maintained in *meis1* morphants, although the r4 domain is smaller (*n*=17/17; Figure 3-9A, B). *efnb3b* and *epha4a* display complementary expression patterns, where *epha4a* is exclusive to r3 and r5 and *efnb3b* is largely excluded from r3 and r5. Again, although the rhombomere domains are smaller, *efnb3b* (*n*=19/19) and *epha4a* (*n*=31/31) are similarly expressed in *meis1* morphants (Figure 3-9C-F). In summary, wild type and Meis1-depleted embryos have similar rhombomere-restricted patterns of *eph* and *ephrin* gene expression at 15 hpf, indicating that Meis1 is not globally required for specifying segmental identity in the zebrafish hindbrain.

3.2.5 Meis1 is required for normal levels of *hoxa2b* expression in the hindbrain

hoxa2b is the only *hox* gene expressed in r2 (Gavalas et al., 1997; Prince et al., 1998), where its expression is controlled by a Hox-Pbx-Meinox responsive element located 3' to the *hoxa2* locus (Lampe et al., 2004). *meis1* and *hoxa2b* have similar expression patterns at 20 hpf, with enriched expression in r2 and r3 and lower levels in r4 and r5 (compare Figures 3-1F and 3-10C). This suggests that *meis1* may play a role in regulating *hoxa2b* expression. At 12.5 hpf, *hoxa2b* expression in r2 and r3 is reduced in *meis1* morphants (*n*=9/10; Figure 3-10A, B). Similarly, at 20 hpf *hoxa2b* expression in r2-5 is downregulated in Meis1-depleted embryos, with the r2 domain being the most severely affected (*n*=40/40; Figure 3-10C, D). To show that the downregulation of *hoxa2b* in *meis1* morphants is specifically due to knockdown of Meis1 protein, I injected *meis1* morphants with *myc-meis1* mRNA and assayed for *hoxa2b* expression. Co-injection of *meis1*

morpholino with *myc-meis1* RNA is able to rescue *hoxa2b* expression (*n*=9/14), supporting the idea that Meis1 positively regulates *hoxa2b* transcription (Figure 3-10E-G).

To further test the hypothesis that Meis1 positively regulates *hoxa2b* expression, I assayed for *hoxa2b* expression in wild type (*pbx4*$^{+/+}$ or *pbx4*$^{+/-}$) and *pbx4*$^{-/-}$ embryos injected with *myc-meis1* mRNA. In wild type embryos, *myc-meis1* RNA causes an upregulation of *hoxa2b* in r2-4 (*n*=2/3; Figure 3-11A, B). In *pbx4*$^{-/-}$ embryos without *myc-meis1* RNA, *hoxa2b* expression is greatly reduced, with only residual staining remaining in r2 and r3 (*n*=3/3; Figure 3-11C). Overexpression of *myc-meis1* is able to partially rescue this defect, though only in r2/3 (*n*=3/3; Figure 3-11D). Taken together with Figure 3-10, these data suggest that Meis1 is critically important for normal *hoxa2b* expression in rhombomeres 2 and 3.

3.2.6 Meis1 knockdown causes r2 to adopt an r1-like identity

Rhombomere 1 is the only hindbrain segment whose identity is not specified by Hox proteins. One of the phenotypes of Pbx-depleted embryos mutants is the posterior expansion of r1 identity resulting from a failure to specify Hox-dependent r2-6 identity (Waskiewicz et al., 2002). The strong reduction of *hoxa2b* expression in *meis1* morphants suggests that r2 identity requires Meis1 function. To test whether r2 adopts an r1-like identity in *meis1* morphants, I looked at the expression of *epha4a*, which marks r1, r3, and r5 in 26 hpf wild type embryos (Figure 3-12A, C). In *meis1* morphants, the r1 domain is expanded posteriorly up to r3 (*n*=33/33; Figure 3-12B, D). The expansion of r1 is not due to a general expansion of anterior hindbrain identity, as the cerebellar domain of *met* (*hepatocyte growth factor receptor*) expression up to r1 is unchanged in *meis1* morphants (*n*=20/20; Figure 3-12E, F). Taken together, *meis1* provides positive input into *hoxa2b* expression, a function that is likely required to specify r2 and restrict r1 identity to its normal domain.

3.2.7 Meis1 positively regulates otic vesicle size and *fgf3* expression in the hindbrain

One of the phenotypes highlighted in Figure 3-8 is the small, round ear of *meis1* morphants. To quantify this change, I measured the area (μM^2) and circularity (4π[area/perimeter^2]) of otic vesicles in 26 hpf wild type and *meis1* morphant embryos (Figure 3-13A, B). Wild type embryos have a mean otic area of 6358±775 μM^2 (*n*=13), which is 20% larger than the 5266±552 μM^2 average of morphant ears (*n*=17; P=0.0001; Figure 3-13C). Besides having a smaller area, *meis1* morphant ears are also rounder than their wild type counterparts. The circularity of a perfect circle is 1, while wild type otic vesicle have an average circularity of 0.80±0.03 (*n*=13). *meis1* morphant vesicles have an average circularity of 0.86±0.03 (*n*=17; P<0.0001; Figure 3-13D). Thus, at 26 hpf, the otic vesicles of *meis1* morphants are smaller and rounder than wild type embryos.

Vertebrate otic placodes are induced by an extraotic combinatorial Fgf signal, part of which originates from the hindbrain. In zebrafish, Fgf3 and Fgf8a from the hindbrain are required for otic induction. In Pbx-depleted embryos, Fgf expression in the hindbrain is reduced, thereby contributing to defects in ear development (Figure 3-8C) (Waskiewicz et al., 2002). The small ear phenotype of *meis1* morphants suggests that Meis1 may contribute to otic induction by regulating *fgf* expression in the hindbrain. To see if this was the case, I examined *fgf3* expression in *meis1* morphants. At 16.5 hpf, *fgf3* is expressed in the MHB, the cerebellum, in r4, and in mesodermal cells surrounding the hindbrain (Figure 3-13E). In *meis1* morphants, the r4 domain of *fgf3* expression is specifically reduced (*n*=41/41; Figure 3-13F). To see if Meis1 was affecting overall Fgf signaling in the hindbrain, I used a transgenic line of fish where the Fgf-responsive promoter for the *dual specificity phosphatase 6* (*dusp6*) gene drives a destabilized eGFP gene, thereby providing a dynamic readout for some aspects of Fgf signaling in the developing zebrafish embryo (Molina et al., 2007). In 16.5 hpf wild type embryos, eGFP expression resembles the sum of *fgf8a* and *fgf3* expression domains (Figure 3-13G), and while eGFP fluorescence intensity is somewhat reduced in *meis1* morphants, this pattern is essentially unchanged

(*n*=5/5; Figure 3-13H). The modest, but significant, reduction in ear size in *meis1* morphants is similar to that observed for *fgf3* morphants (Phillips et al., 2001). Thus, while Meis1 is not having a large effect on hindbrain Fgf signaling at 16.5 hpf, the reduction of *fgf3* expression may contribute to the small ear phenotype.

3.2.8 *meis1* and *pbx* genes cooperatively pattern the hindbrain

Pbx and Meinox proteins are DNA-binding partners that cooperatively regulate hindbrain gene expression in a complex with Hox PG 1-4 proteins (Chang et al., 1997; Knoepfler et al., 1997; Vlachakis et al., 2000). Additionally, the Pbx-Meinox interaction is bidirectionally required to promote both the stability and nuclear accumulation of these proteins (Figure 3-2G-L) (Abu-Shaar et al., 1999; Choe et al., 2002; Rieckhof et al., 1997; Stevens and Mann, 2007; Waskiewicz et al., 2001). To see if Meis1 is required to maintain wild type levels of Pbx proteins, I performed whole mount immunostaining using a polyclonal antibody designed to recognize human Pbx1/2/3/4 proteins. As this antibody had not been previously used in zebrafish, I tested its specificity by comparing staining patterns in 19 hpf wild type and Pbx-depleted embryos. In wild type embryos, the antibody recognizes nuclear-enriched proteins in a pattern that is consistent with previously published data (Figure 3-14A, C) (Popperl et al., 2000; Waskiewicz et al., 2001). This signal is abolished in Pbx-depleted embryos (*n*=2/2; Figure 3-14B), indicating that this antibody is able to recognize endogenous zebrafish Pbx proteins. To see if Meis1 knockdown had an effect on Pbx protein levels, I stained for Pbx proteins in 19 hpf embryos injected with *meis1* morpholino. Compared to equivalently staged wild type embryos, *meis1* morphants have reduced, but not eliminated, levels of Pbx proteins (*n*=5/5; Figure 3-14C, D). This phenotype is consistent with the ability of overexpressed Meis1 to post-transcriptionally stabilize Pbx proteins (Waskiewicz et al., 2001). Another as-of-yet untested possibility is that Meis1 knockdown reduces *pbx2* and / or *pbx4* transcription, similar to what is observed for *meis1* transcription with regard to Pbx depletion (Figure 3-2D-F). However, there is no precedent in either flies or

vertebrates that Meinox proteins regulate *pbx* / *exd* gene transcription. Thus, Pbx protein stabilization is one of the roles that Meis1 plays in hindbrain development.

To determine if *pbx* and *meis1* genes interact with regard to hindbrain patterning, I compared hindbrain gene expression phenotypes at 19 hpf between wild type embryos, *pbx4*$^{-/-}$ mutants, and *pbx4*$^{-/-}$ embryos injected with *pbx2,4* morpholino (Pbx-depleted), all with and without *meis1* morpholino. As shown previously in Figure 3-2D-F, at 19 hpf *meis1* expression is reduced in *pbx4-/-* mutants (*n*=2/2), and further reduced in Pbx-depleted embryos (*n*=5/5; Figure 3-15A, C, E). Knocking down Meis1 protein causes a more severe reduction of *meis1* transcription in each of these genetic backgrounds. *meis1* morphants express less *meis1* than wild type embryos (*n*=3/3; Figure 3-15A, B); *pbx4*$^{-/-}$ mutants injected with *meis1* MO exhibit less *meis1* staining than *pbx4*$^{-/-}$ embryos alone (*n*=2/2; Figure 3-15C, D); and Pbx-depletion plus Meis1 knockdown leads to even less *meis1* expression than that caused by Pbx-depletion alone (*n*=5/5; Figure 3-15E, F). Taken together, these results indicate that Pbx and Meis promote *meis1* gene expression.

A similar Pbx-Meis interaction is observed for other hindbrain markers. I used a *pax2a* / *egr2b* / *unc45b* riboprobe mixture to mark r3 and r5 (*egr2b*), and define the size of the hindbrain between the MHB (*pax2a*) and the first somite (*unc45b*). *meis1* morphants have normal *pax2a*, *egr2b* and *unc45b* expression, although r3 and r5 are narrower in Meis1-depleted embryos (*n*=3/3; Figure 3-15G, H). *pbx4*$^{-/-}$ mutants have a characteristic reduction in r3 *egr2b* expression (*n*=3/3; Figure 3-15I) (Popperl et al., 2000), and this phenotype is mildly exacerbated by Meis1 knockdown (*n*=2/2; Figure 3-15J). Pbx-depleted embryos completely lack r2-r6 identity (Waskiewicz et al., 2002), and have reduced *pax2a* expression at the MHB (*n*=3/3; Figure 3-15K). This MHB phenotype will be fully discussed in Chapter 5 of this thesis. Meis1 knockdown produces no further reduction in *pax2a* expression, but does lead to a dramatic reduction in the size of the hindbrain/ spinal cord region between the MHB and the first somite (*n*=7/7; Figure 3-15L). Thus, Meis1 synergizes with Pbx-depletion with regard to *meis1* expression and in defining the size of the hindbrain.

As illustrated in Figures 3-10 and 3-11, Meis1 plays an important role in activating *hoxa2b* expression. In *meis1* morphants, *hoxa2b* expression is reduced, particularly in the r2-3 domain (*n*=4/4; Figure 3-15M, N). This phenotype is not as severe as a *pbx4*$^{-/-}$ mutant, where *hoxa2b* expression is greatly reduced in r2 and nearly eliminated in r3-5 (*n*=3/3; Figure 3-15O) . Interestingly, *meis1*MO; *pbx4*$^{-/-}$ embryos lack *hoxa2b* expression in the hindbrain (*n*=2/2; Figure 3-15P), and this is the same phenotype as Pbx-depleted embryos (*n*=5/5; Figure 3-15Q). Similarly, Meis1; Pbx-depleted embryos also lack *hoxa2b* expression (*n*= 7/7; Figure 3-15R).

In summary, *meis1* morphants have a hindbrain patterning phenotype, which in the case of *egr2b* and *hoxa2b* expression, is less severe than the *pbx4*$^{-/-}$ phenotype. Knockdown of Meis1 protein in *pbx4*$^{-/-}$ embryos causes more severe patterning defects than either genetic manipulation alone. Interestingly, the genetic interaction between *meis1* and *pbx4* is stronger with regard to *hoxa2b* expression compared to *egr2b*, indicating a differential requirement for *meis1* in regulating hindbrain gene expression. Unexpectedly, *meis1* morphant + Pbx-depleted embryos have even more severe hindbrain patterning phenotype than Pbx-depleted embryos alone, especially with regard to the regulation of hindbrain size and *meis1* expression. This is surprising because Pbx-depleted embryos already lack r2-6 identity, and have a dramatic reduction in Meis1 proteins levels (Figure 3-2G-I). Taken together, these data suggest that Meis1 contributes to hindbrain patterning both as a regulator of Pbx protein stability, and as a regulator of transcription.

3.2.9 The role of *meis1* in patterning the reticulospinal and branchiomotor neurons

An important output of segmental hindbrain patterning is the development of rhombomere-specific neuronal identities. This is nicely illustrated by the segmental organization of the cranial motor and the reticulospinal neurons (reviewed in Chandrasekhar, 2004; Kimmel et al., 1985; Lumsden and Keynes, 1989; Metcalfe et al., 1986). Although the neurons in each class are considered to

be segmental homologues of one another, the neurons from each rhombomere are unique from one another with regard to their morphology, function, and axonal projection patterns. These differences indicate that rhombomere-specific developmental processes are generating unique neuronal identities amongst the segmental homologues. Pbx-Meinox-Hox complexes are required for this process, as Pbx-depleted embryos lack all segmental neuronal identities (A.J.W., unpublished results; Waskiewicz et al., 2002).

To find out what role Meis1 is playing in hindbrain neuronal specification, I compared the organization of the reticulospinal and branchiomotor neurons between wild type and Meis1-depleted embryos at 50 hpf. The rmo44 α-neurofilament-medium monoclonal antibody marks the reticulospinal neurons in r2-7. In wild type embryos, the reticulospinal neurons are segmentally arrayed with the neurons in even-numbered rhombomeres (r2, r4, r6) projecting their axons contralaterally along the medial longitudinal fascicle to the spinal cord, while those in odd numbered rhombomeres project ipsilaterally (Figure 3-16A). The most remarkable of the teleost reticulospinal neurons is the large Mauthner cell located in r4. In zebrafish, Mauthner development depends on *hoxb1a* and *hoxb1b* function. Knockdown of both paralogues together (but not individually) leads to a loss of Mauthner identity (Jozefowicz et al., 2003; McClintock et al., 2002), while the simultaneous overexpression of *hoxb1b*, *pbx4* and *meis3* can generate ectopic r4-specific Mauthners (Vlachakis et al., 2001). In *meis1* morphants, the clear segmental organization of the anterior RNs is lost. Additionally, one or both Mauthners are missing, and the RoL2 neurons in r2 lack their typical contralateral axonal projection pattern (*n*=19/22; Figure 3-16B). However, the RNs posterior to r4 appear relatively normal. These results indicate that Meis1 is particularly important for reticulospinal neuron development in r2-4.

A subset of branchiomotor neurons can be visualized in the *isl1:GFP* transgenic line of fish (Higashijima et al., 2000). The oculomotor and trochlear neurons of cranial nerves III and IV lie in the midbrain, while the vagal neurons of the X nerve are located in r8 and the anterior spinal cord. In the hindbrain, the V nerve is made up of the trigeminal neurons in r2 (Va – anterior) and r3 (Vp –

posterior), while the facial motorneurons (FMNs) of the VII nerve are born in r4 and subsequently undergo a tangential migration to r6/7, followed by a lateral migration (Figure 3-16C). In *meis1* morphants, the clear division between the Va and Vp trigeminal neurons in r2/3 is lost, and the FMNs either partially or wholly fail to migrate posteriorly (*n*=155/156; Figure 3-16D). These defects are limited to the hindbrain cranial nerves, as the oculomotor (III), trochlear (IV), and vagal (X) neurons are normal in Meis1-depleted embryos. Furthermore, similar phenotypes are observed using a second translation-blocking morpholino whose sequence does not overlap with the first (*meis1*NOL), indicating the specificity of the Meis1-knockdown phenotype (*n*=16/59; Figure 3-16E, F). Taken together, *meis1* morphants exhibit reticulospinal and branchiomotor neuron patterning defects, especially in r2-4 where *meis1* is expressed at its highest levels.

Zebrafish Hoxb1a is an important transcriptional regulator of neuronal specification in r4. In combination with Hoxb1b and in partnership with Pbx proteins, it is required for Mauthner identity and for tangential migration of the FMNs (Cooper et al., 2003; McClintock et al., 2002). The similarities between the *meis1* and *hoxb1a* morphant phenotypes could be explained by the Meis1-dependent activation of *hoxb1a* expression in r4. However, at 16 hpf, *hoxb1a* expression is normal in Meis1-depleted embryos (*n*=50/50; Figure 3-16G, H), consistent with the overtly normal specification of r3-6 (Figure 3-9). One of the ways in which Hoxb1a regulates FMN migration is by activating the expression of *prickle1b* (*pk1b*), a planar cell polarity gene that is required cell-autonomously by FMNs to correctly orient their direction of migration (Mapp et al., 2010; Rohrschneider et al., 2007). To see if Meis1 also promotes *pk1b* transcription, I compared *pk1b* expression in 26 hpf wild type and *meis1* morphant embryos. In wild type embryos, *pk1b* is expressed in the migrating FMNs, which at this stage are present in r4-6 (Figure 3-16I). In *meis1* morphants, *pk1b* expression is greatly reduced (*n*=17/19; Figure 3-16J). To show that this loss of *pk1b* expression was not due to a delay in FMN specification, I also examined the expression of *chemokine (C-X-C motif), receptor 4b* (*cxcr4b*), which is also expressed in FMNs and required for their migration (Cubedo et al., 2009). Similar to *pk1b* expression,

wild type FMNs in r4-6 express *cxcr4b* (Figure 3-16K). *cxcr4b* is still expressed in *meis1* morphant FMNs, although it is mostly limited to r4 (*n*=36/36; Figure 3-16L). These data indicate that, like *hoxb1a*, *meis1* is required for the tangential migration of FMNs and provides positive input into *pk1b* expression.

3.3 Discussion

It is known that Hox-Pbx-Meinox transcriptional complexes specify segmental identity to the hindbrain rhombomeres, but the specific contribution of Meis1 to this process has not been previously examined. Using a combination of overexpression and morpholino-based knockdown approaches, I have shown that Meis1 is important for segmental patterning and neuronal specification in rhombomeres 1-4 in the anterior hindbrain. Given the data presented here, together with previous literature on functions of Meinox proteins, it is likely that Meis1 accomplishes these tasks via two mechanistically distinct, yet functionally inseparable roles: [1] homeodomain-independent biochemical stabilization of Pbx proteins; and [2] homeodomain-dependent transcriptional regulation of target genes.

3.3.1 The bidirectional stabilization of Meis1 and Pbx proteins

The initiation of *meis1* expression is independent of Pbx function (Figure 3-2A-C), although similarly staged Pbx-depleted embryos exhibit a dramatic reduction in Meis1 protein levels (Figure 3-2G-L) (Pillay et al., 2010). These data indicate that Pbx proteins post-translationally regulate Meis1 protein stability, a result that is not surprising given previous studies in flies and vertebrates with regard to the stability and subcellular localization of other Meinox proteins (Abu-Shaar and Mann, 1998; Berthelsen et al., 1999; Choe et al., 2002; Deflorian et al., 2004; Kurant et al., 1998; Maeda et al., 2002; Waskiewicz et al., 2001). What is surprising however is the dramatic reduction of Pbx protein levels in Meis1-depleted embryos at 19 hpf (Figure 3-14C, D). This result was unexpected since there are at least five other Meinox protein family members present in the zebrafish hindbrain, all of which are theoretically competent to bind and stabilize

Pbx proteins. A comprehensive analysis of Pbx-Meinox interaction kinetics, together with a quantitative comparison of Meinox protein levels would help to determine if Meis1 is simply more available or more effective at stabilizing Pbx than other Meinox proteins. Another possibility is that all Pbx and Meinox proteins are engaged in a co-stabilization loop, the framework of which is compromised with the removal of any one of its components. Evidence for this comes from analysis of a hypomorphic mutation in the mouse *Pknox1* gene, which causes a reduction in Pbx1, Pbx2 and Meis1 protein levels in the fetal liver (Ferretti et al., 2006). Additionally, I have observed a reduction in Meis1 protein levels in *meis2.2* morphant embryos (Figure S3-1). Thus, it is likely that any major perturbation in the wild type levels of Pbx or Meinox proteins will destabilize the biochemical and transcriptional networks that maintains those levels.

In this light, the phenotype of *meis1* morphants may be viewed as the sum of its biochemical and transcriptional activities, necessarily including the partial loss of function phenotypes of other TALE-class proteins. For example, knocking down Meis1 in *pbx4* mutant or Pbx-depleted embryos worsens the severity of the hindbrain patterning phenotypes in each case (Figure 3-15), and may do so via two non-exclusive mechanisms. The first involves the non-transcriptional role of Meis1 in regulating Pbx protein stability. Zygotic *pbx4* mutants still possess Pbx2, and while *pbx4* mutants injected with *pbx2* and *pbx4* morpholinos lack up to 99% of endogenous Pbx protein (Waskiewicz et al., 2002), the very nature of morpholino knockdown means that some protein will be produced from the targeted mRNA. Meis1 knockdown in *pbx4*$^{-/-}$ or Pbx-depleted embryos may further reduce the remaining pool of Pbx, thereby leading to a more severe hindbrain patterning phenotype.

The second reason why simultaneous knockdown of Pbx and Meis1 proteins leads to more severe patterning phenotypes could involve direct transcriptional regulation by Meis1 protein. A transcriptional role for Meinox proteins in general has already been demonstrated through the use of Meis dominant negative constructs that either can not bind DNA, or are fused to a

transcriptional repressor domain (Dibner et al., 2001; Waskiewicz et al., 2001). With regard to *meis1* specifically, given the similarities between *meis1* and *hoxa2b* expression, the reduction of *hoxa2b* expression in *meis1* morphants suggests that Meis1 provides positive input into *hoxa2b* transcription. Consistent with this possibility, overexpression of *myc-meis1* mRNA causes an increase in *hoxa2b* in r2-4, but is only able to rescue expression in a *pbx4*$^{-/-}$ mutant in r2 and r3 (Figure 3-11A-D). These data, together with the fact that *meis1* morphants do not exhibit the same gross patterning defects as those observed in *pbx4*$^{-/-}$ or Pbx-depleted embryos (Figures 3-9 and 3-15), suggest that there are specific transcriptional requirements for Meis1 in anterior hindbrain patterning.

3.3.2 Meis1 is required for branchiomotor and reticulospinal neuron patterning in the anterior hindbrain

Rhombomere 4 is home to two interesting neuronal subtypes: the facial branchiomotor nucleus of cranial nerve VII, and the bilateral pair of Mauthner reticulospinal neurons. In zebrafish, the *hoxb1* paralogues *hoxb1a* and *hoxb1b* function redundantly to specify Mauthner identity, while knockdown of Hoxb1a alone is sufficient to block the tangential migration of FMNs from their birthplace in r4 to r6/7. Although r2 identity is compromised in *meis1* morphants, the remainder of the hindbrain appears to retain its segmented character as shown by normal patterns of *eph*, *ephrin* and *egr2b* expression in r3-6, and *hoxb1a* expression in r4 (Figures 3-9, 3-15, and 3-16). As such, it was surprising to find that *meis1* morphants exhibit a loss of Mauthner identity and a failure of the FMNs to fully migrate out of r4 (Figure 3-16A-D). As *hoxb1a* expression is normal in Meis1-depleted embryos, *meis1* is acting either downstream, or in parallel to *hoxb1a* with regard to neuronal specification in r4. Since Meis1 can participate in DNA-binding complexes with Pbx and Hox proteins, it is possible that Meis1 cooperates with Hoxb1a through *prickle1b* to positively regulate FMN migration.

3.4 Figures

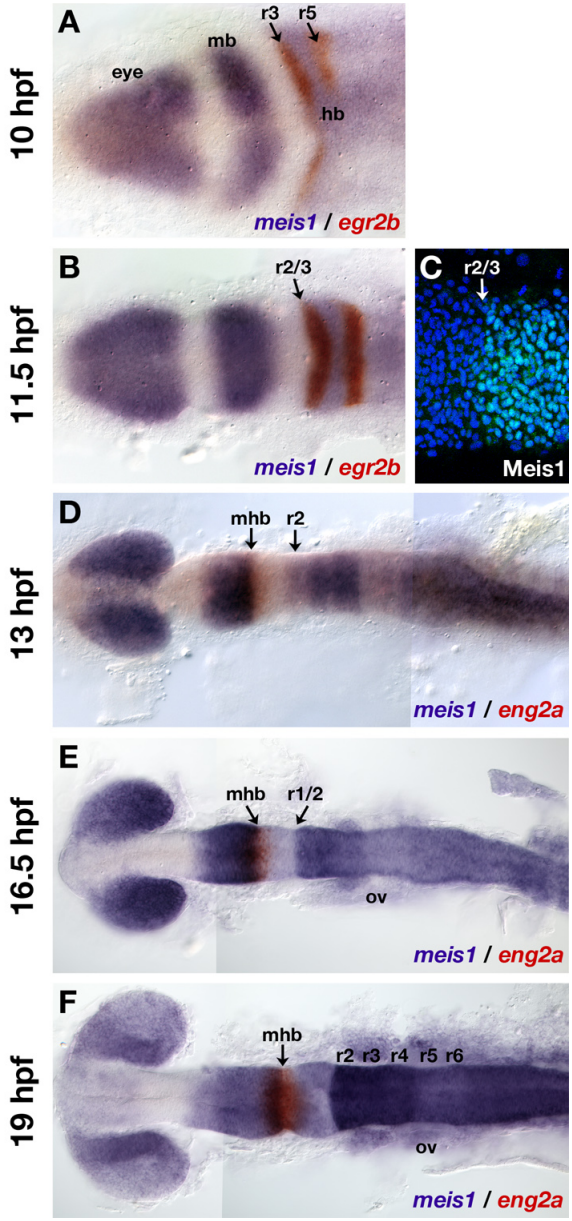

Figure 3-1. mRNA in situ hybridizations detailing *meis1* expression during the hindbrain segmentation period from 10 to 19 hpf. **(A)** *meis1* expression (purple) at 10 hpf in the presumptive eye, midbrain, and hindbrain regions. The embryo is co-stained for *egr2b* mRNA (red) in r3 and r5 of the hindbrain. *meis1* is expressed upto the presumptive r2/3 boundary. **(B)** *meis1* expression (purple) at 11.5 hpf, co-stained with *egr2b*. *meis1* is still expressed upto the r2/3 boundary. **(C)** Optical section of the r2/3 boundary in the hindbrain at 11.5 hpf immunostained using the α-Meis1 P2A6 antibody (green) with nuclei co-stained with Hoechst 33258 (blue). Meis1 protein is primarily nuclear. **(D)** *meis1* expression (purple) at 13 hpf co-stained with *eng2a* (red) at the midbrain-hindbrain boundary (MHB.) At this stage, *meis1* has started to be expressed in r2. **(E, F)** *meis1* expression (purple) at 16.5 hpf **(E)** and 19 hpf **(F)** co-stained with *eng2a* (red) at the MHB. *meis1* is expressed at its highest levels in the anterior hindbrain. Additionally, *meis1* expression has expanded rostrally into the r1 / cerebellar region. All views are dorsal with anterior to the left. Abbreviations: mb – midbrain; hb – hindbrain; r – rhombomere; ov – otic vesicle.

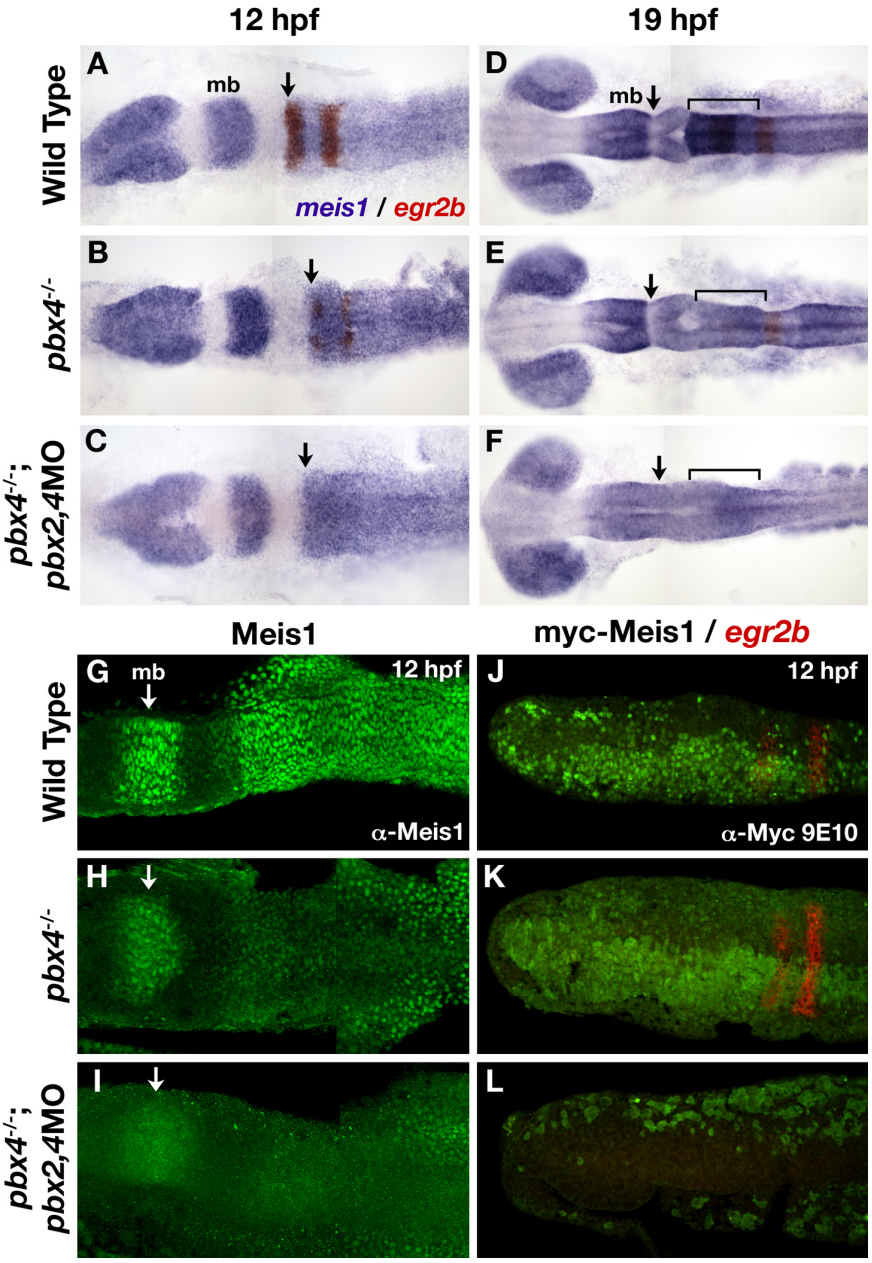

Figure 3-2. The regulation of *meis1* mRNA expression and protein stability by Pbx. **(A-C)** *meis1* mRNA expression (purple) co-stained with *egr2b* (red) in wild type (A), *pbx4*$^{-/-}$ (B), and *pbx4*$^{-/-}$; *pbx2,4*MO (Pbx-depleted; C) at 12 hpf. *egr2b* expression in r3 and r5 is progressively lost as Pbx function is decreased, but *meis1* expression up to the presumptive r2/3 boundary (black arrow) remains unaffected at this stage. **(D-F)** *meis1* mRNA expression (purple) co-stained with *egr2b* (red) in wild type (D), *pbx4*$^{-/-}$ (E), and Pbx-depleted (F) embryos at 19 hpf. *meis1* expression is reduced in the anterior hindbrain of *pbx4*$^{-/-}$ embryos, but

normal elsewhere and still excluded from the MHB (black arrow). In Pbx-depleted embryos, *meis1* expression is reduced throughout the midbrain, hindbrain (brackets), and spinal cord, and is no longer excluded from the MHB (black arrow). **(G-I)** Immunostains for Meis1 protein in wild type (G), *pbx4*$^{-/-}$ (H), and Pbx-depleted (I) embryos at 12 hpf. Relative to wild type, Meis1 protein levels are reduced in *pbx4* mutants, and further reduced in Pbx-depleted embryos. Additionally, the immunostaining is more diffuse, indicating a change in subcellular localization. White arrows indicate the midbrain region. **(J-L)** Immunostains for overexpressed myc-Meis1 protein in wild type (J), *pbx4*$^{-/-}$ (K), and Pbx-depleted (L) embryos at 12 hpf co-stained by mRNA in situ hybridization for *egr2b*. Ectopic myc-Meis1 shows punctate nuclear staining in wild type embryos, by this staining becomes more diffuse as Pbx function is depleted. All views are dorsal with anterior to the left.

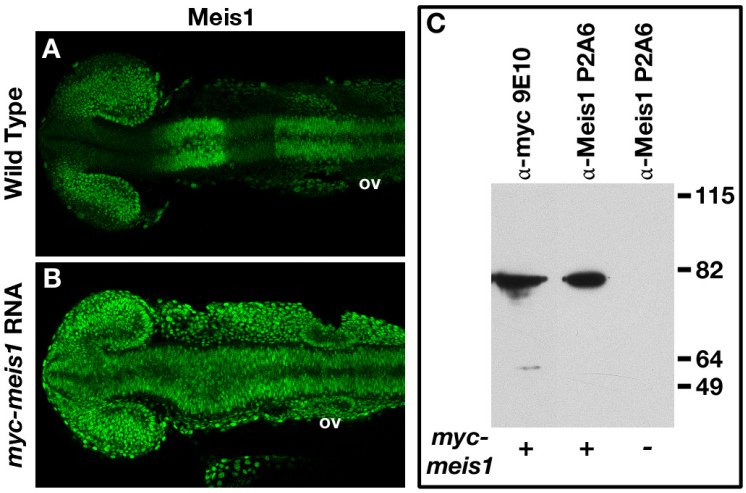

Figure 3-3. myc-Meis1 overexpression controls. **(A-B)** Meis1 protein as detected using the α-Meis1 P2A6 antibody in wild type (A) and *myc-meis1* injected embryos (B) at 17 hpf. Views are dorsal with anterior to the left. **(C)** Western blot showing overexpressed myc-Meis1 protein as detected with the α-Myc 9E10 and α-Meis1 P2A6 antibodies. The α-Meis1 P2A6 does not detect endogenous Meis1 protein in lysates made from uninjected 18 hpf embryos. Abbreviations: ov – otic vesicle.

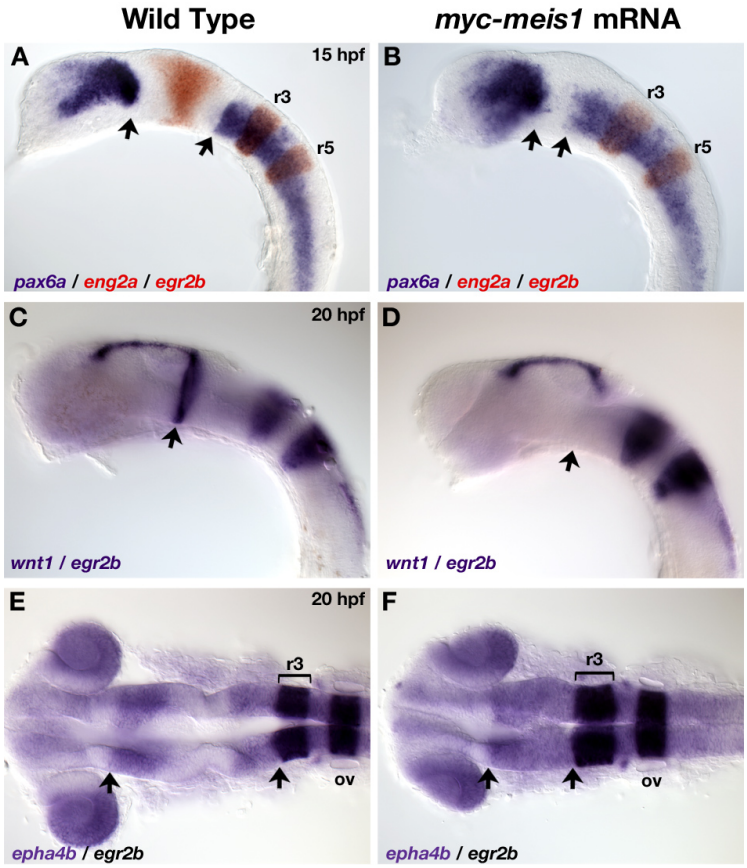

Figure 3-4. *myc-meis1* injected embryos lack the midbrain region. **(A, B)** Wild type and *myc-meis1* injected embryos at 15 hpf stained for *pax6a* (purple) marking the forebrain and hindbrain (black arrows), *eng2a* (red) in the midbrain, and *egr2b* (red) in r3 and r5 of the hindbrain. *eng2a* midbrain expression is missing in *myc-meis1* injected embryos and the forebrain and hindbrain domains of *pax6a* are closer together. **(C-F)** Wild type and *myc-meis1* injected embryos at 20 hpf stained for *wnt1* (C, D) or *epha4b* (E, F) and co-stained with *egr2b*. *wnt1* expression is absent from the MHB (black arrow), but still present in the dorsal midbrain. *epha4b* is expressed in the anterior midbrain and hindbrain, and these domains are fused in *myc-meis1* overexpressing embryos (black arrows). (A-D) are lateral views, (E, F) are dorsal views, all with anterior to the left. Abbreviations: ov – otic vesicle; r – rhombomere.

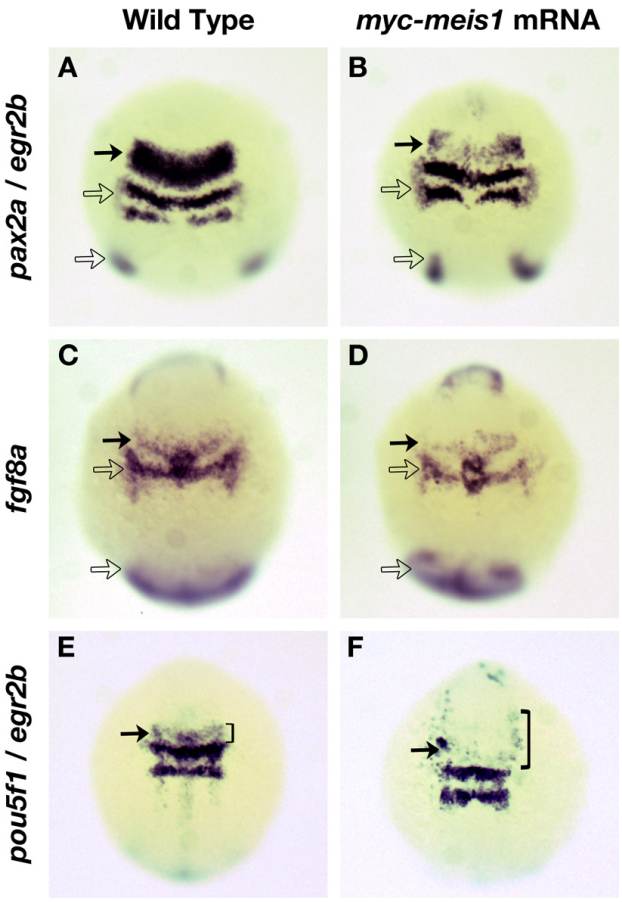

Figure 3-5. *meis1* overexpression perturbs midbrain initiation. Wild type and *myc-meis1* injected embryos at 10-11 hpf stained for midbrain markers (black arrows) *pax2a* (A, B), *fgf8a* (C, D), and *pou5f1* (E, F). In all cases, ectopic Meis1 prevents the proper specification of the midbrain without affecting *egr2b* expression in the hindbrain, or the posterior expression domains of *pax2a* and *fgf8a* (open arrows). The brackets in (E, F) indicate the midbrain expression domain of *pou5f1*. All views are dorsal with anterior at the top.

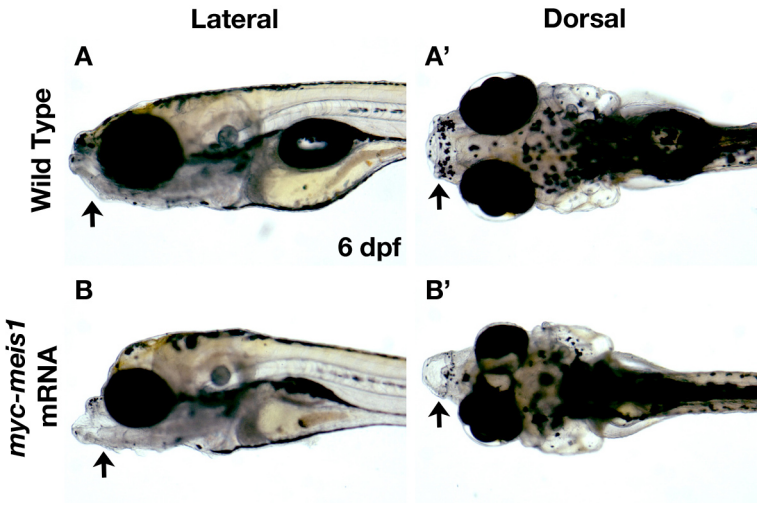

Figure 3-6. *meis1* overexpression causes defects in jaw development. Lateral and dorsal views of live wild type (A, A') and *myc-meis1* injected embryos (B, B') at 6 dpf. Black arrows indicate the jaw region affected by ectopic Meis1.

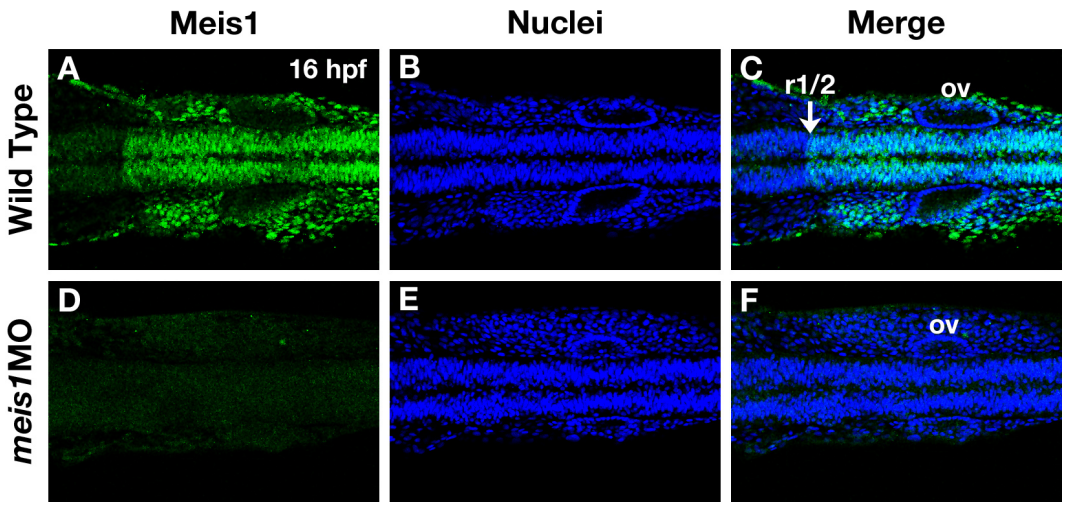

Figure 3-7. The *meis1* translation-blocking morpholino reduces Meis1 protein levels. Immunostains for endogenous Meis1 protein (green) using the α-Meis1 P2A6 antibody in wild type (A-C) and *meis1* morphant (*meis1*MO; D-F) embryos at 16 hpf. Nuclei are stained with Hoechst 33258 (blue). Views are dorsal with anterior to the left. Abbreviations: ov – otic vesicle; r – rhombomere.

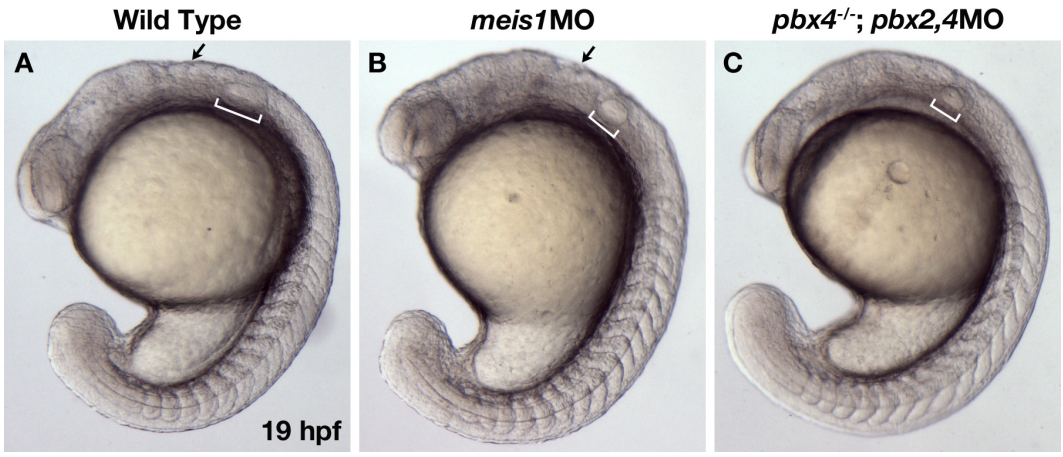

Figure 3-8. Lateral views of live wild type (A), *meis1*MO (B) and Pbx-depleted (C) embryos at 19 hpf. Black arrows indicate rhombomere bulges in wild type and *meis1* morphant embryos. White brackets indicate the otic vesicle.

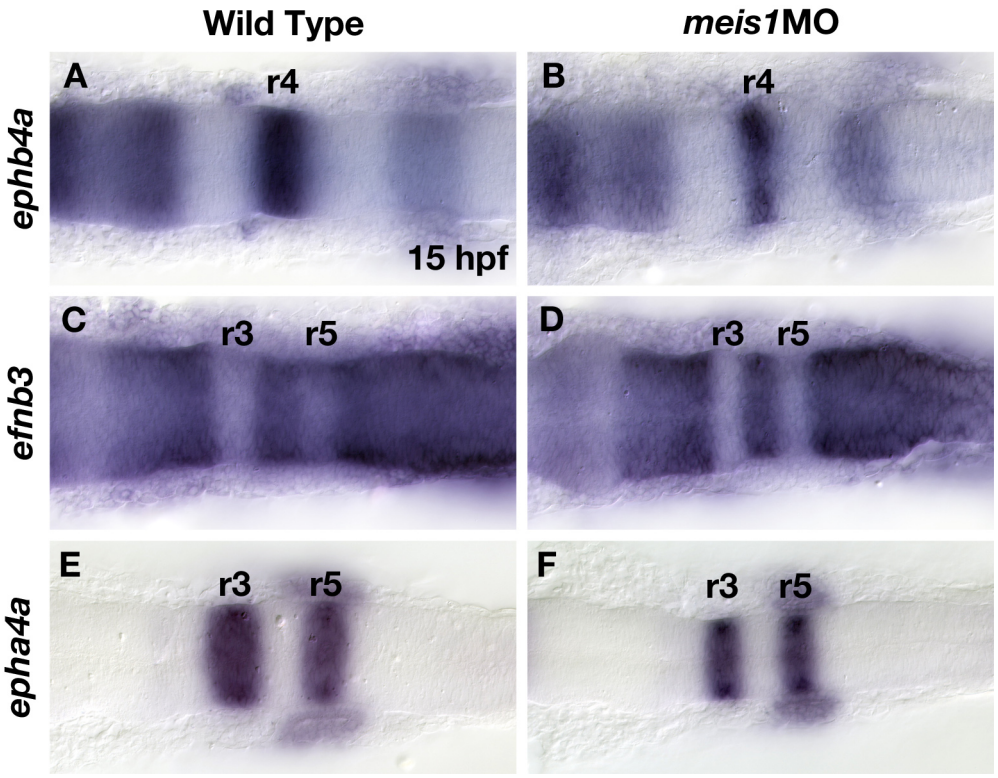

Figure 3-9. The hindbrain retains a segmental organization in *meis1* morphants. Wild type and *meis1* morphant embryos stained for hindbrain segmentation markers *ephb4a* (A, B), *efnb3b* (C, D), and *epha4a* (E, F). All views are dorsal with anterior to the left. Abbreviations: r – rhombomere.

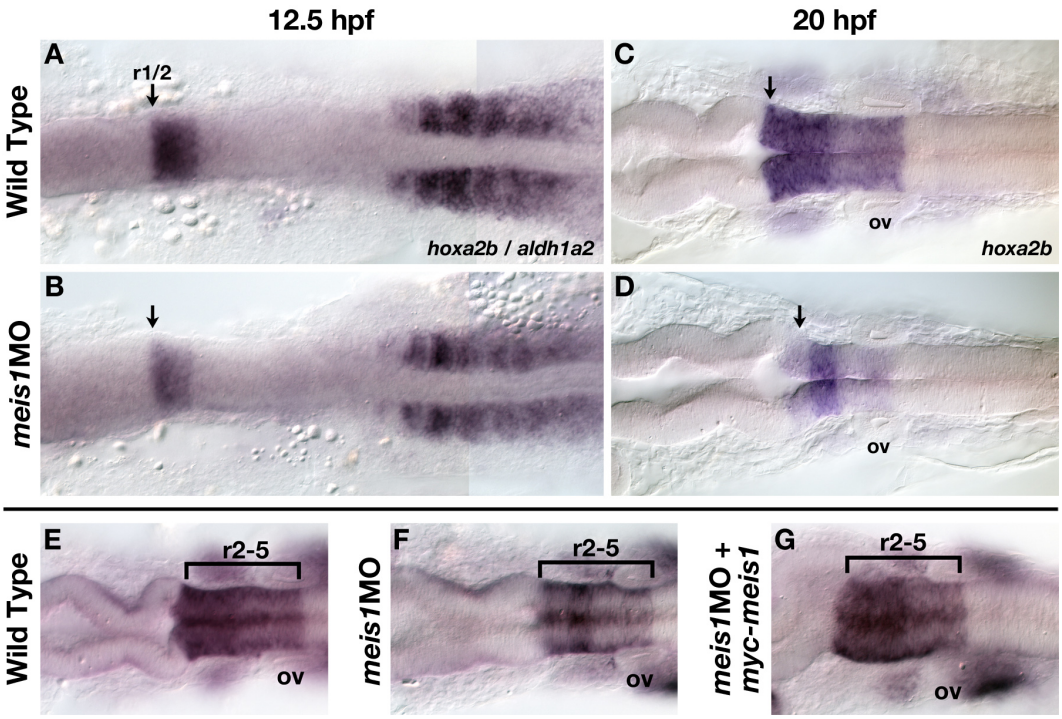

Figure 3-10. *hoxa2b* expression is reduced in *meis1* morphants, and can be rescued by morpholino-insenstive ectopic myc-Meis1. **(A-D)** *hoxa2b* expression in the anterior hindbrain is reduced in *meis1* morphants at 12.5 hpf (A, B) and 20 hpf (C, D). Black arrows indicate the r1/2 boundary. Embryos in A and B are co-stained with *aldh1a2* to mark the somites. **(E-G)** Ectopic Meis1 can rescue the *hoxa2b* expression defects in *meis1* morphants. All views are dorsal with anterior to the left. Abbreviations: ov – otic vesicle; r – rhombomere.

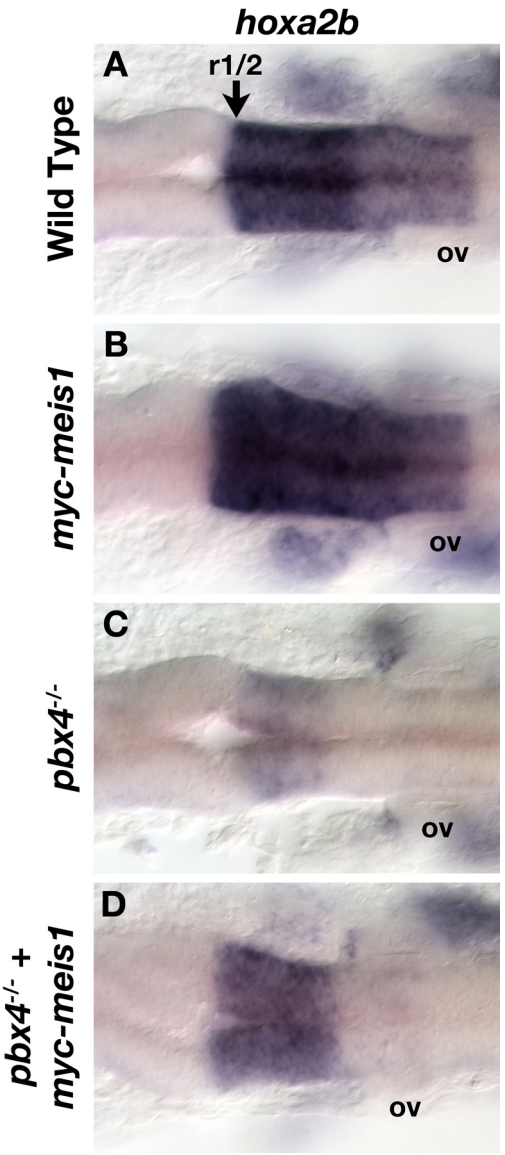

Figure 3-11. *meis1* overexpression can partially rescue *hoxa2b* expression in *pbx4*$^{-/-}$ mutants. *hoxa2b* mRNA expression in wild type (A*), myc-meis1* injected embryos (B), *pbx4*$^{-/-}$ mutants (C), and *pbx4*$^{-/-}$ mutants injected with *myc-meis1* mRNA. Compared to wild type, *myc-meis1* overexpression can increase *hoxa2b* expression, and partially rescue *hoxa2b* levels in r2 and r3 of a *pbx4* mutant. All views are dorsal with anterior to the left. Abbreviations: ov – otic vesicle; r – rhombomere.

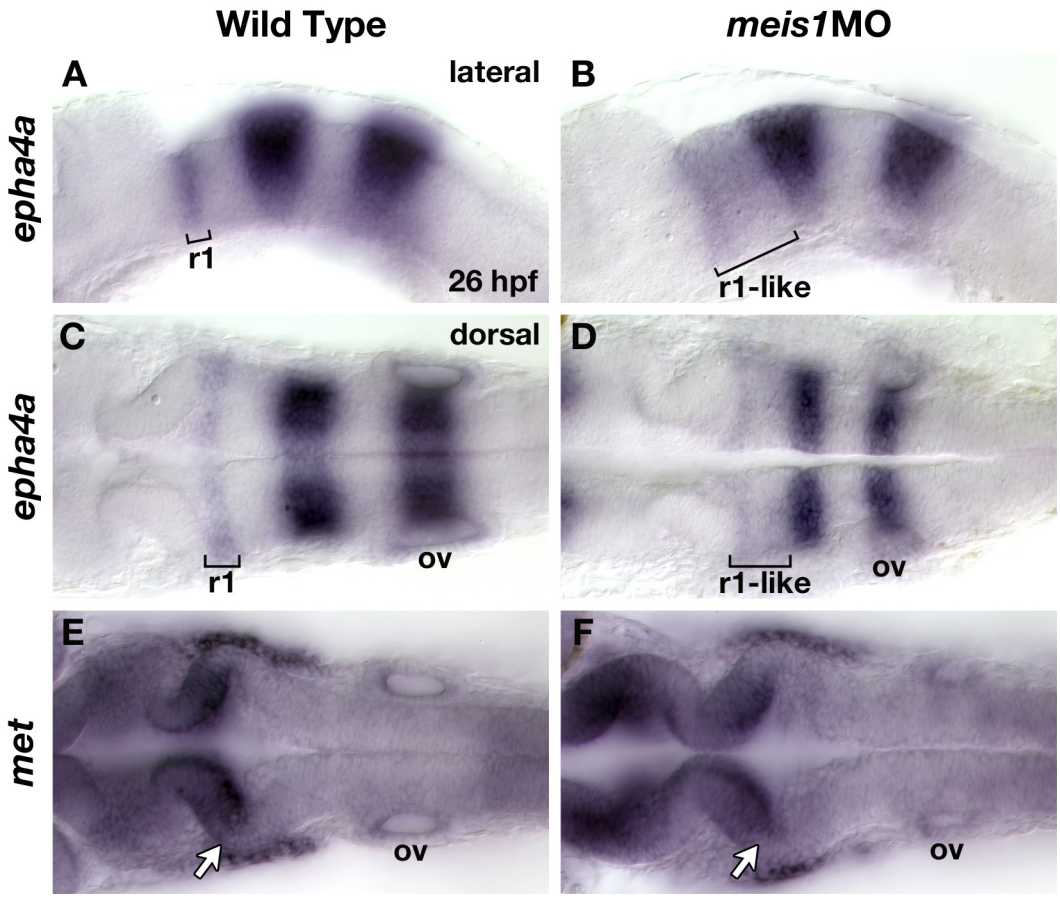

Figure 3-12. Knockdown of Meis1 leads to a posterior expansion of r1 identity. **(A-D)** Lateral and dorsal views of 26 hpf wild type and *meis1* morpants embryos stained for the r1-r3-r5 marker *epha4a*. The r1 domain of *epha4a* is expanded caudally such that it reaches the r3 domain in Meis1-depleted embryos. **(E, F)** Compared to wild type, the cerebellar expression domain of *met proto-oncogene (hepatocyte growth factor receptor)* is unchanged in *meis1* morphants.

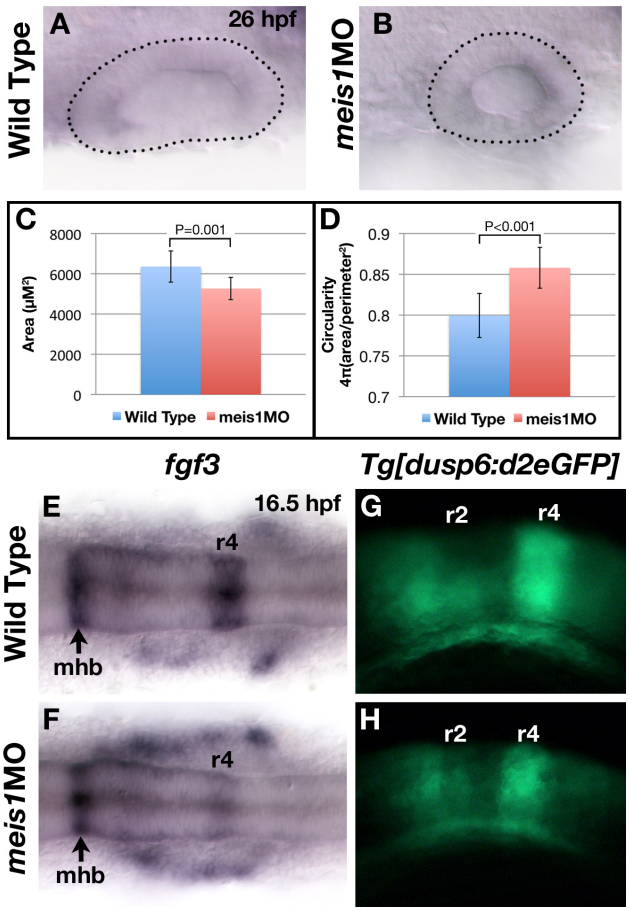

Figure 3-13. *meis1* morphants have smaller otic vesicles (ov) and decreased *fgf3* expression in the hindbrain. **(A, B)** Otic vesicles of wild type and *meis1* morphant embryos at 26 hpf. **(C)** Quantification of ov area in wild type and *meis1* morphant embryos at 26 hpf. Wild type embryos have a mean ov area of 6358 μM^2 ± 775 (*n*=13), while the mean ov area of *meis1* morphants is 5266μM^2 ± 552 (*n*=17; t-test: P=0.0001). Error bars show plus/minus one standard deviation. **(D)** Quantification of ov circularity, as determined by the formula $4\pi(\text{area}/\text{perimeter}^2)$. The circularity of a perfect circle is 1. The mean circularity of wild type ov is 0.8 ± 0.03 (*n*=13), while *meis1* morphant ov have a mean circularity of 0.86± 0.03 (*n*=17; t-test: P<0.0001). Error bars show plus/minus one standard deviation. **(E, F)** *fgf3* expression in wild type and *meis1* morphant embryos at 16.5 hpf. The r4 domain of *fgf3* expression is reduced in *meis1* morphants. **(G, H)** Assay for hindbrain domains of Fgf-signaling using wild type and *meis1* morphant *Tg[dusp6:d2eGFP]* embryos. Compared to wild type, *meis1* morphants have normal domains of Fgf signaling at 16.5 hpf. Views in (A, B, E, F) are dorsal with anterior to the left, while (G, H) are shown in lateral view. Abbreviations: mhb – midbrain-hindbrian boundary; r – rhombomere.

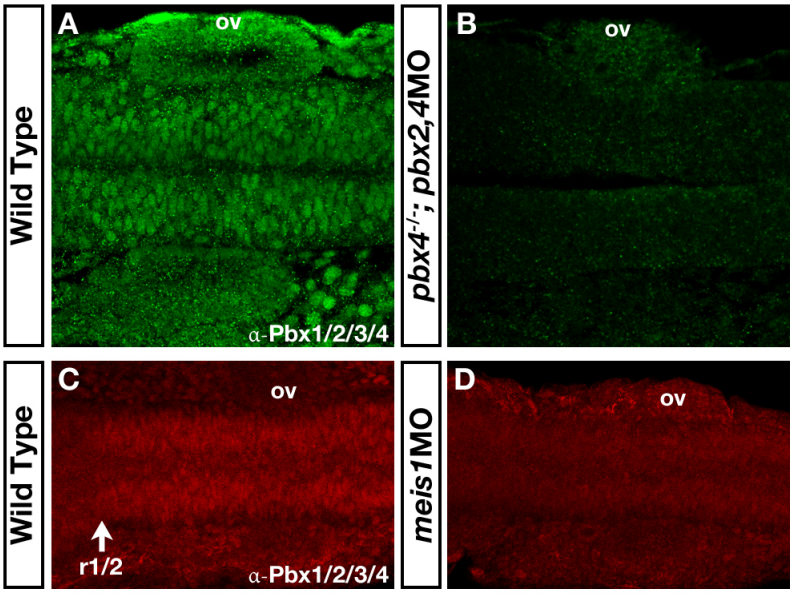

Figure 3-14. Meis1 knockdown causes a decrease in Pbx protein levels. **(A, B)** Immunostains using a polyclonal antibody raised against human PBX1/2/3/4. This antibody recognizes a nuclear-enriched protein in wild type embryos, and specific signal is gone in Pbx-depleted embryos at 19 hpf. **(C, D)** Immunostains for Pbx proteins in wild type and *meis1* morphant embryos. *meis1* morphants have lower levels of Pbx proteins than wild type. All views are dorsal with anterior to the left. A and B are shown at 63X magnification, while C and D are at 20X. Abbreviations: ov – otic vesicle.

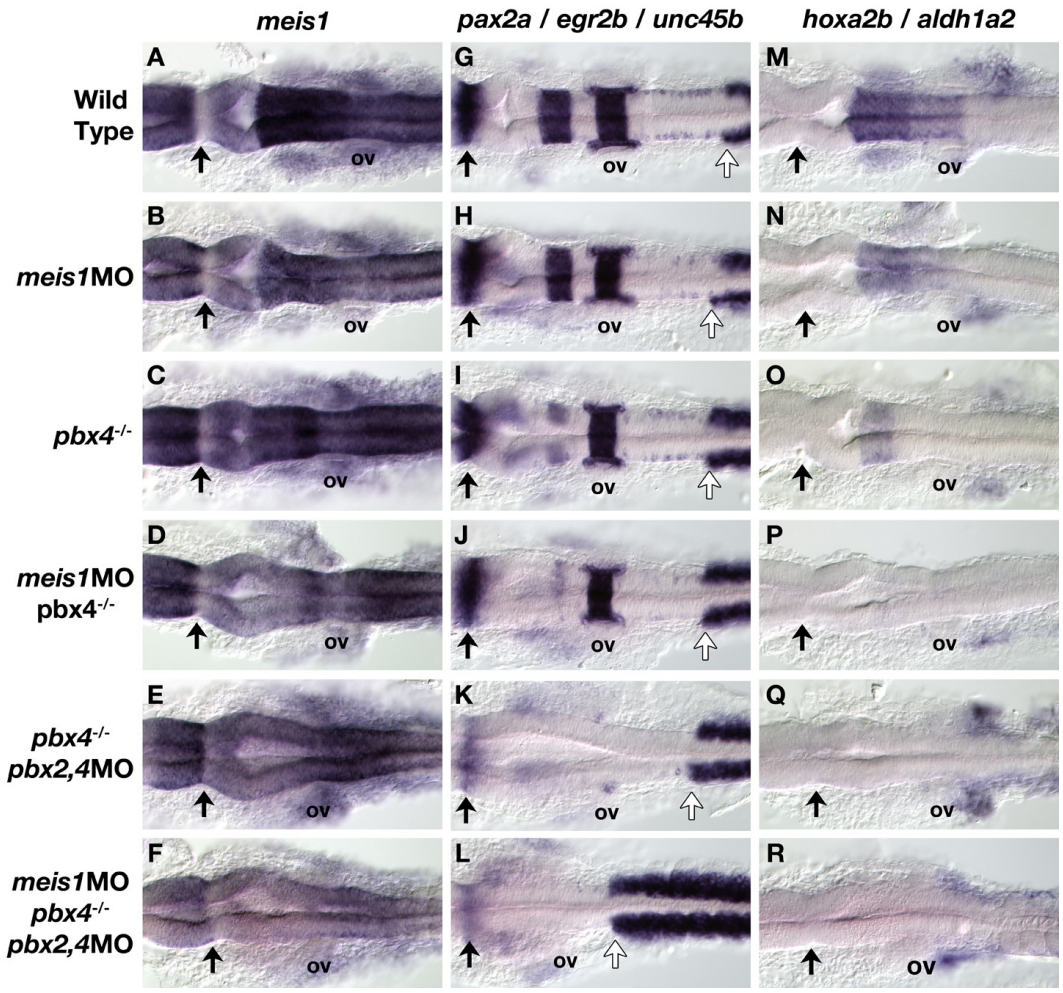

Figure 3-15. Genetic interaction between *meis1* and *pbx* genes. **(A-F)** The expression of *meis1* in wild type, *meis1*MO, *pbx4*$^{-/-}$, *meis1*MO; *pbx4*$^{-/-}$, Pbx-depleted, and *meis1*MO; Pbx-depleted embryos at 19 hpf. Black arrows indication the MHB. **(G, L)** The expression of *pax2a* (MHB, ov), *egr2b* (r3, r5), and *unc45b* (somites) in the same embryo genotypes as (A-F). Black arrows indicate the MHB, while white arrows indicate the position of the anterior-most somite. **(M-R)** The expression of *hoxa2b* (r2-5) and *aldh1a2* (lateral mesoderm) in the same embryo genotypes as (A-F). All views are dorsal with anterior to the left. Abbreviations: ov – otic vesicle.

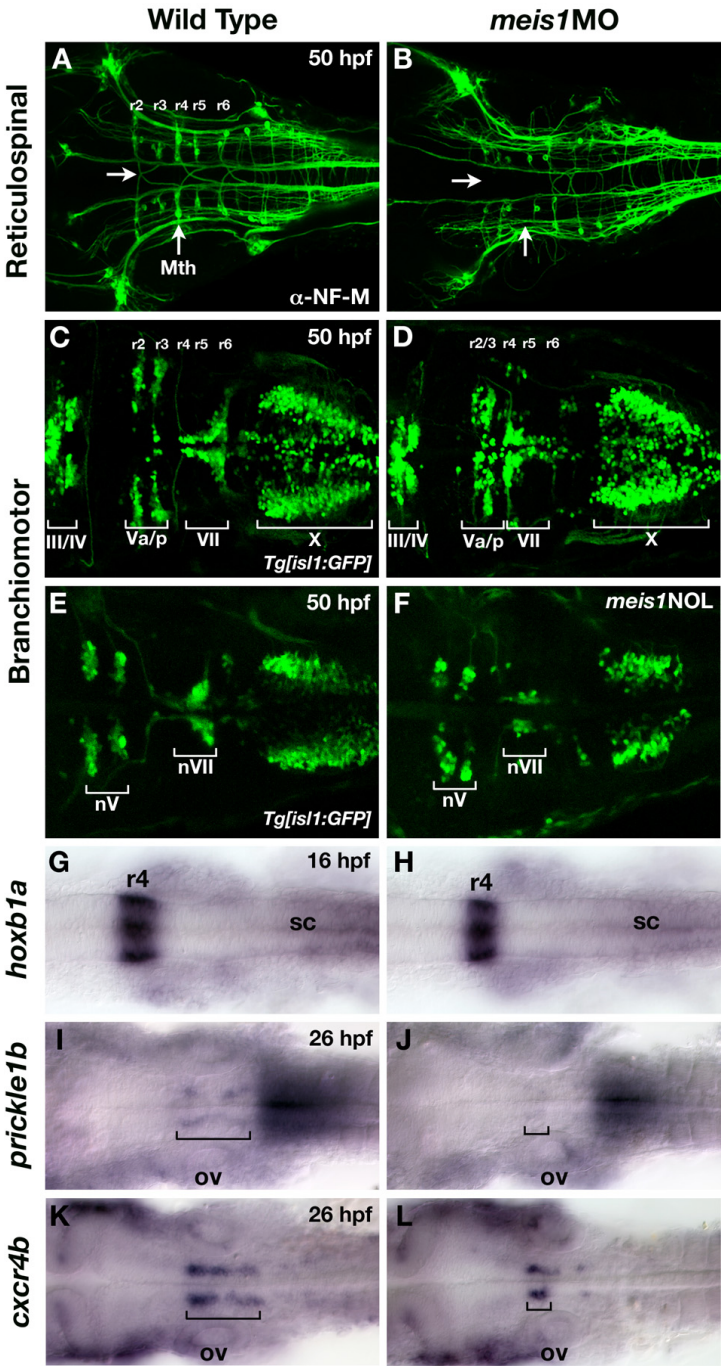

Figure 3-16. *meis1* plays a role in branchiomotor and reticulospinal neuron development. **(A, B)** Reticulospinal neurons (RN) in the hindbrain of wild type and *meis1* morphant embryos at 50 hpf, as detected using the rmo44 α-neurofilament-medium antibody. The anterior RNs of Meis1-depleted embryos are disorganized and the large Mauthner neuron in r4 is frequently missing. White arrow indicates the position at which the RoL2 axons should project

contralaterally. **(C-F)** Cranial motor neurons in wild type and *meis1* morphant embryos at 50 hpf, as visualized using the *Tg[isl1:GFP]* line of zebrafish. The nV cell bodies in r2 and r3 are disorganized in *meis1* morphants and the facial motor neurons (FMN) of the VII nerve fail to completely migrate from r4 to r6. Embryos injected with the ATG-targeted MO are shown in (D), while the non-overlapping (*meis1*NOL) translation blocking morphant phenotype is shown in (F). White brackets and labels indicate the identity of the cranial motor neurons labeled by the *isl1:GFP* transgene. **(G-L)** mRNA in situ hybridizations for *hoxb1a*, *pk1b*, and *cxcr4b* in wild type and *meis1* morphant embryos. **(G, H)** Compared to wild type, *hoxb1a* expression in r4 is unaffected in *meis1* morphants at 16.5 hpf. **(I, J)** The expression of *prickle1b* (*pk1b*) is reduced in the facial motor meurons of Meis1-depleted embryos, while the expression of *cxcr4b* is unaffected **(K, L)**. Black brackets indicate the position of the FMNs. All views are dorsal with anterior to the left. Abbreviations: Mth – Mauthner cell; r – rhombomere; sc – spinal cord.

3.5 References

Abu-Shaar, M., Mann, R. S., 1998. Generation of multiple antagonistic domains along the proximodistal axis during Drosophila leg development. Development. 125**,** 3821-30.

Abu-Shaar, M., Ryoo, H. D., Mann, R. S., 1999. Control of the nuclear localization of Extradenticle by competing nuclear import and export signals. Genes Dev. 13**,** 935-45.

Alexander, T., Nolte, C., Krumlauf, R., 2009. Hox genes and segmentation of the hindbrain and axial skeleton. Annu Rev Cell Dev Biol. 25**,** 431-56.

Berthelsen, J., Kilstrup-Nielsen, C., Blasi, F., Mavilio, F., Zappavigna, V., 1999. The subcellular localization of PBX1 and EXD proteins depends on nuclear import and export signals and is modulated by association with PREP1 and HTH. Genes Dev. 13**,** 946-53.

Chandrasekhar, A., 2004. Turning heads: development of vertebrate branchiomotor neurons. Dev Dyn. 229**,** 143-61.

Chandrasekhar, A., Moens, C. B., Warren, J. T., Jr., Kimmel, C. B., Kuwada, J. Y., 1997. Development of branchiomotor neurons in zebrafish. Development. 124**,** 2633-44.

Chang, C. P., Jacobs, Y., Nakamura, T., Jenkins, N. A., Copeland, N. G., Cleary, M. L., 1997. Meis proteins are major in vivo DNA binding partners for wild-type but not chimeric Pbx proteins. Mol Cell Biol. 17**,** 5679-87.

Choe, S. K., Vlachakis, N., Sagerstrom, C. G., 2002. Meis family proteins are required for hindbrain development in the zebrafish. Development. 129**,** 585-95.

Cooke, J. E., Kemp, H. A., Moens, C. B., 2005. EphA4 is required for cell adhesion and rhombomere-boundary formation in the zebrafish. Curr Biol. 15**,** 536-42.

Cooper, K. L., Leisenring, W. M., Moens, C. B., 2003. Autonomous and nonautonomous functions for Hox/Pbx in branchiomotor neuron development. Dev Biol. 253**,** 200-13.

Cubedo, N., Cerdan, E., Sapede, D., Rossel, M., 2009. CXCR4 and CXCR7 cooperate during tangential migration of facial motoneurons. Mol Cell Neurosci. 40**,** 474-84.

Deflorian, G., Tiso, N., Ferretti, E., Meyer, D., Blasi, F., Bortolussi, M., Argenton, F., 2004. Prep1.1 has essential genetic functions in hindbrain development and cranial neural crest cell differentiation. Development. 131**,** 613-27.

Dibner, C., Elias, S., Frank, D., 2001. XMeis3 protein activity is required for proper hindbrain patterning in Xenopus laevis embryos. Development. 128**,** 3415-26.

Eaton, R. C., Lee, R. K., Foreman, M. B., 2001. The Mauthner cell and other identified neurons of the brainstem escape network of fish. Prog Neurobiol. 63**,** 467-85.

Ferretti, E., Villaescusa, J. C., Di Rosa, P., Fernandez-Diaz, L. C., Longobardi, E., Mazzieri, R., Miccio, A., Micali, N., Selleri, L., Ferrari, G., Blasi, F., 2006. Hypomorphic mutation of the TALE gene Prep1 (pKnox1) causes a major reduction of Pbx and Meis proteins and a pleiotropic embryonic phenotype. Mol Cell Biol. 26**,** 5650-62.

Gavalas, A., Davenne, M., Lumsden, A., Chambon, P., Rijli, F. M., 1997. Role of Hoxa-2 in axon pathfinding and rostral hindbrain patterning. Development. 124**,** 3693-702.

Guthrie, S., 2007. Patterning and axon guidance of cranial motor neurons. Nat Rev Neurosci. 8**,** 859-71.

Hauptmann, G., Belting, H. G., Wolke, U., Lunde, K., Soll, I., Abdelilah-Seyfried, S., Prince, V., Driever, W., 2002. spiel ohne grenzen/pou2 is required for zebrafish hindbrain segmentation. Development. 129**,** 1645-55.

Higashijima, S., Hotta, Y., Okamoto, H., 2000. Visualization of cranial motor neurons in live transgenic zebrafish expressing green fluorescent protein under the control of the islet-1 promoter/enhancer. J Neurosci. 20**,** 206-18.

Jaw, T. J., You, L. R., Knoepfler, P. S., Yao, L. C., Pai, C. Y., Tang, C. Y., Chang, L. P., Berthelsen, J., Blasi, F., Kamps, M. P., Sun, Y. H., 2000. Direct interaction of two homeoproteins, homothorax and extradenticle, is essential for EXD nuclear localization and function. Mech Dev. 91**,** 279-91.

Jozefowicz, C., McClintock, J., Prince, V., 2003. The fates of zebrafish Hox gene duplicates. J Struct Funct Genomics. 3**,** 185-94.

Kimmel, C. B., Metcalfe, W. K., Schabtach, E., 1985. T reticular interneurons: a class of serially repeating cells in the zebrafish hindbrain. J Comp Neurol. 233**,** 365-76.

Knight, R. D., Schilling, T. F., 2006. Cranial neural crest and development of the head skeleton. Adv Exp Med Biol. 589**,** 120-33.

Knoepfler, P. S., Calvo, K. R., Chen, H., Antonarakis, S. E., Kamps, M. P., 1997. Meis1 and pKnox1 bind DNA cooperatively with Pbx1 utilizing an interaction surface disrupted in oncoprotein E2a-Pbx1. Proc Natl Acad Sci U S A. 94**,** 14553-8.

Korn, H., Faber, D. S., 2005. The Mauthner cell half a century later: a neurobiological model for decision-making? Neuron. 47**,** 13-28.

Kurant, E., Pai, C. Y., Sharf, R., Halachmi, N., Sun, Y. H., Salzberg, A., 1998. Dorsotonals/homothorax, the Drosophila homologue of meis1, interacts with extradenticle in patterning of the embryonic PNS. Development. 125**,** 1037-48.

Lampe, X., Picard, J. J., Rezsohazy, R., 2004. The Hoxa2 enhancer 2 contains a critical Hoxa2 responsive regulatory element. Biochem Biophys Res Commun. 316**,** 898-902.

Laue, K., Janicke, M., Plaster, N., Sonntag, C., Hammerschmidt, M., 2008. Restriction of retinoic acid activity by Cyp26b1 is required for proper timing and patterning of osteogenesis during zebrafish development. Development. 135**,** 3775-87.

Lumsden, A., Keynes, R., 1989. Segmental patterns of neuronal development in the chick hindbrain. Nature. 337**,** 424-8.

Maeda, R., Ishimura, A., Mood, K., Park, E. K., Buchberg, A. M., Daar, I. O., 2002. Xpbx1b and Xmeis1b play a collaborative role in hindbrain and neural crest gene expression in Xenopus embryos. Proc Natl Acad Sci U S A. 99**,** 5448-53.

Mapp, O. M., Wanner, S. J., Rohrschneider, M. R., Prince, V. E., 2010. Prickle1b mediates interpretation of migratory cues during zebrafish facial branchiomotor neuron migration. Dev Dyn. 239**,** 1596-608.

McClintock, J. M., Kheirbek, M. A., Prince, V. E., 2002. Knockdown of duplicated zebrafish hoxb1 genes reveals distinct roles in hindbrain patterning and a novel mechanism of duplicate gene retention. Development. 129**,** 2339-54.

Metcalfe, W. K., Mendelson, B., Kimmel, C. B., 1986. Segmental homologies among reticulospinal neurons in the hindbrain of the zebrafish larva. J Comp Neurol. 251**,** 147-59.

Moens, C. B., Prince, V. E., 2002. Constructing the hindbrain: insights from the zebrafish. Dev Dyn. 224**,** 1-17.

Molina, G., Watkins, S., Tsang, M., 2007. Generation of FGF reporter transgenic zebrafish and their utility in chemical screens. BMC Developmental Biology. 7**,** 62.

Nasevicius, A., Ekker, S. C., 2000. Effective targeted gene 'knockdown' in zebrafish. Nat Genet. 26**,** 216-20.

Phillips, B. T., Bolding, K., Riley, B. B., 2001. Zebrafish fgf3 and fgf8 encode redundant functions required for otic placode induction. Dev Biol. 235**,** 351-65.

Pillay, L. M., Forrester, A. M., Erickson, T., Berman, J. N., Waskiewicz, A. J., 2010. The Hox cofactors Meis1 and Pbx act upstream of gata1 to regulate primitive hematopoiesis. Dev Biol. 340**,** 306-17.

Piotrowski, T., Schilling, T. F., Brand, M., Jiang, Y. J., Heisenberg, C. P., Beuchle, D., Grandel, H., van Eeden, F. J., Furutani-Seiki, M., Granato, M., Haffter, P., Hammerschmidt, M., Kane, D. A., Kelsh, R. N., Mullins, M. C., Odenthal, J., Warga, R. M., Nusslein-Volhard, C., 1996. Jaw and

branchial arch mutants in zebrafish II: anterior arches and cartilage differentiation. Development. 123**,** 345-56.

Popperl, H., Rikhof, H., Chang, H., Haffter, P., Kimmel, C. B., Moens, C. B., 2000. lazarus is a novel pbx gene that globally mediates hox gene function in zebrafish. Mol Cell. 6**,** 255-67.

Prince, V. E., Moens, C. B., Kimmel, C. B., Ho, R. K., 1998. Zebrafish hox genes: expression in the hindbrain region of wild-type and mutants of the segmentation gene, valentino. Development. 125**,** 393-406.

Reim, G., Brand, M., 2002. Spiel-ohne-grenzen/pou2 mediates regional competence to respond to Fgf8 during zebrafish early neural development. Development. 129**,** 917-33.

Rhinn, M., Lun, K., Luz, M., Werner, M., Brand, M., 2005. Positioning of the midbrain-hindbrain boundary organizer through global posteriorization of the neuroectoderm mediated by Wnt8 signaling. Development. 132**,** 1261-72.

Rieckhof, G. E., Casares, F., Ryoo, H. D., Abu-Shaar, M., Mann, R. S., 1997. Nuclear translocation of extradenticle requires homothorax, which encodes an extradenticle-related homeodomain protein. Cell. 91**,** 171-83.

Rohrschneider, M. R., Elsen, G. E., Prince, V. E., 2007. Zebrafish Hoxb1a regulates multiple downstream genes including prickle1b. Dev Biol. 309**,** 358-72.

Stevens, K. E., Mann, R. S., 2007. A balance between two nuclear localization sequences and a nuclear export sequence governs extradenticle subcellular localization. Genetics. 175**,** 1625-36.

Summerton, J., 1999. Morpholino antisense oligomers: the case for an RNase H-independent structural type. Biochim Biophys Acta. 1489**,** 141-58.

Trainor, P. A., Krumlauf, R., 2001. Hox genes, neural crest cells and branchial arch patterning. Curr Opin Cell Biol. 13**,** 698-705.

Vlachakis, N., Choe, S. K., Sagerstrom, C. G., 2001. Meis3 synergizes with Pbx4 and Hoxb1b in promoting hindbrain fates in the zebrafish. Development. 128**,** 1299-312.

Vlachakis, N., Ellstrom, D. R., Sagerstrom, C. G., 2000. A novel pbx family member expressed during early zebrafish embryogenesis forms trimeric complexes with Meis3 and Hoxb1b. Dev Dyn. 217**,** 109-19.

Waskiewicz, A. J., Rikhof, H. A., Hernandez, R. E., Moens, C. B., 2001. Zebrafish Meis functions to stabilize Pbx proteins and regulate hindbrain patterning. Development. 128**,** 4139-51.

Waskiewicz, A. J., Rikhof, H. A., Moens, C. B., 2002. Eliminating zebrafish pbx proteins reveals a hindbrain ground state. Dev Cell. 3**,** 723-33.

Chapter Four - Zebrafish *teashirt zinc finger homeobox 3b* plays a role in hindbrain patterning by regulating Hox function.

A version of this chapter has been submitted for publication. Erickson, T., Pillay, L.M., and Waskiewicz, A.J. 2010. Genesis.

4.1 Introduction

During vertebrate brain development, the hindbrain is transiently segmented into lineage-restricted compartments called rhombomeres (reviewed in Fraser et al., 1990; Lumsden and Keynes, 1989; Moens and Prince, 2002; von Baer, 1828). The specification of each rhombomere's identity is homologous to that of Drosophila anterior-posterior embryonic segmentation (reviewed in Pearson et al., 2005), with both developmental processes requiring transcriptional regulation by Hox proteins complexed with their TALE-class homeodomain partners Pbx (Drosophila Extradenticle) and Meinox (Meis/Pknox; Drosophila Homothorax) (Chan et al., 1994; reviewed in Mann and Chan, 1996; reviewed in Moens and Selleri, 2006; van Dijk and Murre, 1994). The anteriorly-expressed Hox paralog groups (PG) 1-4 exhibit very clear homeotic properties in segmental hindbrain patterning, as a gain or loss of Hox function can lead to transformations of rhombomere identity (Bell *et al.*, 1999; Gavalas *et al.*, 1997; McClintock *et al.*, 2001; Studer *et al.*, 1996; Vlachakis *et al.*, 2001; Zhang *et al.*, 1994). Perturbations in Pbx or Meis function also result in profound hindbrain segmentation defects (Dibner *et al.*, 2001; Popperl *et al.*, 2000; Waskiewicz *et al.*, 2001). In zebrafish embryos lacking both Pbx2 and Pbx4 function, the hindbrain loses its segmental character and adopts the fate of the most anterior rhombomere r1, whose specification does not depend on Hox function (Waskiewicz *et al.*, 2002). Similar results are achieved through a triple knockdown of Hox1 paralogues in Xenopus (McNulty *et al.*, 2005). These data suggest that Hox, Pbx and Meis proteins act as homeotic factors during hindbrain segmentation and that, in the absence of Hox function, the entire hindbrain adopts a Hox-independent r1-like fate.

In Drosophila, the zinc-finger protein Teashirt has also been identified as a homeotic transcription factor. Loss-of-function analyses reveal that Tsh can promote trunk identity and repress head characteristics through both Hox-dependent and Hox-independent mechanisms (Fasano *et al.*, 1991; Roder *et al.*, 1992). Complementing the loss of function experiments, overexpression studies of

hox genes Antp, Ubx and Abd in a *tsh*-/- background reveal less severe head-to-trunk transformations than when Tsh is functional (Alexandre *et al.*, 1996; Andrew *et al.*, 1994; Coiffier *et al.*, 2008). Conversely, Tsh overexpression before embryonic stage 11 results in a partial head-to-trunk homeotic transformation (de Zulueta *et al.*, 1994). Ectopic *tsh* is less effective at driving a head-to-trunk transformation in embryos lacking Scr, Antp and BX-C function, although it can partially rescue the trunk-to-head transformation observed in posterior Hox compound-mutant embryos (de Zulueta *et al.*, 1994). Taken together, these studies suggest that Tsh defines a trunk ground state upon which posterior Hox proteins can act to specify the identity of the thoracic segments, and that Tsh can act independently of Hox proteins to promote trunk and repress head identity.

One of the ways in which Tsh promotes trunk identity is by repressing anterior *hox* gene expression in the trunk. *tsh* mutants express transcripts for the anterior Hox 1, 2 and 4 paralogues *labial* (*lab*), *proboscipedia* (*pb*), and *deformed* (*dfd*) in ectopic posterior positions (Roder *et al.*, 1992; Rusch and Kaufman, 2000). Tsh can also regulate the activity of anterior Hox proteins independently of their transcription. For example, the trunk-to-head transformation induced by ectopic expression of Dfd is much more effective in the absence of Tsh function (Robertson *et al.*, 2004). These data indicate that Tsh can antagonize anterior *hox* genes by repressing both their transcription and protein function. Overall, Tsh participates in a complex transcription factor network that establishes functional domains for Hox proteins, thereby regionalizing the fly embryo along the anterior-posterior axis.

Vertebrate *teashirt*-related genes are co-expressed with *hox*, *pbx* and *meis* genes throughout the developing nervous system (Koebernick *et al.*, 2006; Santos *et al.*, 2010; Wang *et al.*, 2007), raising the possibility that vertebrate Hox function is subject to regulation by Teashirt proteins as well. The ability of mouse Tsh homologues to substitute for the endogenous fly *tsh* gene (Manfroid *et al.*, 2004), and studies in Xenopus and mice showing that vertebrate *teashirt*-related genes perform important functions in hindbrain development (Caubit *et al.*, 2010; Koebernick *et al.*, 2006) support this idea. However, the possibility that vertebrate

teashirt genes might regulate Hox function during hindbrain development has not been directly investigated.

In this chapter, I describe a role for zebrafish *teashirt zinc finger homeobox 3b* (*tshz3b*) in hindbrain development. *tshz3b* is expressed in rhombomeres 4-7, and is regulated by a combination of Hox-Pbx-Meis transcriptional input and retinoic acid signaling. Morpholino-mediated knockdown of Tshz3b causes defects in hindbrain morphology and disorganization of the cranial and reticulospinal neurons. Overexpression of *tshz3b* causes a loss of hindbrain segmentation similar to that observed in Hox or Pbx-depleted embryos. Consistent with this loss of segmentation, *tshz3b* overexpression perturbs the specification the hindbrain cranial motorneurons and reticulospinal tract. This effect of *tshz3b* overexpression is likely achieved by antagonizing Hox function, as *tshz3b* overexpression synergizes with the *pbx4*$^{-/-}$ phenotype, and can block the r2-to-r4 homeotic transformation caused by *hoxb1b* overexpression. Lastly, structure-function assays show that Tshz3b likely functions as a transcriptional repressor, and that the overexpression phenotype does not require the vertebrate-specific C-terminal zinc fingers or homeodomain. However, in contrast to the ability of mouse *tshz* genes to functionally rescue Drosophila *tsh* mutants, overexpression of Drosophila *tsh* in zebrafish does not produce the same hindbrain patterning defects as *tshz3b* overexpression. In summary, this work suggests that *tshz3b* contributes to hindbrain patterning by modulating Hox function. Furthermore, it supports the idea that the regulation of Hox function is an evolutionarily conserved function of Teashirt proteins, although some of the mechanisms through which this occurs may differ between flies and vertebrates.

4.2 Results

4.2.1 Embryonic expression of four zebrafish *teashirt*-related genes: *tshz1*, *tshz2*, *tshz3a* and *tshz3b*

To find out which *tshz* genes were expressed in the hindbrain during segmentation, we performed mRNA in situ hybridizations for all four zebrafish *tsh*-related genes. *tshz3b* expression is first detectable is first detectable by in situ hybridization between 9-11 hpf when it is enriched in the presumptive forebrain, in the hindbrain posterior to r3, and in the trunk midline (Figure 4-1A, L). Over the first two days of development, this pattern becomes refined where the early broad forebrain and hindbrain expression domains resolve to specific cells in those regions (Figure 4-1B-H, M, N). Additionally, *tshz3b* is expressed in the developing pectoral fins (arrows in Figure 4-1I-K). We also raised a polyclonal antibody against Tshz3b, and in whole mount immunostains on 20 hpf embryos, it recognizes a nuclear-enriched protein in a pattern that is consistent with *tshz3b* mRNA expression at that stage (Figure 4-1O, P). Taken together, *tshz3b* is expressed up to the r3/4 boundary during the initial stages of hindbrain segmentation, consistent with what has been found in mouse, chick and frog (Caubit *et al.*, 2010; Manfroid *et al.*, 2006; Onai *et al.*, 2007; Santos *et al.*, 2010).

The other zebrafish *teashirt*-related genes also have tissue-specific embryonic expression patterns. Between 16-26 hpf, *tshz1* is expressed in the eyes and forebrain at low levels, and at high levels in the posterior hindbrain and spinal cord up to the r6/7 boundary (Figure 4-1Q-S) (Wang *et al.*, 2007). *tshz2* expression is barely detectable by in situ hybridization during early development, but by 50 hpf it is broadly expressed in the head with enriched expression in the hindbrain and anterior spinal cord (Figure 4-1T-V) (Santos *et al.*, 2010). Lastly, *tshz3a* is the paralogue of *tshz3b* (Santos *et al.*, 2010), and it also exhibits a rhombomere-restricted expression pattern during hindbrain segmentation. At 12 hpf, *tshz3a* is expressed in r2 and r4, and although it becomes expressed throughout r2-6 by 20 hpf, its expression remains enriched in r4 (Figure 4-1W-Y). As a whole, the zebrafish *tshz* genes have unique, but partially overlapping

expression patterns in the neural tube, from the eyes and forebrain, to the midbrain, hindbrain and spinal cord.

4.2.2 *tshz3b* hindbrain expression is regulated by Hox / TALE-class homeodomain transcription factors and retinoic acid signaling

In Drosophila, *tsh* expression is a directly activated by Hox proteins and their TALE-class partners Exd (vertebrate Pbx) and Hth (vertebrate Meis / Pknox) (Mathies *et al.*, 1994; McCormick *et al.*, 1995; Merabet *et al.*, 2007; Rauskolb and Wieschaus, 1994; Roder *et al.*, 1992). In the zebrafish hindbrain at 10.5 hpf, *tshz3b* is co-expressed with *hox* genes, including *hoxb1a, hoxa2*, and *hoxb2*, suggesting that *tshz3b* may be regulated in a Hox-dependent fashion. To test this, we examined *tshz3b* expression in embryos lacking the Hox cofactors Pbx4 and Meis1. In 20 hpf *pbx4*$^{-/-}$ / *lazarus* mutants, *tshz3b* expression is decreased in the midbrain and hindbrain (Figure 4-2A, B). Similarly, the hindbrain expression of *tshz3b* is downregulated in 16 hpf *meis1* morphants (Figure 4-2C, D). These data suggest that *tshz3b* is regulated in a Hox-dependent manner. To test this more directly, we knocked down Hoxb1 function using a combination of *hoxb1a* and *hoxb1b* translation-blocking morpholinos (McClintock *et al.*, 2002). In 10.5 hpf *hoxb1* morphants, *tshz3b* expression is not initiated correctly (*n*=8/8; Figure 4-2E, F). At 20 hpf, *hoxb1* morphants lack *tshz3b* expression specifically in the r4 region, but expression in r5-7 and the spinal cord is normal (*n*=18/18; Figure 4-2G, H). To see if ectopic *hoxb1* can drive *tshz3b* expression, we injected one-cell zebrafish embryos with mRNA coding for Hoxb1b fused to an N-terminal HA tag (Vlachakis *et al.*, 2000). Overexpressed *hoxb1b* can transform r2 to an r4-like identity, as shown by the ectopic expression of *hoxb1a* in the r2 region (compare the red stain in Figure 4-2I, J) (McClintock *et al.*, 2001). Consistent with the results of the *hoxb1* knockdown experiment, *hoxb1b* overexpression drives ectopic *tshz3b* expression in the r4-like region (*n*=38/38; blue stain in Figure 4-2J). These data suggest that *hoxb1* genes play a critical role in regulating the r4 domain of *tshz3b* expression.

Retinoic acid (RA) is a signaling molecule that is essential for anterior-posterior hindbrain patterning. Pharmacological inhibition of RA synthesis causes a loss of r5 and r6 hindbrain identity, while exogenous RA can transform the entire anterior neural tube into posterior hindbrain tissue (Dupe and Lumsden, 2001; reviewed in Gavalas, 2002; reviewed in Gavalas and Krumlauf, 2000; Hernandez et al., 2007; Maves and Kimmel, 2005). To see if RA contributes to *tshz3b* expression, we treated embryos with 10 and 100 nM solutions of RA from 3 hpf until 15 hpf and assayed for *tshz3b* expression by in situ hybridization. Embryos treated with 10 nM RA show an increase in *tshz3b* expression, especially in the dorsal neural tube (*n*=39/39; Figure 4-2K, L). Embryos treated with 100 nM RA exhibit severe morphological defects as well as a dramatic upregulation of *tshz3b* expression (*n*=40/40; Figure 4-2M). To determine what effect the inhibition of RA signaling has on *tshz3b* expression, we treated embryos with 10 μM diethylaminobenzaldehyde (DEAB), a competitive inhibitor of the aldehyde dehydrogenase (Aldh / Raldh) enzymes that synthesize retinoic acid. DEAB-treated embryos lack r5 and r6 identity, and r4 is expanded posteriorly (Figure 4-2N, O) (Maves and Kimmel, 2005). Likewise, the r5/6 domain of *tshz3b* expression is lost in DEAB-treated embryos, and the r4 domain of *tshz3b* is expanded posteriorly to the spinal cord, where *tshz3b* expression is unaffected (*n*=31/31; Figure 4-2O). Taken together, *tshz3b* expression is positively regulated by RA signaling. Given that *tshz3b* is still expressed in r4 and the spinal cord following DEAB-treatment, it is likely that the r5/6 domain of *tshz3b* expression is specifically RA-responsive.

4.2.3 *tshz3b* gene structure and protein domains

To determine the full gene structure and coding sequence of zebrafish *tshz3b*, we performed 5' RACE (rapid amplification of cDNA ends), followed by cloning of the full-length 3444 bp *tshz3b* ORF. In this way, we established that the zebrafish *tshz3b* gene (GenBank HQ116415) is organized as a two exon gene with a short first exon and a large second exon interrupted by a large 48,440 bp intron bounded by a canonical GT-AG splice junction sequence (Figure 4-3A).

This is similar to the mouse *Tshz3* gene (NM_172298), which also has a two exon structure. Determining the 5' structure of the *tshz3b* gene allowed us to design morpholino oligomers designed to block Tshz3b protein production. Morpholino 1 targets the ATG start site, while morpholino 2 is designed to inhibit mRNA splicing by blocking the splice donor site (Figure 4-3B). In summary, the genomic organization of the *tshz3* gene is conserved between mice and zebrafish.

The putative Tshz3b protein produced from this cDNA is 1147 aa in length with 70.8% identity and 81.2% similarity to the 1081 aa mouse Tshz3 protein. As with other vertebrate Teashirt-related proteins (Koebernick et al., 2006; Onai et al., 2007), the putative Tshz3b protein contains three widely-spaced C2H2 zinc fingers in the N-terminal half of the protein, a CtBP-interaction motif just N-terminal to an atypical homeodomain, followed by two more C2H2 zinc fingers at the C-terminal end (Figure 4-3C). The CtBP-interaction motif (PIDLT) mediates binding to the transcriptional co-repressor C-terminal Binding Protein (CtBP), thereby conferring transcriptional repressor activity to both vertebrate and invertebrate Tsh proteins (Manfroid et al., 2004; Saller et al., 2002). The homeodomain is unique to vertebrate Teashirt-related proteins, and its function is not known. Besides having an 11 aa insertion near the middle of the HD (grey letters), overall the Tshz homeodomain has very low amino acid identity with canonical homeodomains, as revealed through an alignment with the Conserved Domains Database consensus homeodomain sequence smart:00389 (Figure 4-3D) (Marchler-Bauer et al., 2009). In particular, the putative third helix of the Tshz3b HD lacks many of the charged and polar residues that are typically required to contact DNA. However, the Tshz3b HD does possess an asparagine (N) residue (black arrow Figure 4-3D) in this region that is critical for DNA binding in other homeodomains (reviewed in Gehring et al., 1994), perhaps suggesting that the *Tshz* HD retains some DNA-binding functionality. Of these *Tshz* domains, only the N-terminal zinc fingers and the CtBP-interaction motif are conserved with the fly Tsh protein (Caubit et al., 2000; Manfroid et al., 2004). However, the vertebrate CtBP-interaction motif is C-terminal to the conserved zinc fingers, while it is located at the N-terminus in the fly protein. Furthermore, even the zinc

finger region of the two proteins share very limited conservation, with only 20% acid identity and 32.8% similarity between fly Tsh and zebrafish Tshz3b (Figure 4-3E). In summary, zebrafish *tshz3b* and mouse *tshz3* genes share a similar genetic organization and protein structure, but their amino acid homology to the fly Tsh protein is very limited.

4.2.4 Knockdown of Tshz3b causes defects in hindbrain morphology

To test whether *tshz3b* plays a role in hindbrain development, I used two morpholinos (MO) to block Tshz3b protein production (Figure 4-3B). The ATG-targeted MO is designed to block protein translation while the second MO is targeted to the exon1-intron1 boundary and should interfere with mRNA splicing. Both morpholinos produce a similar defect in hindbrain morphology (Figure 4-4A-C). In 20 hpf wild type embryos, *pax2a* marks the MHB and the otic vesicle, *egr2b* marks r3 and r5 in the hindbrain, while *unc45b* marks the somites. In *tshz3b* morphants, the MHB and somites appear normal, but the distance between those domains is reduced. As well, the rhombomeres are misshapen, with near fusion between r3 and r5 in some cases. Looking at the expression of *eng2a* and *hoxb1a* at the 10 hpf stage, there is no difference between wild type embryos and *tshz3b*MO-SB morphants (Figure 4-4D, E). Thus, the defects in 20 hpf *tshz3b* morphants must arise during the ensuing period when the hindbrain coalesces and rhombomere boundaries are organized.

To see if these morphological defects persist into later development, I examined live wild type and *tshz3b*MO-ATG morphants at 48 hpf. Compared to wild type embryos, *tshz3b* morphants exhibit severe morphological defects in both the midbrain and hindbrain regions (Figure 4-5A, B). These defects may also have a negative effect on neuronal organization in the hindbrain, as both the branchiomotor and reticulospinal neurons are disorganized in Tshz3b-depleted embryos. In particular, the trigeminal (V) neurons are not neatly compartmentalized into r2 and r3, and facial (VII) neurons partially fail to migrate posteriorly (Figure 4-5C, D). With regard to the reticulospinal neurons, a single Mauthner neuron is occasionally missing in *tshz3b* morphants, and the RN axon

bundles are somewhat defasciculated (Figure 4-5E, F). Consistent with the disorganization of the branchiomotor and reiculospinal neurons, labeling the commissural hindbrain axons with an antibody again the DM-GRASP cell adhesion molecule reveals another level of neuronal disorganization in *tshz3b* morphants (Figure 4-5G, H). In summary, *tshz3b* morphants have normal segmental identity in the hindbrain, but display morphological abnormalities that may contribute to the organizational defects in the branchiomotor, reticulospinal and commissural neurons.

4.2.5 *tshz3b* overexpression produces Hox loss-of-function hindbrain patterning defects

In flies, Tsh promotes trunk identity, in part, by antagonizing the expression and function of anterior Hox PG1, 2, and 4 proteins that specify head segments (Robertson *et al.*, 2004; Roder *et al.*, 1992; Rusch and Kaufman, 2000). Moreover, Tsh can repress anterior *hox* expression in a posterior Hox-independent fashion, as Tsh overexpression has no effect on posterior *hox* gene expression (de Zulueta *et al.*, 1994). To test the hypothesis that *tshz3b* antagonizes vertebrate Hox PG1-4-dependent hindbrain patterning, we assayed for the expression of hindbrain marker genes at 10 and 20 hpf in embryos injected with *tshz3b* mRNA. The α-Tshz3b polyclonal antibody is able to recognize a single band in lysates made from 4 hpf *tshz3b*-injected embryos that is not present in lysates made from equivalently staged uninjected embryos (Figure 4-6A, Lanes 1 and 2). Attempts at identifying endogenous *tshz3b* from 18 hpf embryo lysates were not successful (Figure 4-6A, Lane 3). At 10 hpf, *hoxb1a* marks the presumptive hindbrain up to r3, while *myod* is expressed in the posterior paraxial mesoderm. In *tshz3b* overexpressing embryos, *hoxb1a* expression is downregulated while *myod* expression is undisturbed (*n*=9/10; Figure 4-6B, C). Similar results are observed in 20 hpf embryos, where *tshz3b* overexpression downregulates *hoxa2b* expression in r2-5 (*n*=3/6; Figure 4-6D, E). To determine if this loss of *hox* expression results in a posterior expansion of r1 identity as in Pbx-depleted embryos (Waskiewicz *et al.*, 2002), we also examined the expression of *epha4a*,

which marks r1, r3, and r5 at 20 hpf. Consistent with the hypothesis that *tshz3b* is antagonizing *hox* function, *tshz3b* overexpression leads to an expansion of r1-like identity at the expense of more posterior rhombomere identities (Figure 4-6F, G). A similar result is observed when *tshz3b* mRNA is injected into the Fgf-responsive *dusp6:d2eGFP* transgenic line of fish (Molina *et al.*, 2007). In wild type fish, the *dusp6:d2eGFP* transgene is expressed at high levels in the cerebellum and r1, as well as in r4 and r6. Overexpression of *tshz3b* downregulates the hindbrain domains of Fgf-signaling, and expands the r1-like domain caudally (*n*=49/134; Figure 4-6H, I). Taken together, these results suggest that *tshz3b* overexpression causes a hindbrain patterning phenotype similar to that caused by a loss of Hox function.

4.2.6 The effect of *tshz3b* overexpression on the expression of *tshz1* and *tshz3a*

In flies, *teashirt* is known to positively regulate its own expression (de Zulueta *et al.*, 1994). To see if overexpression of *tshz3b* modulates the expression of other zebrafish *tshz* genes, we compared the expression of *tshz1* and *tshz3a* between wild type and *tshz3b*-injected embryos at 18 hpf. Similar to *hoxb4a* and *hoxd4a*, *tshz1* is expressed in the spinal cord up to the r6/7 boundary (Wang *et al.*, 2007), with additional expression in the caudal forebrain (Figure 4-7A). Ectopic *tshz3b* overexpression leaves *tshz1*'s forebrain and spinal cord domains intact, although the r6/7 boundary is somewhat disorganized (Figure 4-7B). This indicates that *tshz3b* does not positively regulate *tshz1* expression, and furthermore, it demonstrates that the loss of hindbrain segmental identity is not due to a rostral expansion of anterior spinal cord identity. With regard to *tshz3a*, its normal expression in the midbrain, r2 and r4 is downregulated by *tshz3b* overexpression (Figure 4-7C, D). This loss of *tshz3a* expression is also consistent with the *tshz3b* overexpression phenotype being caused by a loss of Hox function, as *pbx2,4* double morphants exhibit a similar loss of *tshz3a* expression (Figure 4-7E, F). This loss of *tshz3a* expression in Pbx-depleted embryos is similar to that observed for *tshz3b* expression (Figure 4-2A, B). In summary, *tshz3b* is not a positive regulator of *tshz1* or *tshz3a* expression, *tshz3b* overexpression does not

cause a rostral expansion of spinal cord identity, and both *tshz3a* and *tshz3b* are positively regulated by Pbx-Hox function.

4.2.7 *tshz3b* overexpression causes mispatterning of the branchiomotor and reticulospinal neurons

One of the outputs of Hox-dependent anterior-posterior hindbrain patterning is the correct positioning, identity and function of the branchiomotor and reticulospinal neurons (reviewed in Chandrasekhar, 2004; Chandrasekhar et al., 1997; Cooper et al., 2003; Ferretti et al., 2000; Gavalas et al., 1998; reviewed in Guthrie, 2007; Kimmel et al., 1985; Metcalfe et al., 1986; reviewed in Moens and Prince, 2002; Waskiewicz et al., 2001; Waskiewicz et al., 2002). To determine if ectopic Tshz3b affects the development of the hindbrain cranial branchiomotor neurons, we overexpressed *tshz3b* in *Tg[isl1:GFP]* embryos, which express GFP in the motor nuclei of the V, VII and X cranial nerves under the control of the *isl1* promoter (Higashijima *et al.*, 2000). Compared to wild type *Tg[isl1:GFP]* embryos, *tshz3b* injected embryos have mispatterned trigeminal (V) and facial (VII) cranial motorneurons, (*n*=15/49; Figure 4-8A, B). However, the oculomotor (III) and trochlear (IV) nuclei in the midbrain are unaffected by *tshz3b* overexpression. Similarly, the vagal (X) nerve in the spinal cord is also unaffected, suggesting that the effect of ectopic Tshz3b is limited to the hindbrain branchiomotor neurons. Additionally, *tshz3b* overexpression has a negative effect on reticulospinal neuron development. The ladder-like array of reticulospinal neurons is disrupted by ectopic *tshz3b*, particularly in r2-4 (*n*=5/9; Figure 4-8C, D). These phenotypes are consistent with the idea that ectopic *tshz3b* antagonizes *hox* function and that the segmental patterning defects in *tshz3b*-overexpressing embryos perturb the specification of neuronal identity in the hindbrain.

4.2.8 *tshz3b* overexpression synergizes with the *pbx4* mutant phenotype

To further explore the hypothesis that *tshz3b* antagonizes *hox* function, we looked for a synergistic interaction between *tshz3b* overexpression and a partial loss of Pbx function by injecting a suboptimal dose of *tshz3b* mRNA into the

progeny of a *pbx4*$^{+/-}$ cross. Compared to wild type embryos, *pbx4* mutants have markedly reduced, but not eliminated, *egr2b* expression in r3 (*n*=3/3, Figure 4-9A, B). 200 pg of *tshz3b* RNA alone produces only a very mild reduction on the size of r3 and r4 (*n*=5/5; Figure 4-9C). The combination of ectopic *tshz3b* and loss of *pbx4* function causes a synergistic effect where r5 *egr2b* is reduced and the r3 domain is eliminated (*n*=3/4; Figure 4-9D). These data support the idea that *tshz3b* is a negative regulator of *hox*-dependent hindbrain patterning.

4.2.9 *tshz3b* overexpression blocks the r2-to-r4 homeotic transformation caused by ectopic *hoxb1b* function

As a final way of demonstrating that *tshz3b* inhibits *hox* function, we examined the interaction between ectopically expressed *hoxb1b* and *tshz3b*. As demonstrated previously, overexpressed *hoxb1b* can transform r2 to an r4-like identity, as shown by *hoxb1a* expression (*n*=20/32; Figure 4-9E, F), while overexpressed *tshz3b* reduces *hoxb1a* expression in r4 (*n*=23/24; Figure 4-9G). When the two mRNAs are injected simultaneously, ectopic *hoxb1a* expression in r2 is never observed (*n*=47), and the r4 domain of *hoxb1a* is typically reduced (*n*= 39/47; Figure 4-9H). Thus, even when *hoxb1b* is ectopically supplied, *tshz3b* overexpression is able to block *hox* function and perturb segmental patterning of the hindbrain. This lends further support to the idea that *tshz3b* negatively regulates Hox function in the hindbrain.

4.2.10 The Tshz3b homeodomain and C-terminal zinc fingers are dispensable for its overexpression phenotype

To determine which domains of Tshz3b are required to antagonize *hox* function in vivo, we created a series of *tshz3b* deletion constructs. N-terminal zinc fingers represent the main region of sequence homology between fly and vertebrate Tsh proteins (Caubit *et al.*, 2000). To test whether these zinc fingers are required for the *tshz3b* overexpression phenotype, we created a construct that codes for the last 700 aa of the Tshz3b protein, which includes a CtBP-interaction (PIDLT) motif associated with transcriptional repression (Manfroid *et al.*, 2004),

the homeodomain and the last two zinc-fingers (Tshz3bΔZnF1-3). Expressing this construct in zebrafish does not cause a hindbrain patterning phenotype (*n*=16/16; compare Figure 4-10A-C). Similarly, overexpression of the first three zinc fingers only, without the PIDLT motif, homeodomain or C-terminal zinc fingers (Tshz3bZnF1-3) also fails to perturb hindbrain patterning (*n*=13/13; Figure 4-10D). However, when the PIDLT motif is included along with the N-terminal zinc fingers (Tshz3bΔHD), this construct can perturb hindbrain patterning with a similar efficiency as the full-length protein (*n*=13/13; Figure 4-10E). Ectopic Tshz3bΔHD also perturbs *hoxa2b* expression and causes a caudal expansion of r1 identity (Figure S4-1), similar to that observed for full length Tshz3b (Figure 4-6E, G). Thus, the homeodomain and C-terminal zinc fingers do not contribute to the *tshz3b* overexpression phenotype. In summary, the ability of ectopic Tshz3b to perturb Hox-dependent hindbrain segmentation requires only the first three zinc finger domains and the PIDLT motif.

4.2.11 *tshz3b* functions as a transcriptional repressor

Evidence from studies done in Drosophila using both fly and mouse *tsh* genes suggest that Teashirt-related proteins act as repressors of transcription (Manfroid *et al.*, 2004; Saller *et al.*, 2002). To confirm that this is also true of *tshz3b*, we created constructs that encode FLAG-tagged Tshz3b fused at its C-terminus to either a repressor domain from the Engrailed protein (EnR), or a transactivation domain from the virion protein 16 (VP16) of the herpes simplex virus type 1. If Tshz3b acts as a repressor, then Tshz3b-EnR should produce the same phenotype as Tshz3b alone, while Tshz3b-VP16 should have either no effect or produce a new phenotype. Consistent with previous findings, overexpressed *tshz3b* and *tshz3b-EnR* cause the same hindbrain patterning phenotype (*n*=13/13 and 13/15 respectively; Figure 4-10F), while embryos injected with *tshz3b-VP16* have no discernable phenotype (*n*=11/11; Figure 4-10G). The observation that Tshz3b-VP16 does not produce a dominant negative phenotype is somewhat surprising, and could be indicative of a structural or

functional incompatibility between Tshz3b and the VP16 domain. Together these data suggest that *tshz3b* functions as a repressor to antagonize *hox* function.

4.2.12 Expressing the fly Tsh protein in zebrafish does not perturb hindbrain patterning

The observation that only the evolutionarily conserved Tsh domains are required for the *tshz3b* overexpression phenotype suggests that the fly Tsh protein might perform the same functions when expressed in fish. The ability of mouse Tshz proteins to rescue the *tsh* mutant phenotype in flies also supports the hypothesis that, although Tsh-related proteins are not well conserved at the sequence level, they exhibit a high level of functional conservation (Manfroid *et al.*, 2004). To test this hypothesis, we injected mRNA encoding Myc-tagged Drosophila Tsh, confirmed its translation by immunostains (Figure 4-11A,B) and analyzed embryos for patterning defects. Injecting 300-600 pg of untagged *tsh* mRNA into one-cell embryos causes defects in tail morphology of a kind that is not observed in *tshz3b*-injected embryos (300 pg *n*=22/40; 600 pg *n*=20/25; Figure 4-11C-E). To determine if *tsh* overpression also perturbs hindbrain patterning, we analyzed the expression of *wnt1* (MHB), *egr2b* (r3 / r5), and *hoxd4a* (r7 / spinal cord). Compared to wild type, *tsh* overexpressing embryos exhibit some morphological defects in the midbrain and hindbrain, but do not have any of the patterning defects associated with *tshz3b* overexpression (*n*=32/32; Figure 4-11F-H). Thus, in spite of previous evidence that fly and vertebrate Tsh-related proteins are functionally conserved, and that the Tshz3b overexpression phenotype does not require any of the characterized vertebrate-specific domains, overexpression of the fly Tsh protein in fish does not antagonize Hox-dependent hindbrain patterning.

4.3 Discussion

In this study, I explore the role of the zebrafish *teashirt*-related gene *tshz3b* in hindbrain segmentation by detailing the regulation of its mRNA expression pattern and examining its loss- and gain-of-function phenotypes. I find

that zebrafish *tshz3b* expression in the hindbrain is positively regulated by Pbx, Meis and Hox function, with additional positive input from retinoic acid signaling (Figure 4-2). Knockdown of Tshz3b causes defects in hindbrain morphology and neuronal organization (Figures 4-4 and 4-5). Furthermore, I observe that Tshz3b acts as a transcriptional repressor to antagonize Hox-dependent hindbrain patterning (Figures 4-6, 4-7, 4-8, 4-9, and 4-10). Taken together, *tshz3b* is both a transcriptional target and a negative regulator of the *hox* genes that are responsible for AP patterning of the vertebrate hindbrain.

4.3.1 The regulation of *tshz3b* expression in the hindbrain

The results of the Pbx, Meis1, and Hoxb1 loss of function experiments, as well as the *hoxb1b* overexpression assay, suggest that both *tshz3b* and *tshz3a* expression is positively regulated by Hox and TALE-class transcription factors (Figures 4-2A-J and 4-7E, F). This is consistent with the situation in flies, where *tsh* expression is directly activated by Antp-Exd-Hth trimeric complexes (McCormick *et al.*, 1995; Merabet *et al.*, 2007). It is possible that Hox-TALE complexes directly regulate *tshz3b* as well, as we have identified putative Pbx-Meis binding sites in evolutionarily conserved blocks of *tshz3b* promoter sequence (T.E. unpublished observations). Definitively demonstrating the direct transcriptional regulation of the *tshz3* paralogues by Hox-Pbx-Meis complexes would add to the small but growing list of direct Hox targets in vertebrates.

Retinoic acid signaling also positively regulates *tshz3b* transcription (Figure 4-2K-O). It is likely that the r5 and r6 domains of *tshz3b* expression require RA input, as these domains of *tshz3b* expression are lost in DEAB-treated embryos. *tshz3b* expression in r4 and the spinal cord is not reduced in DEAB-treated embryos, suggesting that these domains of *tshz3b* expression are not dependent on RA signaling. Previous research has demonstrated that RA also positively regulates *tshz1* expression (Wang *et al.*, 2007). However, not all *tshz* genes are RA-responsive, since *tshz3a* expression in the hindbrain does not respond to exogenous RA treatment (Figure S4-2). Taken together, *tshz3b*

expression in the hindbrain is positively regulated by both Hox and RA transcriptional input.

4.3.2 Ectopic Tshz3b inhibits Hox-dependent hindbrain segmentation

Ectopic *tshz3b* produces hindbrain segmentation defects that resemble those caused by a Hox-Pbx-Meis loss of function. These phenotypes include the downregulation of *hoxb1a*, *hoxa2b* and *egr2b* expression (Figures 4-6; 4-9; 4-10), a posterior expansion of Hox-independent r1 identity (Figure 4-6; Figure S4-1), and a mispatterning of the hindbrain cranial and reticulospinal neurons (Figure 4-8). Furthermore, ectopic *tshz3b* can block the r2-to-r4 homeotic transformation caused by *hoxb1b* overexpression (Figure 4-9E-H). This *tshz3b*-mediated loss of segmental identity is not caused by ectopic activity of posterior Hox genes, since r1 identity is expanded caudally (Figure 4-6G), and the genetic and neuronal markers of spinal cord identity are not expanded rostrally (Figures 4-7B and 4-8B). These data are consistent with the anterior Hox-repressing activities of the Drosophila Tsh protein, and suggest that the inhibition of Hox PG1-4 function is a conserved characteristic of Tsh-related proteins.

The question now becomes one of how *tshz3b* is able to inhibit Hox function in the hindbrain. Structure-function analyses suggest that Tshz3b functions as a repressor and requires the evolutionarily conserved N-terminal zinc fingers and CtBP-binding motif in order to antagonize Hox function (Figure 4-10). Addition of a VP16 activation domain, or removal of the CtBP-interaction motif abrogates the Hox-antagonizing activity of ectopic Tshz3b. This suggests that Tshz3b represses the transcription of Hox target genes. Of course, some of these targets could be *hox* genes themselves. In Drosophila, the Wnt-mediated repression of Ultrabithorax transcription (Ubx / Hox7) is accomplished by a complex of Tsh and the co-repressors CtBP and Brinker (Saller *et al.*, 2002; Waltzer *et al.*, 2001). In this example, it is thought that Tsh does not directly bind DNA, but rather is recruited to its target gene via its interaction with the DNA-binding protein Brinker. Could Tshz3b use a similar piggybacking mechanism for recruitment to Hox target sequences? Fly Tsh is able to bind Hox proteins such as

Scr and its vertebrate orthologue Hoxa5 via its N-terminal acidic domain (Taghli-Lamallem *et al.*, 2007). Additionally, Tsh can bind to the Hox6 orthologue Antp, though the interaction domain has not been mapped. Similar to the fly acidic domain, Tshz3b contains an N-terminal stretch of 23 amino acids with 12 acidic residues, hinting at the possibility that Tshz3b can bind Hox proteins. Additionally, fly Tsh has been shown to interact directly with Exd (Pbx) and Hth (Meis) in vitro, and this interaction between Hth and Tsh may be important to repress the transcription of *eyes absent* (*eya*) during eye development (Bessa *et al.*, 2002). These data suggest that zebrafish Tshz3b may be recruited to Hox-regulated promoters through a direct interaction with Hox proteins and their TALE-class partners. Alternatively, *tshz3b* may function independently of *hox* genes to repress shared target genes, as has been also been observed in Drosophila (Alexandre *et al.*, 1996; de Zulueta *et al.*, 1994; Taghli-Lamallem *et al.*, 2007). Although these hypotheses remain to be tested, it is possible that Tshz3b antagonizes Hox function via both mechanisms.

Given the ability of mouse Tshz genes to rescue *tsh* mutant flies, and the observation that the Tshz3b overexpression phenotype does not require the vertebrate-specific homeodomain or C-terminal zinc fingers, it was surprising to find that overexpressing fly Tsh in zebrafish did not produce similar hindbrain patterning defects (Figure 4-11). However, fly and vertebrate Teashirt proteins have not been well conserved over evolution (Caubit *et al.*, 2000). Thus, while both zebrafish *tshz3b* and fly *tsh* can repress anterior Hox function in their respective organisms, they may do so via distinct mechanisms that reflects their evolutionary divergence. Alternatively, they may function by homologous mechanisms, albeit one where the fly Tsh protein is incompatible with the vertebrate system.

4.3.3 Hox-repressing activities of other Teashirt-related proteins

Other vertebrate *teashirt*-related genes can also negatively regulate Hox function, as overexpression of Xtsh1 in Xenopus perturbs *Hox* expression in the hindbrain and cranial neural crest (Koebernick *et al.*, 2006). However, the results

from that study differ from ours in that their overexpression phenotype was not limited to perturbations in hindbrain segmentation. Whereas *tshz3b* overexpression in zebrafish primarily affects hindbrain patterning, ectopic Xtsh1 in frogs also eliminates Engrailed-2 expression at the midbrain-hindbrain boundary (MHB) and mildly downregulates Otx-2 in the forebrain, both of which are regulated by *hox*-independent mechanisms. Although Hox proteins are not involved in anterior neural patterning, maintenance of the MHB does require a functional complex of Pbx and Engrailed proteins (Erickson *et al.*, 2007). However, other than downregulating *tshz3a* expression in the midbrain (Figure 4-7), ectopic *tshz3b* does not phenocopy a loss of Pbx function in the midbrain (see *eng2a* expression in Figure 4-9A-D and *pax2a* expression in Figure 4-10). Thus, while both fish *tshz3b* and frog Xtsh1 can perturb hindbrain segmentation, it appears that the effects of *tshz3b* are largely limited to the hindbrain, while Xtsh1 provokes more widespread neural patterning defects. Whether this reflects functional differences between Tshz1 and Tshz3 proteins, or differences between model organisms remains to be seen.

4.3.4 Loss-of-function studies on vertebrate *teashirt*-related genes

Loss-of-function studies of vertebrate *teashirt*-related genes also suggest that they play a role in hindbrain development. Morpholino-mediated knockdown of Xenopus Xtsh1 protein causes severe hindbrain segmentation defects that, like Xtsh1 overexpression, resemble a Hox loss-of-function phenotype (Koebernick *et al.*, 2006). The exact mechanisms by which both a gain and loss of Xtsh1 function produce similar hindbrain phenotypes have not been determined.

In contrast, morpholino knockdown of Tshz3b causes defects in hindbrain morphology (Figure 4-4A-C and Figure 4-5A, B), but not obvious patterning phenotypes associated with changes in Hox function. Loss of Tshz3b function can lead to defects in hindbrain neuronal development and organization (Figure 4-5C-H), but these are likely a consequence of altered morphology rather than defects in Hox-dependent pattern formation. Consistent with this idea, there are brain morphology mutants in zebrafish which exhibit defects in reticulospinal

organization that are similar to those observed in *tshz3b* morphants (Lowery et al., 2009). Thus, it is possible that Tshz3b is playing a Hox-independent role in regulating cell movement and / or adhesion during neural tube development.

Tshz3 mutant mice do not exhibit defects in hindbrain segmental identity (Caubit *et al.*, 2010), data that is consistent with our own morpholino-based Tshz3b knockdown studies (Figure 4-4). These data suggest that *tshz3* genes in mice and zebrafish do not play a broad role in regulating early Hox function during hindbrain segmentation. However, Tshz3 inactivation does lead to defects in the hindbrain motorneurons that control respiratory rhythm, causing these mice to suffocate at birth. Hox proteins are known regulators of the developmental pathways involved in breathing behaviour (Champagnat *et al.*, 2009; Chatonnet *et al.*, 2003). Whether Tshz3 inactivation directly perturbs Hox-dependent development of the respiratory system remains to be elucidated. However, the ability of ectopic Tshz3b to inhibit Hox function in the hindbrain presents the interesting possibility that the *Tshz3*-null phenotype is caused by a failure to negatively regulate Hox function during the development of respiratory neural circuitry.

4.3.5 The involvement of *tshz3b* with non-Hox developmental pathways

Teashirt-related proteins are multifunctional transcription factors, able to directly interact with transcriptional repressor complexes (Manfroid *et al.*, 2004; Saller *et al.*, 2002), with Hox and TALE-class homeodomain transcription factors (Bessa *et al.*, 2002; Taghli-Lamallem *et al.*, 2007), and with transcriptional effectors of the Wnt pathway such as β-catenin and Tcf3 (Gallet *et al.*, 1999; Gallet *et al.*, 1998; Onai *et al.*, 2007). Although ectopic Tshz3b could potentially disrupt numerous developmental processes, the most obvious phenotype is a disruption of Hox-dependent hindbrain segmentation. Our results stand in contrast to the Xtsh3 studies in frogs, where ectopic Xtsh3 dorsalizes the embryonic axis by enhancing canonical Wnt signaling, and morpholino knockdown of Xtsh3 causes a severe ventralized phenotype (Onai *et al.*, 2007). However, this discrepancy does not eliminate the possibility that endogenous zebrafish *tshz3b*

also participates on the Wnt pathway. Genetic interaction experiments between *tshz3b* and members of the Wnt pathway, along with biochemical evidence of a functionally relevant interaction between Tshz3b and β-catenin or Tcf3 in the hindbrain would help to clarify the relationship between *tshz3b* and the Wnt pathway. Definitive evidence that *tshz3b* acted on both the Wnt and Hox pathways could define *tshz3b* as point of integration between these two pathways during hindbrain development.

4.4 Figures

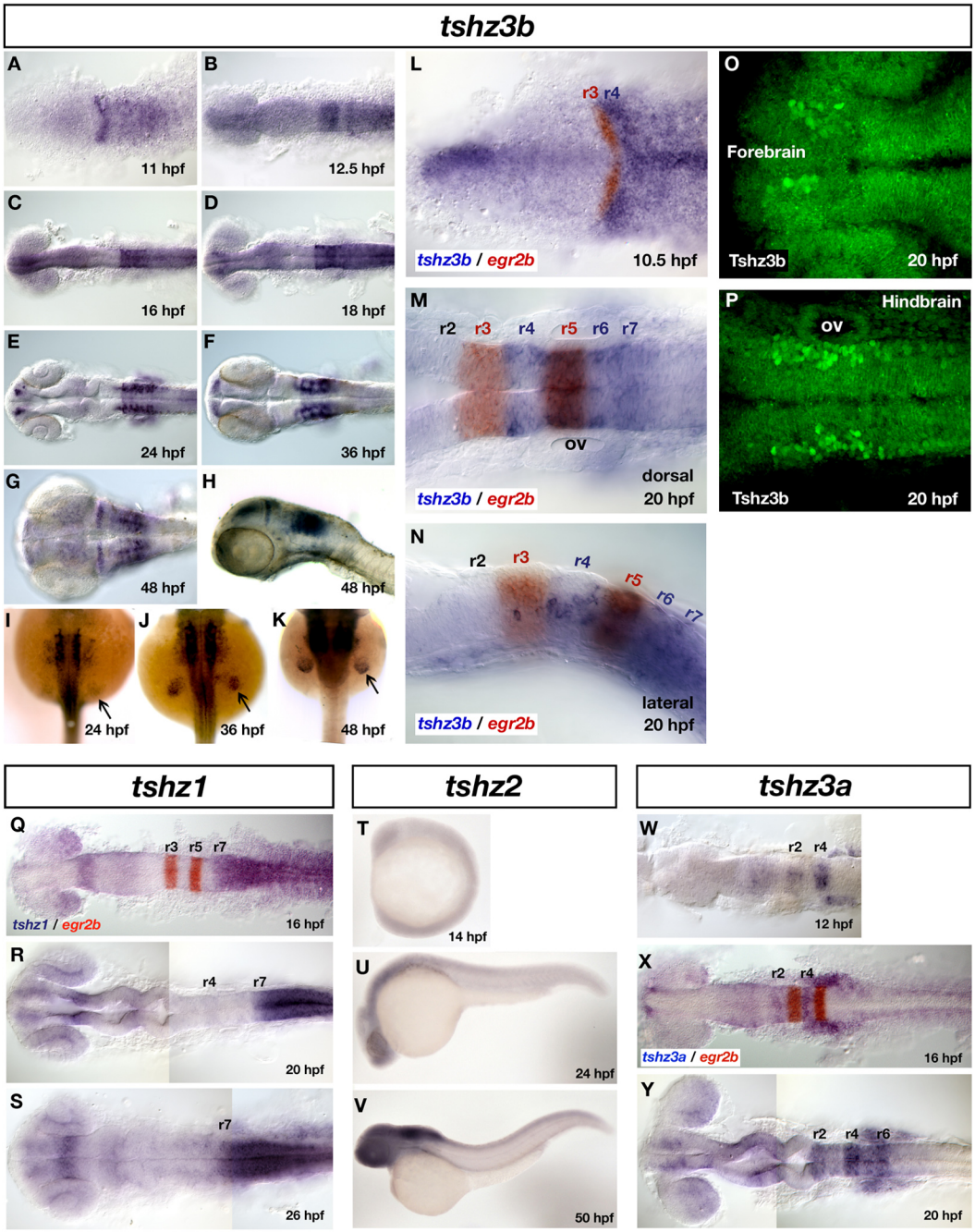

Figure 4-1. mRNA expression of zebrafish *teashirt*-related genes *tshz1*, *tshz2*, *tshz3a*, and *tshz3b*. **(A-H)** mRNA in situ hybridizations (ISH) for *tshz3b* from 11 – 48 hpf showing expression in the forebrain, midbrain, hindbrain and anterior spinal cord. **(I-K)** *tshz3b* ISH in the developing pectoral fins (black arrows) from 24-48 hpf. **(L-N)** mRNA ISH for *tshz3b* (purple) co-stained with *egr2b* (red) in r3

(L) and r3 and r5 (M, N) detailing *tshz3b* expression in the hindbrain. **(O, P)** Whole mount immunostains for Tshz3b showing protein accumulation in the forebrain and hindbrain of 20 hpf embryos. **(Q-S)** mRNA ISH for *tshz1* (purple) showing expression in the posterior hindbrain / spinal cord and forebrain between 16 – 26 hpf. **(T-V)** mRNA ISH for *tshz2* showing weak, diffuse expression between 14-24 hpf, and enriched hindbrain expression at 50 hpf. **(W-Y)** mRNA ISH for *tshz3a* (purple) between 12 – 20 hpf showing tissue-specific expression in the forebrain, midbrain and hindbrain. All views are dorsal with anterior to the left, except for (I-K; anterior at the top), and (H, N, T-V; lateral). Embryos in (L-N, Q, X) are co-stained with the r3/r5 marker *egr2b* (red). Abbreviations: hpf - hours post fertilization; ov – otic vesicle; r – rhombomere.

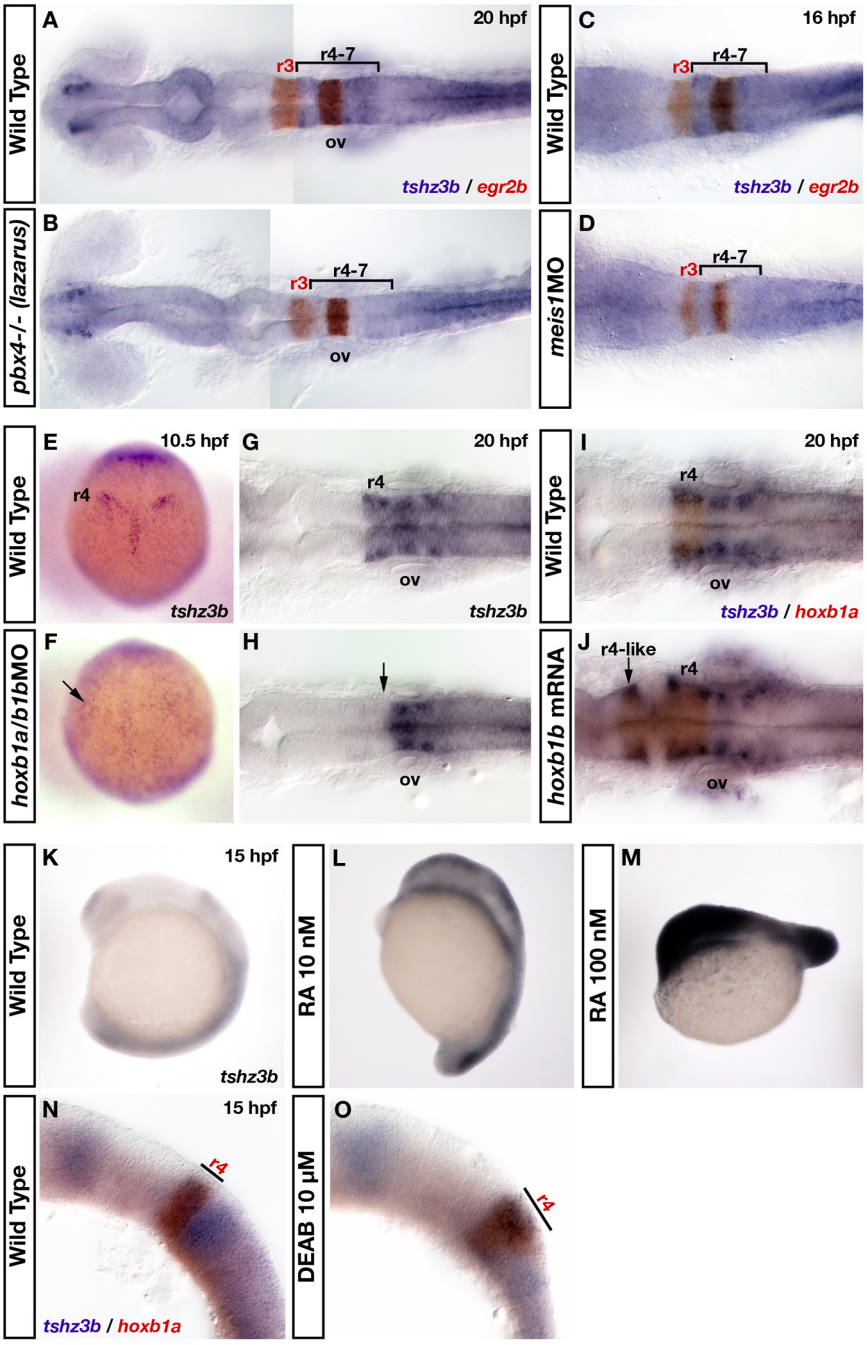

Figure 4-2. *tshz3b* expression in the hindbrain is positively regulated by Hox/Pbx/Meis proteins and retinoic acid signaling. **(A, B)** mRNA in situ hybridizations (ISH) for *tshz3b* in wild type and *pbx4*$^{-/-}$ mutant embryos at 20 hpf. *tshz3b* is reduced in the midbrain and r4-7 of the hindbrain in *pbx4* mutants. **(C, D)** *tshz3b* ISH in wild type and *meis1* morphant embryos at 16 hpf. *tshz3b* expression is reduced in the hindbrain of Meis1-depleted embryos. Embryos in

(A-D) are co-stained with the r3/r5 marker *egr2b* (red) and shown in dorsal view with anterior to the left. **(E-H)** *tshz3b* ISH in wild type and *hoxb1a/b1b* (*hoxb1*) morphant embryos. (E) At 10.5 hpf, *tshz3b* is expressed in the presumptive r4 domain, and in the midline. This expression pattern is not initiated correctly in *hoxb1* morphants (F; black arrow). At 20 hpf, the r4 domain of *tshz3b* expression is lost in *hoxb1* morphants (G, H; black arrow). Embryos in (E, F) are shown in dorsal view with anterior up; embryos in (G, H) are shown in dorsal view with anterior to the left. **(I, J)** mRNA ISH for *tshz3b* (purple) and *hoxb1a* (red) in wild type and *hoxb1b* overexpressing embryos at 20 hpf. Ectopic Hoxb1b drives *hoxb1a* expression in the r2 region, where *tshz3b* is also ectopically expressed. Embryos are shown in dorsal view with anterior to the left. **(K-M)** mRNA ISH for *tshz3b* expression in 15 hpf embryos treated with DMSO, 10 nM retinoic acid (RA) or 100 nM RA. Increasing concentrations of RA lead to increased *tshz3b* expression. **(N, O)** mRNA ISH for *tshz3b* (purple) and *hoxb1a* (red) expression in 15 hpf embryos treated with DMSO or 10 μM DEAB (an inhibitor of Aldh1 enzymes that synthesize RA). DEAB-treatment leads to a caudal expansion of r4 identity, and a concomitant expansion of r4 *tshz3b* expression. Embryos in (K-O) are lateral views with anterior to the upper left. Abbreviations: DEAB – diethylaminobenzaldehyde; hpf - hours post fertilization; ov – otic vesicle; r – rhombomere; RA – retinoic acid.

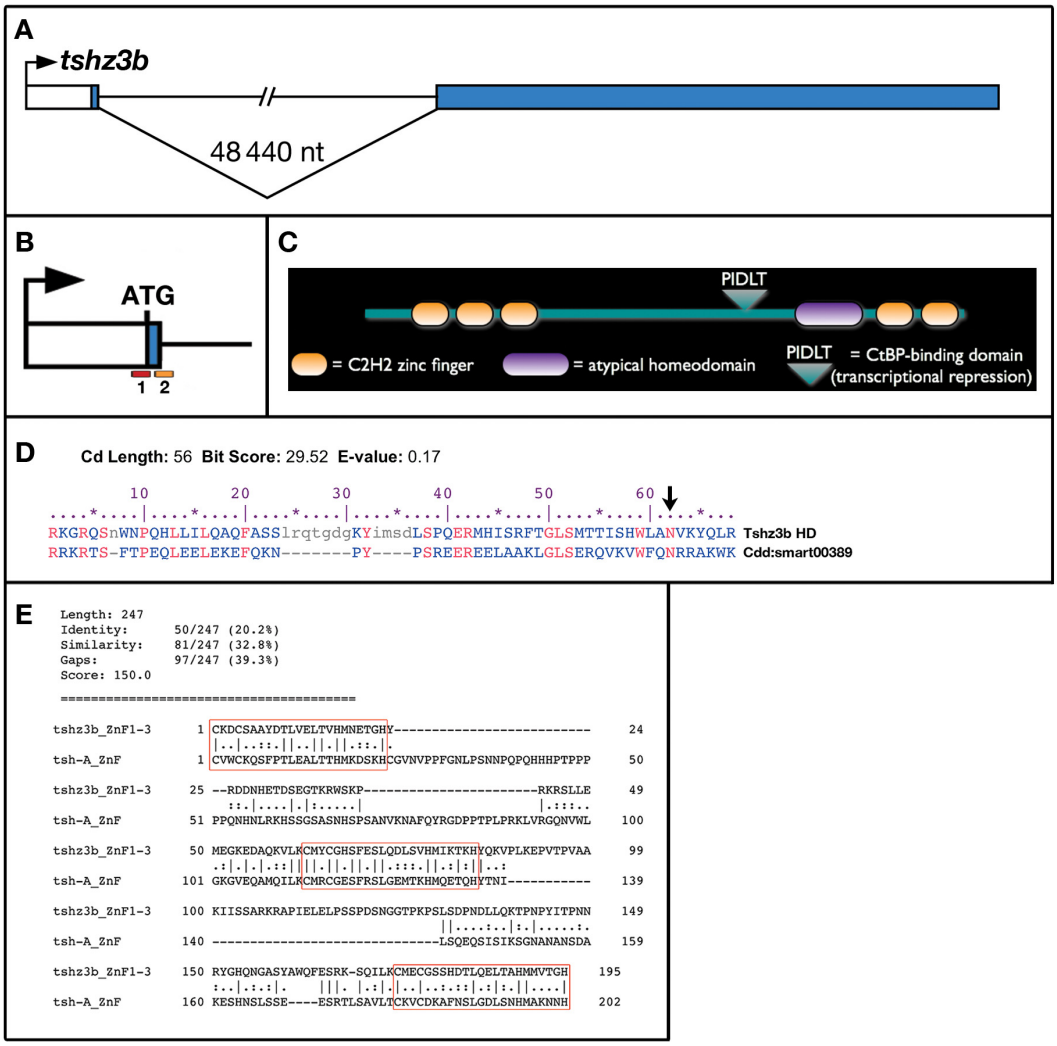

Figure 4-3. *tshz3b* gene structure and protein domains. **(A)** As determined by 5' RACE and full-length ORF cloning, the zebrafish *tshz3b* locus consists of two coding exons separated by a 48,440 bp intron. **(B)** Detail of the first *tshz3b* exon showing the locations of the ATG translation blocking (red) and splice blocking (yellow) morpholinos used in this study. **(C)** Illustration of the Tshz3b protein domains and their relative positions within the polypeptide. **(D)** Amino acid alignment of the Tshz3b homeodomain (HD) with the consensus Cdd:smart00389 HD (NCBI Conserved Domains database). The black arrow indicates the position of a conserved asparagine (N) residue that is important for the DNA-binding properties of HDs. **(E)** Amino acid alignment between the first three Tshz3b zinc fingers with those of the fly Tsh protein. Red boxes indicate the C2H2 zinc finger domains.

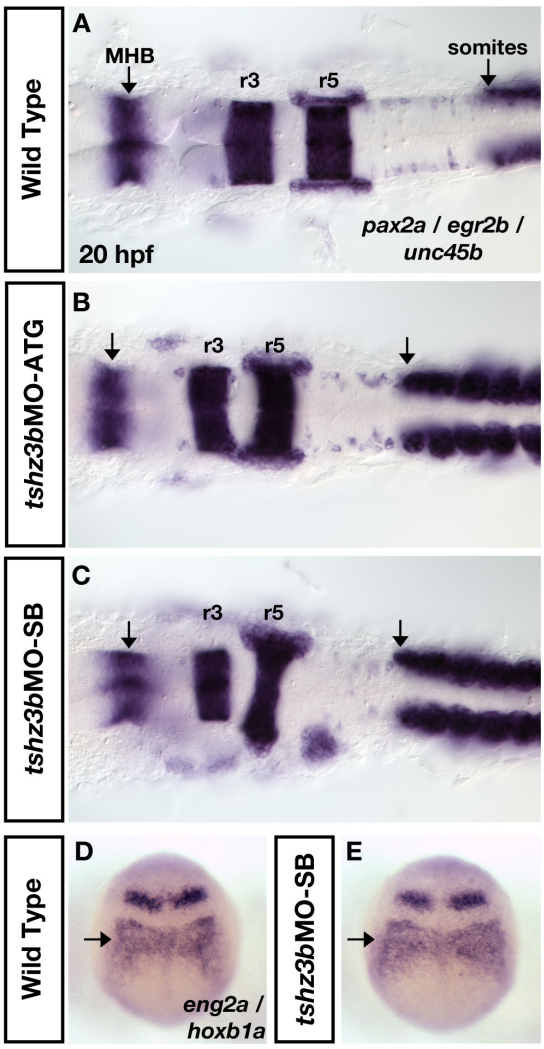

Figure 4-4. Knockdown of Tshz3b causes defects in hindbrain morphology. **(A-C)** Using either the ATG translation blocking morpholino (MO), or the splice blocking MO, targeted knockdown of Tshz3b leads to disorganized and misshapen rhombomeres (r). 20 hpf embryos are stained for *pax2a* (MHB, ov), *egr2b* (r3 and r5) and *unc45b* (somites). Black arrows indicate the MHB and most anterior somite. Views are dorsal with anterior to the left. **(D, E)** *eng2a* (MHB) and *hoxb1a* (hindbrain - black arrow) in situs on 10 hpf wild type and *tshz3b*MO embryos. The *hoxb1a* expression domain is normal at this stage.

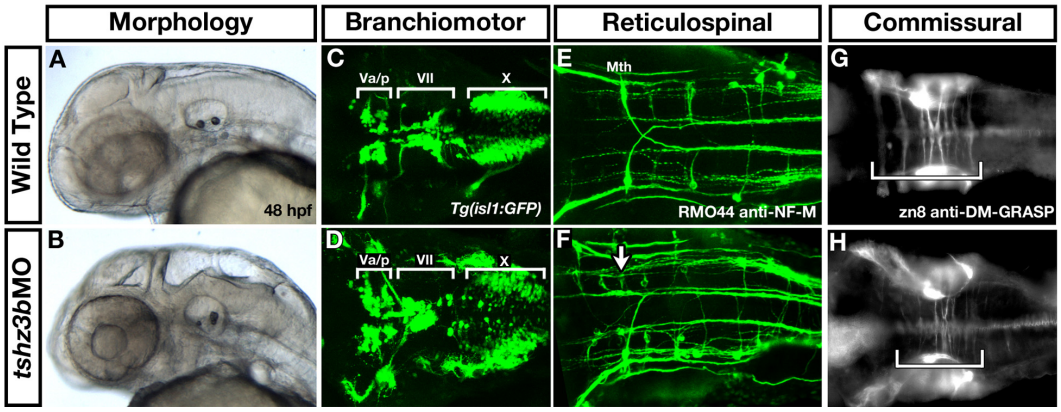

Figure 4-5. *tshz3b* morphants exhibit disorganized hindbrain neurons. **(A, B)** Live lateral views of wild type and *tshz3b* morphant embryos at 48 hpf. The morphants have abnormal brain morphology. **(C, D)** Branchiomotor cranial neurons as visualized in *Tg[isl1:GFP]* embryos at 48 hpf. Tshz3b-knockdown leads to disorganization of the segmental arrangement of these neurons. **(E, F)** Reticulospinal neurons (RN) as detected by immunostaining with the rmo44 α-neurofilament-medium antibody. Similar to the branchiomotor neurons, the RNs are disorganized in Tshz3b-depleted embryos. The white arrow indicates the position of a missing Mauthner (Mth) neuron. **(G, H)** DM-GRASP immunostaining for hindbrain commissural axons. The segmental arrangement of commissural axons is disorganized in *tshz3b* morphants. Embryos in (C-H) are shown in dorsal view with anterior to the left.

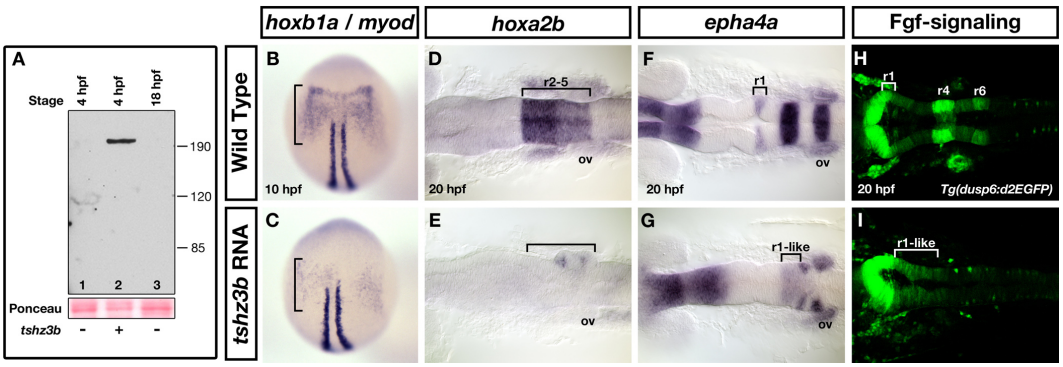

Figure 4-6. Ectopic Tshz3b perturbs segmental patterning of the hindbrain. **(A)** Western blot for Tshz3b using an α-Tshz3b polyclonal antibody. Lysates were made from wild type and *tshz3b* mRNA-injected embryos at 4 hpf (Lanes 1 and 2), as well as from 18 hpf wild type embryos (Lane 3). The antibody recognizes a single band at >190 kDa in the lysates made from *tshz3b* injected embryos. Ponceau stain of the membrane is shown as a loading control. **(B, C)** *hoxb1a* (brackets) and *myoD* expression in 10 hpf wild type and *tshz3b* injected embryos. *hoxb1a* expression in the hindbrain is reduced while myoD expression is unchanged by ectopic Tshz3b. **(D, E)** *hoxa2b* expression in 20 hpf wild type and *tshz3b* injected embryos. *hoxa2b* expression in r2-5 is reduced by ectopic Tshz3b. **(F, G)** *epha4a* expression in 20 hpf wild type and *tshz3b* injected embryos. *epha4a* expression in 3 and r5 is reduced by ectopic Tshz3b, and the r1 domain is expanded caudally. **(H, I)** Fgf-signaling domains in wild type and *tshz3b* injected *Tg[dusp6:d2eGFP]* embryos. Ectopic Tshz3b perturbs the r4 and r6 Fgf-responsive domains, while expanding an r1-like level of Fgf-responsiveness into the anterior hindbrain. All views are dorsal with anterior to the left, except in B and C where anterior is at the top. Abbreviations: ov – otic vesicle; r – rhombomere.

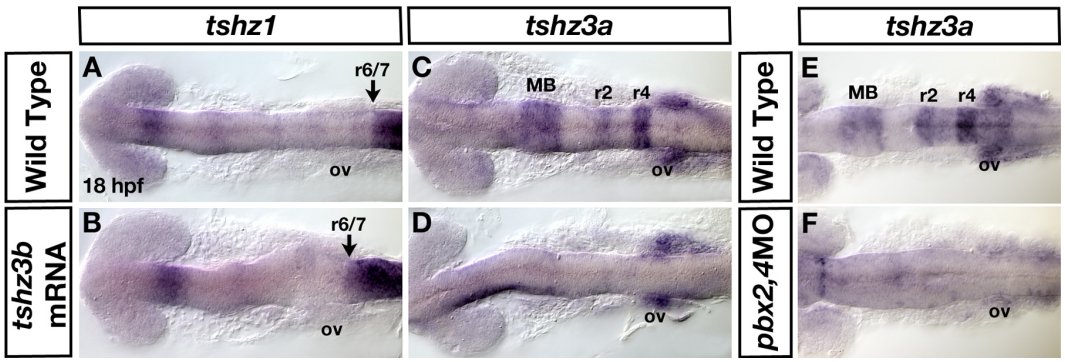

Figure 4-7. The effect of ectopic Tshz3b on *tshz1* and *tshz3a* expression at 18 hpf. **(A, B)** Although the faint hindbrain expression of *tshz1* is perturbed in *tshz3b*-injected embryos, the forebrain and caudal hindbrain / spinal cord domains are unaffected by ectopic Tshz3b. **(C, D)** *tshz3a* expression in the midbrain and hindbrain is downregulated in *tshz3b* overexpressing embryos, and this phenotype is similar to that observed in *pbx2,4* morphant embryos **(E, F)**. All views are dorsal with anterior to the left. Abbreviations: MB – midbrain; ov – otic vesicle; r – rhombomere.

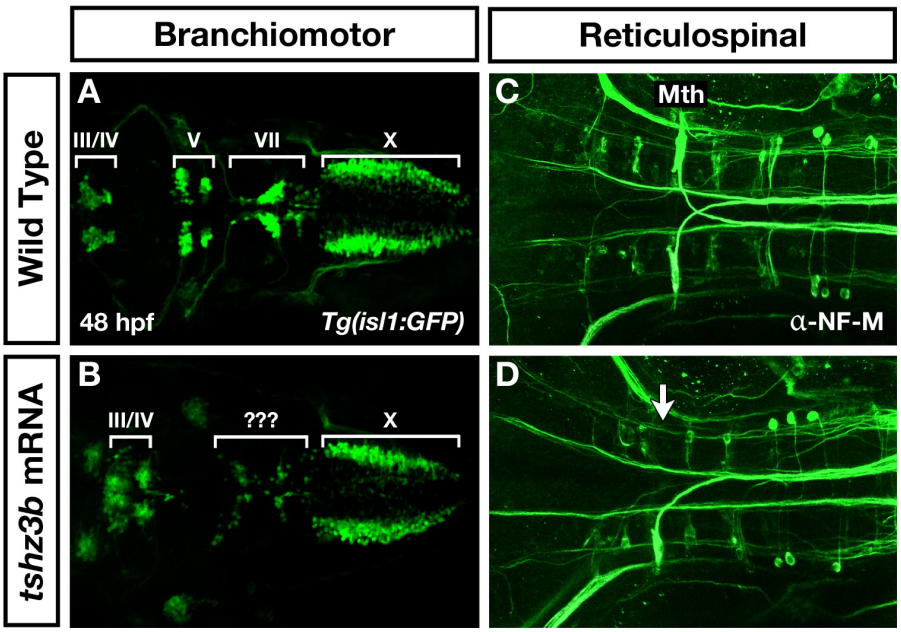

Figure 4-8. The branchiomotor and reticulospinal hindbrain neurons are mispatterned in *tshz3b* overexpressing embryos. **(A, B)** Branchiomotor cranial neurons as visualized in *Tg[isl1:GFP]* embryos at 48 hpf. Ectopic Tshz3b disrupts the specification of the trigeminal (V) and facial (VII) motor neurons. White brackets and labels indicate the identities of the cranial motor neurons. **(C, D)** Reticulospinal neurons (RN) as detected by immunostaining with the rmo44 α-neurofilament-medium antibody. *tshz3b*-overexpressing embryos exhibit disorganized anterior RNs. White arrow indicates a missing Mauthner (Mth) cell in r4. All views are dorsal with anterior to the left.

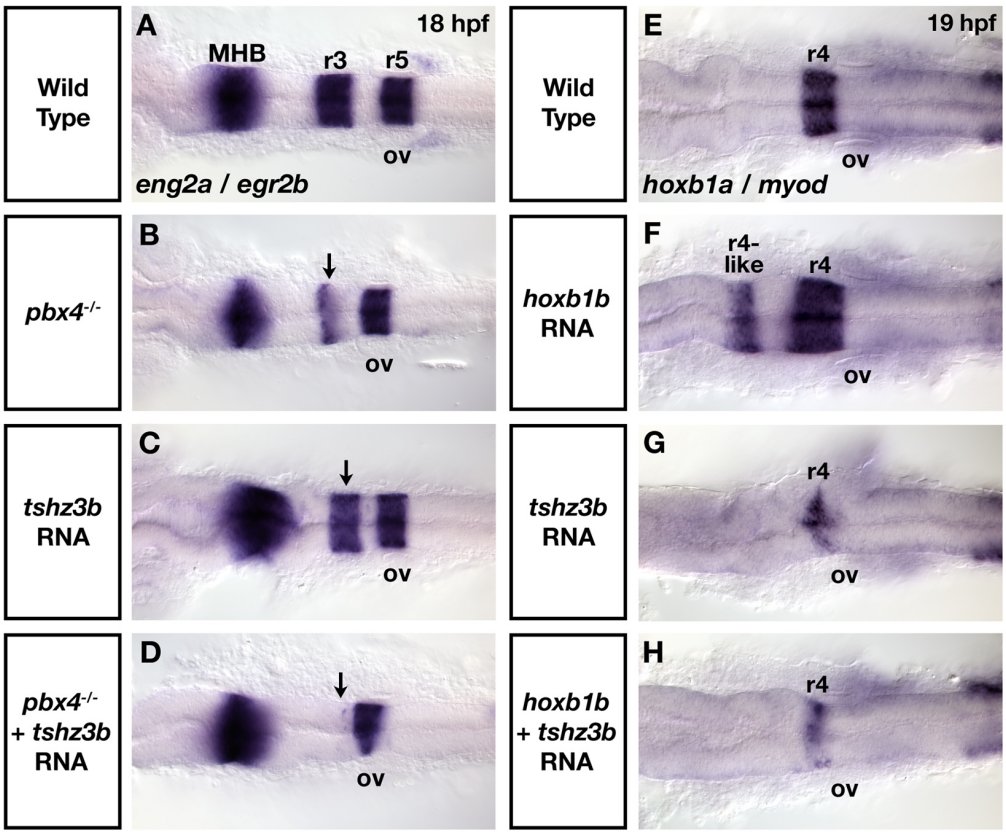

Figure 4-9. (A-D) *tshz3b* overexpression synergizes with the *pbx4* mutant hindbrain phenotype. mRNA in situ hybridization (ISH) for *eng2a* (MHB) and *egr2b* (r3 and r5) in wild type (A), *pbx4*$^{-/-}$ (B), *tshz3b*-injected (C), and *pbx4*$^{-/-}$ embryos injected with *tshz3b* mRNA (D). The low dose of *tshz3b* mRNA produces little phenotype on its own, but, in a *pbx4* mutant background, can further reduce r3 expression of *egr2b*. **(E-H)** Ectopic Tshz3b blocks the r2-to-r4 homeotic transformation caused by *hoxb1b* overexpression. mRNA ISH for *hoxb1a* in 19 hpf wild type (E), *hoxb1b*-injected (F), *tshz3b*-injected (G), and *hoxb1b+tshz3b* injected (H) embryos. Ectopic Hoxb1b is able to drive *hoxb1a* expression an ectopic r4-like region (B), but is unable to do so when co-expressed with Tshz3b (D). Ectopic Tshz3b alone reduces *hoxb1a* expression in r4 (C).

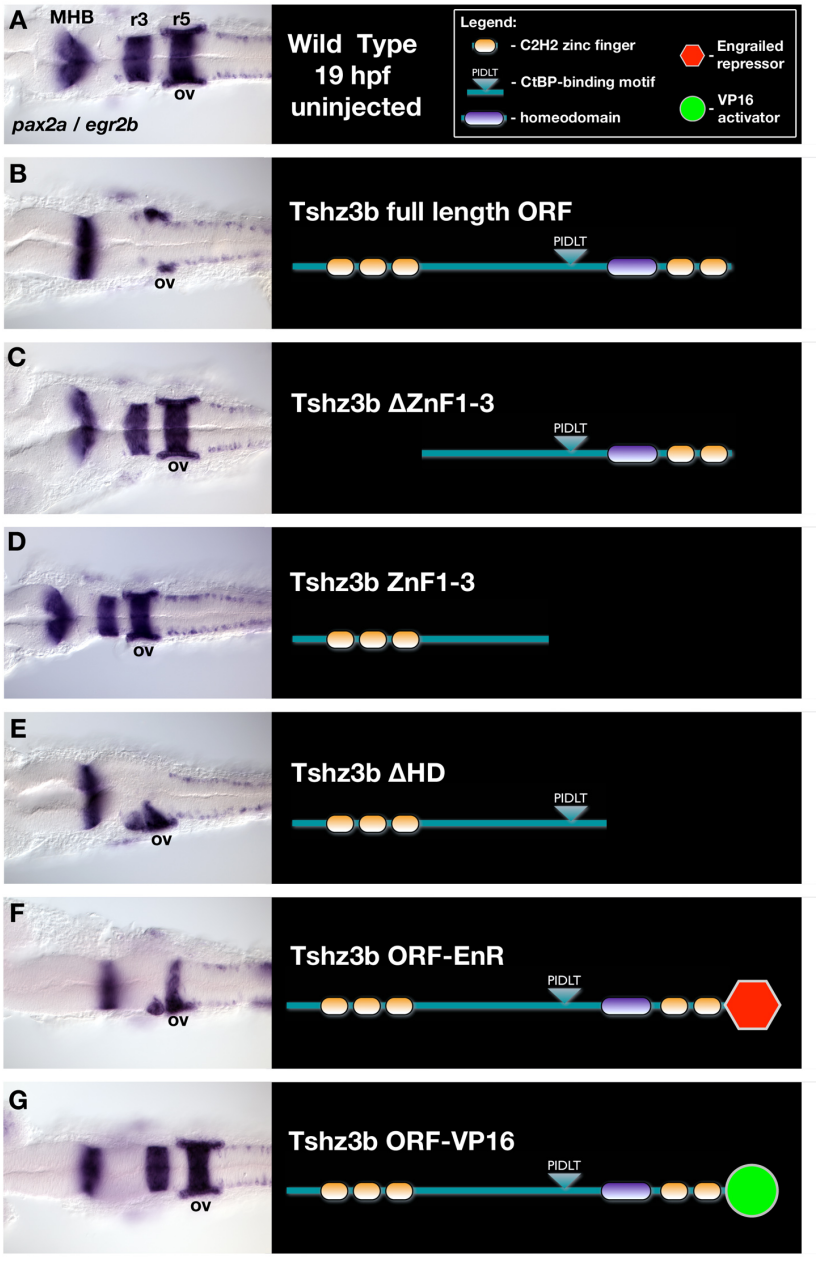

Figure 4-10. (A-E) Deletion construct analysis for Tshz3b. mRNA in situ hybridizations (ISH) for *pax2a* (MHB, ov) and *egr2b* (r3 and r5) in 19 hpf embryos injected with mRNAs coding for (B) full length Tshz3b, (C) Tshz3bΔZn1-3, (D) Tshz3bZn1-3, or (E) Tshz3bΔHD. Ectopic Tshz3bΔZn1-3 or Tshz3bZn1-3 produces little effect on hindbrain patterning, while Tshz3bΔHD has the same phenotype as full length Tshz3b. **(E, F)** Tshz3b act as a repressor to disrupt hindbrain patterning. mRNA ISH for *pax2a* (MHB, ov) and *egr2b* in embryos injected with mRNA coding for FLAG-tagged (E) Tshz3b-EnR (fused to

an engrailed repressor domain), or (F) Tshz3b-VP16 (fused to a Virion protein 16 activation domain). Tshz3b-EnR produces the same hindbrain patterning defect as Tshz3b, while Tshz3b-VP16 has no effect. All views are dorsal with anterior to the left. Abbreviations: ORF – open reading frame; MHB – midbrain-hindbrain boundary; ov – otic vesicle; r – rhombomere; ZnF – zinc finger.

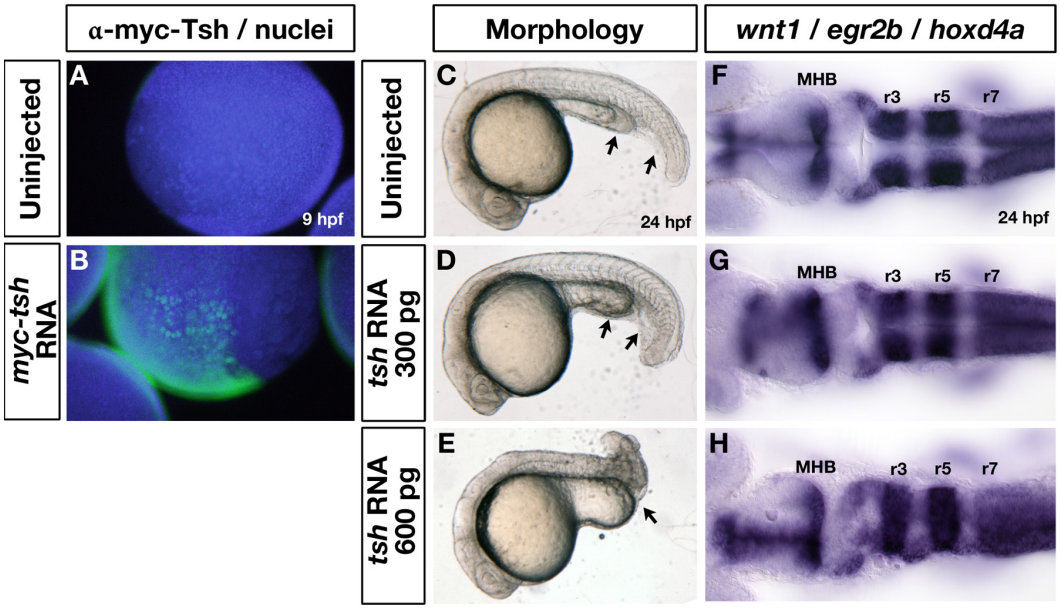

Figure 4-11. Overexpressed fly Tsh does not perturb Hox-dependent hindbrain patterning. **(A, B)** Immunostain for Myc-tagged Teashirt protein (green) using the α-Myc 9E10 monclonal antibody on 8 hpf uninjected and *myc-tsh* mRNA injected embryos. Uninjected embryos are negative for immunoreactivity. Nuclei are co-stained with Hoechst 33258. **(C-E)** Dose-dependent effects on the morphology of *tsh* mRNA injected embryos. Embryos injected with 300 pg of *tsh* mRNA exhibit defects in the ventral tail and yolk-extension region (black arrows), while embryos injected with 600 pg of *tsh* mRNA exhibit more severe tail defects. **(F-H)** The expression of *wnt1* (MHB, HB), *egr2b* (r3 and r5) and *hoxd4a* (r7 and spinal cord) in wild type and *tsh*-overexpressing embryos at 24 hpf. Although the morphology of the midbrain and hindbrain regions are disorganized, ectopic fly Tsh does not produce the same hindbrain patterning defects as ectopic Tshz3b. Embryos in C-E are lateral views of live embryos with anterior to the left, while views in F-H are dorsal.

4.5 References

Alexandre, E., Graba, Y., Fasano, L., Gallet, A., Perrin, L., De Zulueta, P., Pradel, J., Kerridge, S., Jacq, B., 1996. The Drosophila teashirt homeotic protein is a DNA-binding protein and modulo, a HOM-C regulated modifier of variegation, is a likely candidate for being a direct target gene. Mech Dev. 59**,** 191-204.

Andrew, D. J., Horner, M. A., Petitt, M. G., Smolik, S. M., Scott, M. P., 1994. Setting limits on homeotic gene function: restraint of Sex combs reduced activity by teashirt and other homeotic genes. EMBO J. 13**,** 1132-44.

Bell, E., Wingate, R. J., Lumsden, A., 1999. Homeotic transformation of rhombomere identity after localized Hoxb1 misexpression. Science. 284**,** 2168-71.

Bessa, J., Gebelein, B., Pichaud, F., Casares, F., Mann, R. S., 2002. Combinatorial control of Drosophila eye development by eyeless, homothorax, and teashirt. Genes Dev. 16**,** 2415-27.

Caubit, X., Core, N., Boned, A., Kerridge, S., Djabali, M., Fasano, L., 2000. Vertebrate orthologues of the Drosophila region-specific patterning gene teashirt. Mech Dev. 91**,** 445-8.

Caubit, X., Thoby-Brisson, M., Voituron, N., Filippi, P., Bevengut, M., Faralli, H., Zanella, S., Fortin, G., Hilaire, G., Fasano, L., 2010. Teashirt 3 regulates development of neurons involved in both respiratory rhythm and airflow control. J Neurosci. 30**,** 9465-76.

Champagnat, J., Morin-Surun, M. P., Fortin, G., Thoby-Brisson, M., 2009. Developmental basis of the rostro-caudal organization of the brainstem respiratory rhythm generator. Philos Trans R Soc Lond B Biol Sci. 364**,** 2469-76.

Chan, S. K., Jaffe, L., Capovilla, M., Botas, J., Mann, R. S., 1994. The DNA binding specificity of Ultrabithorax is modulated by cooperative interactions with extradenticle, another homeoprotein. Cell. 78**,** 603-15.

Chandrasekhar, A., 2004. Turning heads: development of vertebrate branchiomotor neurons. Dev Dyn. 229**,** 143-61.

Chandrasekhar, A., Moens, C. B., Warren, J. T., Jr., Kimmel, C. B., Kuwada, J. Y., 1997. Development of branchiomotor neurons in zebrafish. Development. 124**,** 2633-44.

Chatonnet, F., Dominguez del Toro, E., Thoby-Brisson, M., Champagnat, J., Fortin, G., Rijli, F. M., Thaeron-Antono, C., 2003. From hindbrain segmentation to breathing after birth: developmental patterning in rhombomeres 3 and 4. Mol Neurobiol. 28**,** 277-94.

Coiffier, D., Charroux, B., Kerridge, S., 2008. Common functions of central and posterior Hox genes for the repression of head in the trunk of Drosophila. Development. 135**,** 291-300.

Cooper, K. L., Leisenring, W. M., Moens, C. B., 2003. Autonomous and nonautonomous functions for Hox/Pbx in branchiomotor neuron development. Dev Biol. 253**,** 200-13.

de Zulueta, P., Alexandre, E., Jacq, B., Kerridge, S., 1994. Homeotic complex and teashirt genes co-operate to establish trunk segmental identities in Drosophila. Development. 120**,** 2287-96.

Dibner, C., Elias, S., Frank, D., 2001. XMeis3 protein activity is required for proper hindbrain patterning in Xenopus laevis embryos. Development. 128**,** 3415-26.

Dupe, V., Lumsden, A., 2001. Hindbrain patterning involves graded responses to retinoic acid signalling. Development. 128**,** 2199-208.

Erickson, T., Scholpp, S., Brand, M., Moens, C. B., Waskiewicz, A. J., 2007. Pbx proteins cooperate with Engrailed to pattern the midbrain-hindbrain and diencephalic-mesencephalic boundaries. Dev Biol. 301**,** 504-17.

Fasano, L., Roder, L., Core, N., Alexandre, E., Vola, C., Jacq, B., Kerridge, S., 1991. The gene teashirt is required for the development of Drosophila embryonic trunk segments and encodes a protein with widely spaced zinc finger motifs. Cell. 64**,** 63-79.

Ferretti, E., Marshall, H., Popperl, H., Maconochie, M., Krumlauf, R., Blasi, F., 2000. Segmental expression of Hoxb2 in r4 requires two separate sites that integrate cooperative interactions between Prep1, Pbx and Hox proteins. Development. 127**,** 155-66.

Fraser, S., Keynes, R., Lumsden, A., 1990. Segmentation in the chick embryo hindbrain is defined by cell lineage restrictions. Nature. 344**,** 431-5.

Gallet, A., Angelats, C., Erkner, A., Charroux, B., Fasano, L., Kerridge, S., 1999. The C-terminal domain of armadillo binds to hypophosphorylated teashirt to modulate wingless signalling in Drosophila. Embo J. 18**,** 2208-17.

Gallet, A., Erkner, A., Charroux, B., Fasano, L., Kerridge, S., 1998. Trunk-specific modulation of wingless signalling in Drosophila by teashirt binding to armadillo. Curr Biol. 8**,** 893-902.

Gavalas, A., 2002. ArRAnging the hindbrain. Trends Neurosci. 25**,** 61-4.

Gavalas, A., Davenne, M., Lumsden, A., Chambon, P., Rijli, F. M., 1997. Role of Hoxa-2 in axon pathfinding and rostral hindbrain patterning. Development. 124**,** 3693-702.

Gavalas, A., Krumlauf, R., 2000. Retinoid signalling and hindbrain patterning. Curr Opin Genet Dev. 10**,** 380-6.

Gavalas, A., Studer, M., Lumsden, A., Rijli, F. M., Krumlauf, R., Chambon, P., 1998. Hoxa1 and Hoxb1 synergize in patterning the hindbrain, cranial nerves and second pharyngeal arch. Development. 125**,** 1123-36.

Gehring, W. J., Qian, Y. Q., Billeter, M., Furukubo-Tokunaga, K., Schier, A. F., Resendez-Perez, D., Affolter, M., Otting, G., Wuthrich, K., 1994. Homeodomain-DNA recognition. Cell. 78**,** 211-23.

Guthrie, S., 2007. Patterning and axon guidance of cranial motor neurons. Nat Rev Neurosci. 8**,** 859-71.

Hernandez, R. E., Putzke, A. P., Myers, J. P., Margaretha, L., Moens, C. B., 2007. Cyp26 enzymes generate the retinoic acid response pattern necessary for hindbrain development. Development. 134**,** 177-87.

Higashijima, S., Hotta, Y., Okamoto, H., 2000. Visualization of cranial motor neurons in live transgenic zebrafish expressing green fluorescent protein under the control of the islet-1 promoter/enhancer. J Neurosci. 20**,** 206-18.

Kimmel, C. B., Metcalfe, W. K., Schabtach, E., 1985. T reticular interneurons: a class of serially repeating cells in the zebrafish hindbrain. J Comp Neurol. 233**,** 365-76.

Koebernick, K., Kashef, J., Pieler, T., Wedlich, D., 2006. Xenopus Teashirt1 regulates posterior identity in brain and cranial neural crest. Dev Biol. 298**,** 312-26.

Lowery, L. A., De Rienzo, G., Gutzman, J. H., Sive, H., 2009. Characterization and classification of zebrafish brain morphology mutants. Anat Rec (Hoboken). 292**,** 94-106.

Lumsden, A., Keynes, R., 1989. Segmental patterns of neuronal development in the chick hindbrain. Nature. 337**,** 424-8.

Manfroid, I., Caubit, X., Kerridge, S., Fasano, L., 2004. Three putative murine Teashirt orthologues specify trunk structures in Drosophila in the same way as the Drosophila teashirt gene. Development. 131**,** 1065-73.

Manfroid, I., Caubit, X., Marcelle, C., Fasano, L., 2006. Teashirt 3 expression in the chick embryo reveals a remarkable association with tendon development. Gene Expr Patterns. 6**,** 908-12.

Mann, R. S., Chan, S. K., 1996. Extra specificity from extradenticle: the partnership between HOX and PBX/EXD homeodomain proteins. Trends Genet. 12**,** 258-62.

Marchler-Bauer, A., Anderson, J. B., Chitsaz, F., Derbyshire, M. K., DeWeese-Scott, C., Fong, J. H., Geer, L. Y., Geer, R. C., Gonzales, N. R., Gwadz, M., He, S., Hurwitz, D. I., Jackson, J. D., Ke, Z., Lanczycki, C. J., Liebert, C. A., Liu, C., Lu, F., Lu, S., Marchler, G. H., Mullokandov, M., Song, J. S., Tasneem, A., Thanki, N., Yamashita, R. A., Zhang, D., Zhang, N., Bryant, S. H., 2009. CDD: specific functional annotation with the Conserved Domain Database. Nucleic Acids Res. 37**,** D205-10.

Mathies, L. D., Kerridge, S., Scott, M. P., 1994. Role of the teashirt gene in Drosophila midgut morphogenesis: secreted proteins mediate the action of homeotic genes. Development. 120**,** 2799-809.

Maves, L., Kimmel, C. B., 2005. Dynamic and sequential patterning of the zebrafish posterior hindbrain by retinoic acid. Dev Biol. 285**,** 593-605.

McClintock, J. M., Carlson, R., Mann, D. M., Prince, V. E., 2001. Consequences of Hox gene duplication in the vertebrates: an investigation of the zebrafish Hox paralogue group 1 genes. Development. 128**,** 2471-84.

McClintock, J. M., Kheirbek, M. A., Prince, V. E., 2002. Knockdown of duplicated zebrafish hoxb1 genes reveals distinct roles in hindbrain patterning and a novel mechanism of duplicate gene retention. Development. 129**,** 2339-54.

McCormick, A., Core, N., Kerridge, S., Scott, M. P., 1995. Homeotic response elements are tightly linked to tissue-specific elements in a transcriptional enhancer of the teashirt gene. Development. 121**,** 2799-812.

McNulty, C. L., Peres, J. N., Bardine, N., van den Akker, W. M., Durston, A. J., 2005. Knockdown of the complete Hox paralogous group 1 leads to dramatic hindbrain and neural crest defects. Development. 132**,** 2861-71.

Merabet, S., Saadaoui, M., Sambrani, N., Hudry, B., Pradel, J., Affolter, M., Graba, Y., 2007. A unique Extradenticle recruitment mode in the Drosophila Hox protein Ultrabithorax. Proc Natl Acad Sci U S A. 104**,** 16946-51.

Metcalfe, W. K., Mendelson, B., Kimmel, C. B., 1986. Segmental homologies among reticulospinal neurons in the hindbrain of the zebrafish larva. J Comp Neurol. 251**,** 147-59.

Moens, C. B., Prince, V. E., 2002. Constructing the hindbrain: insights from the zebrafish. Dev Dyn. 224**,** 1-17.

Moens, C. B., Selleri, L., 2006. Hox cofactors in vertebrate development. Dev Biol. 291**,** 193-206.

Molina, G. A., Watkins, S. C., Tsang, M., 2007. Generation of FGF reporter transgenic zebrafish and their utility in chemical screens. BMC Dev Biol. 7**,** 62.

Onai, T., Matsuo-Takasaki, M., Inomata, H., Aramaki, T., Matsumura, M., Yakura, R., Sasai, N., Sasai, Y., 2007. XTsh3 is an essential enhancing factor of canonical Wnt signaling in Xenopus axial determination. EMBO J. 26**,** 2350-60.

Pearson, J. C., Lemons, D., McGinnis, W., 2005. Modulating Hox gene functions during animal body patterning. Nat Rev Genet. 6**,** 893-904.

Popperl, H., Rikhof, H., Chang, H., Haffter, P., Kimmel, C. B., Moens, C. B., 2000. lazarus is a novel pbx gene that globally mediates hox gene function in zebrafish. Mol Cell. 6**,** 255-67.

Rauskolb, C., Wieschaus, E., 1994. Coordinate regulation of downstream genes by extradenticle and the homeotic selector proteins. EMBO J. 13**,** 3561-9.

Robertson, L. K., Bowling, D. B., Mahaffey, J. P., Imiolczyk, B., Mahaffey, J. W., 2004. An interactive network of zinc-finger proteins contributes to regionalization of the Drosophila embryo and establishes the domains of HOM-C protein function. Development. 131**,** 2781-9.

Roder, L., Vola, C., Kerridge, S., 1992. The role of the teashirt gene in trunk segmental identity in Drosophila. Development. 115**,** 1017-33.

Rusch, D. B., Kaufman, T. C., 2000. Regulation of proboscipedia in Drosophila by homeotic selector genes. Genetics. 156**,** 183-94.

Saller, E., Kelley, A., Bienz, M., 2002. The transcriptional repressor Brinker antagonizes Wingless signaling. Genes Dev. 16**,** 1828-38.

Santos, J. S., Fonseca, N. A., Vieira, C. P., Vieira, J., Casares, F., 2010. Phylogeny of the teashirt-related zinc finger (tshz) gene family and analysis of the developmental expression of tshz2 and tshz3b in the zebrafish. Dev Dyn. 239**,** 1010-8.

Studer, M., Lumsden, A., Ariza-McNaughton, L., Bradley, A., Krumlauf, R., 1996. Altered segmental identity and abnormal migration of motor neurons in mice lacking Hoxb-1. Nature. 384**,** 630-4.

Taghli-Lamallem, O., Gallet, A., Leroy, F., Malapert, P., Vola, C., Kerridge, S., Fasano, L., 2007. Direct interaction between Teashirt and Sex combs reduced proteins, via Tsh's acidic domain, is essential for specifying the identity of the prothorax in Drosophila. Dev Biol. 307**,** 142-51.

van Dijk, M. A., Murre, C., 1994. extradenticle raises the DNA binding specificity of homeotic selector gene products. Cell. 78**,** 617-24.

Vlachakis, N., Choe, S. K., Sagerstrom, C. G., 2001. Meis3 synergizes with Pbx4 and Hoxb1b in promoting hindbrain fates in the zebrafish. Development. 128**,** 1299-312.

Vlachakis, N., Ellstrom, D. R., Sagerstrom, C. G., 2000. A novel pbx family member expressed during early zebrafish embryogenesis forms trimeric complexes with Meis3 and Hoxb1b. Dev Dyn. 217**,** 109-19.

von Baer, K. E., 1828. Entwicklungsgeschichte der Thiere: Beobachtung und Reflexion. Bornträger, Königsberg.

Waltzer, L., Vandel, L., Bienz, M., 2001. Teashirt is required for transcriptional repression mediated by high Wingless levels. Embo J. 20**,** 137-45.

Wang, H., Lee, E. M., Sperber, S. M., Lin, S., Ekker, M., Long, Q., 2007. Isolation and expression of zebrafish zinc-finger transcription factor gene tsh1. Gene Expr Patterns. 7**,** 318-22.

Waskiewicz, A. J., Rikhof, H. A., Hernandez, R. E., Moens, C. B., 2001. Zebrafish Meis functions to stabilize Pbx proteins and regulate hindbrain patterning. Development. 128**,** 4139-51.

Waskiewicz, A. J., Rikhof, H. A., Moens, C. B., 2002. Eliminating zebrafish pbx proteins reveals a hindbrain ground state. Dev Cell. 3**,** 723-33.

Zhang, M., Kim, H. J., Marshall, H., Gendron-Maguire, M., Lucas, D. A., Baron, A., Gudas, L. J., Gridley, T., Krumlauf, R., Grippo, J. F., 1994. Ectopic Hoxa-1 induces rhombomere transformation in mouse hindbrain. Development. 120**,** 2431-42.

Chapter Five - Pbx proteins cooperate with Engrailed to pattern the midbrain–hindbrain and diencephalic–mesencephalic boundaries.

A version of this chapter has been published. Erickson, T., Scholpp, S., Brand, M., Moens, C.B., and Waskiewicz, A.J. 2007. Developmental Biology 301: 504-517.

5.1 Introduction

Over the course of vertebrate development, the neural plate is progressively subdivided into functionally specialized, lineage restricted compartments (reviewed in Kiecker and Lumsden, 2005). Tissue compartmentalization is important to specify cell position, identity and function during vertebrate patterning. The seven rhombomeres of the hindbrain were the first observed lineage-restricted compartments in the vertebrate nervous system (Fraser et al., 1990; von Baer, 1828). Hindbrain segmentation has since been shown to occur downstream of Hox proteins and their DNA binding partners Pbx and Meis. Lineage-restriction has also been observed at the diencephalic-mesencephalic boundary (DMB) and the midbrain-hindbrain boundary (MHB), which enclose the midbrain at its rostral and caudal ends respectively. In this regard, the vertebrate neural tube is an excellent system in which to study the formation and maintenance of lineage-restricted boundaries.

The Pbx (pre-B-cell leukemia transcription factor) family of TALE class homeodomain transcription factors are best characterized as heterodimeric partners for Hox proteins (reviewed in Mann and Chan, 1996; reviewed in Moens and Selleri, 2006). Pbx proteins are hypothesized to reveal intrinsic DNA-binding specificity within the Hox proteins, as well as to coordinately bind an adjacent Pbx recognition site in the promoter of target genes (Chan et al., 1996; Knoepfler et al., 1996; reviewed in Mann and Chan, 1996). As such, Pbx-Hox complexes often have a much higher DNA binding specificity and affinity than either Pbx or Hox alone. A zebrafish mutant in the *pbx4* gene (*lazarus* or *lzr*) was identified in a genetic screen for embryos that fail to properly express the rhombomere 3 (r3) and r5-specific transcription factor *egr2b (krox20)* (Popperl et al., 2000). Two partially redundant zebrafish *pbx* genes, *pbx2* and *pbx4*, are expressed during early embryogenesis at a time when the hindbrain is being patterned. These two Pbx proteins cooperate with Hox proteins to drive expression of early hindbrain patterning genes such as *fgf3*, *fgf8*, *hoxb1a*, and *vhnf1* (Hernandez et al., 2004; Maves et al., 2002; Popperl et al., 1995; Walshe et al., 2002; Waskiewicz et al.,

2002). In the absence of Pbx2 and Pbx4 proteins, the region of hindbrain normally fated to give rise to r2-r6 is deprogrammed to adopt the default groundstate identity of r1, a segment that lacks expression of any *hox* gene (Waskiewicz et al., 2002). As such, the hindbrain region of Pbx-less embryos mimics the loss of all hindbrain *hox* gene function, demonstrating the importance of Pbx proteins in tissue compartmentalization during vertebrate hindbrain development. However, although Pbx genes are expressed ubiquitously throughout the developing zebrafish nervous system, no role for Pbx proteins in the formation or patterning of either forebrain or midbrain has been described.

Within the Hox proteins themselves, a motif called the hexapeptide is required for cooperative DNA binding with Pbx (Chang et al., 1995; Neuteboom et al., 1995). This evolutionarily conserved consensus motif, located just N-terminal of the Hox homeodomain, consists of the residues YQWPM. The hexapeptide motif, particularly the tryptophan residue, binds within a hydrophobic pocket formed by the extended loop between helix 1 and 2 in the Pbx homeodomain (LaRonde-LeBlanc and Wolberger, 2003; Piper et al., 1999). The mechanism of the homeodomain-hexapeptide interaction is conserved in fly Exd and Hox proteins as well (Passner et al., 1999), illustrating the importance of Pbx-Hox interactions during development.

Other hexapeptide-containing transcription factors have been found to bind Pbx proteins (In der Rieden et al., 2004). Amongst these Pbx-interacting proteins is the homeodomain transcription factor Engrailed (abbreviated Eng or En). In Engrailed proteins, a hexapeptide motif (WPAWVY) is located just upstream of the EH2 (Eng Homology-2) domain. The hexapeptide, along with the EH2 and EH3 domains, is required for the Pbx - Eng interaction (Peltenburg and Murre, 1996). Within the Engrailed hexapeptide itself, the two tryptophan residues are of particular importance in mediating cooperative binding between Pbx and Eng. Additionally, the three amino acid extension of the Pbx homeodomain is also required for the Pbx–Eng interaction (Peltenburg and Murre, 1997). All domains necessary for the Pbx-Eng interaction are conserved in flies

and vertebrates, pointing to the importance of this interaction for metazoan development.

Engrailed was originally identified in *Drosophila* as a factor required for the maintenance of cellular compartments during fly development (reviewed in Hidalgo, 1996). In *Drosophila*, a genetic interaction between *engrailed* and the *pbx* orthologue *extradenticle* (*exd)* has been established based on the similarity in phenotypes between maternal, zygotic *exd* mutants and those of *en* mutant flies (Alexandre and Vincent, 2003; Kobayashi et al., 2003; Peifer and Wieschaus, 1990). Biochemical evidence suggests that the Pbx / Exd family of TALE-class homeodomain proteins can directly bind Engrailed in vitro and in vivo (Kobayashi et al., 2003; Peltenburg and Murre, 1996; Serrano and Maschat, 1998; van Dijk and Murre, 1994; van Dijk et al., 1995). Experimentally, Engrailed's role as a transcriptional regulator has been shown to require the presence of functional Exd and Homothorax (Hth; vertebrate Meis) proteins (Alexandre and Vincent, 2003; Kobayashi et al., 2003; Rieckhof et al., 1997). A trimeric complex of En, Exd, and Hth can cooperatively bind DNA and either activate or repress transcription of target genes (Alexandre and Vincent, 2003; Kobayashi et al., 2003). En expression is autoregulatory and is not maintained in maternal, zygotic *exd* mutants, suggesting that *en* requires *exd* to positively regulate its own expression (Peifer and Wieschaus, 1990). These studies have established a genetic and biochemical pathway involving Engrailed and TALE-class transcription factors. However, vertebrate developmental pathways involving a Pbx-Eng interaction have not been investigated.

In vertebrates, the best-described role for Engrailed is in patterning the mesencephalic region of the developing neural tube, especially the midbrain-hindbrain boundary (MHB). Formed at the interface between anterior (*otx2*-expressing) and posterior (*gbx2*-expressing) neural tissue, the isthmic organizer (IsO) at the MHB has been identified as an important source of signals required for specification of the mesencephalon and the rostral metencephalon, as well as formation and maintenance of the DMB and MHB (Alvarado-Mallart et al., 1990; reviewed in Raible and Brand, 2004; reviewed in Wurst and Bally-Cuif, 2001).

Fgf8 is likely the main IsO signaling molecule as ectopic Fgf8 protein can mimic the organizer activity of the MHB (Crossley et al., 1996; Martinez et al., 1999) Although the interface of *otx2* and *gbx2* expression correlates with the position of the MHB, it is unclear how gene expression at the MHB organizer is initiated. In mice, expression of MHB markers can be initiated in the absence of *otx2* and *gbx2* function (Giudicelli et al., 2001). This suggests that other factors are involved in MHB establishment, such as Wnt8 signals originating from the lateral mesendodermal cells (Rhinn et al., 2005), and transcriptional regulation by *pou5f1* (*spg)* and *sp5* (*bts1*) (Burgess et al., 2002; Tallafuss et al., 2001). Although MHB initiation is not well understood, it is clear that following establishment there is considerable transcriptional interdependence amongst the MHB patterning factors. Maintenance appears to involve a complicated cross-regulatory loop involving the secreted factors Wnt1 and Fgfs 8, 17, and 18, as well as transcriptional regulators including the Pax2/5/8 family, Irx1b, Irx7, Lmx1b.1, Lmx1b.2, and Engrailed proteins (Brand et al., 1996; Itoh et al., 2002; McMahon and Bradley, 1990; McMahon et al., 1992; O'Hara et al., 2005; Reifers et al., 1998). Functional perturbations in any of these genes can lead to a depletion of all other MHB markers and a loss of tectal and cerebellar structures.

Besides being a primary player in the cross-regulatory loop that maintains the isthmic organizer, Engrailed also performs more specialized functions in midbrain development. Specifically, Engrailed is required to position the caudal extent of the forebrain by maintaining the DMB and to polarize gene expression in the optic tectum (Araki and Nakamura, 1999; Liu and Joyner, 2001; Logan et al., 1996; Scholpp and Brand, 2001; Scholpp et al., 2003). Additionally, Engrailed can act as a cell-cell signaling molecule to guide retinal ganglion cell axons via a novel secretory mechanism (Brunet et al., 2005; Maizel et al., 1999). In mouse and zebrafish embryos lacking Engrailed function, expression of the forebrain markers *pax6a* and *epha4a* are expanded caudally, implying Eng proteins are required to maintain the integrity of the DMB. Conversely, ectopic overexpression of Engrailed can repress *pax6* expression in the forebrain and cause a rostral expansion of midbrain identity (Araki and Nakamura, 1999;

Scholpp and Brand, 2001; Scholpp et al., 2003). Furthermore, Araki and Nakamura present evidence in chick that the repression of *pax6* by ectopic En-2 occurs prior to the induction of *pax2*, *pax5* and *fgf8*, suggesting that the foremost function of Engrailed is to maintain the DMB. Taken together, these studies highlight the importance of Engrailed protein function in the formation, patterning and maintenance of the vertebrate midbrain.

Here we present evidence that zebrafish Pbx proteins are important regulators of MHB and DMB formation by acting as biochemical partners with Engrailed proteins. Zebrafish embryos that lack Pbx2 and Pbx4 function initiate MHB development normally, but progressively lose *eng2a*, *pax2a, fgf8, gbx2, and wnt1* expression as well as the corresponding midbrain-derived structures. Likewise, we show that in the absence of Pbx function, the forebrain domain of *pax6a* expression is caudally expanded, suggesting that Pbx proteins are required to maintain the integrity of the DMB. We also show in vitro that zebrafish Pbx4 interacts biochemically with the zebrafish Eng2a protein and that this physical interaction is required for the biological activity of *eng2a* overexpression in vivo. Based on these results, we favor a model where Eng requires Pbx as a co-factor in the midbrain to properly pattern the MHB and DMB.

5.2 Results

5.2.1 Pbx proteins are required for the proper formation of the midbrain and for maintenance of gene expression at the MHB

Given the established genetic and biochemical interactions between Engrailed and Exd proteins in flies, we wanted to see if Pbx proteins cooperated with Engrailed to pattern the vertebrate midbrain. As a first step, we examined midbrain morphology in live wild type, *lazarus* (*lzr* / *pbx4*$^{-/-}$), and Pbx-depleted embryos at 24 hours post-fertilization (hpf). In wild type embryos, the characteristic isthmic constriction has formed at the MHB with the tectum and the cerebellum located rostrally and caudally to the MHB respectively. (Figure 5-1A, A′). In *lzr* embryos, the isthmus is poorly formed and the size of tectum is diminished (Figure 5-1 B, B′; *n*=15). To further reduce Pbx function, we injected *lzr* embryos with both

pbx2 and *pbx4* morpholinos (*lzr;pbx2,4*MO). In all Pbx-depleted embryos examined, the isthmic constriction is almost completely absent and the tectum is further reduced (Figure 5-1C, C′; *n*=10). The phenotype of the Pbx-depleted embryos is similar to that of *eng2a* morphants, although not as severe as *eng2a/2b* double morphants or *noi* (*no isthmus / pax2a*$^{-/-}$) embryos (Figure 5-1D, D′) (Brand et al., 1996; Scholpp and Brand, 2001). These results suggest that vertebrate midbrain development requires Pbx proteins in a dose dependent fashion, and that *pbx* genes may act on the same genetic or biochemical MHB patterning pathway as the *engrailed* family of genes.

The MHB promotes separation between midbrain and hindbrain identities by restricting cell movements between the mesencephalon and metencephalon (Langenberg and Brand, 2005). MHB development consists of two early phases: initiation and maintenance. The genes involved in MHB maintenance are initiated largely independently of one another, and later become transcriptionally interdependent (reviewed in Raible and Brand, 2004). To determine if Pbx proteins are required to initiate MHB gene expression, we compared the expression of *eng2a, pax2a, fgf8, gbx2*, and *wnt1* in wild type and Pbx-depleted embryos at 11 hpf (3 somite stage; Figure 5-2A-J). Pbx-depleted embryos were identified by the absence of *egr2b* (*krox20*) expression in rhombomeres 3 and 5 of the presumptive hindbrain. *eng2a* and *pax2a* are expressed broadly across the MHB region, *fgf8* and *gbx2* are expressed in the posterior half of the MHB, while *wnt1* is expressed in the anterior region of the mesencephalon. We can detect no difference in the level or pattern of MHB gene expression between wild type and Pbx-depleted embryos at this stage (*n*=30). These data suggest that Pbx-proteins are not involved in the specification or positioning of the MHB and the immediately adjacent regions. Therefore, the loss of tectal and isthmic structures observed at 24 hpf may be due to a subsequent failure to maintain MHB gene expression.

In 18 hpf wild type embryos, a cross-regulatory loop between *eng2a, eng2b, pax2a*, *fgf8*, and *wnt1* maintains gene expression at the MHB and shapes the morphology of the isthmic constriction. We tested whether Pbx function is

required to maintain the MHB by examining the expression of MHB marker genes in wild type, *lzr* and Pbx-depleted embryos (Figure 5-3A-O). We used *eng2a* to mark the mesencephalon, MHB and metencephalon. In wild type embryos, *eng2a* is expressed in a wedge shape centered about the MHB (Figure 5-3A). This domain is diminished slightly in *lzr* embryos (Figure 5-3B). In Pbx-depleted embryos, this wedge-shaped domain of expression is greatly reduced and expression anterior to the MHB (the presumptive tectum) is absent (Figure 5-3C). A similar loss of ventral expression is observed for *pax2a* expression at the MHB (Figure 5-3D-F). We also performed in situ hybridizations for *fgf8* and *gbx2* to examine the effects of Pbx depletion on the rostral metencephalon. *fgf8* expression is not changed in *lzr* mutants as compared to wild type (Figure 5-3G, H). However, in Pbx-depleted embryos, the ventral domain is expanded caudally while medial expression is absent (Figure 5-3I). Similar results were recorded for *gbx2* expression, although it appears to be more sensitive to Pbx-depletion (Figure 5-3J-L). In wild type embryos, *wnt1* is expressed in the caudal mesencephalon and dorsal midbrain (Figure 5-3M). In *lzr* and Pbx-depleted embryos, *wnt1* ventral expression is progressively lost, while the dorsal domain is unchanged. To summarize, in all cases where *egr2b* expression was completely or nearly absent in hindbrain rhombomeres 3 and 5, we observed a general decrease in the level of MHB marker expression and loss of medio-ventral gene expression at the MHB (n>300). Although less severe, the perturbation of MHB gene expression in Pbx-depleted embryos is similar to a *pax2a*, *fgf8* or *eng2a/2b* loss-of-function (Lun and Brand, 1998; Reifers et al., 1998; Scholpp and Brand, 2001). This comprehensive decrease in MHB gene expression supports the hypothesis that Pbx proteins act within the same regulatory pathway as *eng* to maintain the MHB.

5.2.2 The diencephalic-mesencephalic boundary is compromised in Pbx-depleted embryos

The diencephalic-mesencephalic boundary (DMB) is a lineage-restricted boundary that maintains separation between forebrain and midbrain identities. A loss of *eng*, *pax2a* or *fgf8* expression at the MHB has been shown to cause a

caudal expansion of the forebrain at the expense of midbrain territory (Araki and Nakamura, 1999; Liu and Joyner, 2001; Scholpp and Brand, 2001; Scholpp and Brand, 2003; Scholpp et al., 2003). To determine the effect of Pbx-depletion on the DMB, we analyzed *epha4a*, *pax6a*, and *fgf8* expression by in situ hybridization on wild type and Pbx-depleted embryos (Figure 5-4). In 16.5 hpf and 18 hpf Pbx-depleted embryos, forebrain-specific expression of *epha4a* (Figure 5-4A, B) and *pax6a* (Figure 5-4C, D) extends beyond its normal posterior limit while the distance between the DMB and MHB is reduced (all Pbx-null embryos affected, $n>100$). To quantify this, we compared the rostro-caudal extent of the *pax6a* domain and found it to be expanded by an average of 15% in Pbx-depleted embryos ($P<0.025$; $n=5$). Similarly, the distance between the MHB (*fgf8* expression) and the caudal limit of *pax6a* expression is reduced by 44% in Pbx-depleted embryos ($P<0.01$; $n=5$). Zebrafish embryos depleted of both Eng2a and Eng2b also exhibit a caudal expansion of forebrain markers *pax6a* and *epha4a* and a loss of midbrain territory. This demonstrates a strong similarity between the DMB defects in Pbx-depleted embryos and those lacking Engrailed function, implying that *pbx* and *eng* genes may function on a common genetic pathway in vertebrates.

To more closely examine the integrity of the DMB in Pbx-depleted embryos, we analyzed the expression of *pax6a* and *eng2a* in 16.5 hpf embryos (Figure 5-4E-H′). In wild type embryos, cells expressing forebrain (*pax6a*) and midbrain (*eng2a*) markers exist as separate populations (arrows in Figure 5-4E, G). In 16.5 hpf Pbx-depleted embryos, the integrity of the DMB has been compromised, as indicated by the region of overlap between forebrain and midbrain cells due to a caudal expansion of *pax6a* and a rostral expansion of *eng2a* (brackets in Figure 5-4F, F′, H, H′) Analysis of *eng2a* expression using fluorescent visualization of Fast Red-labeled *eng2a* probe details this anterior-ward expansion of the midbrain domain (Figure 5-4E′-H′). These results demonstrate that Pbx proteins are required to maintain separate populations of forebrain and midbrain cells, a critical element of DMB formation and positioning.

Given the overlap between forebrain and midbrain genetic markers at 16.5 hpf, we examined 20 hpf and 28 hpf embryos to determine if cells were able to subsequently reorganize into proper domains. In 20 hpf Pbx-depleted embryos, the overlap between *pax6a* and *eng2a* expressing cells observed earlier at 16.5 hpf has diminished (Figure 5-4J). *pax6a*-expressing cells from the diencephalon and hindbrain have encroached into the former mesencephalon and *eng2a* expression has retreated to small dorsal and ventral domains (compare brackets in Figure 5-4I, J). At 28 hpf, we used *pax6a* as a marker for forebrain identity and included *isl1* to label interneurons of the posterior commissure, located just anterior to the DMB. In wild type embryos, the forebrain and hindbrain expression domains of *pax6a* are separated by the midbrain (Figure 5-4K). However, like the 20 hpf Pbx-depleted embryos, these two domains of *pax6a* expression are nearly fused in 28 hpf Pbx-depleted embryos, and the caudal limit of forebrain *pax6a* has an obvious bulge midway along the dorsal-ventral axis (Figure 5-4J, L). Additionally, the number and caudal position of the posterior commissure cell bodies are markedly expanded (brackets in Figure 5-4I-L), whereas the neuronal cell population at the epiphysis is mostly unaffected (marked with an asterisk). This suggests, that the dorsal pretectal area (marked by the posterior commissure) expands posteriorly in Pbx-depleted embryos, whereas the more anteriorly positioned epithalamus (epiphysis) is less affected.

These data show that Pbx function is required to maintain the distinction between the forebrain and midbrain. In Pbx-depleted embryos, MHB development is initiated correctly, but expression of MHB patterning genes is not maintained. There is a transient period during which *pax6a* and *eng2a* expressing cells can share the same region of the midbrain, but eventually the mesencephalic region adopts a forebrain fate. It has been demonstrated in *noi* and *eng2a/2b*MO embryos that the midbrain adopts a forebrain fate (Scholpp and Brand, 2003; Scholpp et al., 2003). Other studies have demonstrated that a loss of MHB gene expression leads to a decrease in cell proliferation and / or an increase in cell death in the mesencephalon (Brand et al., 1996; Chi et al., 2003; Jaszai et al., 2003), and this may account for the eventual replacement of the mesencephalon with forebrain

cells in Pbx-depleted embryos. In wild type embryos, Engrailed proteins are believed to be the principle factor that prevents the rostral midbrain from adopting a forebrain identity. From an early stage, *eng2a* is expressed immediately adjacent to the forebrain *pax6a* domain, thus placing it in an excellent position to repress diencephalic gene expression (Scholpp et al., 2003). Furthermore, in chick, ectopic Engrailed can repress *pax6a* expression in the forebrain, and does so before leading to the activation of other MHB genes (Araki and Nakamura, 1999). Therefore, together with the established genetic and biochemical interactions between fly Engrailed and Exd / Pbx proteins, the failure to maintain the MHB and DMB in Pbx-depleted embryos strongly suggests that zebrafish Pbx and Engrailed proteins cooperate to pattern the midbrain region of the neural tube.

5.2.3 Eng protein activity is dependent on the presence of Pbx proteins

Our finding that Pbx-depleted embryos resemble a loss of Engrailed function suggests a biochemical dependence of Eng function on Pbx proteins. To test this hypothesis directly, we determined whether Eng function is dependent on the presence of Pbx. We used an Eng overexpression assay in which we injected *eng2a* mRNA into single-cell zebrafish embryos and examined the resulting change in forebrain *pax6a* expression (Figure 5-5) (Araki and Nakamura, 1999; Scholpp et al., 2003). Injection of low doses of *eng2a* mRNA caused strong reduction of *pax6a* expression, with only a vestigial stripe of *pax6a* typically remaining at the anterior-most region of the injected embryo (67.7%, *n*=341; Figure 5-5A, B). The *eng2a*-dependent repression of *pax6a* in the forebrain was accompanied by a marked shortening of the forebrain region and a loss of eye formation. To determine whether the biological activity of ectopic Eng2a is dependent on the presence of Pbx4 protein, we also injected *eng2a* into maternal, zygotic *lzr* (mz*lzr*) mutant embryos. We chose to use mz*lzr* embryos to avoid the difficulty in scoring expression domains caused by the expansion of *pax6a* that is seen in Pbx-less embryos. The loss of maternal and zygotic Pbx4 potently attenuated the biological activity of injected *eng2a* mRNA. mz*lzr*, *eng2a*-injected embryos possessed both eyes, and near-normal levels of *pax6a* expression

(strongly reduced in only 1.3% of injected embryos, *n*=75; Figure 5-5C, D). The presence of Pbx2 protein in these embryos may account for some of the residual *pax6a* repressing activity of ectopic Eng2a. These results show that the ability of overexpressed Eng2a to repress *pax6a* expression is largely dependent upon the presence of Pbx4 protein. These data suggest that Eng and Pbx proteins act together to repress diencephalic fate in the vertebrate midbrain.

5.2.4 A biochemical interaction between Pbx and Eng is required for Eng function

A biochemical interaction between both vertebrate and *Drosophila* Eng and Pbx/Exd proteins has been documented previously (Peltenburg and Murre, 1996; van Dijk et al., 1995). This interaction requires an intact hexapeptide motif (WPAWVY) in Eng and the TALE-motif in Pbx (Figure 5-6A). To confirm that the zebrafish proteins possess similar biochemical properties, we performed EMSA using in vitro translated zebrafish Eng2a (fused to a 6X Myc epitope) and Pbx4 (Figure 5- 6B). We assayed for cooperative binding by mixing proteins together with a ^{32}P-labeled oligonucleotide that binds both Eng2a and Pbx4 (van Dijk et al., 1995). Whereas Eng2a has the ability to bind the oligo in the absence of Pbx4, we find that zebrafish Pbx4 will bind the oligo only in the presence of Eng2a proteins (compare lanes 1, 2 and 7 in Figure 5-6B). To examine which residues are required for an interaction between zebrafish Pbx and Eng, we mutated the orthologous residues to those which are required for mouse Pbx-Eng interactions, tryptophan residues 145 and 148 within the hexapeptide motif of Eng2a. We found that mutation of either tryptophan (W145K, W145S, or W148K) completely eliminated cooperative DNA binding with Pbx4 protein, implying that these mutated Eng proteins cannot bind effectively to Pbx (Figure 5-6B lanes 8-11). The ability of Eng2a to bind the oligo was not affected by mutation of either tryptophan residue. However, we observed a general decrease in the ability of Eng2a with non-functional hexapeptide motifs to bind the oligo in the presence of Pbx4 (Figure 5-6B lanes 8-11). We expect that this is a result of a residual in vitro interaction between Pbx4 and Eng2a that leaves both proteins in a

conformation that is unfavorable for binding DNA. This incomplete interaction may involve the EH2 and EH3 domains just N-terminal to the Eng homeodomain (Figure 5-6A) that have previously been shown to be required for the Eng-Pbx interaction (Peltenburg and Murre, 1996). Our EMSA results show that there is an evolutionarily conserved biochemical interaction between zebrafish Eng2a and Pbx4 mediated by the tryptophan residues of the hexapeptide domain, agreeing with previous work performed on the orthologous murine and *Drosophila* proteins.

According to our experiments with Pbx-depleted embryos, reduction of *pax6a* expression by overexpressed Eng2a requires the presence of Pbx proteins (Figure 5-5). To directly test whether ectopically expressed Eng2a must have the ability to bind Pbx proteins in order to reduce *pax6a* expression, we injected one-cell wild type embryos with the same mRNAs used in our gel shift assays. We then assayed for *pax6a* expression to compare the biological activity of wild type Eng2a with that of the hexapeptide mutants which cannot bind directly to Pbx proteins. We find that all of the Eng2a hexapeptide mutants have dramatically lowered biological activity. Whereas 76.2% (n=126) of *eng2a* WT injected embryos show reduced expression of *pax6a* (Figure 5-7B, G), only 6.6% of embryos injected with *eng2a*-W148K and 17.2% of embryos injected with *eng2*a-W148S show any observable reduction of *pax6a* (Figure 5-7C, F, G). Mutation of both tryptophan residues together (WWKK) was similar to mutation of the W148 alone (7.9% showing reduced expression; Figure 5-7E, G). Mutation of the other conserved Eng2a tryptophan residue alone (W145) leads to a subtly smaller attenuation of biological activity (24% showing reduced *pax6a*; Figure 5-7D, G). All *eng2a* mRNA constructs were expressed as full-length proteins and translated at similar efficiencies (Figure 5-7H), showing that the point mutations introduced into the *eng2a* coding region did not affect the translation or stability of the protein product. Taken together, these results agree with our in vitro gel-shift assays and show that the repression of *pax6a* expression by Eng2a in vivo requires the ability to directly bind Pbx4.

To establish whether Eng and Pbx proteins cooperate to pattern the MHB, we examined the ability of wild type and tryptophan-mutant forms of *eng2a* mRNA to rescue the MHB defects of *eng2a,2b* morphants and *pbx2,4* morphants (Figure 5-8). First, we examined the effects of overexpressing the WT and WWKK forms of *eng2a* mRNA on the MHB by assaying for *pax2a* expression. As shown previously, the ectopic expression of wild type *eng2a* causes a loss of eye formation. In 65% embryos that exhibit this phenotype, we also observe a slight expansion of *pax2a* expression at the MHB (*n*=37) (Figure 5-8B). On the other hand, overexpression of *eng2a* WWKK does not lead to an expansion of the MHB. Furthermore, in 47% of these embryos (*n*=73) we observe a decrease in *pax2a* expression, suggesting the tryptophan-mutant forms of Eng2a can act as a dominant negative (Figure 5-8C). We speculate that Eng2a WWKK can bind to promoter sites normally occupied by Eng-Pbx heterodimers and prevent the normal regulation of target genes, thereby causing the dominant negative effect. These results suggest that Eng2a requires an intact hexapeptide motif in order to properly regulate MHB development. To further test this, we attempted to rescue *eng2a* and *eng2b* double morphants (*eng2a,2b*MO) with wild type and WWKK forms of *eng2a* mRNA. At the dose of morpholino we used (8ng of each MO), knockdown of both Eng2a and Eng2b lead to a dramatic decrease in *pax2a* expression at the MHB (Figure 5-8D). Injection of wild type *eng2a* RNA resulted in near normal levels of *pax2a* expression in 67% of *eng2a,2b*MO embryos (*n*=15) (Figure 5-8E). *eng2a* WWKK was unable to rescue the MHB phenotype of *eng2a,2b*MO embryos (100%, *n*=20) (Figure 5-8F). To see if *eng2a* RNA is able to rescue the MHB phenotype of Pbx-depleted embryos, we injected *pbx2* and *pbx4* double morphant embryos with either WT or WWKK forms of *eng2a* mRNA. The loss of *pax2a* expression at the MHB in Pbx-depleted embryos (Figure 5-8G) cannot be fully rescued by injection of WT *eng2a* mRNA (*n*=14), though we do observe a partial rescue in 36% of embryos (Figure 5-8H). We attribute this partial rescue to incomplete knockdown of Pbx proteins by morpholino treatment in some embryos, since the degree of rescue correlates with the amount of *egr2b* remaining in the hindbrain of Pbx-depleted embryos.

Injection of Pbx-depleted embryos with *eng2a* WWKK cannot rescue *pax2a* expression at the MHB (100%, *n*=26) (Figure 5-8I). Taken together, the dominant negative effect of *eng2a* WWKK mRNA at the MHB, its inability to rescue *eng2a,2b* morphants, and the inability of WT *eng2a* mRNA to rescue Pbx-depleted embryos all suggest that Engrailed function at the MHB requires a biochemical interaction with Pbx proteins.

5.3 Discussion

In this paper, we present evidence that zebrafish Pbx2 and Pbx4 proteins act as biochemical partners with Eng proteins to pattern the mesencephalic territory of the developing vertebrate neural tube. This new role as a midbrain patterning factor expands upon the previously reported role of zebrafish Pbx2 and Pbx4 as Hox co-factors in patterning the hindbrain. We show that the expression of MHB markers is initiated, but not maintained in Pbx-depleted embryos, suggesting that Pbx participates in the cross-regulatory loop that maintains MHB gene expression. Furthermore, diencephalic markers *pax6a* and *epha4a* are expanded caudally and that there is an anomalous overlap between *pax6a* and *eng2a* expressing cells at the DMB in Pbx-depleted embryos. We used an Eng2a overexpression assay to demonstrate that the *pax6a* repressing activity of Eng2a depends largely upon the presence of Pbx4 protein. Lastly, we show that zebrafish Pbx4 and Eng2a interact biochemically in vitro via Engrailed's hexapeptide motif, and that this biochemical interaction is required for Engrailed's role in regulating MHB development. Taken together, these data suggest a model whereby Pbx and Eng proteins cooperate biochemically to pattern the developing vertebrate midbrain.

5.3.1 The interaction between Eng and Pbx/Exd is conserved in vertebrates

Drosophila Engrailed is an important factor in establishing and maintaining cellular compartments during development (reviewed in Hidalgo, 1996). Engrailed fulfills this role in part through its biochemical interaction with Exd, the fly orthologue of Pbx (Alexandre and Vincent, 2003; Kobayashi et al.,

2003; Peifer and Wieschaus, 1990). Engrailed's role in forming lineage restricted compartments is highly conserved in vertebrates, as evidenced by the Engrailed loss-of-function phenotype in the mesencephalon (Scholpp and Brand, 2001; Wurst et al., 1994). In this paper, we show that the ability of Engrailed to pattern the MHB and DMB is dependent on its interaction with Pbx proteins. Thus, the partnership between Engrailed and Pbx/Exd, their mechanism of biochemical interaction, and their role in the transcriptional regulation of boundary formation are all conserved between flies and vertebrates.

5.3.2 Pbx proteins act outside of the hindbrain to pattern the zebrafish embryo

Pbx proteins are well characterized as Hox co-factors that function to compartmentalize the vertebrate hindbrain. However, previous research has demonstrated that Pbx proteins do function outside of the hindbrain, sometimes in a Hox-independent fashion. *Pbx*-deficient mice have defects in Hox-dependent processes such as organogenesis (Manley et al., 2004; Schnabel et al., 2003), hematopoiesis (DiMartino et al., 2001), limb formation (Capellini et al., 2006), and skeletal and cartilage formation (Selleri et al., 2001). Other studies in zebrafish and mouse have demonstrated Hox-independent functions for Pbx proteins as cofactors for MyoD in muscle cells (Berkes et al., 2004), Pdx1/Ipf1 in pancreatic development (Dutta et al., 2001; Kim et al., 2002; Peers et al., 1995), and for the metaHox protein Rnx/Hox11L2/Tlx-3 to control development of the medullary respiratory control mechanisms (Rhee et al., 2004). Our finding that Pbx cooperates with Eng proteins to pattern the midbrain adds to this growing body of evidence that vertebrate Pbx proteins are involved in a myriad of developmental processes in multiple tissue types, and that some functions of Pbx proteins are Hox-independent.

Our results also suggest that Pbx proteins are key regulators of compartmental boundaries. In the absence of Pbx function, the primary division of the neuroectoderm into presumptive fore-, mid-, and hindbrain regions still occurs normally. Subsequent to this, these boundaries are reinforced and maintained

while the tissues are secondarily subdivided. Our results show that, in the absence of Pbx function, the midbrain region is initiated correctly, but that secondary maintenance of the MHB and DMB is compromised. This result is consistent with the role already described for Pbx in the hindbrain. A Pbx (Waskiewicz et al., 2002), Meis (Choe and Sagerstrom, 2004) or Pknox (Deflorian et al., 2004) loss-of-function prevents the rhombomere boundaries from ever forming, but does not prevent the initial specification of the hindbrain region. Thus, it appears that a general role for Pbx proteins during vertebrate development is to act as transcriptional co-factors throughout the midbrain and hindbrain in the formation and maintenance of lineage-restricted boundaries. Whether or not Pbx participates in lineage restriction between compartments within the forebrain has not been investigated.

5.3.3 The requirement for zebrafish Pbx proteins in regulating midbrain gene expression

A loss of *pax2a* or *engrailed* function in the vertebrate midbrain is characterized by a reduction of the tectum and cerebellum, and a failure to maintain the morphological and genetic characteristics of the isthmic organizer at the MHB. In fish, it is possible to study a partial loss of *engrailed* function by using morpholinos against one of the two *eng* paralogues, *eng2a* (*eng2*) or *eng2b* (*eng3*) (Scholpp and Brand, 2001). Eng2b knockdown has very limited phenotypic effects, but the loss of *eng2a* function leads to a morphological phenotype that is intermediate between wild type and *eng2a/2b*MO or *noi* embryos. The ventral region of the MHB is especially sensitive to Eng2a knockdown, as the ventral domains of *pax2a* and *eng2b* expression are lost. Similar DV patterning defects can be observed in weak alleles of *pax2a* (Lun and Brand, 1998). We observe similar defects in Pbx-depleted embryos. The medio-ventral domain of MHB gene expression preferentially lost (Figure 5-3), and the isthmic constriction is diminished, but not completely eliminated (Figure 5-1). This result shows that a Pbx loss-of-function is not equivalent to a complete Engrailed loss-of-function, suggesting that some activities of Engrailed are Pbx-

independent. The idea that Engrailed can act independently of Pbx is also supported by the observation that Engrailed proteins with mutated hexapeptide domains still possess some ability to repress *pax6a* expression in zebrafish embryos (Figure 5-7). These data suggest either of two possibilities: that Engrailed can act independently of Pbx, or that the Pbx-Engrailed interaction in vivo is not solely dependent on a functional hexapeptide domain in Engrailed. Although either theory is possible, it has been demonstrated in flies that En requires Exd for activation of some targets, but not the repression of others (Alexandre and Vincent, 2003; Kobayashi et al., 2003; Serrano and Maschat, 1998). Therefore, it is likely that some functions of Eng are Pbx-independent.

5.3.4 Downstream effects of Pbx depletion on midbrain structures and function

Besides patterning the DMB and MHB regions of the neural tube, Engrailed function is also required to establish spatial polarity in the optic tectum. A rostrocaudal gradient of Engrailed expression in the tectum is necessary for correct topographic targeting of the retinal ganglion cell axons (Friedman and O'Leary, 1996; Itasaki et al., 1991; Itasaki and Nakamura, 1996; Logan et al., 1996; reviewed in Nakamura and Sugiyama, 2004). Engrailed likely exerts that effect by regulating the gradient expression of Ephs and Ephrins in the tectum (Logan et al., 1996). The Eph family of RTKs and their Ephrin ligands are essential components in establishing tectal polarity, mediating axon guidance and forming the retinotectal topographic map (reviewed in Drescher et al., 1997). Our analysis of Pbx-depleted embryos shows that the rostrocaudal gradient of *eng2a* is abolished by 21 hpf, suggesting that Pbx-depletion may cause tectal patterning defects later in development. We found that the normal patterns of *epha4a* (Figure 5-1A-D) and *efna2* gene expression in the presumptive tectum are disrupted in Pbx-depleted embryos (French et al., 2007). Both *epha4a* and *efna2* have been implicated in retinal ganglion axon guidance (Marin et al., 2001; Pfeiffenberger et al., 2005; Walkenhorst et al., 2000). This result implies that, together with defects

in the DMB, Pbx-depleted embryos may also exhibit abnormalities in tectal patterning and retinal ganglion cell axon projection defects.

5.4 Figures

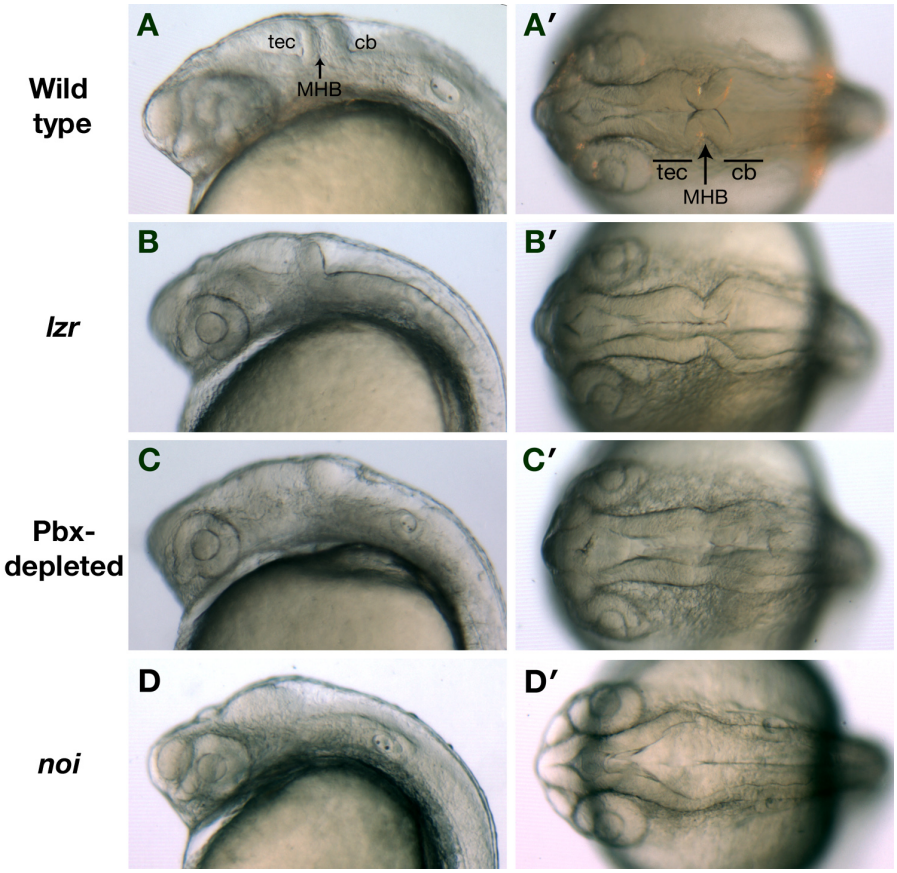

Figure 5-1. The morphology of the MHB, tectum and cerebellum is defective in Pbx-depleted embryos at 24 hpf. **(A, A′)** Wild type embryos at 24 hpf possess a well formed tectum (tec) and cerebellum (cb) separated by the isthmic constriction at the MHB. **(B, B′)** *lzr* (*pbx4*$^{-/-}$) embryos have a normal cerebellum, but the size of the tectum is diminished and the isthmus is not as well formed. **(C, C′)** In Pbx-depleted embryos, the isthmic constriction at the MHB is indistinct, and neither the tectum nor cerebellum has formed properly. **(D, D′)** By way of comparison, *noi* (*pax2a*$^{-/-}$) embryos lack all midbrain-derived structures. The isthmus is completely absent and the tectum and cerebellum are unrecognizable. Anterior is to the left; panels A-D are lateral views and panels A′- D′ are dorsal views.

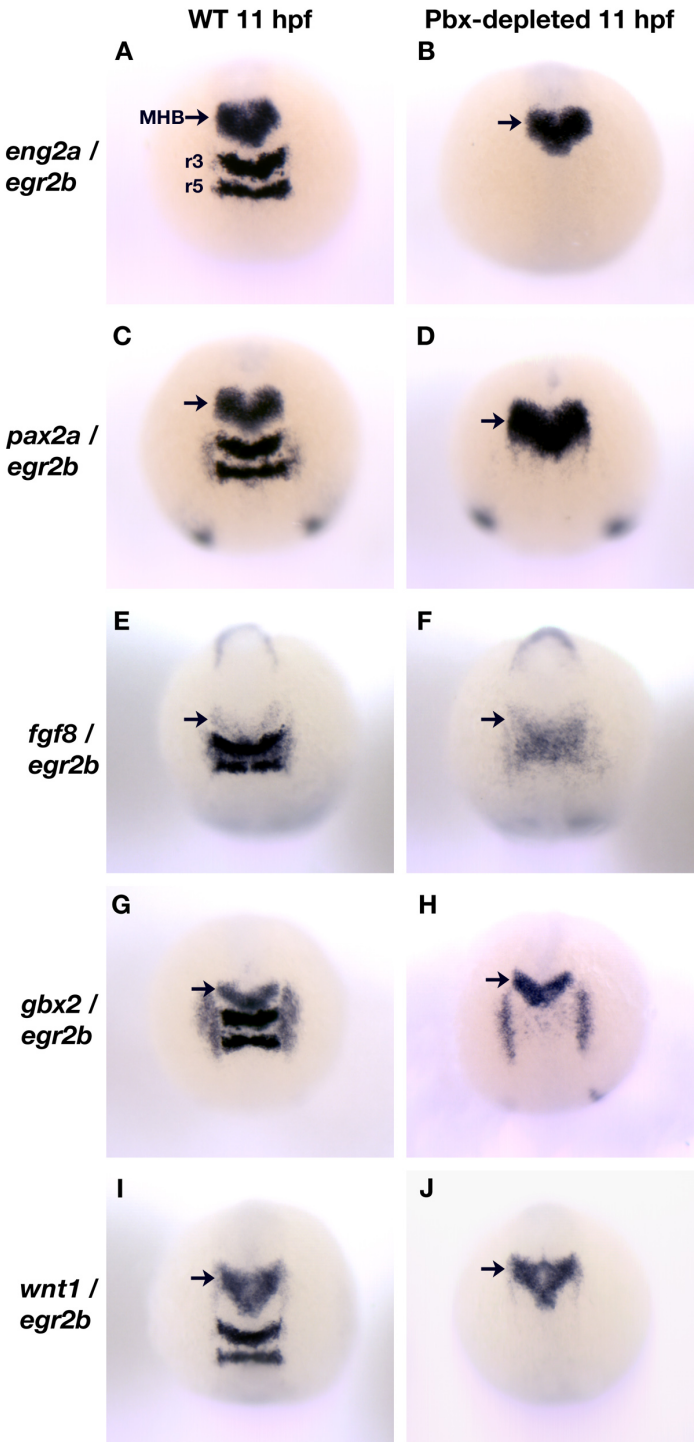

Figure 5-2. The establishment of the midbrain region of the neural tube is normal in Pbx-depleted embryos. *eng2a* (A, B), *pax2a* (C, D), *fgf8* (E, F), *gbx2* (G, H) and *wnt1* (I, J) expression at the MHB is normal in both wild type (WT) and Pbx-depleted embryos at 11 hpf. The absence of *egr2b* (*krox20*) expression in the rhombomeres 3 and 5 of the presumptive hindbrain was used as an indicator of Pbx loss-of-function. All embryos are shown in dorsal view with anterior at the top. Abbreviations: MHB - midbrain-hindbrain boundary; r3 - rhombomere 3; r5 - rhombomere 5. Arrows indicate the MHB.

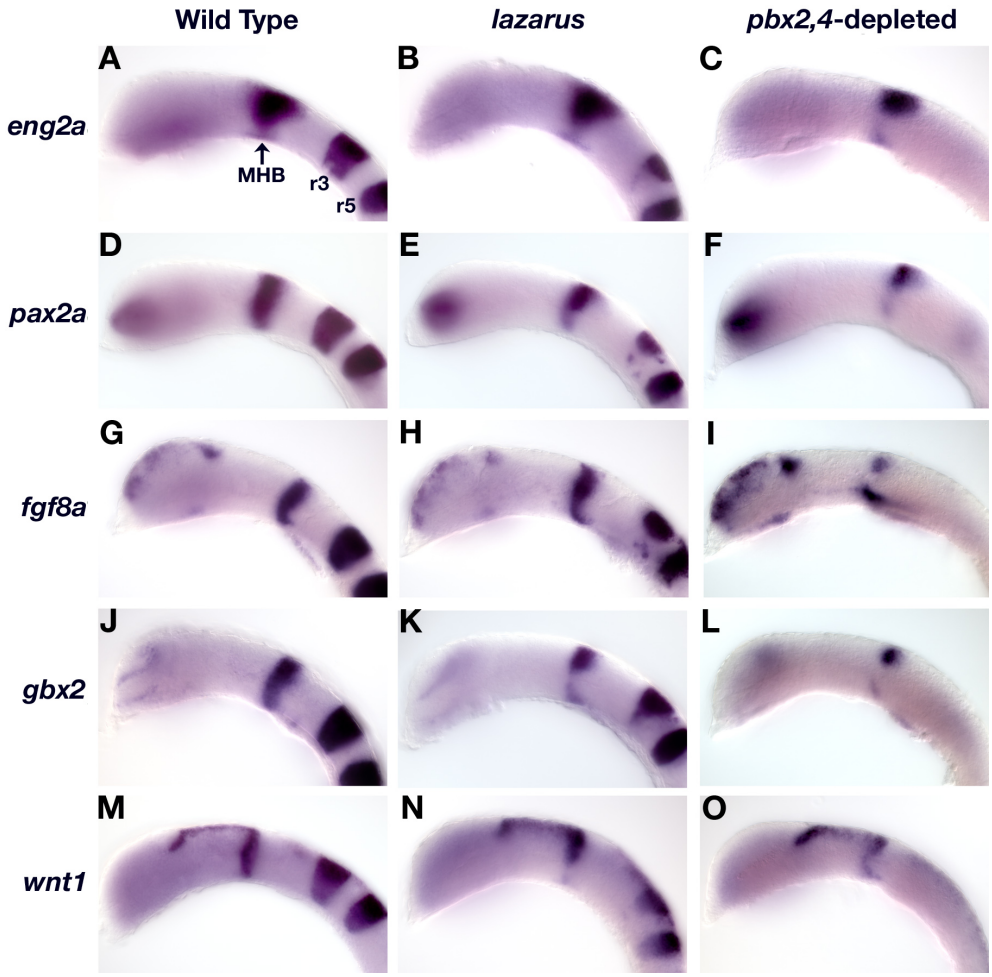

Figure 5-3. Pbx-depleted embryos do not maintain gene expression at the MHB. **(A-C)** *eng2a*: In 18 hpf wild type embryos, *eng2a* is expressed broadly across the MHB in a wedge-shaped domain (A). *eng2a* expression is decreased slightly in *lzr* embryos (B). In Pbx-depleted embryos, the ventral expression of *eng2a* is greatly decreased and the rostral domain is diminished. **(D-F)** *pax2a*: At 18 hpf, *pax2a* expression at the MHB is normally restricted to a narrow stripe with approximately equal expression over the dorsal-ventral axis (D). In *lzr* embryos, *pax2a* expression is decreased in the ventral domain (E). In Pbx-depleted embryos, the ventral expression of *pax2a* is also completely absent (F). **(G-L)** *fgf8* and *gbx2*: Both *fgf8* and *gbx2* are expressed in the caudal half of the MHB at 18 hpf (G, J). *fgf8* expression is normal in *lzr* embryos (H), whereas the ventral domain of *gbx2* expression is decreased (K). In Pbx-depleted embryos, the medial domain of *fgf8* expression is lost, while the dorsal domain is decreased and the

ventral domain is expanded caudally (I). The effect of Pbx-depletion on *gbx2* expression is more severe with only a residual dorsal patch remaining (L). **(M-O)** *wnt1*: In 18 hpf wild type embryos, *wnt1* is expressed in the rostral half of the MHB and the dorsal diencephalons (M). The ventral domain of wnt1 expression at the MHB is decreased in *lzr* embryos, whereas the dorsal domains remain unchanged (N). In Pbx-depleted embryos, *wnt1* expression is decreased at the MHB and expanded caudally, but is expressed in the dorsal diencephalon at near normal levels. All embryos are shown in lateral view with anterior to the left. Abbreviations: MHB – midbrain-hindbrain boundary; r3 – rhombomere 3; r5 – rhombomere 5. Arrows indicate the MHB.

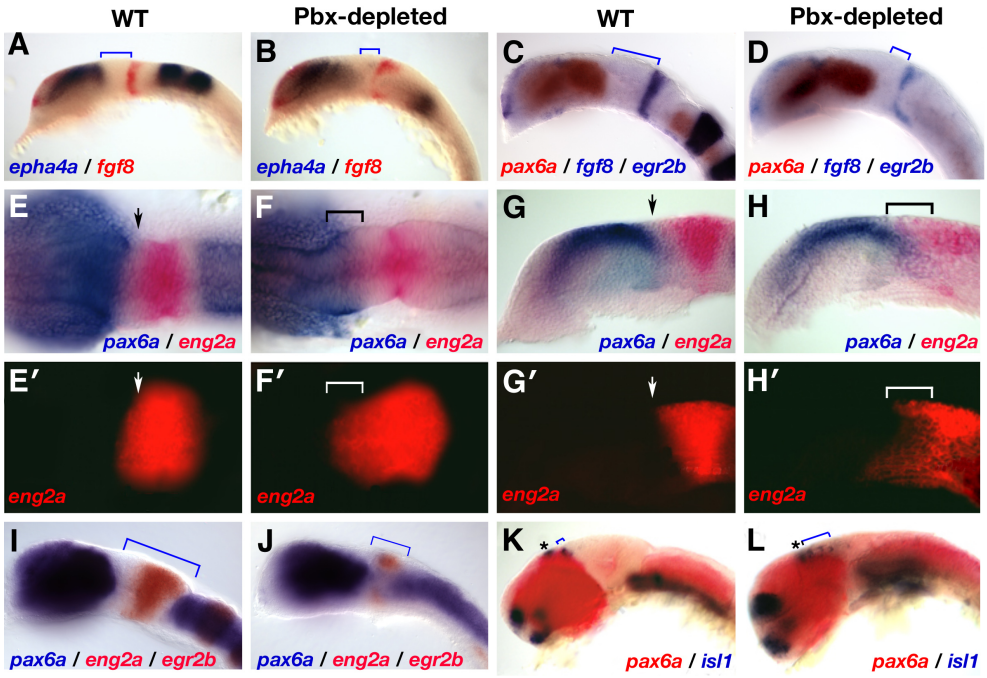

Figure 5-4. The boundary between diencephalon and mesencephalon (DMB) is not formed properly in Pbx-depleted embryos. **(A-D)**: We examined the size of forebrain and midbrain domains in 16.5 hpf (A, B) and 18 hpf (C, D) Pbx-depleted embryos. The expression domains of *epha4a* (A, B) and *pax6a* (C, D) are expanded caudally at the expense of midbrain territory, as indicated by the blue brackets. **(E-H′)**: Forebrain and midbrain cells no longer exist as separate populations in Pbx-depleted embryos. In wild type (WT) 16.5 hpf embryos, *pax6a* (blue) and *eng2a* (red) expressing cells are separated by a sharp boundary at the DMB (arrow heads E, E′, G, G′). 16.5 hpf Pbx-depleted embryos exhibit a loss of DMB integrity, a caudal expansion of *pax6a* and a rostral expansion of *eng2a* expression (F, F′, H, H′). There is a region of overlap between these two cell populations as indicated by the brackets in F, F′, H, and H′. Note that identical embryos are shown in E-H and E′-H′. **(I - L)**: Midbrain territory is lost in older Pbx-depleted embryos. Wild type 20 hpf embryos have well defined forebrain and hindbrain *pax6a* domains separated by *eng2a* positive cells of the midbrain. In 20 hpf Pbx-depleted embryos, the forebrain and hindbrain domains of *pax6a* expression have moved into the mesencephalic region (compare brackets in I and J) while *eng2a* expression is limited to residual dorsal and ventral patches. To

determine the state of the DMB in 28 hpf Pbx-depleted embryos, we analyzed the expression of *pax6a* (red) and visualized the position of the epiphysis (marked with an asterisk) and posterior commissure interneurons by analyzing expression of *isl1* (blue). In wild type embryos, the *isl1*-positive neurons of the posterior commissure are tightly grouped (blue brackets in K). In 28 hpf Pbx-depleted embryos, the position of the posterior commissure neurons is caudally expanded (marked by blue brackets in L), while the *isl1*-positive neurons of the epiphysis are unaffected. Embryos were imaged either using DIC microscopy (A-H, I-L) or using fluorescent emission of Fast-Red stain (E′-H′). All embryos are deyolked and shown as either lateral or dorsal views with anterior to the left, except the embryos shown in G, G′, H, and H′, which are saggital sections. Note: experiments in panels A, B, E-H', K and L were performed by Stefen Scholpp and Andrew Waskiewicz.

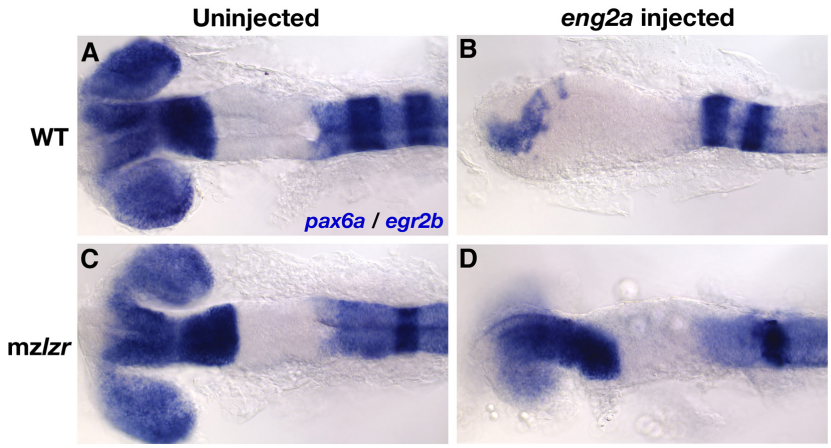

Figure 5-5. Activity of ectopically expressed *eng2a* mRNA is dependent on presence of Pbx4 protein. We analyzed the expression of *pax6a* by in situ hybridization to visualize the effect of ectopic *eng2a* overexpression in both 18 hpf wild type (WT) (A,B) or mz*lzr* embryos (C,D). We also analyzed the expression of the rhombomere 3 and 5 marker *egr2b* to distinguish which embryos had the mz*lzr* genotype (lack of r3 *egr2b* expression). Injection of 50 pg *eng2a* mRNA causes profound defects in the formation of the forebrain, including a reduction in *pax6a* expression and the loss of eye formation (compare A and B). These effects are strongly attenuated in embryos lacking Pbx4 (compare C and D). All views are dorsal with anterior to the left. Note: this experiment was performed by Andrew Waskiewicz.

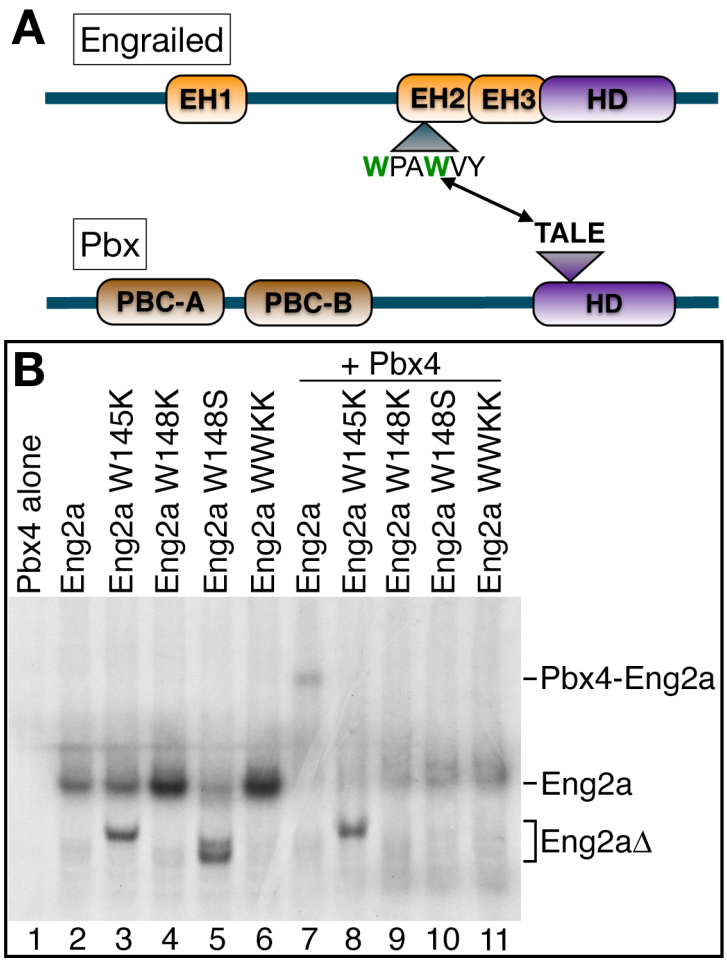

Figure 5-6. Eng2a requires a functional Pbx-binding hexapeptide to bind Pbx4 in vitro. **(A)** Schematic of the biochemical interaction between the Engrailed hexapeptide (WPAWVY) and the Pbx TALE motif. **(B)** EMSA demonstrating a hexapeptide-dependent interaction between Zebrafish Pbx4 and Eng2a. By site-directed mutagenesis, zebrafish Eng2a tryptophan residues W145 and W148 were changed to either lysine (W145K, W148K, WWKK), or a serine (W148S) residues, and tested for cooperative binding with Pbx4. In lanes containing Pbx4 (Lanes1, 7-11), only the sample containing both Pbx4 and myc-Eng2a was capable of binding the ^{32}P-labeled oligo (Lane 7). Mutations in the Eng2a hexapeptide abrogated cooperative Eng2a-Pbx4 binding to the oligo (Lanes 8-11). Note: this experiment was performed by Andrew Waskiewicz.

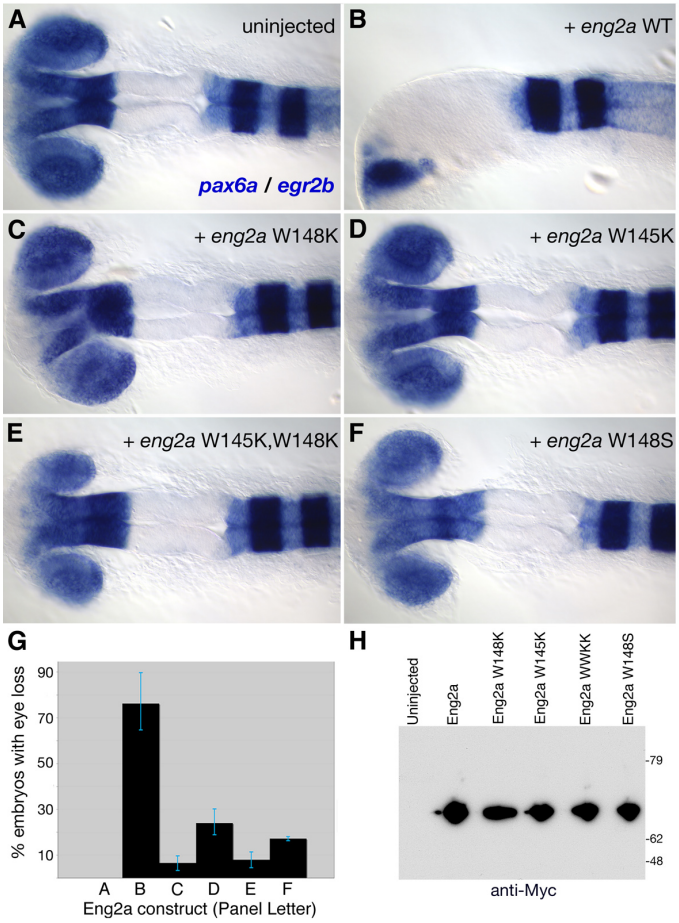

Figure 5-7. Eng2a proteins with point mutations in the hexapeptide exhibit attenuated *pax6a*-reducing activity. To determine whether mutations in the Eng2a hexapeptide affected the in vivo activity of overexpressed *eng2a*, we injected mRNAs coding for the same myc-Eng2a proteins that we used in our EMSA assay and assayed for *pax6a* and *egr2b* expression by in situ analysis. **(A, B)** Uninjected wild type embryos never exhibited eye loss, while the majority of embryos injected with *eng2a* mRNA displayed a loss of eye formation and greatly reduced *pax6a* expression. **(C-F)** Mutations in the Eng2a hexapeptide, W148K (C), W145K (D), W145KW148K (WWKK) (E), W148S (F), resulted in strongly reduced biological activity compared to the wild type Eng2a (B). **(G)** Biological effects of each construct were quantified and are shown with the error bars denoting the range of values from two separate experiments. Compared to the activity of wild type Eng2a, mutations in the hexapeptide caused a 3-11X reduction in activity. **(H)** Western blot analysis of overexpressed Myc-tagged Eng2a proteins using the monoclonal α-myc 9E10 antibody (9E10). All Eng2a proteins were full length and present at similar levels, showing that the point mutations introduced into the *eng2a* coding region did not affect protein translation or stability. Note: experiments in Panels A-G performed by Andrew Waskiewicz.

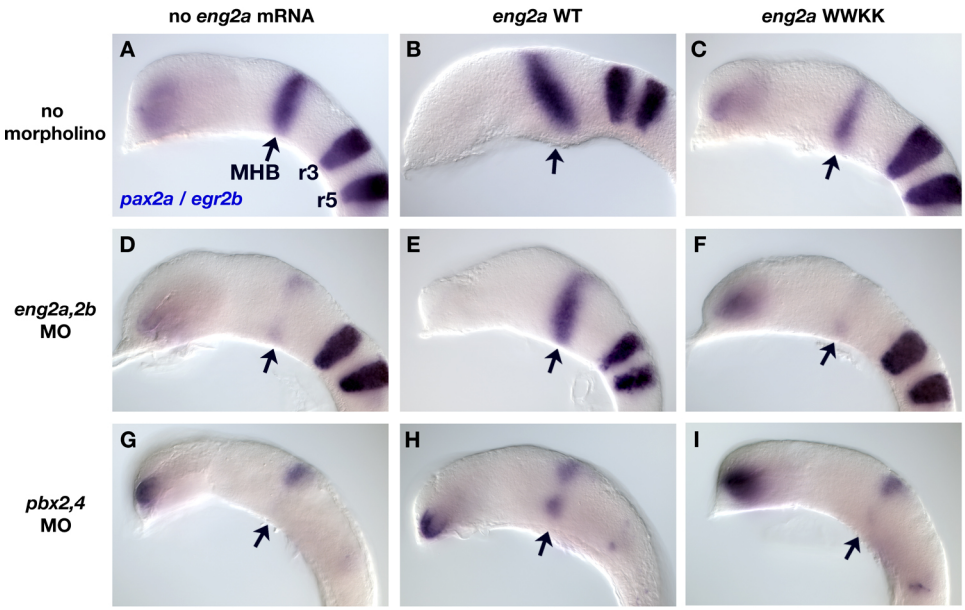

Figure 5-8. Engrailed and Pbx cooperatively regulate midbrain-hindbrain boundary development. **(A-C)** We used *pax2a* as a marker for the MHB in wild type, *eng2a* WT, and *eng2a* WWKK injected embryos. Overexpression of wild type Eng2a causes a slight expansion of the MHB, together with a loss of eye formation (compare A and B). Overexpression of a hexapeptide mutated form of Eng2a (WWKK) has a dominant negative effect on MHB development, as shown by the decrease in *pax2a* expression (compare A and C). **(D-F)** *eng2a,2b* morphant embryos (D) can be rescued by injection with wild type *eng2a* mRNA (E), but not by *eng2a* WWKK (F). **(G-I)** The MHB defect in Pbx-depleted embryos (G) cannot be rescued by injection of either *eng2a* WT (H) or *eng2a* WWKK (I). All embryos are deyolked and mounted laterally with anterior to the left. Abbreviations: MHB – midbrain-hindbrain boundary; r3 – rhombomere 3; r5 – rhombomere 5. Arrows indicate the MHB.

5.5 References

Alexandre, C., Vincent, J. P., 2003. Requirements for transcriptional repression and activation by Engrailed in Drosophila embryos. Development. 130**,** 729-39.

Alvarado-Mallart, R. M., Martinez, S., Lance-Jones, C. C., 1990. Pluripotentiality of the 2-day-old avian germinative neuroepithelium. Dev Biol. 139**,** 75-88.

Araki, I., Nakamura, H., 1999. Engrailed defines the position of dorsal di-mesencephalic boundary by repressing diencephalic fate. Development. 126**,** 5127-35.

Berkes, C. A., Bergstrom, D. A., Penn, B. H., Seaver, K. J., Knoepfler, P. S., Tapscott, S. J., 2004. Pbx marks genes for activation by MyoD indicating a role for a homeodomain protein in establishing myogenic potential. Mol Cell. 14**,** 465-77.

Brand, M., Heisenberg, C. P., Jiang, Y. J., Beuchle, D., Lun, K., Furutani-Seiki, M., Granato, M., Haffter, P., Hammerschmidt, M., Kane, D. A., Kelsh, R. N., Mullins, M. C., Odenthal, J., van Eeden, F. J., Nusslein-Volhard, C., 1996. Mutations in zebrafish genes affecting the formation of the boundary between midbrain and hindbrain. Development. 123**,** 179-90.

Brunet, I., Weinl, C., Piper, M., Trembleau, A., Volovitch, M., Harris, W., Prochiantz, A., Holt, C., 2005. The transcription factor Engrailed-2 guides retinal axons. Nature. 438**,** 94-8.

Burgess, S., Reim, G., Chen, W., Hopkins, N., Brand, M., 2002. The zebrafish spiel-ohne-grenzen (spg) gene encodes the POU domain protein Pou2 related to mammalian Oct4 and is essential for formation of the midbrain and hindbrain, and for pre-gastrula morphogenesis. Development. 129**,** 905-16.

Capellini, T. D., Di Giacomo, G., Salsi, V., Brendolan, A., Ferretti, E., Srivastava, D., Zappavigna, V., Selleri, L., 2006. Pbx1/Pbx2 requirement for distal limb patterning is mediated by the hierarchical control of Hox gene spatial distribution and Shh expression. Development. 133**,** 2263-73.

Chan, S. K., Popperl, H., Krumlauf, R., Mann, R. S., 1996. An extradenticle-induced conformational change in a HOX protein overcomes an inhibitory function of the conserved hexapeptide motif. Embo J. 15**,** 2476-87.

Chang, C. P., Shen, W. F., Rozenfeld, S., Lawrence, H. J., Largman, C., Cleary, M. L., 1995. Pbx proteins display hexapeptide-dependent cooperative DNA binding with a subset of Hox proteins. Genes Dev. 9**,** 663-74.

Chi, C. L., Martinez, S., Wurst, W., Martin, G. R., 2003. The isthmic organizer signal FGF8 is required for cell survival in the prospective midbrain and cerebellum. Development. 130**,** 2633-44.

Choe, S. K., Sagerstrom, C. G., 2004. Paralog group 1 hox genes regulate rhombomere 5/6 expression of vhnf1, a repressor of rostral hindbrain fates, in a meis-dependent manner. Dev Biol. 271**,** 350-61.

Crossley, P. H., Martinez, S., Martin, G. R., 1996. Midbrain development induced by FGF8 in the chick embryo. Nature. 380**,** 66-8.

Deflorian, G., Tiso, N., Ferretti, E., Meyer, D., Blasi, F., Bortolussi, M., Argenton, F., 2004. Prep1.1 has essential genetic functions in hindbrain development and cranial neural crest cell differentiation. Development. 131**,** 613-27.

DiMartino, J. F., Selleri, L., Traver, D., Firpo, M. T., Rhee, J., Warnke, R., O'Gorman, S., Weissman, I. L., Cleary, M. L., 2001. The Hox cofactor and proto-oncogene Pbx1 is required for maintenance of definitive hematopoiesis in the fetal liver. Blood. 98**,** 618-26.

Drescher, U., Bonhoeffer, F., Muller, B. K., 1997. The Eph family in retinal axon guidance. Curr Opin Neurobiol. 7**,** 75-80.

Dutta, S., Gannon, M., Peers, B., Wright, C., Bonner-Weir, S., Montminy, M., 2001. PDX:PBX complexes are required for normal proliferation of pancreatic cells during development. Proc Natl Acad Sci U S A. 98**,** 1065-70.

Fraser, S., Keynes, R., Lumsden, A., 1990. Segmentation in the chick embryo hindbrain is defined by cell lineage restrictions. Nature. 344**,** 431-5.

French, C. R., Erickson, T., Callander, D., Berry, K. M., Koss, R., Hagey, D. W., Stout, J., Wuennenberg-Stapleton, K., Ngai, J., Moens, C. B., Waskiewicz, A. J., 2007. Pbx homeodomain proteins pattern both the zebrafish retina and tectum. BMC Dev Biol. 7**,** 85.

Friedman, G. C., O'Leary, D. D., 1996. Retroviral misexpression of engrailed genes in the chick optic tectum perturbs the topographic targeting of retinal axons. J Neurosci. 16**,** 5498-509.

Giudicelli, F., Taillebourg, E., Charnay, P., Gilardi-Hebenstreit, P., 2001. Krox-20 patterns the hindbrain through both cell-autonomous and non cell-autonomous mechanisms. Genes Dev. 15**,** 567-80.

Hernandez, R. E., Rikhof, H. A., Bachmann, R., Moens, C. B., 2004. vhnf1 integrates global RA patterning and local FGF signals to direct posterior hindbrain development in zebrafish. Development. 131**,** 4511-20.

Hidalgo, A., 1996. The roles of engrailed. Trends Genet. 12**,** 1-4.

In der Rieden, P. M., Mainguy, G., Woltering, J. M., Durston, A. J., 2004. Homeodomain to hexapeptide or PBC-interaction-domain distance: size apparently matters. Trends Genet. 20**,** 76-9.

Itasaki, N., Ichijo, H., Hama, C., Matsuno, T., Nakamura, H., 1991. Establishment of rostrocaudal polarity in tectal primordium: engrailed expression and subsequent tectal polarity. Development. 113**,** 1133-44.

Itasaki, N., Nakamura, H., 1996. A role for gradient en expression in positional specification on the optic tectum. Neuron. 16**,** 55-62.

Itoh, M., Kudoh, T., Dedekian, M., Kim, C. H., Chitnis, A. B., 2002. A role for iro1 and iro7 in the establishment of an anteroposterior compartment of the ectoderm adjacent to the midbrain-hindbrain boundary. Development. 129**,** 2317-27.

Jaszai, J., Reifers, F., Picker, A., Langenberg, T., Brand, M., 2003. Isthmus-to-midbrain transformation in the absence of midbrain-hindbrain organizer activity. Development. 130**,** 6611-23.

Kiecker, C., Lumsden, A., 2005. Compartments and their boundaries in vertebrate brain development. Nat Rev Neurosci. 6**,** 553-64.

Kim, S. K., Selleri, L., Lee, J. S., Zhang, A. Y., Gu, X., Jacobs, Y., Cleary, M. L., 2002. Pbx1 inactivation disrupts pancreas development and in Ipf1-deficient mice promotes diabetes mellitus. Nat Genet. 30**,** 430-5.

Knoepfler, P. S., Lu, Q., Kamps, M. P., 1996. Pbx-1 Hox heterodimers bind DNA on inseparable half-sites that permit intrinsic DNA binding specificity of the Hox partner at nucleotides 3' to a TAAT motif. Nucleic Acids Res. 24**,** 2288-94.

Kobayashi, M., Fujioka, M., Tolkunova, E. N., Deka, D., Abu-Shaar, M., Mann, R. S., Jaynes, J. B., 2003. Engrailed cooperates with extradenticle and homothorax to repress target genes in Drosophila. Development. 130**,** 741-51.

Langenberg, T., Brand, M., 2005. Lineage restriction maintains a stable organizer cell population at the zebrafish midbrain-hindbrain boundary. Development. 132**,** 3209-16.

LaRonde-LeBlanc, N. A., Wolberger, C., 2003. Structure of HoxA9 and Pbx1 bound to DNA: Hox hexapeptide and DNA recognition anterior to posterior. Genes Dev. 17**,** 2060-72.

Liu, A., Joyner, A. L., 2001. EN and GBX2 play essential roles downstream of FGF8 in patterning the mouse mid/hindbrain region. Development. 128**,** 181-91.

Logan, C., Wizenmann, A., Drescher, U., Monschau, B., Bonhoeffer, F., Lumsden, A., 1996. Rostral optic tectum acquires caudal characteristics following ectopic engrailed expression. Curr Biol. 6**,** 1006-14.

Lun, K., Brand, M., 1998. A series of no isthmus (noi) alleles of the zebrafish pax2.1 gene reveals multiple signaling events in development of the midbrain-hindbrain boundary. Development. 125**,** 3049-62.

Maizel, A., Bensaude, O., Prochiantz, A., Joliot, A., 1999. A short region of its homeodomain is necessary for engrailed nuclear export and secretion. Development. 126**,** 3183-90.

Manley, N. R., Selleri, L., Brendolan, A., Gordon, J., Cleary, M. L., 2004. Abnormalities of caudal pharyngeal pouch development in Pbx1 knockout mice mimic loss of Hox3 paralogs. Dev Biol. 276**,** 301-12.

Mann, R. S., Chan, S. K., 1996. Extra specificity from extradenticle: the partnership between HOX and PBX/EXD homeodomain proteins. Trends Genet. 12**,** 258-62.

Marin, O., Blanco, M. J., Nieto, M. A., 2001. Differential expression of Eph receptors and ephrins correlates with the formation of topographic projections in primary and secondary visual circuits of the embryonic chick forebrain. Dev Biol. 234**,** 289-303.

Martinez, S., Crossley, P. H., Cobos, I., Rubenstein, J. L., Martin, G. R., 1999. FGF8 induces formation of an ectopic isthmic organizer and isthmocerebellar development via a repressive effect on Otx2 expression. Development. 126**,** 1189-200.

Maves, L., Jackman, W., Kimmel, C. B., 2002. FGF3 and FGF8 mediate a rhombomere 4 signaling activity in the zebrafish hindbrain. Development. 129**,** 3825-37.

McMahon, A. P., Bradley, A., 1990. The Wnt-1 (int-1) proto-oncogene is required for development of a large region of the mouse brain. Cell. 62**,** 1073-85.

McMahon, A. P., Joyner, A. L., Bradley, A., McMahon, J. A., 1992. The midbrain-hindbrain phenotype of Wnt-1-/Wnt-1- mice results from stepwise deletion of engrailed-expressing cells by 9.5 days postcoitum. Cell. 69**,** 581-95.

Moens, C. B., Selleri, L., 2006. Hox cofactors in vertebrate development. Dev Biol. 291**,** 193-206.

Nakamura, H., Sugiyama, S., 2004. Polarity and laminar formation of the optic tectum in relation to retinal projection. J Neurobiol. 59**,** 48-56.

Neuteboom, S. T., Peltenburg, L. T., van Dijk, M. A., Murre, C., 1995. The hexapeptide LFPWMR in Hoxb-8 is required for cooperative DNA binding with Pbx1 and Pbx2 proteins. Proc Natl Acad Sci U S A. 92**,** 9166-70.

O'Hara, F. P., Beck, E., Barr, L. K., Wong, L. L., Kessler, D. S., Riddle, R. D., 2005. Zebrafish Lmx1b.1 and Lmx1b.2 are required for maintenance of the isthmic organizer. Development. 132**,** 3163-73.

Passner, J. M., Ryoo, H. D., Shen, L., Mann, R. S., Aggarwal, A. K., 1999. Structure of a DNA-bound Ultrabithorax-Extradenticle homeodomain complex. Nature. 397**,** 714-9.

Peers, B., Sharma, S., Johnson, T., Kamps, M., Montminy, M., 1995. The pancreatic islet factor STF-1 binds cooperatively with Pbx to a regulatory element in the somatostatin promoter: importance of the FPWMK motif and of the homeodomain. Mol Cell Biol. 15**,** 7091-7.

Peifer, M., Wieschaus, E., 1990. Mutations in the Drosophila gene extradenticle affect the way specific homeo domain proteins regulate segmental identity. Genes Dev. 4**,** 1209-23.

Peltenburg, L. T., Murre, C., 1996. Engrailed and Hox homeodomain proteins contain a related Pbx interaction motif that recognizes a common structure present in Pbx. Embo J. 15**,** 3385-93.

Peltenburg, L. T., Murre, C., 1997. Specific residues in the Pbx homeodomain differentially modulate the DNA-binding activity of Hox and Engrailed proteins. Development. 124**,** 1089-98.

Pfeiffenberger, C., Cutforth, T., Woods, G., Yamada, J., Renteria, R. C., Copenhagen, D. R., Flanagan, J. G., Feldheim, D. A., 2005. Ephrin-As and neural activity are required for eye-specific patterning during retinogeniculate mapping. Nat Neurosci. 8**,** 1022-7.

Piper, D. E., Batchelor, A. H., Chang, C. P., Cleary, M. L., Wolberger, C., 1999. Structure of a HoxB1-Pbx1 heterodimer bound to DNA: role of the hexapeptide and a fourth homeodomain helix in complex formation. Cell. 96**,** 587-97.

Popperl, H., Bienz, M., Studer, M., Chan, S. K., Aparicio, S., Brenner, S., Mann, R. S., Krumlauf, R., 1995. Segmental expression of Hoxb-1 is controlled by a highly conserved autoregulatory loop dependent upon exd/pbx. Cell. 81**,** 1031-42.

Popperl, H., Rikhof, H., Chang, H., Haffter, P., Kimmel, C. B., Moens, C. B., 2000. lazarus is a novel pbx gene that globally mediates hox gene function in zebrafish. Mol Cell. 6**,** 255-67.

Raible, F., Brand, M., 2004. Divide et Impera--the midbrain-hindbrain boundary and its organizer. Trends Neurosci. 27**,** 727-34.

Reifers, F., Bohli, H., Walsh, E. C., Crossley, P. H., Stainier, D. Y., Brand, M., 1998. Fgf8 is mutated in zebrafish acerebellar (ace) mutants and is required for maintenance of midbrain-hindbrain boundary development and somitogenesis. Development. 125**,** 2381-95.

Rhee, J. W., Arata, A., Selleri, L., Jacobs, Y., Arata, S., Onimaru, H., Cleary, M. L., 2004. Pbx3 deficiency results in central hypoventilation. Am J Pathol. 165**,** 1343-50.

Rhinn, M., Lun, K., Luz, M., Werner, M., Brand, M., 2005. Positioning of the midbrain-hindbrain boundary organizer through global posteriorization of the neuroectoderm mediated by Wnt8 signaling. Development. 132**,** 1261-72.

Rieckhof, G. E., Casares, F., Ryoo, H. D., Abu-Shaar, M., Mann, R. S., 1997. Nuclear translocation of extradenticle requires homothorax, which encodes an extradenticle-related homeodomain protein. Cell. 91**,** 171-83.

Schnabel, C. A., Selleri, L., Cleary, M. L., 2003. Pbx1 is essential for adrenal development and urogenital differentiation. Genesis. 37**,** 123-30.

Scholpp, S., Brand, M., 2001. Morpholino-induced knockdown of zebrafish engrailed genes eng2 and eng3 reveals redundant and unique functions in midbrain--hindbrain boundary development. Genesis. 30**,** 129-33.

Scholpp, S., Brand, M., 2003. Integrity of the midbrain region is required to maintain the diencephalic-mesencephalic boundary in zebrafish no isthmus/pax2.1 mutants. Dev Dyn. 228**,** 313-22.

Scholpp, S., Lohs, C., Brand, M., 2003. Engrailed and Fgf8 act synergistically to maintain the boundary between diencephalon and mesencephalon. Development. 130**,** 4881-93.

Selleri, L., Depew, M. J., Jacobs, Y., Chanda, S. K., Tsang, K. Y., Cheah, K. S., Rubenstein, J. L., O'Gorman, S., Cleary, M. L., 2001. Requirement for Pbx1 in skeletal patterning and programming chondrocyte proliferation and differentiation. Development. 128**,** 3543-57.

Serrano, N., Maschat, F., 1998. Molecular mechanism of polyhomeotic activation by Engrailed. Embo J. 17**,** 3704-13.

Tallafuss, A., Wilm, T. P., Crozatier, M., Pfeffer, P., Wassef, M., Bally-Cuif, L., 2001. The zebrafish buttonhead-like factor Bts1 is an early regulator of pax2.1 expression during mid-hindbrain development. Development. 128**,** 4021-34.

van Dijk, M. A., Murre, C., 1994. extradenticle raises the DNA binding specificity of homeotic selector gene products. Cell. 78**,** 617-24.

van Dijk, M. A., Peltenburg, L. T., Murre, C., 1995. Hox gene products modulate the DNA binding activity of Pbx1 and Pbx2. Mech Dev. 52**,** 99-108.

von Baer, K. E., 1828. Entwicklungsgeschichte der Thiere: Beobachtung und Reflexion. Bornträger, Königsberg.

Walkenhorst, J., Dutting, D., Handwerker, C., Huai, J., Tanaka, H., Drescher, U., 2000. The EphA4 receptor tyrosine kinase is necessary for the guidance of nasal retinal ganglion cell axons in vitro. Mol Cell Neurosci. 16**,** 365-75.

Walshe, J., Maroon, H., McGonnell, I. M., Dickson, C., Mason, I., 2002. Establishment of hindbrain segmental identity requires signaling by FGF3 and FGF8. Curr Biol. 12**,** 1117-23.

Waskiewicz, A. J., Rikhof, H. A., Moens, C. B., 2002. Eliminating zebrafish pbx proteins reveals a hindbrain ground state. Dev Cell. 3**,** 723-33.

Wurst, W., Auerbach, A. B., Joyner, A. L., 1994. Multiple developmental defects in Engrailed-1 mutant mice: an early mid-hindbrain deletion and patterning defects in forelimbs and sternum. Development. 120**,** 2065-75.

Wurst, W., Bally-Cuif, L., 2001. Neural plate patterning: upstream and downstream of the isthmic organizer. Nat Rev Neurosci. 2**,** 99-108.

Chapter Six - Meis1 specifies positional information in the retina and tectum to organize the zebrafish visual system.

A version of this chapter has been accepted for publication. Erickson, T., French, C.R., and Waskiewicz, A.J. 2010. Neural Development.

6.1 Introduction

In order to preserve the spatial coordinates of visual input, retinal ganglion cell (RGC) axons are topographically organized in the visual processing centres of the midbrain. Retinotopic mapping has been most extensively studied in the optic tectum of fish, amphibians, and chick, and in the superior colliculus of mice. Within both the retina and the tectum, axially restricted expression of the *Eph* and *Ephrin* family of axon guidance molecules provides some of the positional information required for retinotectal map formation. Interactions between Eph receptor tyrosine kinases and their cognate Ephrin ligands result in cytoskeletal rearrangements and changes in cell adhesion, thereby eliciting either repulsive or attractive responses. By interpreting the molecular Eph and Ephrin code, RGC axons form a precisely ordered arrangement within the optic tectum that accurately reflect their axial position within the retina (reviewed in Lemke and Reber, 2005; reviewed in Scicolone et al., 2009).

Axial patterning of the retina is required to establish the correct domains of *Eph* and *Ephrin* expression. During eye development, retinal patterning occurs along both the dorsal-ventral (DV) and nasal-temporal (NT) axes (reviewed in Harada et al., 2007; reviewed in McLaughlin et al., 2003). The DV axis is established through an antagonistic relationship between the Bone morphogenetic protein (Bmp) and Hedgehog signaling pathways. In the dorsal retina, Smad-dependent Bmp/Gdf signaling initiates expression of the dorsal-specific T-box transcription factors *tbx5* and *tbx2b*, which in turn activate *ephrinB* expression (Behesti et al., 2006; French et al., 2009; Gosse and Baier, 2009; Koshiba-Takeuchi et al., 2000). Additionally, Wnt signaling is required to maintain dorsal identity (Veien et al., 2008; Zhou et al., 2008). In the ventral retina, Hedgehog signals from the ventral midline induce the expression of Vax homeodomain transcription factors (Lupo et al., 2005; Take-uchi et al., 2003; Zhang and Yang, 2001), thereby establishing ventral *ephB* expression (Barbieri et al., 2002; Mui et al., 2002; Mui et al., 2005; Schulte et al., 1999). Restricted *ephrinB* and *ephB*

expression along the DV axis is required for normal formation of the retinotectal map (Hindges et al., 2002; Mann et al., 2002).

The nasal-temporal axis is defined by the restricted expression of forkhead transcription factors *foxG1* (*bf1*) and *foxD1* (*bf2*) in the nasal and temporal retina, respectively (Hatini et al., 1994; Takahashi et al., 2009; Takahashi et al., 2003). These factors function antagonistically to promote the expression of *ephrinA* ligands in the nasal retina and a subset of *ephA* receptors in the temporal domain. Altering the normal domains of *ephrinA* and *ephA* expression causes defects in retinotectal map formation (Feldheim et al., 2000; Feldheim et al., 2004; Hornberger et al., 1999). Similarly to the DV axis, secreted signaling proteins are also involved in NT patterning. Fgf signals from the telencephalon and periocular mesenchyme promote nasal (*ephrinA*) and repress temporal fates (*ephA*) (Nakayama et al., 2008; Picker and Brand, 2005; Picker et al., 2009). At this time, it is not clear whether temporal identity represents a retinal ground state or if it is induced by an unidentified factor.

Proper patterning of the tectum / superior colliculus is also a critical component of proper retinotectal mapping. In the midbrain, *eph* and *ephrin* genes are expressed in opposing gradients. *EphrinA* ligands are expressed in a posterior to anterior gradient, while *EphA* receptors are expressed in an opposing anterior to posterior gradient (Rashid et al., 2005). Likewise, along the medial-lateral axis, *EphrinB* ligands are expressed in a medial to lateral gradient while *EphB* receptors exhibit an opposing lateral to medial gradient (Hindges et al., 2002). These opposing gradients, together with the repulsive interactions between Eph-Ephrin molecules, suggested a gradient matching model of retinotectal map formation (reviewed in Goodhill and Richards, 1999). This model is supported by experiments showing, for example, that *EphA3*-expressing temporal RGCs tend not to innervate posterior regions of the tectum expressing high levels of EphrinA ligands (Cheng et al., 1995; Nakamoto et al., 1996). However, this model does not explain all facets of retinotectal map formation, and other factors such as attractive Eph-Ephrin interactions, axon competition (Gosse et al., 2008), and other molecular cues may refine the process (reviewed in Goodhill and Richards,

1999). It is clear, however, that the precise topographic mapping of RGCs onto the tectum / superior colliculus is a highly regulated process in which Eph and Ephrin interactions play a key role.

Eph and Ephrin proteins have been well studied in the hindbrain where they are involved in cell sorting and restricting cell movements between rhombomeres (Cooke et al., 2005; Kemp et al., 2009; Xu et al., 1999). Of particular importance in regulating hindbrain *eph* and *ephrin* expression are the TALE-class homeodomain transcription factors Meis/Pknox and Pbx, which act in trimeric complexes with Hox proteins to impart segmental identity to the hindbrain rhombomeres (Choe et al., 2002; Deflorian et al., 2004; reviewed in Moens and Selleri, 2006; Waskiewicz et al., 2001; Waskiewicz et al., 2002). However, Pbx and Meis also perform Hox-independent roles in eye, lens, midbrain, heart and muscle development (Erickson et al., 2007; French et al., 2007; Maves et al., 2009; Maves et al., 2007; Zhang et al., 2002).

Meis1 is a particularly attractive candidate for playing an important role in patterning the visual system. *meis1* expression in the developing eye and midbrain is conserved across multiple species, and Meis1-deficiency causes microphthalmia in mice, chickens and zebrafish (Bessa et al., 2008; Heine et al., 2008; Hisa et al., 2004). The Drosophila Meis homolog Homothorax (Hth) also plays an important role in insect eye development (Bessa et al., 2002; Pai et al., 1998). Structurally, Meis proteins contain a Pbx-interaction domain in the N-terminus, a DNA-binding homeodomain and a C-terminal activation domain (Huang et al., 2005). In addition to the trimeric Meis-Pbx-Hox complexes that regulate hindbrain patterning, Meis proteins can form heterodimeric complexes with Pbx and with a subset of posterior Hox proteins (Chang et al., 1997; Shen et al., 1997). Meis and its binding partners have been identified as important regulators of *eph* and *ephrin* gene expression in the midbrain and hindbrain through both direct and indirect mechanisms (Agoston and Schulte, 2009; Chen and Ruley, 1998; Choe et al., 2002; French et al., 2007; Shim et al., 2007; Sohl et al., 2009; Theil et al., 1998). However, despite this well-characterized role in hindbrain axial patterning and the regulation of *eph* and *ephrin* gene expression,

the function of Meis1 in axial patterning of the retina and in the formation of the retinotectal map not been fully addressed.

In this study, we use morpholino-mediated knockdown of Meis1 protein in zebrafish to determine if Meis1 patterns the retinotectal system. In the DV axis, Meis1 functions to promote ocular Bmp signaling through the positive regulation of *smad1* expression and the negative regulation of *follistatin a* (*fsta*). With regard to NT patterning, Meis1-knockdown causes a loss of temporal identity in the retina. This phenotype can be attributed to an increase in retinal Fgf signaling and a decrease in *foxd1* expression in the temporal retina. We also demonstrate that Meis1 positively regulates *ephrin* gene expression in the tectum. Consistent with these patterning defects, Meis1-depleted embryos also exhibit retinotectal mapping defects in both the NT and DV axes. We conclude that Meis1 contributes to retinotectal map formation by specifying positional information in both the retina and tectum.

6.2 Results

6.2.1 *meis1* expression and morpholino knockdown

Zebrafish *meis1* is expressed in the presumptive eye, midbrain and hindbrain regions between 11-15 hours post fertilization (hpf) (Figure 6-1A-F) (Waskiewicz et al., 2001). A transverse section through the optic vesicle of a 13 hpf embryo stained by a Meis1 monoclonal antibody reveals the presence of Meis1 protein in both the dorsal and ventral leaflets of the eye (Figure 6-1D). At 15 hpf, *meis1* mRNA is expressed in the dorsal midbrain that will go on to form the optic tectum (Figure 6-1F). At 20 hpf, Meis1 protein is present in the retinal progenitor cells, in the presumptive tectum, and in the hindbrain (Figure 6-1G). By 50 hpf, the early pattern of *meis1* mRNA expression has changed dramatically. *meis1* is robustly expressed in the hindbrain and cerebellum (Figure 6-1H), but its tectal expression has retreated to the dorsal midline and to a deeper layer of the tectum (Figure 6-1I). In the retina, *meis1* expression is largely restricted to the ciliary marginal zone (CMZ; Figure 6-1I). The robust expression of *meis1* in the

eye and tectum at early developmental stages (10-20 hpf) suggests that Meis1 may be playing an early role in patterning the zebrafish visual system.

To examine the function of Meis1 in eye and midbrain development, we used an ATG-targeted translation-blocking morpholino to knockdown Meis1 protein expression (French et al., 2007). This morpholino was used in all experiments unless otherwise noted. To determine the effectiveness of this morpholino, we compared the levels of Meis1 protein between 16 hpf wild type and *meis1* morphant embryos by whole-mount immunohistochemistry using a monoclonal antibody against zebrafish Meis1 (Figure S6-1A, B). In *meis1* morphant embryos, the specific Meis1 signal is lost, showing that the morpholino effectively reduces Meis1 protein levels. We also observe a similar knockdown of Meis1 protein using a second, non-overlapping translation blocking morpholino (*meis1*NOL; Figure S6-1C, D). Furthermore, *meis1*NOL gives similar phenotypes to the ATG-morpholino (compare Figure S6-1E-H with Figure 6-5A-D and Figure 6-6F, G). Together, these results suggest that the *meis1* morpholino represents an accurate Meis1 loss of function model.

6.2.2 Meis1-knockdown results in a downregulation of *ephrin* gene expression in the tectum

Axial patterning of the tectum is an important element in retinotectal map formation. Precise patterns of *eph* and *ephrin* expression within the tectum establish positional cues that, together with the *eph* and *ephrin* genes expressed in the retina, instruct the innervation patterns of the RGC axons. Since Meis1 is expressed in the developing tectum, and Meis proteins have been shown to regulate *eph* and *ephrin* expression in the midbrain (Agoston and Schulte, 2009; Shim et al., 2007; Sohl et al., 2009), we tested whether zebrafish Meis1 also plays a critical role in tectal patterning by examining the expression of *ephrin* genes. In 32 hpf embryos, the *efna* genes (*efna2*, *efna3b*, *efna5a*) are all expressed in posterior high – anterior low gradients in the presumptive tectum, along with a dorsal-ventral domain of expression in the anterior region of the midbrain-hindbrain boundary (MHB; Figure 6-2A, C, E). In *meis1* morphants, the tectal

expression of *efna2* (*n*=11/11), *efna3b* (*n*=13/13) and *efna5a* (*n*=57/57) are severely reduced (Figure 6-2B, D, F). *efnb3*, a member of the *ephrinB* family of ligands, is expressed broadly across the medial-lateral axis of the presumptive tectum in 32 hpf wild type embryos (Figure 6-2G). This expression depends upon Meis1 function, as the level of transcript is greatly reduced in Meis1-depleted embryos (*n*=12/14; Figure 6-2H). These defects in *ephrin* gene expression are not due to failings in MHB formation, as *fgf8a* (*n*=35/35), *eng2a* (*n*=31/31), and *pax2a* (*n*=18/18) expression at the MHB is normal in *meis1* morphants (Figure S6-2). Together, these results suggest that Meis1 regulates *ephrin* gene expression in the presumptive tectum.

By 48 hpf, the tectum has adopted a more mature morphology and the RGC axons have started to innervate their target zones (Stuermer, 1988). Therefore, we examined *ephrin* gene expression in *meis1* morphants again at this developmental stage. Consistent with the results obtained at 32 hpf, the expression of *efna2* (*n*=23/25), *efna3b* (*n*=16/19), and *efna5a* (*n*=26/30) expression is reduced in Meis1-depleted embryos (Figure 6-2I-N). At 48 hpf, *efnb3* expression has refined into a medial high – lateral low gradient in wild type embryos (Figure 6-2O). Meis1-depleted embryos display a similar pattern of expression, albeit at a much lower level (*n*=13/13; Figure 6-2P). Taken together, these results suggest that Meis1 is required for proper tectal patterning, a role that may contribute to the retinotopic organization of the zebrafish visual system.

6.2.3 Meis1 knockdown affects early retinal DV patterning and results in a partial ventralization of the retina

The role of Meis1 in patterning the retina has not been previously examined. To determine if Meis1 is involved in specifying DV identity the retina, we compared the expression of the DV markers *tbx5* and *vax2* between wild type and Meis1-depleted embryos. At 15 hpf, *tbx5* is expressed in the presumptive dorsal retina (Figure 6-3A). Knockdown of Meis1 reduces both the domain and intensity of *tbx5* expression (*n*=27/30; Figure 6-3B). To examine the domain of ventral identity at 15 hpf, we looked at the expression of *vax2*. Compared to wild

type embryos, the retinal domain of *vax2* expression is expanded upon Meis1 depletion (*n*=14/19; Figure 6-3I, J). Taken together, these data suggest that a loss of Meis1 function results in a reduction in presumptive dorsal retinal identity together with an expansion of ventral identity.

To determine if these early defects in DV patterning persist into later eye development, we examined dorsal *tbx5* and *efnb2a* and ventral *vax2* and *ephb2* expression in 28 hpf retinas. By this stage, the wild type zebrafish eye has adopted a more definitive morphology where the neural retina wraps around the lens and meets at the ventral choroid fissure to form a 360° circle. To quantify changes in retinal axial patterning, we analyzed in situ staining intensity in flat-mounted retinas from 28 hpf wild type and *meis1* morphants and compared the radial position at which gene expression intensity falls to the halfway point between its minimum and maximum values (see Methods) (Picker and Brand, 2005). Consistent with the defects observed at 15 hpf, we find that the extent of *tbx5* expression is reduced in 28 hpf *meis1* morphants (Figure 6-3C-E). This reduction in *tbx5* expression is primarily at its dorso-nasal boundary, where *meis1* morphants exhibit a 26° retraction in expression ($P<0.0001$; Figure 6-3E). In contrast, the dorso-temporal border of *tbx5* does not statistically differ between wild type and *meis1* morphants ($P=0.0124$; Figure 6-3E). *ephrin b2a* (*efnb2a*) is a transcriptional target of *tbx5* in the dorsal retina. Similar to the changes we observe for *tbx5* expression, we find that the dorso-nasal border of *efnb2a* is retracted by 22° in *meis1* morphants ($P<0.0001$), and the dorso-temporal border is unchanged ($P=0.3301$; Figure 6-3F-H). With regard to ventral identity at 28 hpf, we find that the ventro-nasal borders of both *vax2* and *ephb2* are expanded dorsally by 25° and 31° respectively in *meis1* morphants ($P<0.0001$; Figure 6-3K-P). While the ventro-temporal border of *vax2* is not statistically different between wild type and morphants ($P=0.2046$), the ventro-temporal border of *ephb2* is retracted ventrally by 18° in *meis1* morphants ($P<0.0001$). Overall, these results demonstrate that Meis1 plays a role in specifying DV identity, and that Meis1 knockdown leads to a partial ventralization of the retina, especially in the ventro-nasal domain.

6.2.4 Meis1 promotes retinal BMP signaling by regulating *smad1* and *follistatin a* expression

The Bmp signaling pathway plays an evolutionarily conserved role in specifying dorsal identity in the retina (Behesti et al., 2006; French et al., 2009; Gosse and Baier, 2009; Koshiba-Takeuchi et al., 2000). The DV patterning defects in *meis1* morphants could be due to misregulation of a vital component of the BMP pathway. Smad transcription factors play an essential role in this process by mediating the transcriptional response to Bmp signaling. We hypothesized that Meis1 might regulate retinal s*mad1* expression since its domain in the early zebrafish optic vesicle is similar to that of Meis1 protein, and *meis1* mRNA expression precedes that of *smad1* (Figure S6-3A-D). To test this hypothesis, we compared *smad1* expression between wild type and *meis1* morphants at 15 hpf and found that *smad1* expression is strongly downregulated in the retina of Meis1-depleted embryos (*n*=65/65; Figure 6-4A, B). This phenotype can be rescued by the co-injection of morpholino-insensitive, myc-tagged *meis1* mRNA (*n*=14/15; Figure S6-4A-D), demonstrating the specificity of the *meis1* morpholino phenotype. Furthermore, *gdf6a* morphants have normal levels of *smad1* transcript in the presumptive retina at 13 hpf (Figure S6-5A, B), demonstrating that early *smad1* transcription is not regulated by Bmp signaling. Taken together, these data suggest that Meis1 is a specific regulator of *smad1* transcription.

The phosphorylation of Smads 1, 5, and 8 by Type I Bmp receptors is an essential step in transducing the Bmp signal into a transcriptional response. To see if the downregulation of *smad1* expression had an effect on the total amount of phosphorylated Smads in the retina, we performed whole mount immunohistochemistry using a phospho-Smad1/5/8-specific antibody. At 12 hpf, phospho-Smad staining is reduced in Meis1-depleted embryos (*n*=17/21; Figure 6-4C, D). Taken together with the downregulation of Bmp-dependent *tbx5* in Meis1-depleted embryos (Figure 6-3A, B), these data suggest that Meis1 has a positive effect on the level of Bmp signaling during early retinal patterning.

Although the level of *smad1* mRNA remains low in *meis1* morphants, the reduced level of phospho-Smad1/5/8 at 12 hpf largely recovers by 15 hpf

(compare Figures 6-4E and F). The presence of other Smad proteins could account for this discrepancy. *smad5* is ubiquitously expressed during early development, can act redundantly with *smad1* (Arnold et al., 2006; Pangas et al., 2008; Retting et al., 2009), and is not transcriptionally regulated by Meis1 (Figure S6-6A-D). To determine if the presence of Smad5 is masking the loss of *smad1* expression in Meis1-depleted embryos at 15 hpf, we performed an interaction experiment using *meis1* and *smad5* morpholinos. Using the level of phospho-Smads1/5/8 and *tbx5* transcription as an assay for Smad5 function, we observe a decrease in the level of retinal Bmp signaling in *smad5* morphants. Knocking down Smad5 protein lowers the overall level of phospho-Smads1/5/8 (*n*=4/4; compare Figure 6-4E and G), and reduces *tbx5* transcript to levels comparable to that of Meis1-depleted embryos (*n*=34/34; compare Figure 6-4J with I and K). However, by combining the two morpholinos, there is a synergistic effect where the level of phospho-Smads1/5/8 is nearly eliminated (*n*=6/6; Figure 6-4H) and *tbx5* transcript is often undetectable by in situ hybridization (*n*=28/39; Figure 6-4L). These results are consistent with the hypothesis that Meis1-regulated transcription of *smad1* is important for retinal DV patterning, and that Smad1 and Smad5 perform at least partially redundant functions in the eye.

In addition to positive regulators of retinal Bmp signaling, we also examined the role of Meis1 in regulating the expression of Bmp inhibitors. In particular, we observe that Meis1 knockdown results in an upregulation of *follistatin a* (*fsta*) expression throughout much of the brain and anterior spinal cord (*n*=48/48; Figure 6-5A-D). Especially striking is the ectopic *fsta* expression in the retina at 13 hpf (Figure 6-5B). As with *smad1*, injection of *myc-meis1* mRNA can partially rescue the *fsta* expression defects in *meis1* morphants (*n*=7/10; Figure S6-7A-D). Additionally, this phenotype cannot be attributed to a downregulation of Bmp signaling, as *gdf6a* morphants do not exhibit increased *fsta* expression at 13 hpf (Figure S6-5C, D). These data suggest that, in addition to positively regulating *smad1* transcription, Meis1 inhibits *fsta* expression.

Follistatin is a secreted protein known to bind directly to several different Bmp ligands to prevent Bmp receptor activation (Amthor et al., 2002; Fainsod et

al., 1997; Iemura et al., 1998). Although Follistatin can downregulate Gdf6 transcription in Xenopus animal caps (Chang and Hemmati-Brivanlou, 1999), a functional antagonism between Follistatin and Gdf6 proteins has not been demonstrated. To determine if the upregulation of *fsta* expression in *meis1* morphants can inhibit *gdf6a* function in the retina, we tested the ability of ectopic *fsta* to inhibit the embryonic ventralization phenotype caused by the injection of human *GDF6* mRNA into 1-cell embryos (Figure 6-5E). As little as 10 pg of *GDF6* mRNA is sufficient to cause a ventralized phenotype in 92% of the embryos, with 50% of embryos lacking all anterior head structures (*n*=38; Column 3). Conversely, 200 pg of *fsta* mRNA alone causes a dorsalized phenotype in 38% (*n*=37) of the injected embryos (Column 2). Injecting 200 pg of *fsta* mRNA together with 10 pg of *GDF6* mRNA effectively inhibits the ventralizing effects of GDF6 (Column 4). Following this treatment, no severely ventralized embryos were observed, and only 14% had a mildly ventralized phenotype (*n*=32). To test if *fsta* can inhibit endogenous Gdf6a signaling in the zebrafish retina, we injected 100 pg of *fsta* mRNA into a single cell of two-cell embryos and examined the level phospho-Smads1/5/8 at 14 hpf by whole-mount immunohistochemistry. This asymmetrical injection of *fsta* mRNA into only one of two cells causes uniocular reductions of phospho-Smads1/5/8 (*n*=5/8; Figure 6-5F, G). Together, these results suggest that Fsta can inhibit Gdf6a-mediated signaling, and that the upregulation of *fsta* expression in *meis1* morphants may contribute to the retinal DV patterning defects observed in these embryos.

In summary, Meis1 knockdown causes a dorsal-to-ventral shift in retinal identity that correlates with a reduced level of Bmp signaling in the optic vesicle. This decreased Bmp signal in *meis1* morphants can be attributed to a loss of *smad1* expression and an upregulation of *fsta*. Thus, Meis1 plays an important role in retinal DV patterning by facilitating retinal Bmp signaling.

6.2.5 Meis1-knockdown causes a partial loss of temporal identity in the retina

During early zebrafish eye development, the nasal and temporal axes are initially established in the dorsal and ventral leaflets of the optic vesicle,

respectively (Picker et al., 2009). As the retina develops, *foxd1*-expressing cells in the ventral leaflet move into the dorsal leaflet to form the temporal domain of the neural retina. To determine if Meis1 regulates positional identity along the nasal-temporal (NT) axis, we examined *foxg1a* and *foxd1* mRNA expression in the presumptive nasal and temporal domains. In 15 hpf wild type embryos, *foxg1a* is expressed in the dorsal leaf of the optic vesicle, specifically the proximal region fated to form the nasal retina (Figure 6-6A). In *meis1* morphants, this domain of *foxg1a* expression is expanded distally, suggesting an expansion of nasal identity (*n*=31/54; Figure 6-6B). Likewise, in 15 hpf wild type embryos, *foxd1* is also expressed in the dorsal optic vesicle, but in a domain underlying, and more distal to, that of *foxg1a* (Figure 6-6F). In 15 hpf *meis1* morphants, cells in the dorsal optic vesicle do not express *foxd1* (*n*=44/52; Figure 6-6G). Instead, faint *foxd1* expression is observed in the ventral leaflet of the eye, suggesting that *foxd1*-expressing cells have failed to move into the dorsal leaflet of the optic vesicle. We also examined the temporally-restricted expression of *epha7* at 16 hpf and found that *epha7* expression is similarly reduced in Meis1-depleted embryos (Figure 6-7A, B). Together, these results suggest that Meis1 is an important regulator of early nasal-temporal patterning.

To see how these early defects in NT patterning translate into later phenotypes, we quantified the expression domains of *foxg1a* and *foxd1* in dissected 28 hpf retinas. At this later stage, there is no significant expansion of nasal *foxg1a* expression towards the dorsal pole in Meis1-depleted retinas (P=0.5457; Figure 6-6C-E). Conversely, the dorso-temporal border of *foxd1* expression is retracted ventrally by 25° in Meis1-depleted retinas (P<0.0001; Figure 6-6H-J). Consistent with this latter observation, we also find that the expression domains of *epha7* (*n*=14/14) and *epha4b* (*n*=18/20) in the temporal retina are also reduced in *meis1* morphants (Figure 6-7C-F). Together, these data support the idea that Meis1 plays a role in nasal-temporal patterning, especially with regard to the establishment of *foxd1* and *ephA* expression in the temporal retina.

6.2.6 The contribution of Fgf signaling to the nasal-temporal patterning defects in Meis1-depleted embryos

The Fgf signaling pathway establishes nasal identity in the developing retina (Nakayama et al., 2008; Picker and Brand, 2005; Picker et al., 2009). Ectopic Fgf signaling expands nasal identity at the expense of temporal fate, while inhibition of the pathway has the opposite effect. Since some aspects of the *meis1* morphant phenotype resemble that of ectopic Fgf signaling, we examined the effect of Meis1-depletion on *il17rd* / *sef* and *dusp6* expression, two genes whose transcription is positively controlled by the Fgf pathway (Furthauer et al., 2002; Li et al., 2007; Molina et al., 2007; Tsang et al., 2002). As seen in dorsal view, both *il17rd* (Figure 6-8A) and *dusp6* (Figure 6-8C) are expressed in the dorsal forebrain, optic stalk and faintly in the presumptive nasal retina of 15 hpf wild type embryos. Meis1 knockdown results in broader domains of *il17rd* (*n*=27/48; Figure 6-8B) and *dusp6* (*n*=18/30; Figure 6-8D) expression in the dorsal forebrain and presumptive nasal retina, suggesting that this region of the eye experiences higher levels of Fgf signaling in *meis1* morphants. Transverse cross sections also reveal that the nasal expression domains of *il17rd* and *dusp6* are expanded laterally in 15 hpf Meis1-depleted embryos (*il17rd* - Figure 6-8E, E', F, F'; *dusp6* - Figure 6-8G, G', H, H'). Thus, we can conclude from these experiments that there is a subtly higher level of Fgf signaling in the eyes and forebrain of *meis1* morphant embryos.

To determine whether the expanded range of Fgf signaling contributes to the NT patterning defects in *meis1* morphants, we antagonized Fgf signaling in *meis1* morphants using a pharmaceutical inhibitor of Fgf receptors (PD173074). Changes in NT patterning were assayed by in situ hybridization for the nasal marker *efna5a* and the temporal marker *epha3* and quantified by radial profiling of in situ intensity. Consistent with the NT patterning defects shown in Figure 6-6 and Figure 6-7, *meis1* morphants exhibit an expansion of nasal *efna5a* (mean shift of 14º; $P<0.0001$; Figure 6-9A, C, E) and a reduction in temporal *epha3* expression compared to wild type (20º; $P<0.0001$; Figure 6-9F, H, J). Fgf receptor (FgfR) inhibitor-treated embryos exhibit a partial loss of nasal identity (56º;

P<0.0001; Figure 6-9B, E), and an expansion of the temporal domain (49º; P<0.0001; Figure 6-9G, J). Compared to the *meis1* morphant phenotype alone, morphants treated with the FgfR inhibitor exhibit reduced *efna5a* expression (46º difference; P<0.0001; Figure 6-9D, E), and have an expanded domain of *epha3* expression (19º difference; P<0.0001; Figure 6-9I, J). However, neither of these phenotypes are as profound as those caused by the FgfR inhibitor treatment alone. This is true with regard to both *efna5a* and *epha3* expression, where inhibition of Fgf signaling in *meis1* morphants does not cause the same robust shifts in axial identity as it does in uninjected embryos. Similar results were observed in experiments using the Fgf receptor inhibitor SU5402 (Figure S6-8). Together, these data suggest that the subtle expansion of Fgf signaling in Meis1-depleted embryos is unlikely to be the sole reason for the observed shifts in nasal-temporal identity.

6.2.7 Meis1 knockdown results in retinotectal map defects

Having established that Meis1 plays an early developmental role in patterning the retina and tectum, we next determined whether the early role of Meis1 had a later effect on tectal development and the formation of the retinotectal map. To compare the size of the tectal neuropil, we stained 5 dpf wild type and *meis1* morphant embryos an antibody against acetylated tubulin to mark axons and with Hoechst 33258 to mark nuclei (Figure 6-10A-F). Morphant neuropil (*n*=34 individual neuropil) are 50% smaller on average than their wild type counterparts (*n*=13 individual neuropil; P<0.0001; Figure 6-10B'). However, acetylated tubulin-positive axons are still present in morphant tecta (*n*=19/19; Figure 6-10C-F), suggesting that RGC axons still innervate the tectum in Meis1-depleted embryos.

To find out if Meis1-depleted embryos have retinotectal mapping defects, we injected DiI and DiO fluorescent lipophilic dyes into specific axial regions of 5 dpf retinas and visualized the mapping patterns of the RGC axons by confocal microscopy. With regard to the retinal DV axis, wild type dorsal RGCs (red) innervate the lateral tectum, while ventral RGCs (green) project to the medial

region (Figure 6-11A-C). Along the NT axis, wild type nasal RGCs (red) innervate the posterior tectum, while temporal RGCs (green) project to the anterior region (Figure 6-11G-I). Meis1-depleted embryos exhibit defects in DV mapping, where the innervation zones of the dorsal and ventral RGC axons partially overlap in the tectum (*n*=18/47; Figure 6-11D-F). Although, the normal medial-lateral restriction is lost in morphants for both dorsal and ventral axons, the ventral axons tend to exhibit a broader innervation pattern than dorsal axons (compare Figure 6-11B with 6-11E). We observe a similar situation with regard to the nasal-temporal retinotectal map in *meis1* morphants. In Meis1-depleted embryos, innervation zones of the nasal and temporal RGC axons overlap in the tectum (*n*=25/64; Figure 6-11J-L). Again, while normal anterior-posterior segregation of axons is lost for both the nasal and temporal axons, temporal axons tend to be more broadly distributed in the tectum (compare Figure 6-11H and 6-11K). Although overlapping innervation patterns are a common phenotypic class in *meis1* morphants, we also frequently observe a partial or complete axon stalling phenotype (Figure 6-11M; Figure S6-9). These data demonstrate that Meis1 function is required to correctly organize the retinotectal map.

6.3 Discussion

6.3.1 Meis1 is required to establish tissue polarity throughout the anterior neural tube

meis1 is expressed in the eye field, the midbrain and hindbrain during the crucial period in which axial cell identities are established in these tissues. Consistent with the known role for Meis proteins in patterning the hindbrain (This thesis - Chapter 3) (Choe et al., 2002; Vlachakis et al., 2001; Waskiewicz et al., 2001), in this work we demonstrate a specific role for Meis1 in establishing axial polarity in the presumptive tectum and retina. The tectum exhibits a strong anterior-posterior polarity that is reflected in opposing gradients of *eph* and *ephrin* expression (Rashid et al., 2005). In this work, we show that Meis1 establishes polarity in the zebrafish tectum by regulating *efna2*, *efna3b*, *efna5a*, and *efnb3* expression. This is consistent with what has been found in other model organisms

where murine Meis2 patterns the superior colliculus by directly activating *ephA8* expression (Shim et al., 2007) and chick Meis2 promotes tectal *ephrin B1* expression, possibly via a direct interaction with Otx2 (Agoston and Schulte, 2009). The functions of Meis in regulating *eph* and *ephrin* expression are independent of any role in midbrain-hindbrain boundary development, again consistent with Meis2 function in chick (Agoston and Schulte, 2009). Lastly, while *meis1* is also expressed in the developing eye, its role in patterning this tissue has not been explored. In this paper, we show that Meis1 influences the specification of the dorsal-ventral and nasal-temporal axes in the retina. Taken together, these studies demonstrate that Meis1 contributes to the establishment of axial polarity in anterior neural tissues such as the hindbrain, midbrain and retina.

6.3.2 The axial patterning roles of Meis1 contribute to formation of the retinotectal map

Meis1-depleted embryos exhibit a range of aberrant retinotectal pathfinding phenotypes, the most common of which are topographic mapping defects in the tectum (Figure 6-11) and axon stalling (Figure S6-9). While it is clear that Meis1 plays a role in the early patterning of the presumptive DV and NT axes, these patterning phenotypes are not as robust by the time the retinal axes have assumed their final anatomical positions (Figures 6-3 and 6-6). Indeed, by 28 hpf, the axial patterning defects in *meis1* morphants are milder than what is seen in embryos with decreased levels of Gdf6a or increased Fgf function (French et al., 2009; Gosse and Baier, 2009; Picker and Brand, 2005; Picker et al., 2009). However, the retinotectal mapping defects in *meis1* morphants are more profound than expected on the basis of observed retinal patterning defects. These data suggest that the loss of Meis1 causes pleiotropic effects throughout the zebrafish visual system. Meis1 is also a regulator of retinal progenitor cell proliferation (Bessa et al., 2008; Heine et al., 2008), the relevance of which to eye patterning is not yet understood. Furthermore, Meis2 has been shown to regulate the patterning and morphogenesis of the optic tectum in chick (Agoston and Schulte, 2009). In addition to axial patterning defects, we also observe defects in tectal size and

morphology in *meis1* morphant zebrafish (Figure 6-10) and an expansion of the optic stalk (Figure S6- 2). Taken together, while it is clear that Meis1 plays a part in specifying positional information in both the neural retina and tectum, it is possible that this patterning role is but one way that Meis1 contributes to the organization of the retinotectal map.

6.3.3 Meis1 is a positive regulator of retinal Bmp signaling

The requirement for Bmp activity in regulating dorsal retinal identity and the retinotectal map has been well established (Behesti et al., 2006; French et al., 2009; Gosse and Baier, 2009; Koshiba-Takeuchi et al., 2000; Murali et al., 2005; Plas et al., 2008; Sakuta et al., 2001; Sakuta et al., 2006). A decrease in Bmp signaling leads to a loss of dorsal markers such as *tbx5* and an expansion of ventral identity as marked by *vax2*. We observe similar changes in *meis1* morphants suggesting that Meis1 can potentiate Bmp signaling in the retina (Figure 6-3). Meis1 regulates the Bmp pathway in at least two ways: first, by positively regulating *smad1* transcription (Figure 6-4); and second, by repressing *fsta* expression (Figure 6-5). Meis proteins have not been previously characterized as positive regulators of Bmp signaling, and as such, these results point to a new role for Meis1 in the regulation of neural patterning.

Meis proteins are known to act as transcriptional activators by facilitating histone acetylation at target promoters (Choe et al., 2009; Goh et al., 2009; Huang et al., 2005). For this reason, the ectopic *fsta* expression observed in *meis1* morphants is likely not due to Meis1 directly regulating *fsta*. On the other hand, the downregulation of *smad1* transcription in *meis1* morphants is consistent with it being a direct target of Meis1. *meis1* and *smad1* are co-expressed in the presumptive retina during early development, and we observe that *smad1* expression is never initiated properly in *meis1* morphants. Furthermore, we have identified two putative Meis binding sites in a region upstream of the *smad1* coding sequence that is conserved between zebrafish (*Danio rerio)*, Medaka (*Oryzias latipes*), the green spotted pufferfish (*Tetraodon nigroviridis*), and the three-spined stickleback (*Gasterosteus aculeatus*) (T.E. unpublished

observations). Further analyses will determine whether these sites are functionally significant. Very few studies of *smad1* transcriptional regulation have been done (Freudenberg and Chen, 2007; Sun et al., 2007), thus the Meis1-dependent activation of *smad1* transcription is an important finding in this area, and represents a novel mechanism of tissue-specificity in Bmp regulation.

Smads1 and 5 have been shown to act redundantly is some processes such as bone formation and tumour suppression (Arnold et al., 2006; Pangas et al., 2008; Retting et al., 2009), yet perform distinct functions during embryonic dorsal-ventral patterning and blood development (Dick et al., 1999; McReynolds et al., 2007). The delayed onset of Smad1/5/8 phosphorylation in *meis1* morphants suggests that Smad1 may be especially important during the initiation of retinal Bmp signaling. However, the results of the *meis1-smad5* morpholino interaction experiment suggest that Smad1 and Smad5 function redundantly, at least with regard to activating *tbx5* expression. These results suggest that Smad1 and 5 have differential and overlapping roles in patterning the zebrafish retina.

6.3.4 Meis1 is an important factor in the specification of the temporal retina

Vertebrate eye patterning is characterized by a complex series of interactions in which cell proliferation and morphogenesis (Li et al., 2000; Schmitt and Dowling, 1994) must be spatially and temporally coordinated. This has been best described with regard to nasal specification in the zebrafish retina by Fgfs 3, 8, and 24 (Picker and Brand, 2005; Picker et al., 2009). In this case, the movement of temporally-fated cells from the ventral leaflet of the optic vesicle are required to compact the future nasal domain, thereby defining the relative sizes of these two axes. Thus, patterning of the nasal-temporal axis is intimately linked with eye morphogenesis.

Meis1-depleted embryos display defects in NT patterning, especially with regard to the specification of the temporal retina. The early expression of *foxd1*, an essential regulator of temporal identity, is downregulated in *meis1* morphants (Figure 6-6F, G). Furthermore, the dorsal-ventral position of *foxd1*-expressing cells is altered in Meis1-depleted embryos compared to equivalently staged wild

type embryos. By 15 hpf, *foxd1*-expressing cells have largely moved from the ventral optic vesicle leaflet to the dorsal leaflet in wild type embryos. However, in *meis1* morphants, *foxd1*-expressing cells are still located in the ventral leaflet, suggesting that temporal cell movements into the neural retina are impaired in Meis1-depleted embryos. Foxd1 is known to regulate *ephA* expression in the temporal retina (Takahashi et al., 2009). Since Ephs and Ephrins are involved in cell sorting and adhesion (reviewed in Cooke and Moens, 2002), the decrease in temporal *epha3*, *epha4b*, and *epha7* expression (Figure 6-7 and 6-9) is likely to alter cohesive cell behaviours amongst temporal retinal progenitors and may contribute to hampered cell movements in *meis1* morphants.

We also observe a subtle expansion of Fgf signaling in the optic vesicle of *meis1* morphants (Figure 6-8A-H') that could contribute to the NT patterning defects. Indeed, a partial inhibition of Fgf signaling in *meis1* morphants is sufficient to restore temporal identity to at least wild type levels (Figure 6-9, Figure S6-8). However, the nasal-to-temporal shift in axial identity caused by FgfR-inhibitor treatment is not as robust in Meis1-depleted embryos as in uninjected controls. As such, these data suggest that expanded Fgf signaling is unlikely to be the only contributing factor to the NT patterning defects in Meis1-depleted embryos. The balance between nasal and temporal identity is mechanistically complex and interdependent (Picker et al., 2009), and the early expansion of Fgf signaling and *foxg1a* expression in 15 hpf *meis1* morphants could be a consequence, rather than a cause, of decreased temporal identity. Consistent with this idea is the observation that temporal identity is robustly reduced in *meis1* morphants at both 15 hpf and 28 hpf (Figure 6-6F-J, Figure 6-7), whereas the expansion of nasal identity and Fgf signaling is less consistent at these same stages (Figure 6-6A-E, Figure 6-8). Furthermore, we do not observe any consistent change in the expression of *fgf3*, *fgf8*, or *fgf24* between the stages of 12-15 hpf (data not shown). It is currently unknown if the temporal retina is actively specified, and future studies will determine whether Meis1 plays a specific role in regulating temporal retinal identity.

6.4 Figures

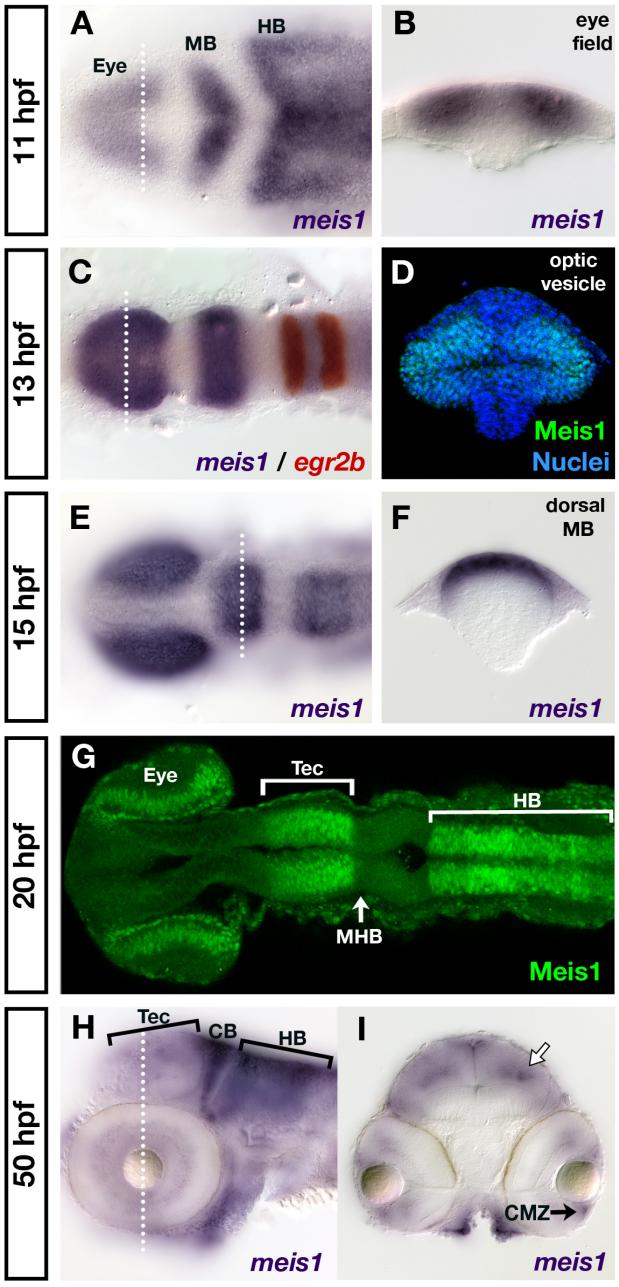

Figure 6-1. *meis1* mRNA and protein expression. **(A)** At 11 hpf, *meis1* is expressed in the eye field, and in the presumptive midbrain (MB) and hindbrain (HB). **(B)** Transverse section through an 11 hpf embryo shows *meis1* mRNA expression in the presumptive eye field. **(C, E)** *meis1* mRNA continues to be expressed in the optic vesicles, midbrain and hindbrain. *egr2b* / *krox20* expression (red) marks rhombomeres (r) 3 and 5 of the hindbrain in C. **(D)** Transverse section

through a 13 hpf stained with a Meis1 antibody shows Meis1 protein in the dorsal and ventral leaves of the optic vesicle. Hoechst 33258 stain marks the nuclei. **(F)** Transverse section through the midbrain of a 15 hpf embryo showing *meis1* mRNA expression in the dorsal midbrain. **(G)** Meis1 protein expression at 20 hpf. Meis1 protein is present in the eye, presumptive tectum (Tec), and in the posterior to the r1-r2 boundary. Meis1 is excluded from the midbrain-hindbrain boundary (MHB). (H) At 50 hpf, *meis1* mRNA is strongly expressed in the hindbrain (HB) and cerebellum (CB), but is only faintly detectable in the tectum. **(I)** Transverse section through a 50 hpf embryo showing *meis1* expression in the ciliary marginal zone (CMZ) of the retina. *meis1* expression is also observed in the dorsal midline and in a deeper layer of the tectum (white arrows). Embryos in A, C, E, and G are shown in dorsal view with anterior to the left. Embryo in H is shown in lateral view with anterior to the left. Transverse section in B, D, F, and I are oriented dorsal up. The dotted lines in A, C, E, and H indicate the position of the corresponding transverse sections in B, D, F, and I. Scale bars = 50 μM.

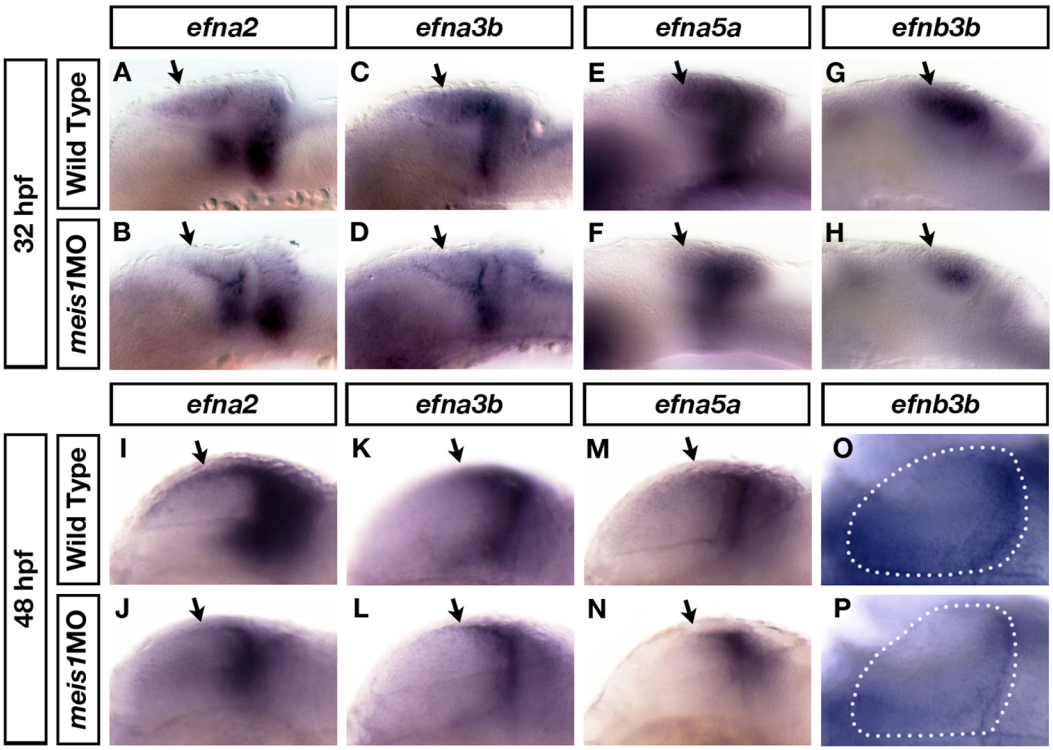

Figure 6-2. Tectal *ephrin* gene expression is reduced in *meis1* morphants. **(A-H)** mRNA in situ hybridizations for *efna2* (A, B), *efna3b* (C, D), *efna5a* (E, F) and *efnb3* (G, H) in 32 hpf wild type (A, C, E, G) and *meis1* morphant (B, D, F, H) embryos. Meis1-knockdown leads to a downregulation in the tectal expression of these *ephrin* genes. Arrows mark the tectum. **(I-P)** mRNA in situ hybridizations for *efna2* (I, J), *efna3b* (K, L), *efna5a* (M, N) and *efnb3* (O, P) in 48 hpf wild type (I, K, M, O) and *meis1* morphant (J, L, N, P) embryos. The defects in tectal *ephrin* gene expression remain in 48 hpf *meis1* morphants. Arrows mark the tectum. The dotted lines in O and P outline one of the tectal lobes in each embryo. Embryos in A-F and I-N are shown in lateral view with anterior left, while embryos in G, H, O, and P are shown in dorsal view with anterior left.

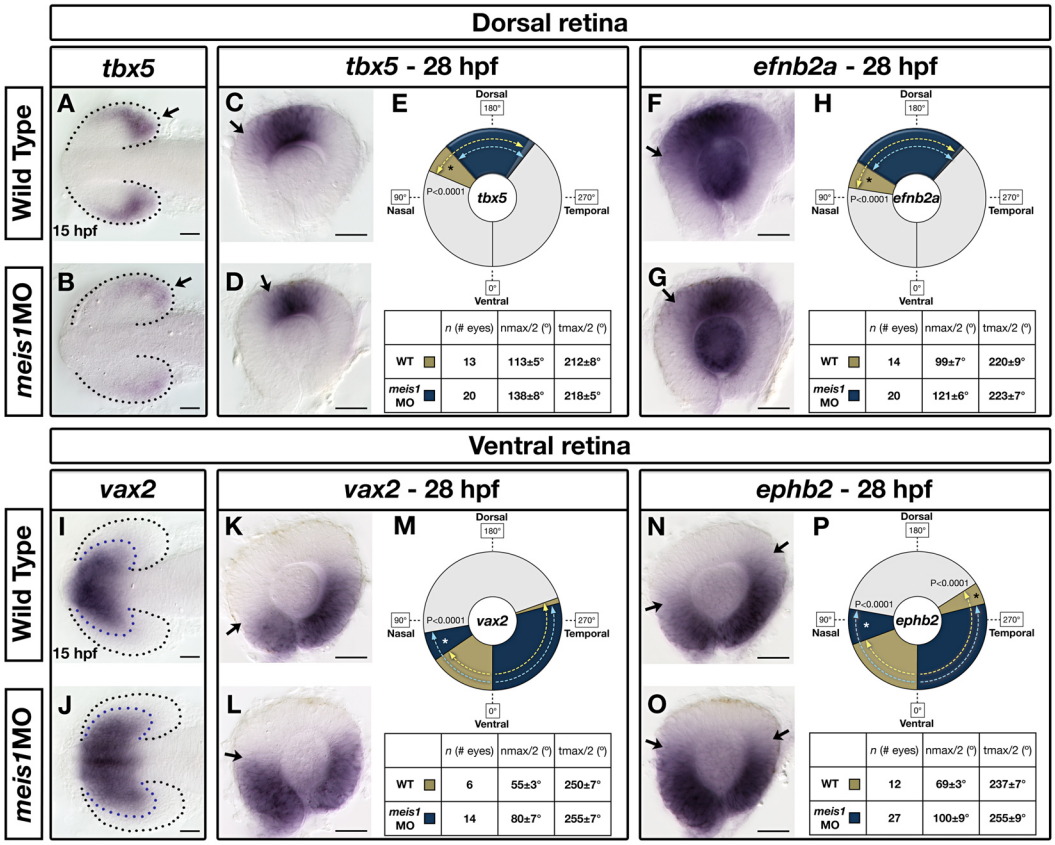

Figure 6-3. Meis1 contributes to dorsal-ventral patterning in the retina. mRNA in situ hybridization (ISH) for the dorsal marker *tbx5* **(A, B)** and the ventral marker *vax2* **(I, J)** in 15 hpf wild type and *meis1* morphant embryos. Dotted lines outline the optic vesicle. All views are dorsal with anterior left. **(C-P)** mRNA ISH for dorsal genes *tbx5* **(C-E)** and *efnb2a* **(F-H),** and ventral genes *vax2* **(K-M)** and *ephb2* **(N-P)** in dissected, flat-mounted eyes from 28 hpf wild type and *meis1* morphant embryos. The domains of gene expression were quantified by determining a 360° profile of in situ staining intensity and graphing the radial position at which gene expression intensity falls to the halfway point between its minimum and maximum values (see Methods). The nmax/2 and tmax/2 values are given as the mean radial position in degrees plus/minus one standard deviation. Asterisks indicate regions in which there are statistically significant differences in axial identity between wild type and *meis1* morphants as determined by an unpaired, two-tailed t-test using a P value of 0.01 as a cutoff for significance. Representative dissected eyes are shown. Scale bars = 50 µM.

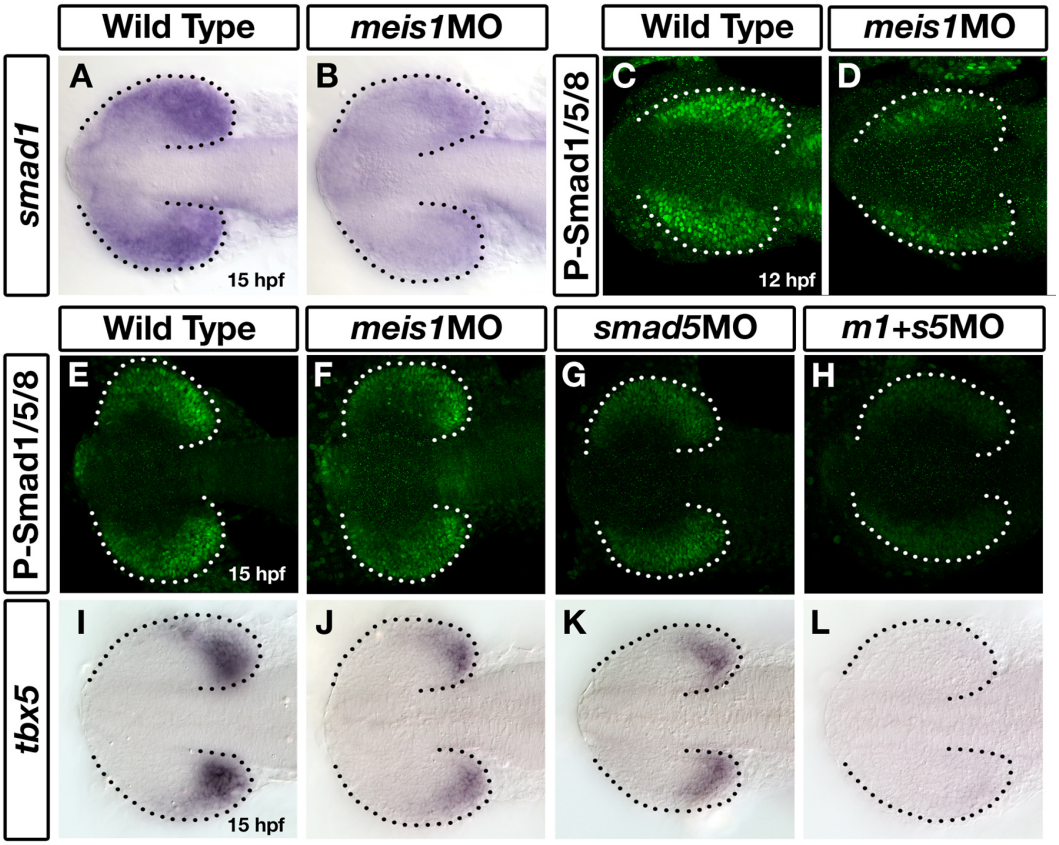

Figure 6-4. Meis1 positively regulates *smad1* expression in the developing eye. **(A, B)** mRNA in situ hybridization for *smad1*in 15 hpf wild type and *meis1* morphant embryos. **(C, D)** Confocal images of whole mount 12 hpf embryos stained for phosphorylated Smad1/5/8. **(E-H)** Phospho-Smad1/5/8 stains on whole mount 15 hpf embryos treated with *meis1* morpholino (F), *smad5* morpholino (G) or a combination of both morpholinos (H). **(I-L)** mRNA in situ hybridization for *tbx5* in 15 hpf wild type (I), *meis1* morphant (J), *smad5* morphant (K), and *meis1-smad5* double morphant (L) embryos. Dotted lines outline the optic vesicle. All views are dorsal with anterior to the left.

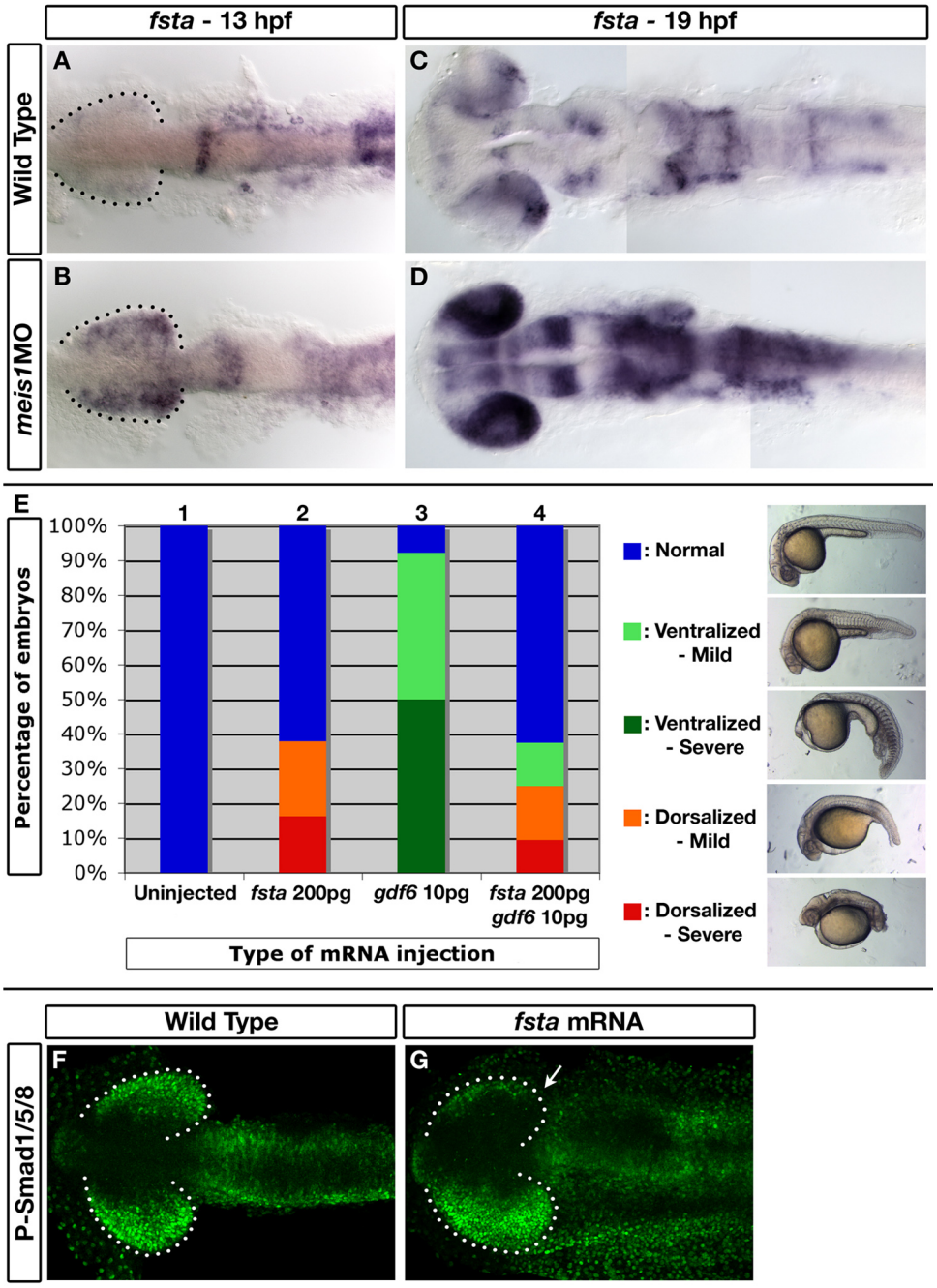

Figure 6-5. *follistatin a* is ectopically expressed in Meis1-depleted embryos and can inhibit Gdf6-mediated Bmp signaling. **(A-D)** mRNA in situ hybridizations for *follistatin a* (*fsta*) on 13 hpf (A, B) and 19 hpf (C, D) wild type and *meis1* morphant embryos. Dotted lines outline the optic vesicle. All views are dorsal with anterior to the left. **(E)** Results of the GDF6-Fsta interaction experiments. One-cell embryos were injected with either 200 pg of zebrafish *fsta* mRNA (Bar 2), human *GDF6* mRNA (Bar 3), or both mRNAs (Bar 4), raised until 28 hpf, and

scored for dorsalized and ventralized phenotypes (see legend on the right for classification). **(F, G)** Confocal images of whole mount immunostains for phospho-Smad1/5/8 in wild type and *fsta* mRNA-injected embryos at 14 hpf. Injection of *fsta* mRNA into one cell of a two-cell embryo causes a unilateral reduction in phospho-Smad1/5/8 staining (arrow in G). Dotted lines outline the optic vesicle. Views are dorsal with anterior to the left.

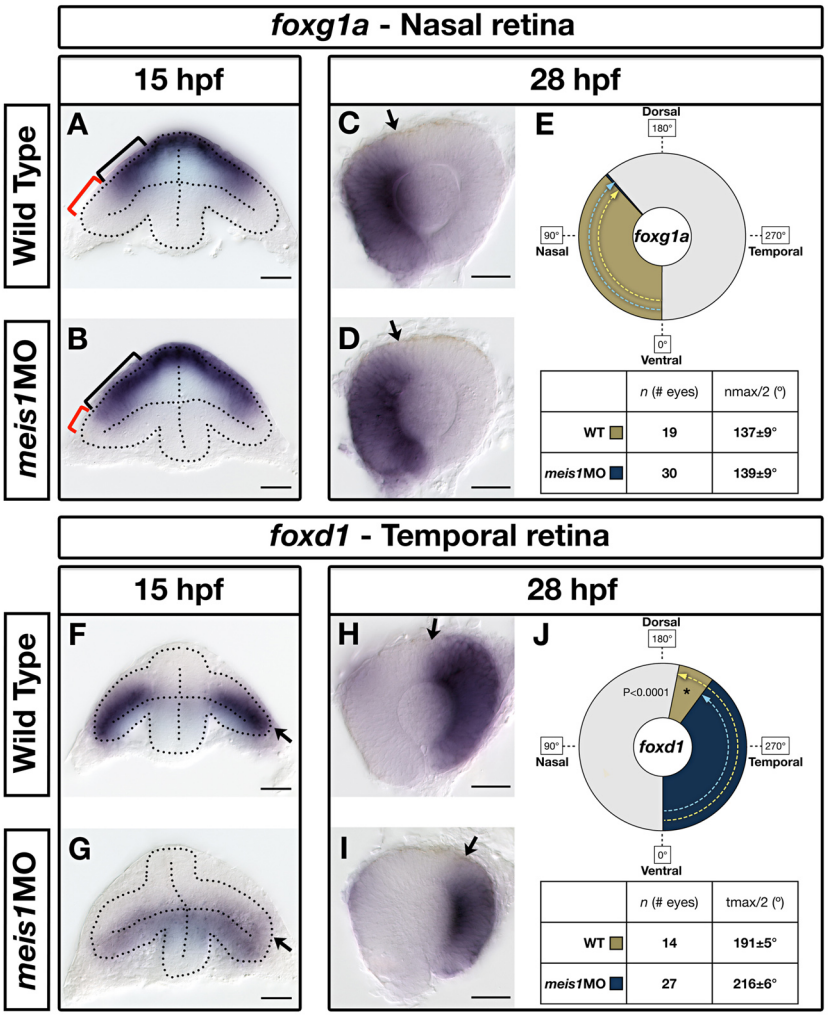

Figure 6-6. Meis1-depleted embryos exhibit a partial loss of temporal identity in the retina. mRNA in situ hybridization (ISH) for the nasal marker *foxg1a* **(A, B)** and the temporal marker *foxd1* **(F, G)** in 15 hpf wild type and *meis1* morphant embryos. Dotted lines outline the optic vesicle. Brackets in A and B indicate the proximal-distal extent of *foxg1a* expression. Arrows in F and G indicate the dorsal leaflet of the optic vesicle. Transverse sections are oriented dorsal up. **(C-J)** mRNA ISH for the nasal marker *foxg1a* **(C-E)** and the temporal marker *foxd1* **(H-J)** in dissected, flat-mounted eyes from 28 hpf wild type and *meis1* morphant embryos. The domains of gene expression were quantified by determining a 360° profile of in situ staining intensity and graphing the radial position at which gene expression intensity falls to the halfway point between its minimum and maximum values (see Methods). The nmax/2 and tmax/2 values are given as the

mean radial position in degrees plus/minus one standard deviation. Asterisks indicate regions in which there are statistically significant differences in axial identity between wild type and *meis1* morphants as determined by an unpaired, two-tailed t-test using a P value of 0.01 as a cutoff for significance. Representative dissected eyes are shown. Scale bars = 50 μM.

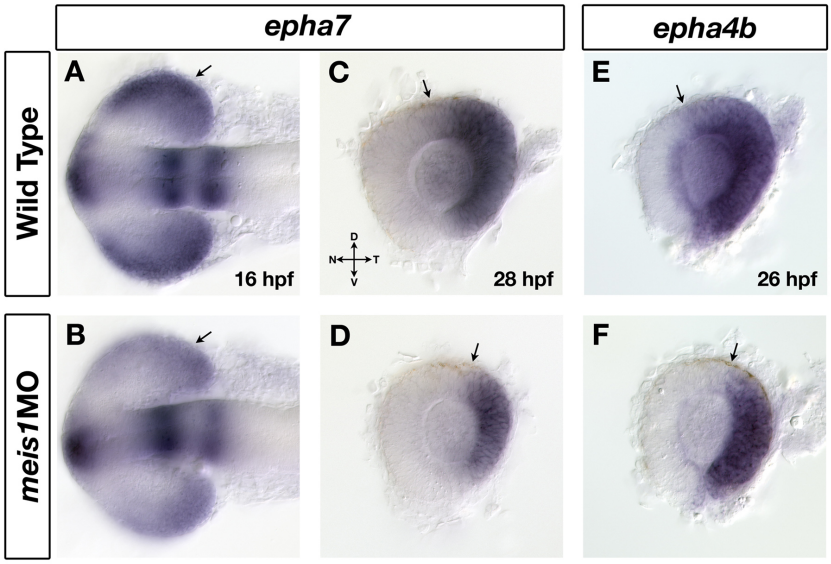

Figure 6-7. The temporal expression domains of *epha7* and *epha4b* are reduced in *meis1* morphants. **(A, B)** mRNA in situ hybridization (ISH) for *epha7* on wild type (A) and *meis1* morphant (B) embryos at 16 hpf. Arrows indicate the expression of *epha7* in the presumptive temporal retina. Embryos are shown in dorsal view with anterior to the left. **(C-F)** mRNA ISH for the temporal markers *epha7* **(C, D)** and *epha4b* **(E, F)** in dissected, flat-mounted eyes from 26-28 hpf wild type and *meis1* morphant embryos. Arrows indicate the dorsal extent of gene expression. Representative dissected eyes are shown. Legend for retinal axial orientation: D- dorsal, V – ventral, N – nasal, T – temporal.

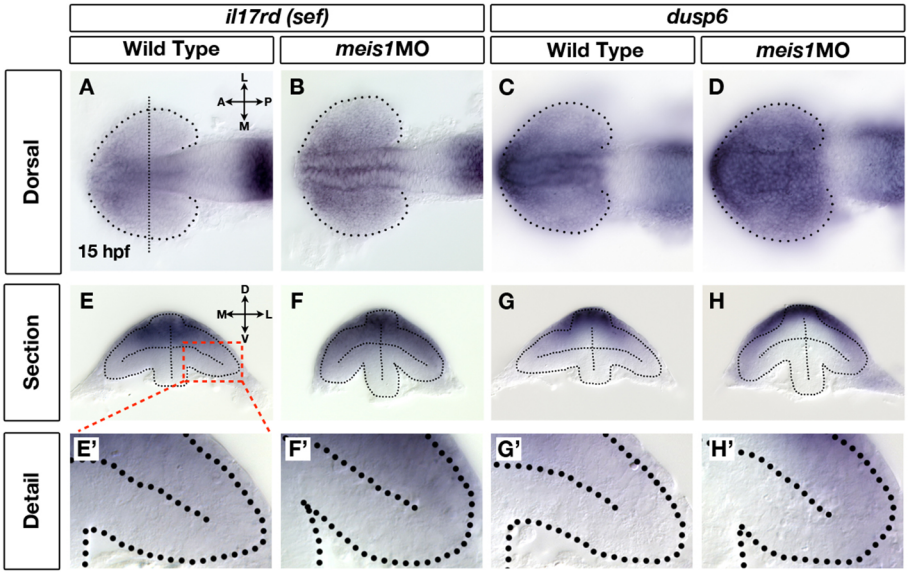

Figure 6-8. Fgf signaling in the retina is upregulated in *meis1* morphants. **(A-D)** mRNA in situ hybridization (ISH) for Fgf-responsive genes *il17rd* / *sef* (A, B) and *dusp6* (C, D) in wild type (A, C) and *meis1* morphant (B, D) embryos. Dotted lines outline the optic vesicle. The vertical dotted line in A indicates the estimated position of the transverse sections in E-H. Views are dorsal with anterior left. **(E-H)** Transverse sections through the eyes of 15 hpf wild type and *meis1* morphant embryos stained for *il17rd* and *dusp6*. **(E'-H')** Detailed views of the corresponding sections in E-H. The region of interest is indicated by the red dashed-line box. Dotted lines outline the optic vesicles. All transverse sections are oriented with dorsal up. Legend for retinal axial position: D - dorsal, V- ventral, N – nasal, T- temporal, L – lateral, M – medial, A – anterior, P - posterior.

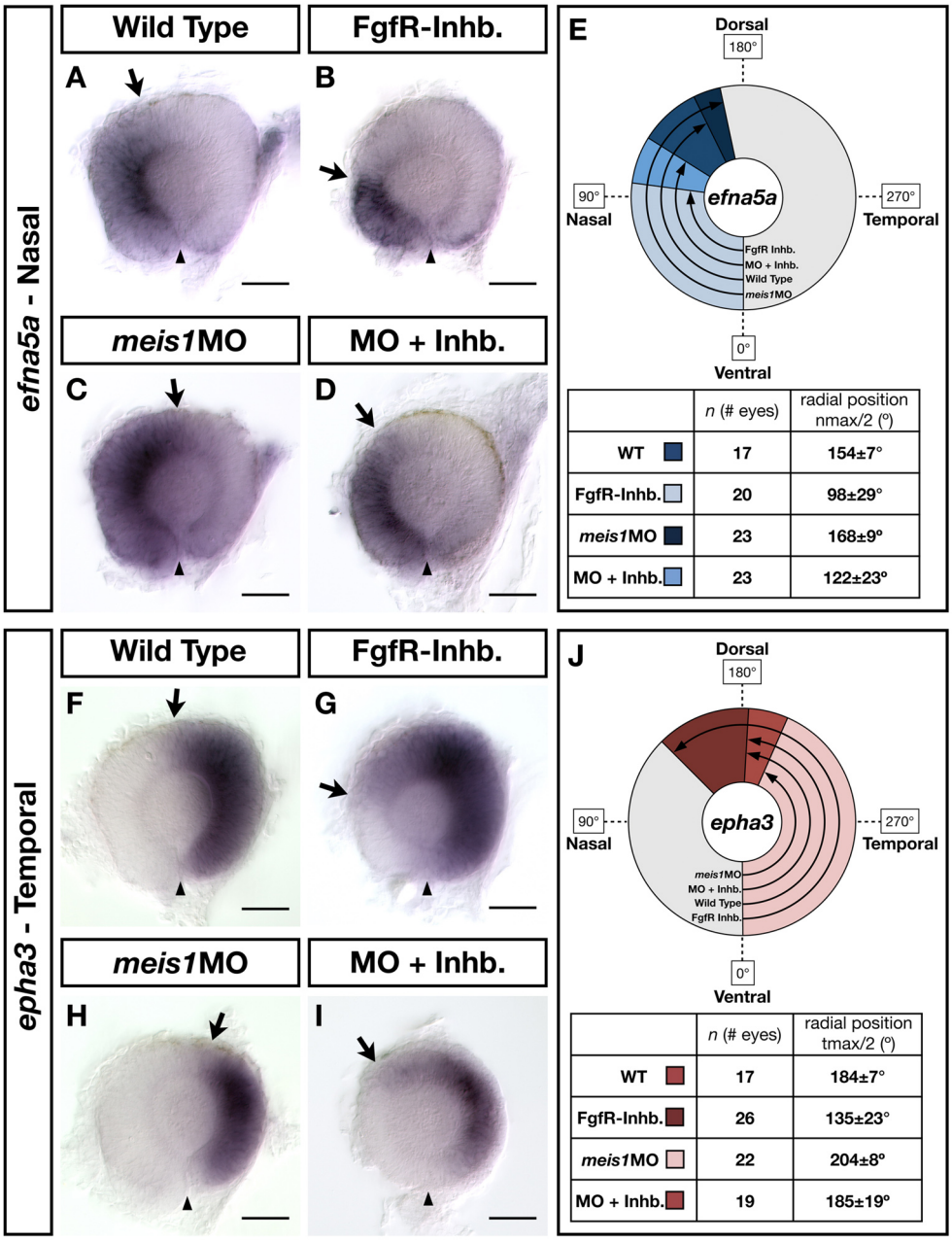

Figure 6-9. The contribution of Fgf signaling to the nasal-temporal patterning defects in Meis1-depleted embryos. **(A-D, F-I)** mRNA in situ hybridizations for the NT markers *efna5a* and *epha3* in wild type, Meis1-depleted, Fgf receptor-inhibitor treated, and FgfR-inhibited/Meis1-depleted retinas. Arrows indicate the extent of the gene expression domain, while the arrowheads indicate the position of the ventral choroid fissure. Representative dissected eyes are shown oriented with dorsal up and nasal to the left. Scale bars = 50 µM. **(E, J)** Quantification of the changes in *efna5a* and *epha3* expression, as quantified by measuring a 360°

profile of in situ staining intensity and graphing the mean radial position at which gene expression intensity falls to the halfway point between its minimum and maximum values. The nmax/2 and tmax/2 values are given as the mean radial position in degrees plus/minus one standard deviation.

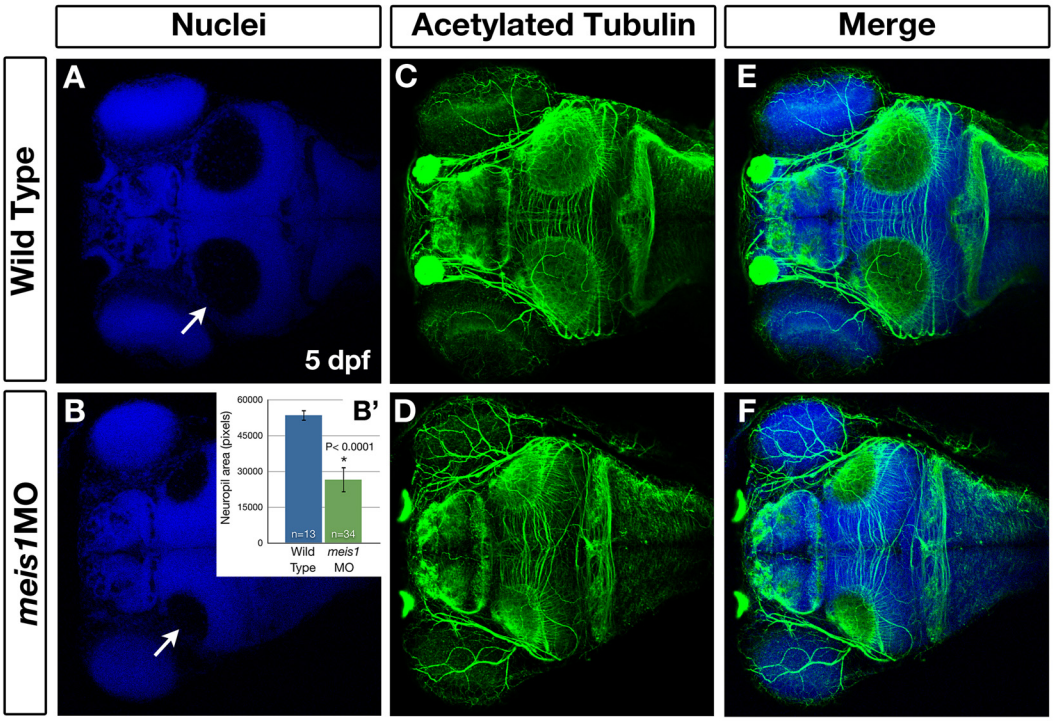

Figure 6-10. Meis1-depleted embryos have smaller tectal neuropil. **(A-F)** Whole mount immunohistochemistry using anti-acetylated tubulin (axons) and Hoechst 33258 (nuclei) to compare the size of the tectal neuropil in 5 dpf WT (A, C, E) and *meis1* morphant (B, D, F) embryos. White arrows in A and B indicate the tectal neuropil. **(B')** The area (in pixels) of the neuropil from wild type and *meis1* morphant embryos was measured using ImageJ. The *n*-values represent individual neuropil regions. The asterisk indicates a statistically significant reduction the size of morphant neuropil as determined by an unpaired, two-tailed t-test.

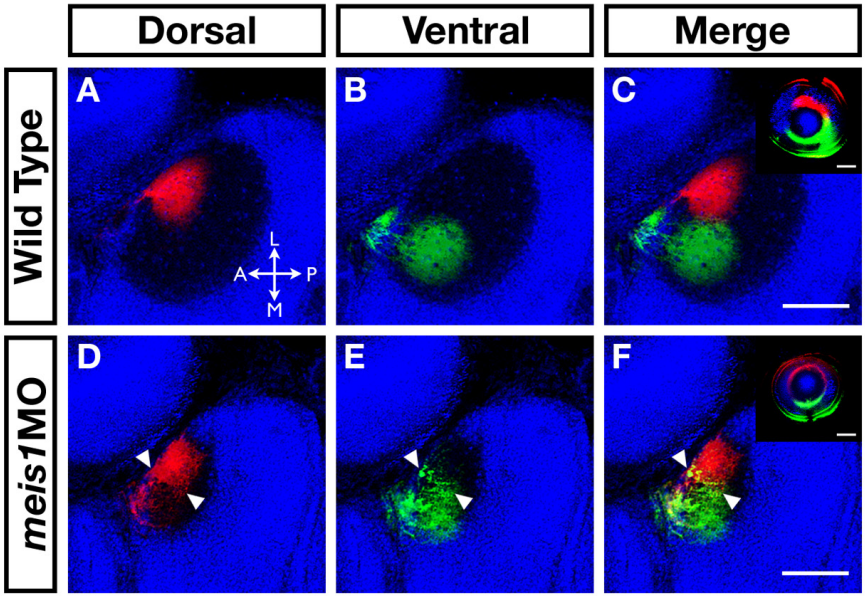

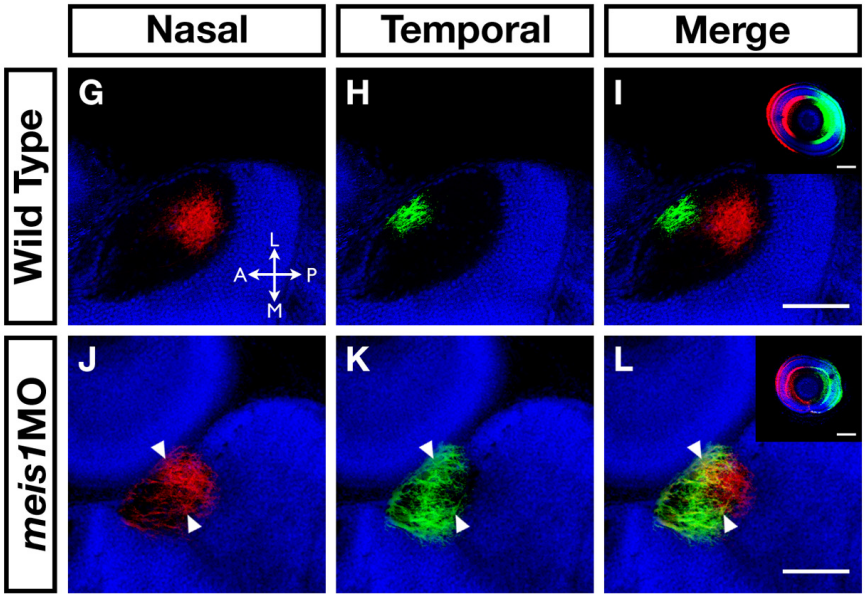

M

*meis1*MO phenotype	Dorsal-Ventral	Nasal-Temporal
Patterning Defect (overlap)	18	25
Axons overshoot the tectum	1	3
No tectal innervation (stalling)	15	23
Wild type-like	13	13
Total (*n*)	47	64

Figure 6-11. The retinotectal map is disorganized in Meis1-depleted embryos. **(A-L)** Lipophilic fluorescent dyes DiI (red) and DiO (green) were injected into specific axial positions of the retina of fixed 5 dpf wild type and *meis1* morphant

embryos and innervation patterns of the ganglion cell axons on the tectum were imaged by confocal microscopy. Nuclei are stained with Hoechst 33258 (blue). The wild type (A-C) medial-lateral segregation of dorsal (red) and ventral (green) ganglion cell axons in the tectum is lost in *meis1* morphants (white arrowheads in D-F). Similarly, the wild type (G-I) anterior-posterior segregation of nasal (red) and temporal (green) ganglion cell axons in the tectum is disorganized in *meis1* morphants (white arrowheads in J-L). The insets in C, F, I, and L are lateral views of injected retinas from the embryos shown in the corresponding panels. Retinas are oriented with dorsal up and nasal to the left, while all tectal views are dorsal with anterior to the left. Legend for axial position in the tectum: L – lateral, M – medial, A – anterior, P – posterior. All scale bars = 75 μM. **(M)** Table describing the frequency of various retinotectal mapping phenotypes observed in *meis1* morphants. No retinotectal mapping defects were observed in any wild type embryos examined. Note: this experiment was performed by Curtis French.

6.5 References

Agoston, Z., Schulte, D., 2009. Meis2 competes with the Groucho co-repressor Tle4 for binding to Otx2 and specifies tectal fate without induction of a secondary midbrain-hindbrain boundary organizer. Development. 136**,** 3311-22.

Amthor, H., Christ, B., Rashid-Doubell, F., Kemp, C. F., Lang, E., Patel, K., 2002. Follistatin regulates bone morphogenetic protein-7 (BMP-7) activity to stimulate embryonic muscle growth. Dev Biol. 243**,** 115-27.

Arnold, S. J., Maretto, S., Islam, A., Bikoff, E. K., Robertson, E. J., 2006. Dose-dependent Smad1, Smad5 and Smad8 signaling in the early mouse embryo. Developmental Biology. 296**,** 104.

Barbieri, A. M., Broccoli, V., Bovolenta, P., Alfano, G., Marchitiello, A., Mocchetti, C., Crippa, L., Bulfone, A., Marigo, V., Ballabio, A., Banfi, S., 2002. Vax2 inactivation in mouse determines alteration of the eye dorsal-ventral axis, misrouting of the optic fibres and eye coloboma. Development. 129**,** 805-13.

Behesti, H., Holt, J. K., Sowden, J. C., 2006. The level of BMP4 signaling is critical for the regulation of distinct T-box gene expression domains and growth along the dorso-ventral axis of the optic cup. BMC Dev Biol. 6**,** 62.

Bessa, J., Gebelein, B., Pichaud, F., Casares, F., Mann, R. S., 2002. Combinatorial control of Drosophila eye development by eyeless, homothorax, and teashirt. Genes Dev. 16**,** 2415-27.

Bessa, J., Tavares, M. J., Santos, J., Kikuta, H., Laplante, M., Becker, T. S., Gomez-Skarmeta, J. L., Casares, F., 2008. meis1 regulates cyclin D1 and c-myc expression, and controls the proliferation of the multipotent cells in the early developing zebrafish eye. Development. 135**,** 799-803.

Chang, C., Hemmati-Brivanlou, A., 1999. Xenopus GDF6, a new antagonist of noggin and a partner of BMPs. Development. 126**,** 3347-57.

Chang, C. P., Jacobs, Y., Nakamura, T., Jenkins, N. A., Copeland, N. G., Cleary, M. L., 1997. Meis proteins are major in vivo DNA binding partners for wild-type but not chimeric Pbx proteins. Mol Cell Biol. 17**,** 5679-87.

Chen, J., Ruley, H. E., 1998. An enhancer element in the EphA2 (Eck) gene sufficient for rhombomere-specific expression is activated by HOXA1 and HOXB1 homeobox proteins. J Biol Chem. 273**,** 24670-5.

Cheng, H. J., Nakamoto, M., Bergemann, A. D., Flanagan, J. G., 1995. Complementary gradients in expression and binding of ELF-1 and Mek4 in development of the topographic retinotectal projection map. Cell. 82**,** 371-81.

Choe, S.-K., Lu, P., Nakamura, M., Lee, J., Sagerstrˆm, C. G., 2009. Meis Cofactors Control HDAC and CBP Accessibility at Hox-Regulated Promoters during Zebrafish Embryogenesis. Developmental Cell. 17**,** 561-567.

Choe, S. K., Vlachakis, N., Sagerstrom, C. G., 2002. Meis family proteins are required for hindbrain development in the zebrafish. Development. 129**,** 585-95.

Cooke, J. E., Kemp, H. A., Moens, C. B., 2005. EphA4 is required for cell adhesion and rhombomere-boundary formation in the zebrafish. Curr Biol. 15**,** 536-42.

Cooke, J. E., Moens, C. B., 2002. Boundary formation in the hindbrain: Eph only it were simple. Trends Neurosci. 25**,** 260-7.

Deflorian, G., Tiso, N., Ferretti, E., Meyer, D., Blasi, F., Bortolussi, M., Argenton, F., 2004. Prep1.1 has essential genetic functions in hindbrain development and cranial neural crest cell differentiation. Development. 131**,** 613-27.

Dick, A., Meier, A., Hammerschmidt, M., 1999. Smad1 and Smad5 have distinct roles during dorsoventral patterning of the zebrafish embryo. Dev Dyn. 216**,** 285-98.

Erickson, T., Scholpp, S., Brand, M., Moens, C. B., Waskiewicz, A. J., 2007. Pbx proteins cooperate with Engrailed to pattern the midbrain-hindbrain and diencephalic-mesencephalic boundaries. Dev Biol. 301**,** 504-17.

Fainsod, A., Deissler, K., Yelin, R., Marom, K., Epstein, M., Pillemer, G., Steinbeisser, H., Blum, M., 1997. The dorsalizing and neural inducing gene follistatin is an antagonist of BMP-4. Mech Dev. 63**,** 39-50.

Feldheim, D. A., Kim, Y. I., Bergemann, A. D., Frisen, J., Barbacid, M., Flanagan, J. G., 2000. Genetic analysis of ephrin-A2 and ephrin-A5 shows their requirement in multiple aspects of retinocollicular mapping. Neuron. 25**,** 563-74.

Feldheim, D. A., Nakamoto, M., Osterfield, M., Gale, N. W., DeChiara, T. M., Rohatgi, R., Yancopoulos, G. D., Flanagan, J. G., 2004. Loss-of-function analysis of EphA receptors in retinotectal mapping. J Neurosci. 24**,** 2542-50.

French, C. R., Erickson, T., Callander, D., Berry, K. M., Koss, R., Hagey, D. W., Stout, J., Wuennenberg-Stapleton, K., Ngai, J., Moens, C. B., Waskiewicz, A. J., 2007. Pbx homeodomain proteins pattern both the zebrafish retina and tectum. BMC Dev Biol. 7**,** 85.

French, C. R., Erickson, T., French, D. V., Pilgrim, D. B., Waskiewicz, A. J., 2009. Gdf6a is required for the initiation of dorsal-ventral retinal patterning and lens development. Dev Biol. 333**,** 37-47.

Freudenberg, J. A., Chen, W. T., 2007. Induction of Smad1 by MT1-MMP contributes to tumor growth. Int J Cancer. 121**,** 966-77.

Furthauer, M., Lin, W., Ang, S. L., Thisse, B., Thisse, C., 2002. Sef is a feedback-induced antagonist of Ras/MAPK-mediated FGF signalling. Nat Cell Biol. 4**,** 170-4.

Goh, S. L., Looi, Y., Shen, H., Fang, J., Bodner, C., Houle, M., Ng, A. C., Screaton, R. A., Featherstone, M., 2009. Transcriptional activation by MEIS1A in response to protein kinase A signaling requires the transducers of regulated CREB family of CREB co-activators. J Biol Chem. 284**,** 18904-12.

Goodhill, G. J., Richards, L. J., 1999. Retinotectal maps: molecules, models and misplaced data. Trends Neurosci. 22**,** 529-34.

Gosse, N. J., Baier, H., 2009. An essential role for Radar (Gdf6a) in inducing dorsal fate in the zebrafish retina. Proc Natl Acad Sci U S A. 106**,** 2236-41.

Gosse, N. J., Nevin, L. M., Baier, H., 2008. Retinotopic order in the absence of axon competition. Nature. 452**,** 892-5.

Harada, T., Harada, C., Parada, L. F., 2007. Molecular regulation of visual system development: more than meets the eye. Genes Dev. 21**,** 367-78.

Hatini, V., Tao, W., Lai, E., 1994. Expression of winged helix genes, BF-1 and BF-2, define adjacent domains within the developing forebrain and retina. J Neurobiol. 25**,** 1293-309.

Heine, P., Dohle, E., Bumsted-O'Brien, K., Engelkamp, D., Schulte, D., 2008. Evidence for an evolutionary conserved role of homothorax/Meis1/2 during vertebrate retina development. Development. 135**,** 805-11.

Hindges, R., McLaughlin, T., Genoud, N., Henkemeyer, M., O'Leary, D. D., 2002. EphB forward signaling controls directional branch extension and arborization required for dorsal-ventral retinotopic mapping. Neuron. 35**,** 475-87.

Hisa, T., Spence, S. E., Rachel, R. A., Fujita, M., Nakamura, T., Ward, J. M., Devor-Henneman, D. E., Saiki, Y., Kutsuna, H., Tessarollo, L., Jenkins, N. A., Copeland, N. G., 2004. Hematopoietic, angiogenic and eye defects in Meis1 mutant animals. Embo J. 23**,** 450-9.

Hornberger, M. R., Dutting, D., Ciossek, T., Yamada, T., Handwerker, C., Lang, S., Weth, F., Huf, J., Wessel, R., Logan, C., Tanaka, H., Drescher, U., 1999. Modulation of EphA receptor function by coexpressed ephrinA ligands on retinal ganglion cell axons. Neuron. 22**,** 731-42.

Huang, H., Rastegar, M., Bodner, C., Goh, S. L., Rambaldi, I., Featherstone, M., 2005. MEIS C termini harbor transcriptional activation domains that respond to cell signaling. J Biol Chem. 280**,** 10119-27.

Iemura, S., Yamamoto, T. S., Takagi, C., Uchiyama, H., Natsume, T., Shimasaki, S., Sugino, H., Ueno, N., 1998. Direct binding of follistatin to a complex of bone-morphogenetic protein and its receptor inhibits ventral and epidermal cell fates in early Xenopus embryo. Proc Natl Acad Sci U S A. 95**,** 9337-42.

Kemp, H. A., Cooke, J. E., Moens, C. B., 2009. EphA4 and EfnB2a maintain rhombomere coherence by independently regulating intercalation of progenitor cells in the zebrafish neural keel. Dev Biol. 327**,** 313-26.

Koshiba-Takeuchi, K., Takeuchi, J. K., Matsumoto, K., Momose, T., Uno, K., Hoepker, V., Ogura, K., Takahashi, N., Nakamura, H., Yasuda, K., Ogura, T., 2000. Tbx5 and the retinotectum projection. Science. 287**,** 134-7.

Lemke, G., Reber, M., 2005. Retinotectal Mapping: New Insights from Molecular Genetics. Annual Review of Cell and Developmental Biology. 21**,** 551-580.

Li, C., Scott, D. A., Hatch, E., Tian, X., Mansour, S. L., 2007. Dusp6 (Mkp3) is a negative feedback regulator of FGF-stimulated ERK signaling during mouse development. Development. 134**,** 167-76.

Li, Z., Joseph, N. M., Easter, S. S., Jr., 2000. The morphogenesis of the zebrafish eye, including a fate map of the optic vesicle. Dev Dyn. 218**,** 175-88.

Lupo, G., Liu, Y., Qiu, R., Chandraratna, R. A. S., Barsacchi, G., He, R.-Q., Harris, W. A., 2005. Dorsoventral patterning of the Xenopus eye: a collaboration of Retinoid, Hedgehog and FGF receptor signaling. Development. 132**,** 1737-1748.

Mann, F., Ray, S., Harris, W., Holt, C., 2002. Topographic mapping in dorsoventral axis of the Xenopus retinotectal system depends on signaling through ephrin-B ligands. Neuron. 35**,** 461-73.

Maves, L., Tyler, A., Moens, C. B., Tapscott, S. J., 2009. Pbx acts with Hand2 in early myocardial differentiation. Dev Biol. 333**,** 409-18.

Maves, L., Waskiewicz, A. J., Paul, B., Cao, Y., Tyler, A., Moens, C. B., Tapscott, S. J., 2007. Pbx homeodomain proteins direct Myod activity to promote fast-muscle differentiation. Development. 134**,** 3371-82.

McLaughlin, T., Hindges, R., O'Leary, D. D., 2003. Regulation of axial patterning of the retina and its topographic mapping in the brain. Curr Opin Neurobiol. 13**,** 57-69.

McReynolds, L. J., Gupta, S., Figueroa, M. E., Mullins, M. C., Evans, T., 2007. Smad1 and Smad5 differentially regulate embryonic hematopoiesis. Blood. 110**,** 3881-90.

Moens, C. B., Selleri, L., 2006. Hox cofactors in vertebrate development. Dev Biol. 291**,** 193-206.

Molina, G., Watkins, S., Tsang, M., 2007. Generation of FGF reporter transgenic zebrafish and their utility in chemical screens. BMC Developmental Biology. 7**,** 62.

Mui, S. H., Hindges, R., O'Leary, D. D., Lemke, G., Bertuzzi, S., 2002. The homeodomain protein Vax2 patterns the dorsoventral and nasotemporal axes of the eye. Development. 129**,** 797-804.

Mui, S. H., Kim, J. W., Lemke, G., Bertuzzi, S., 2005. Vax genes ventralize the embryonic eye. Genes Dev. 19**,** 1249-59.

Murali, D., Yoshikawa, S., Corrigan, R. R., Plas, D. J., Crair, M. C., Oliver, G., Lyons, K. M., Mishina, Y., Furuta, Y., 2005. Distinct developmental programs require different levels of Bmp signaling during mouse retinal development. Development. 132**,** 913-23.

Nakamoto, M., Cheng, H. J., Friedman, G. C., McLaughlin, T., Hansen, M. J., Yoon, C. H., O'Leary, D. D., Flanagan, J. G., 1996. Topographically specific effects of ELF-1 on retinal axon guidance in vitro and retinal axon mapping in vivo. Cell. 86**,** 755-66.

Nakayama, Y., Miyake, A., Nakagawa, Y., Mido, T., Yoshikawa, M., Konishi, M., Itoh, N., 2008. Fgf19 is required for zebrafish lens and retina development. Dev Biol. 313**,** 752-66.

Pai, C. Y., Kuo, T. S., Jaw, T. J., Kurant, E., Chen, C. T., Bessarab, D. A., Salzberg, A., Sun, Y. H., 1998. The Homothorax homeoprotein activates the nuclear localization of another homeoprotein, extradenticle, and suppresses eye development in Drosophila. Genes Dev. 12**,** 435-46.

Pangas, S. A., Li, X., Umans, L., Zwijsen, A., Huylebroeck, D., Gutierrez, C., Wang, D., Martin, J. F., Jamin, S. P., Behringer, R. R., Robertson, E. J., Matzuk, M. M., 2008. Conditional deletion of Smad1 and Smad5 in somatic cells of male and female gonads leads to metastatic tumor development in mice. Mol Cell Biol. 28**,** 248-57.

Picker, A., Brand, M., 2005. Fgf signals from a novel signaling center determine axial patterning of the prospective neural retina. Development. 132**,** 4951-62.

Picker, A., Cavodeassi, F., Machate, A., Bernauer, S., Hans, S., Abe, G., Kawakami, K., Wilson, S. W., Brand, M., 2009. Dynamic coupling of pattern formation and morphogenesis in the developing vertebrate retina. PLoS Biol. 7**,** e1000214.

Plas, D. T., Dhande, O. S., Lopez, J. E., Murali, D., Thaller, C., Henkemeyer, M., Furuta, Y., Overbeek, P., Crair, M. C., 2008. Bone morphogenetic proteins, eye patterning, and retinocollicular map formation in the mouse. J Neurosci. 28**,** 7057-67.

Rashid, T., Upton, A. L., Blentic, A., Ciossek, T., Knoll, B., Thompson, I. D., Drescher, U., 2005. Opposing gradients of ephrin-As and EphA7 in the superior colliculus are essential for topographic mapping in the mammalian visual system. Neuron. 47**,** 57-69.

Retting, K. N., Song, B., Yoon, B. S., Lyons, K. M., 2009. BMP canonical Smad signaling through Smad1 and Smad5 is required for endochondral bone formation. Development. 136**,** 1093-104.

Sakuta, H., Suzuki, R., Takahashi, H., Kato, A., Shintani, T., Iemura, S., Yamamoto, T. S., Ueno, N., Noda, M., 2001. Ventroptin: a BMP-4 antagonist expressed in a double-gradient pattern in the retina. Science. 293**,** 111-5.

Sakuta, H., Takahashi, H., Shintani, T., Etani, K., Aoshima, A., Noda, M., 2006. Role of bone morphogenic protein 2 in retinal patterning and retinotectal projection. J Neurosci. 26**,** 10868-78.

Schmitt, E. A., Dowling, J. E., 1994. Early eye morphogenesis in the zebrafish, Brachydanio rerio. J Comp Neurol. 344**,** 532-42.

Schulte, D., Furukawa, T., Peters, M. A., Kozak, C. A., Cepko, C. L., 1999. Misexpression of the Emx-related homeobox genes cVax and mVax2 ventralizes the retina and perturbs the retinotectal map. Neuron. 24**,** 541-53.

Scicolone, G., Ortalli, A. L., Carri, N. G., 2009. Key roles of Ephs and ephrins in retinotectal topographic map formation. Brain Res Bull. 79**,** 227-47.

Shen, W. F., Montgomery, J. C., Rozenfeld, S., Moskow, J. J., Lawrence, H. J., Buchberg, A. M., Largman, C., 1997. AbdB-like Hox proteins stabilize DNA binding by the Meis1 homeodomain proteins. Mol Cell Biol. 17**,** 6448-58.

Shim, S., Kim, Y., Shin, J., Kim, J., Park, S., 2007. Regulation of EphA8 gene expression by TALE homeobox transcription factors during development of the mesencephalon. Mol Cell Biol. 27**,** 1614-30.

Sohl, M., Lanner, F., Farnebo, F., 2009. Characterization of the murine Ephrin-B2 promoter. Gene. 437**,** 54-9.

Stuermer, C. A., 1988. Retinotopic organization of the developing retinotectal projection in the zebrafish embryo. J Neurosci. 8**,** 4513-30.

Sun, Y., Fan, J., Shen, H., Li, P., Cattini, P., Gong, Y., 2007. Cloning and promoter activity of rat Smad1 5'-flanking region in rat hepatic stellate cells. Mol Cell Biochem. 304**,** 227-34.

Takahashi, H., Sakuta, H., Shintani, T., Noda, M., 2009. Functional mode of FoxD1/CBF2 for the establishment of temporal retinal specificity in the developing chick retina. Dev Biol. 331**,** 300-10.

Takahashi, H., Shintani, T., Sakuta, H., Noda, M., 2003. CBF1 controls the retinotectal topographical map along the anteroposterior axis through multiple mechanisms. Development. 130**,** 5203-15.

Take-uchi, M., Clarke, J. D., Wilson, S. W., 2003. Hedgehog signalling maintains the optic stalk-retinal interface through the regulation of Vax gene activity. Development. 130**,** 955-68.

Theil, T., Frain, M., Gilardi-Hebenstreit, P., Flenniken, A., Charnay, P., Wilkinson, D. G., 1998. Segmental expression of the EphA4 (Sek-1) receptor tyrosine kinase in the hindbrain is under direct transcriptional control of Krox-20. Development. 125**,** 443-52.

Tsang, M., Friesel, R., Kudoh, T., Dawid, I. B., 2002. Identification of Sef, a novel modulator of FGF signalling. Nat Cell Biol. 4**,** 165-9.

Veien, E. S., Rosenthal, J. S., Kruse-Bend, R. C., Chien, C. B., Dorsky, R. I., 2008. Canonical Wnt signaling is required for the maintenance of dorsal retinal identity. Development. 135**,** 4101-11.

Vlachakis, N., Choe, S. K., Sagerstrom, C. G., 2001. Meis3 synergizes with Pbx4 and Hoxb1b in promoting hindbrain fates in the zebrafish. Development. 128**,** 1299-312.

Waskiewicz, A. J., Rikhof, H. A., Hernandez, R. E., Moens, C. B., 2001. Zebrafish Meis functions to stabilize Pbx proteins and regulate hindbrain patterning. Development. 128**,** 4139-51.

Waskiewicz, A. J., Rikhof, H. A., Moens, C. B., 2002. Eliminating zebrafish pbx proteins reveals a hindbrain ground state. Dev Cell. 3**,** 723-33.

Xu, Q., Mellitzer, G., Robinson, V., Wilkinson, D. G., 1999. In vivo cell sorting in complementary segmental domains mediated by Eph receptors and ephrins. Nature. 399**,** 267-71.

Zhang, X., Friedman, A., Heaney, S., Purcell, P., Maas, R. L., 2002. Meis homeoproteins directly regulate Pax6 during vertebrate lens morphogenesis. Genes Dev. 16**,** 2097-107.

Zhang, X. M., Yang, X. J., 2001. Temporal and spatial effects of Sonic hedgehog signaling in chick eye morphogenesis. Dev Biol. 233**,** 271-90.

Zhou, C. J., Molotkov, A., Song, L., Li, Y., Pleasure, D. E., Pleasure, S. J., Wang, Y. Z., 2008. Ocular coloboma and dorsoventral neuroretinal patterning defects in Lrp6 mutant eyes. Dev Dyn. 237**,** 3681-9.

Chapter Seven - General Discussion and Conclusions

7. Conclusions

7.1 Summary

During early embryonic development, neural tissue is broadly subdivided along the anterior-posterior (AP) axis. Subsequently, these forebrain, midbrain and hindbrain domains are further subdivided into morphologically and molecularly distinct compartments that allow for the emergence of functionally specialized cell types and tissues (reviewed in Kiecker and Lumsden, 2005). How the nervous system becomes compartmentalized is one of the most interesting and fundamental questions in developmental biology. The hindbrain, with its clear metameric organization, is an excellent model in which to study this process. After almost thirty years of research on the molecular and genetic mechanisms of hindbrain segmentation, it is clear that this process requires the precise temporal and spatial integration of multiple transcriptional and signaling pathways. At the heart of this process are the Hox and TALE-class homeodomain transcription factors. The transcriptional output of Hox-Pbx-Meinox complexes is required for all aspects of AP hindbrain patterning, for when their function is disrupted, the hindbrain loses its segmental character (reviewed in Moens and Prince, 2002). Although a lot is known about what Hox-Pbx-Meinox complexes do in the broad sense of AP hindbrain patterning, not as much is known about the individual roles of these proteins. This is particularly true of the Meinox family of TALE-class homeodomain transcription factors, seven of which are expressed in the hindbrain during its segmentation period. Another area of hindbrain research that has not received due attention is the role of non-homeodomain transcription factors in regulating Hox function. In Drosophila, the zinc-finger protein Teashirt modulates Hox-dependent AP patterning of the fly body plan, but the role of vertebrate Teashirt-related proteins in hindbrain patterning has not been examined. To increase our understanding in these areas, I studied the roles of *meis1* (Chapter 3) and the *teashirt* homologue *tshz3b* (Chapter 4) in regulating AP patterning of the hindbrain.

The hindbrain is not the only tissue where axial patterning is important for tissue function. Correct functioning of the visual system also requires that axial position be specified within the retina and midbrain (mesencephalon). Although the axial polarity of these tissues is not as obvious as that of the hindbrain, the same signaling pathways that pattern the hindbrain along its AP and DV axes are also responsible for retinal and mesencephalic patterning. As a group, *pbx* and *meinox* genes are expressed throughout the developing vertebrate embryo, sometimes in tissues that do not express *hox* genes. In particular, the broad expression of *pbx2* and *pbx4* extends far beyond the anterior limit of *hox* gene expression in the hindbrain, and *meis1* is specifically expressed in the developing eyes and midbrain. This suggested that Pbx and Meis1 might be acting in a Hox-independent fashion to pattern the visual system. In support of this idea, I found that Pbx proteins cooperate with Engrailed homeodomain proteins to maintain lineage-restriction at the forebrain-midbrain and midbrain-hindbrain boundaries (Chapter 5), and that Meis1 plays a critical role in establishing axial position within the retina and tectum (Chapter 6). In summary, these studies clarify the role of *meis1* in Hox-dependent hindbrain patterning, and suggest a new level of Hox regulation by *tshz3b*. Additionally, I have demonstrated novel Hox-independent functions for the TALE-class proteins Pbx and Meis1 with regard to mesencephalic and retinal patterning (Figure 7-1). Overall, this thesis highlights the importance of Pbx and Meis in compartmentalizing the nervous system.

7.2 Insights into the study of TALE-class protein function

The Drosophila genome contains only a single PBC gene (*extradenticle*), and a single Meinox gene (*homothorax*). The simplicity of this system makes genetic and biochemical analyses of TALE-class function relatively easy to interpret. In contrast, most vertebrates have at least four *pbx* genes, most of which can be alternatively spliced. In the case of human PBX3 (ENSG00000167081), up to thirteen different transcripts can be produced, resulting in at least eight different peptides. Similarly, vertebrates possess multiple *meinox* genes (seven in zebrafish) that can also be alternatively processed to produce different coding and

non-coding transcripts (reviewed in Geerts et al., 2005). Thus, when studying TALE-class function, the issue of partial genetic redundancy complicates analysis of developmental function.

It is a fortunate state of affairs that there are only two *pbx* genes expressed during hindbrain segmentation in zebrafish, allowing for a Pbx loss-of-function phenotype to be reasonably approximated. On the downside, *meis1*, *meis2.1*, *meis2.2*, *meis3* and *pknox1* all show high levels of expression during early hindbrain patterning. As such, it is difficult to model a complete loss of *meinox* function by either forward or reverse genetic approaches. Furthermore, it is not clear to what extent the different Meinox proteins can compensate for one another in terms of their transcriptional activities and with regard to Pbx stabilization. On a related note, *hox* and TALE-class transcription and protein stability are regulated by auto- and para-regulatory loops. For example, Pbx regulates both *meis1* transcription and protein stability (Figure 3-2), while Meis1 is required both for its own transcription and for normal levels of Pbx protein (Figures 3-14, 3-15). Perturbations in the Pbx - Meis1 bidirectional stability loop may destabilize similar networks that exist between Pbx and other Meinox proteins. For these reasons, it is difficult to dissect the relative contributions of Pbx and Meinox proteins to hindbrain patterning, much less determine the individual transcriptional and biochemical functions of the various Meinox genes using an in vivo model system.

With these caveats in mind, knockdown of Meis1 does produce specific hindbrain patterning phenotypes that represent a subset of known Pbx and Hox functions. These include segmentation defects with regard to the identity of rhombomere 2 and maintenance of *hoxa2b* expression in this region (Figure 3-10, 3-12). Interestingly, although *meis1* morphants do not show a loss of r4 segmental identity, Meis1-depletion does lead to neuronal defects in rhombomere 4 that are normally associated with a loss of *hoxb1a* and *hoxb1b* function (Figure 3-16). This latter observation suggests that *meis1* contributes to hindbrain development in specific contexts. For example, Meis1 may be specifically required in a complex with Pbx and Hoxb1a to specify the Mauthner cell, or to promote the

tangential migration of facial motor neurons by activating the expression of *prickle1b*.

The challenge for the future will be to determine if these Meis1-knockdown phenotypes represent a specific requirement for transcriptional input from Meis1, or if they are the culmination of Meis1's biochemical and transcriptional activities. One of the ways to begin answering this question is to determine whether *meis1* is co-expressed with other *meis* genes in all cells of the hindbrain. For example, *meis2.2* is expressed in many of the same broad domains as *meis1*, but whether they are spatially and temporally co-expressed in the specific cells that are relevant for Mauthner cell specification or facial motor neuron migration has not been examined. Another way to approach this issue is to determine whether other *meis* genes can rescue the *meis1* loss of function phenotype. If *meis1* performs unique biochemical or transcriptional activities, then one would expect that overexpressing other *meinox* genes would not be able to restore Mauthner identity to FMN migration. Such studies would greatly enrich our knowledge about the Meinox family of transcription factors and their roles in hindbrain development.

Similarly, one of the major unanswered questions in the field of TALE-class biology is whether Pbx and Meinox proteins perform Hox-independent functions in tissues where Hox proteins are present. A growing body of evidence supports the idea that they function in tissues that do not express *hox* genes, but perhaps due to the problems of *hox* gene redundancy, confounding auto- and cross-regulatory loops, and a scarcity of bona fide direct Pbx-Meis target genes, this difficult and interesting question has not yet been addressed.

7.3 *tshz3b* may be a novel regulator of Hox-dependent hindbrain patterning

Teashirt-related proteins are multifunctional transcription factors, able to directly interact with transcriptional repressor complexes (Manfroid et al., 2004; Saller et al., 2002), with Hox and TALE-class homeodomain transcription factors (Bessa et al., 2002; Taghli-Lamallem et al., 2007), and with transcriptional effectors of the Wnt pathway such as β-catenin and Tcf3 (Gallet et al., 1999;

Gallet et al., 1998; Onai et al., 2007). As such, knockdown of Tshz3b could potentially disrupt numerous developmental processes. The genetic interactions between *tsh* and *hox* in flies (Fasano et al., 1991; Roder et al., 1992), together with the apparent functional conservation between fly and mouse Tsh-related proteins, prompted the hypothesis that Tshz3b would help to specify segmental identity in the hindbrain by modulating Hox / TALE-class protein function. While the overexpression phenotype for *tshz3b* is consistent with this hypothesis (Figures 4-6 – 4-9,), the loss of function phenotypes are less informative in this regard (Figures 4-4, 4-5). If *tshz3b* was playing a role in segmental patterning by tempering Hox function in rhombomeres 4-7, then we would expect a loss of Tshz3b function to resemble a Hox gain of function, perhaps resulting in expanded posterior rhombomeres, or a posteriorization of the hindbrain. However, the phenotype of *tshz3b* morphants is not consistent with this hypothesis, and as such, it is currently unclear if endogenous Tshz3b modulates Hox function during hindbrain patterning.

One of the major questions in the field of hindbrain patterning is how Hox proteins define one rhombomere as being different from a neighbouring rhombomere. An even more complicated question is how a cell, once defined as having a specific rhombomere identity, becomes different from other cells within that same rhombomere. As such, I propose a model where Tshz3b plays a gene- or cell-specific role in antagonizing Hox / TALE function, thereby making *tshz3b*-expressing cells in one rhombomere different from neighbouring non-expressing cells (Figure 7-2). In this example, I use the rhombomere 3-4 interface, since by 24 hpf, the anterior limit of *tshz3b* expression is primarily restricted to a subset of r4 cells (Figure 4-1E, M, N, P). At endogenous levels, Tshz3b may antagonize Hox-Pbx-Meis complexes at specific target promoters allowing for differential Hox activity within r4. Thus, Tshz3b activity may promote the heterogeneity of cellular identity in r4. A Tshz3b loss of function (LOF) would relieve this inhibition of Hox function, perhaps causing a homogenization of r4 cellular identity. High levels of Tshz3b, such as that caused by global mRNA overexpression, would block Hox activity at all Hox-regulated promoters, thereby

resulting in a global loss of segmental identity in the hindbrain. While experimental evidence for this model is currently lacking, myself and others (Santos et al., 2010) have noticed a remarkable correlation between the mRNA expression patterns of zebrafish *tsh*-related genes and *meis* family members at later developmental stages, supporting the idea that there is a genetic and / or biochemical interaction between these transcription factors.

As mentioned in the Chapter 4 Discussion section, the morphological and neuronal defects in Tshz3b-depleted embryos resemble those of embryos where Wnt signaling has been compromised. This phenotype may reflect an early role for *tshz3b* on the Wnt pathway. Genetic interaction experiments between *tshz3b* and members of the Wnt pathway, along with biochemical evidence of a functionally relevant interaction between Tshz3b and β-catenin or Tcf3 in the hindbrain would help to support this hypothesis. Definitive evidence that *tshz3b* acted on both the Wnt and Hox pathways would perhaps define *tshz3b* as point of integration between these two pathways during hindbrain development.

7.4 Hox-independent roles of Pbx and Meis1 in patterning the zebrafish visual system

Although first defined as Hox co-factors, the PBC and Meinox families of TALE-class proteins are now being appreciated for their Hox-independent roles in both vertebrate and invertebrate development (reviewed in Mann et al., 2009; reviewed in Moens and Selleri, 2006). In addition to defining the role of Meis1 in hindbrain patterning and examining the regulation of Hox-Pbx-Meis function by Tshz3b, a major goal of my work was to examine the Hox-independent functions of Pbx and Meis1, especially with regard to visual system development. To this end, I have found that Pbx proteins play a critical role in midbrain development via their interactions with Engrailed homeodomain transcription factors (Chapter 5), and have identified multiple points at which Meis1 regulates the specification of positional information in the midbrain and retina (Chapter 6). An overview of Pbx and Meis1 function in the visual system is shown in Figure 7-5. Taken together with their previously defined roles in hindbrain patterning, these studies

define Pbx and Meis1 as having a broad role in axial specification throughout the anterior neural tube.

7.5 Pbx proteins are part of the regulatory network that maintains the MHB signaling center

As discussed in the Introduction of this thesis, the biochemical interaction between Drosophila Extradenticle (Exd) and Engrailed (En) is necessary to regulate En target genes (Alexandre and Vincent, 2003; Kobayashi et al., 2003). In vertebrates, *Engrailed* genes are expressed at the midbrain-hindbrain boundary (MHB) where they are required for multiple aspects of midbrain development, including visual system function (Brunet et al., 2005; Friedman and O'Leary, 1996; Itasaki et al., 1991), and maintenance of lineage-restricted boundaries at the diencephalic-mesencephalic boundary (DMB) and the MHB (Araki and Nakamura, 1999; Scholpp et al., 2003; Wurst et al., 1994). Our work showing that Pbx and Engrailed cooperate to maintain the DMB and MHB signaling centre was the first to demonstrate a biological role for the Pbx and Engrailed interaction in vertebrates (Erickson et al., 2007). As such, Pbx can now be integrated into a model of MHB development where Pbx is not required for MHB initiation, but does cooperate with Engrailed to support the cross-regulatory network that maintains MHB integrity (Figure 7-3A, B).

7.6 The role of *meinox* genes in midbrain initiation, maintenance and axial patterning

In flies, Homothorax (Hth) can participate in trimeric complexes with En and Exd to regulate transcription (Kobayashi et al., 2003). What role, if any, do Meinox proteins play in MHB development? Three lines of evidence suggest that Meis1 is not a factor in MHB specification. First of all, although expressed in the midbrain region, *meis1* expression is specifically excluded from MHB (Figure 3-1, 3-2, and 6-1). Thus, it is unlikely that Meis1 can participate in a trimeric complex with Pbx and Engrailed at the MHB, though it does not exclude the possibility of such an interaction elsewhere in the midbrain. Secondly, *meis1*

morphants do not exhibit defects in MHB marker gene expression (Figure S6-2). Lastly, and perhaps most surprisingly, ectopic Meis1 inhibits specification of the midbrain region and leads to a deletion of the MHB (Figures 3-4 and 3-5). This result suggests that *meis1* is excluded from the MHB for a reason, and that ectopic Meis1 is causing either genetic or biochemical perturbations in the pathways that are responsible for MHB initiation (Figure 7-3A).

While these results exclude Meis1 as a candidate partner for Pbx and Engrailed at the MHB, there is a strong possibility that this trimeric complex actively regulates gene expression elsewhere in the midbrain. The tectal region of the midbrain is characterized by anterior-posterior (AP) and medial-lateral gradients of *eph* and *ephrin* gene expression. Engrailed is known to act downstream of MHB-derived Fgf8 signals to positively regulate the expression of *ephrinA* genes along the AP axis (Chen et al., 2009; Friedman and O'Leary, 1996; Logan et al., 1996; Shigetani et al., 1997). In addition to previously described roles for Meis proteins in regulating *eph* and *ephrin* expression in the tectum (Agoston and Schulte, 2009; Shim et al., 2007), I have shown that Meis1-depleted embryos have reduced tectal expression of *efna2*, *efna3b*, and *efna5a* (Figure 6-2). While further experiments are required to confirm the existence of endogenous Pbx-Eng-Meis1 complexes, these data are consistent with the hypothesis that Meis1 functions with Pbx and Engrailed to pattern the tectum (Figure 7-5).

The Meinox family is comprised of *meis* and *pknox* / *prep* genes. Although members of both groups can bind to Pbx and participate in trimeric complexes with Hox proteins, the transcriptional activities of Meis and Pknox proteins may be quite different. For example, the C-terminus of Meis1 is responsive to protein kinase A activation and TSA (histone deacetylase inhibitor) treatment, while the Pknox1 C-terminus is not (Huang et al., 2005). Given this distinction between *meis* and *pknox* activities, together with the fact that zebrafish *pknox* genes are broadly expressed throughout the neural tube (including the MHB), it is possible that Pknox is the Pbx-Eng partner in MHB development (Figure 7-3B). This hypothesis is supported by preliminary experiments using a *pknox1.1* / *pknox1.2* / *pknox2* triple morpholino cocktail that, while not perturbing hindbrain

segmentation, did result in a reduction of *pax2a* expression at the MHB in a manner very similar to that of Pbx-depleted embryos (Figure S7-1). Thus, *meis* and *pknox* genes may play distinct roles in midbrain development.

In many ways, the midbrain and hindbrain are very similar with regard to the problem of assigning unique functions to the individual members of the *meinox* gene family (see section 7.2). Both tissues express multiple *meinox* genes during early development, and a detailed comparative analysis of their mRNA expression patterns at these stages has not been performed. The future challenge will be to dissect how each *meinox* family member contributes to midbrain development. An especially interesting avenue of research would be to address the possibility that Pbx-Engrailed complexes utilize different Meinox partners to perform different transcriptional tasks. For example, a trimeric complex of Pknox, Pbx, and Engrailed may function to maintain the MHB signaling centre, while Meis-Pbx-Engrailed complexes may be involved in specifying AP polarity in the tectum.

7.7 Meis1 regulates multiple aspects of visual system development

The signaling pathways that specify the retinal nasal-temporal (NT) and dorsal-ventral (DV) axes are generally thought to operate independently of one another. For example, inhibition of Fgf signaling between the stages of 5-10 somites in zebrafish causes temporalization of the retina without affecting DV specification (Picker and Brand, 2005), while the loss of dorsal identity in the *gdf6a* zebrafish mutant does not alter NT polarity (Gosse and Baier, 2009). However, there are a few hints that the two pathways may be integrated in some respects. The dorsal domain of the retina in *fgf8* / *ace* mutant fish is smaller than their wild type counterparts, suggesting that at some point after the 10 somite stage, Fgf signaling is involved in maintaining dorsal identity (Picker and Brand, 2005). In *vax2* mutant mice, the retina is dorsalized as expected, but NT gradient of *efna5a* is also flattened (Mui et al., 2002). Likewise, expression of the nasal-specific transcription factor *hmx1* is lost in *gdf6a* mutants (C.R. French, personal communication). I have found that, in addition to its role in tectal patterning,

Meis1 contributes to the specification of both nasal-temporal (NT) and dorsal-ventral (DV) polarity in the retina (Chapter 6). As such, Meis1 can be integrated into a model of retinal patterning in which it represents a common regulatory factor in the specification of NT and DV identity (Figure 7-4).

Cell proliferation and adhesion are important forces in the process of tissue morphogenesis and pattern formation (reviewed in Ingber, 2005; Nelson et al., 2005), but the link between proliferation, adhesion and axial patterning of the retina has not been sufficiently addressed. Meis proteins are known to promote retinal progenitor cell proliferation by positively regulating the expression of cell cycle factors such as *cyclin D1* and *myca* (*c-myc*) (Bessa et al., 2008; Heine et al., 2008), and Meis1 or Pknox1 deficiency causes microphthalmia and defects in ocular morphology (Ferretti et al., 2006; Hisa et al., 2004). To what extent the proliferation defects in Meis1-depleted embryos contribute to changes in positional information is currently unclear. Additionally, because Ephs and Ephrins are involved in cell sorting and adhesion (reviewed in Cooke and Moens, 2002), the downregulation of *epha3*, *epha4b*, and *epha7* expression in *meis1* morphants is likely to alter cohesive cell behaviours amongst temporal retinal progenitors and hamper morphogenic cell movements. As such, it is plausible that Meis1 acts as a link between cell proliferation, adhesion, eye morphogenesis and axial patterning.

The dorsal, ventral, and nasal axes are specified by the Bmp, Hedgehog, and Fgf signaling pathways, respectively (French et al., 2009; Macdonald et al., 1995; Picker and Brand, 2005). However, it is currently unknown whether the temporal axis is actively specified, or if it represents a groundstate axial identity for retinal progenitor cells. As such, one of the most exciting Meis1-knockdown phenotypes is the decrease in *foxd1* expression in the presumptive temporal retina (Figure 6-6). If *meis1* is functioning upstream of *foxd1* to promote temporal identity, then, to my knowledge, it represents the only known factor to do so. For this reason, a more detailed study on the mechanism of Meis1 function in establishing temporal identity is warranted.

Although the study of *meis1* may provide insight into how the temporal retina is specified, *meis1* cannot be the whole answer. If *meis1* was the only factor regulating *foxd1* expression, then one would expect a complete loss of *foxd1* expression and temporal identity in Meis1-depleted embryos. The partial loss of temporal identity in *meis1* morphants may be due to redundancy with other Meinox genes expressed in the retina such as *meis2.2* or *pknox1.1*. Another possibility is that Meis1 represents one of multiple inputs that promote temporal identity. In order to discover what these other inputs are, I advocate performing a forward genetic screen using the HGn42A:GFP transgenic line of fish that express GFP in the presumptive temporal retina under the control of *foxd1* enhancer element (Picker et al., 2009). In this way, the F3 generation could be rapidly screened for recessive mutations that affect temporal specification. Although this line of research is not directly relevant to *meis1* function, it represents an approach that could provide answers for one of the major outstanding questions in retina patterning.

7.8 Pbx and Meis1 are required to establish lineage-restricted compartments throughout the anterior neural tube

One of the ways in which Hox and TALE-class proteins pattern the hindbrain is by establishing restricted domains of *eph* and *ephrin* expression along the anterior-posterior axis (Chen and Ruley, 1998; Taneja et al., 1996). This creates regions of differential cell adhesion and limits cell mixing between adjoining rhombomeres, thereby leading to the morphological and molecular segmentation of the hindbrain (Cooke et al., 2005; reviewed in Cooke and Moens, 2002; Kemp et al., 2009; Xu et al., 1999). Such lineage-restricted boundaries are not unique to the hindbrain; they are also observed at the midbrain-hindbrain boundary (MHB), the diencephalic-mesencephalic boundary (DMB), and in the forebrain, both anterior and posterior to the zona limitans intrathalamica (ZLI), as well as at the pallial–subpallial boundary (PSB) (reviewed in Kiecker and Lumsden, 2005). Although lineage restriction in the retina is not widely appreciated, the dorsal and ventral domains exhibit characteristics of lineage-

restricted compartments (Peters and Cepko, 2002), and this is likely true for the nasal-temporal axis as well (Picker et al., 2009). While there is currently no evidence that TALE-class proteins are required at the PSB, a member of the Iroquois family of TALE-class genes is required for ZLI establishment in fish (Scholpp et al., 2007). Thus, in light of my findings which implicate Pbx and Meinox proteins in MHB, DMB, and retinal lineage restriction, it has become apparent that the TALE-class of homeodomain transcription factors are key regulators of regional compartmentalization in the vertebrate nervous system.

7.9 Pbx and Meis proteins cooperate with tissue-specific co-factors to pattern the anterior neural tube

The initial characterization of Pbx and Meis TALE-class proteins emphasized their roles as "Hox co-factors", a reputation that has unfortunately minimized the perceived importance of their contributions to embryonic development. While the roles of Meis and Pbx in regulating hindbrain patterning and blood development are, as far as we know, Hox-dependent, it has become increasingly evident that Pbx and Meis perform equally important Hox-independent roles. In these cases, Pbx and Meis enlist the services of a third transcription factor that takes the place of the Hox partner in the complex. For example, trimeric complexes of Pknox, Pbx and the orphan Hox protein Pdx1 cooperatively regulate gene expression in the pancreas (Goudet et al., 1999), while the bHLH protein MyoD forms PID-dependent complexes with Pbx and Meis to promote skeletal muscle differentiation (Berkes et al., 2004). Although trimeric Pknox-Pbx-Engrailed complexes have not yet been directly demonstrated, my data support the hypothesis that Pbx-Pknox dimers use Engrailed as a cofactor to maintain the MHB signaling centre. It is also tempting to speculate that Meis1-Pbx-Engrailed complexes establish AP polarity in the tectum. Taken together, rather than describe Pbx and Meinox proteins as Hox cofactors, it would be more accurate to acknowledge their general role in pattern formation, a role they perform in partnership with tissue-specific cofactors that bind to Pbx in a PID-dependent fashion.

Interestingly, although Pbx and Meis proteins are also involved in axial patterning of the retina (Chapter 6; French et al., 2007), a third partner in the relationship has yet to be described. In zebrafish, leading candidates for this role are the *muscle segment homeobox* (*msx*) genes *msxc* and *msxe*, both of which code for proteins that contain putative PID motifs N-terminal to their homeodomains (In der Rieden et al., 2004). The retinal expression of these two genes is restricted to the dorsal retina (Thisse and Thisse, 2005), and as such could be acting as dorsal-specific co-factors for Pbx and Meis. The paired box transcription factor *pax6* is another retinally-expressed gene that contains a putative PID (In der Rieden et al., 2004). In zebrafish, *pax6b* is expressed throughout the eye field during early development (Thisse and Thisse, 2004), allowing for the possibility that it acts as a general co-factor for Pbx and Meinox proteins in the neural retina. Intriguingly, *msx* and *pax6* genes, as well as other putative PID-containing transcription factors, are also expressed outside of the eye. Thus, a major question for the future is whether Pbx and Meinox proteins can form complexes with these putative partners, and if so, what is the biological relevance of their partnership? The answers to these questions may enrich our knowledge of not only Pbx and Meis protein function, but also of the tissues they pattern.

7.10 Figures

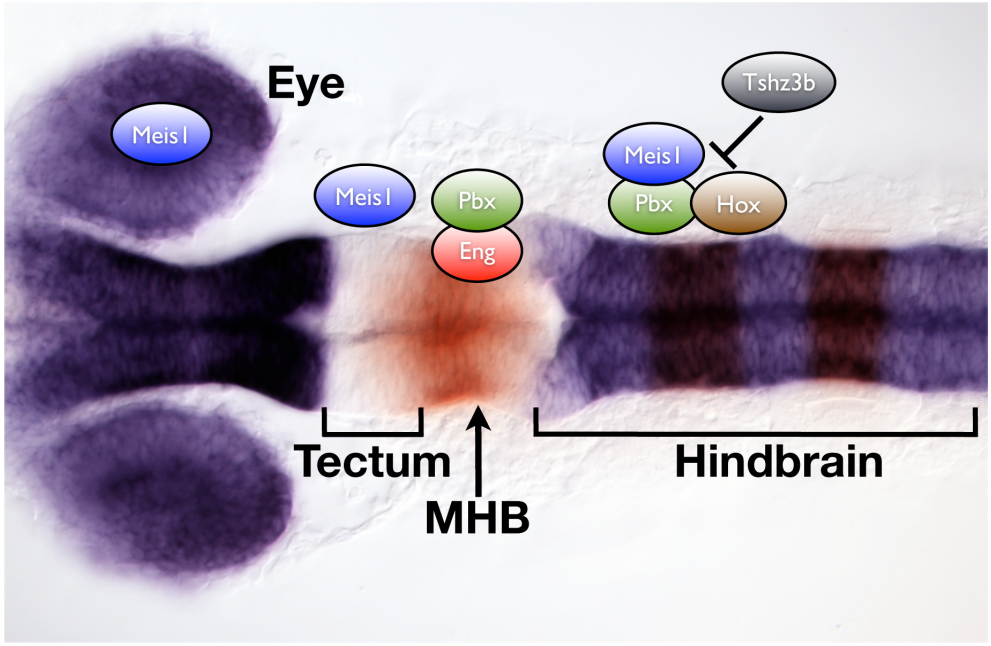

Figure 7-1. Summary of Pbx- and Meis-dependent tissue patterning events described in this thesis. Chapter 3 describes the role of Meis1 in patterning the hindbrain. Chapter 4 provides evidence that Tshz3b inhibits Hox-dependent hindbrain segmentation. Chapter 5 describes how Pbx and Engrailed proteins cooperatively pattern the midbrain-hindbrian boundary. Chapter 6 highlights multiple roles for Meis1 in patterning tissues involved in the visual system, including the tectum and retina.

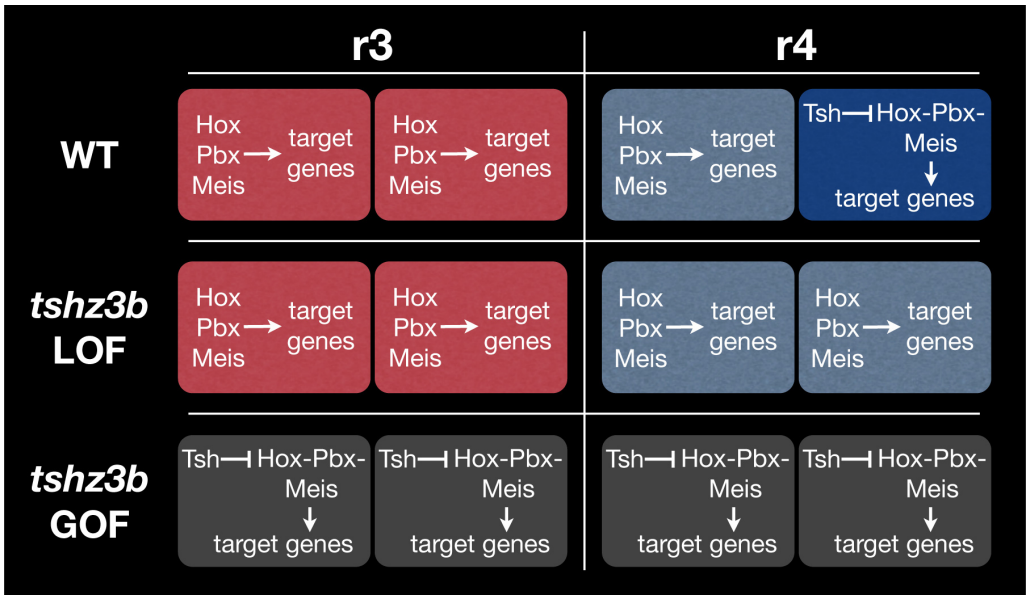

Figure 7-2. Model for the role of *tshz3b* in modulating Hox function during hindbrain patterning. The overexpression phenotype for *tshz3b* suggests that its endogenous role in hindbrain patterning may be to modulate Hox function, thereby contributing to heterogenous cell identities within rhombomeres.

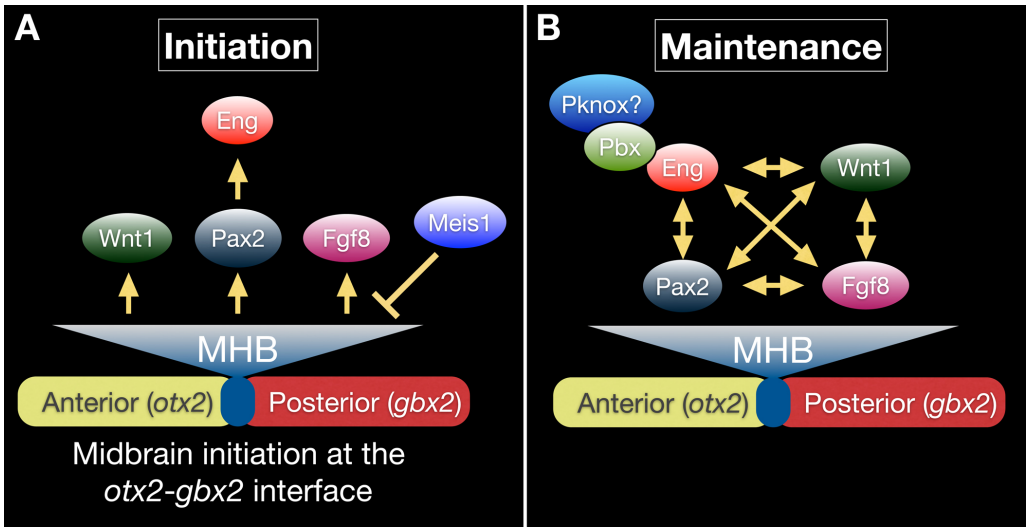

Figure 7-3. Model for Pbx and Meinox function in midbrain-hindbrain boundary (MHB) patterning. (A) Pbx is not involved in MHB inititation, but ectopic Meis1 can block specification of the midbrain region. (B) Pbx, in partnership with Engrailed, is an important component of the regulatory network that maintains the MHB. Meis1 is not involved in MHB maintenance, but Pknox proteins may contribute to this network.

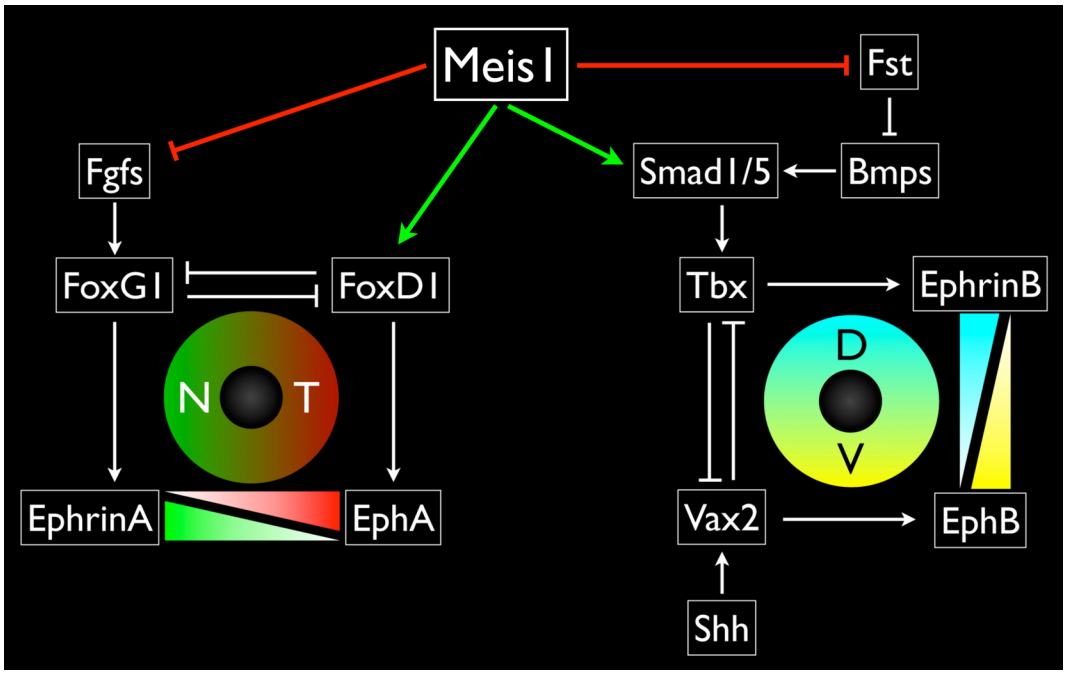

Figure 7-4. Model for the role of Meis1 in axial patterning of the retina. Meis1 contributes to nasal-temporal patterning by promoting *foxd1* expression during retinal development. Meis1 promotes dorsal identity in the retina through the positive regulation of *smad1* expression and the negative regulation of *follistatin*.

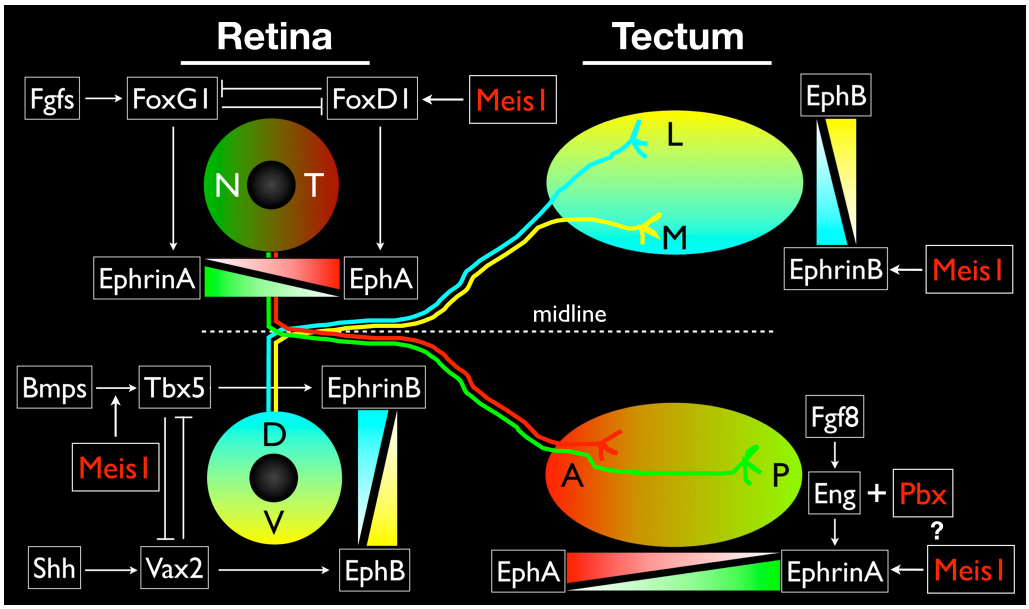

Figure 7-5. Summary of the Hox-independent roles for Pbx and Meis1 in visual system development. Meis1 promotes nasal and dorsal identity in the retina. In the tectum, Meis1 positively regulates *ephrin* gene expression. Together, these roles for Meis1 contribute to the organization of the retinotectal map. Pbx and Engrailed regulate ephrin A expression in the tectum, leaving open the possibility that Eng-Pbx-Meis complexes cooperate to perform this task.

7.11 References

Agoston, Z., Schulte, D., 2009. Meis2 competes with the Groucho co-repressor Tle4 for binding to Otx2 and specifies tectal fate without induction of a secondary midbrain-hindbrain boundary organizer. Development. 136**,** 3311-22.

Alexandre, C., Vincent, J. P., 2003. Requirements for transcriptional repression and activation by Engrailed in Drosophila embryos. Development. 130**,** 729-39.

Araki, I., Nakamura, H., 1999. Engrailed defines the position of dorsal di-mesencephalic boundary by repressing diencephalic fate. Development. 126**,** 5127-35.

Berkes, C. A., Bergstrom, D. A., Penn, B. H., Seaver, K. J., Knoepfler, P. S., Tapscott, S. J., 2004. Pbx marks genes for activation by MyoD indicating a role for a homeodomain protein in establishing myogenic potential. Mol Cell. 14**,** 465-77.

Bessa, J., Gebelein, B., Pichaud, F., Casares, F., Mann, R. S., 2002. Combinatorial control of Drosophila eye development by eyeless, homothorax, and teashirt. Genes Dev. 16**,** 2415-27.

Bessa, J., Tavares, M. J., Santos, J., Kikuta, H., Laplante, M., Becker, T. S., Gomez-Skarmeta, J. L., Casares, F., 2008. meis1 regulates cyclin D1 and c-myc expression, and controls the proliferation of the multipotent cells in the early developing zebrafish eye. Development. 135**,** 799-803.

Brunet, I., Weinl, C., Piper, M., Trembleau, A., Volovitch, M., Harris, W., Prochiantz, A., Holt, C., 2005. The transcription factor Engrailed-2 guides retinal axons. Nature. 438**,** 94-8.

Chen, J., Ruley, H. E., 1998. An enhancer element in the EphA2 (Eck) gene sufficient for rhombomere-specific expression is activated by HOXA1 and HOXB1 homeobox proteins. J Biol Chem. 273**,** 24670-5.

Chen, Y., Mohammadi, M., Flanagan, J. G., 2009. Graded levels of FGF protein span the midbrain and can instruct graded induction and repression of neural mapping labels. Neuron. 62**,** 773-80.

Cooke, J. E., Kemp, H. A., Moens, C. B., 2005. EphA4 is required for cell adhesion and rhombomere-boundary formation in the zebrafish. Curr Biol. 15**,** 536-42.

Cooke, J. E., Moens, C. B., 2002. Boundary formation in the hindbrain: Eph only it were simple. Trends Neurosci. 25**,** 260-7.

Erickson, T., Scholpp, S., Brand, M., Moens, C. B., Waskiewicz, A. J., 2007. Pbx proteins cooperate with Engrailed to pattern the midbrain-hindbrain and diencephalic-mesencephalic boundaries. Dev Biol. 301**,** 504-17.

Fasano, L., Roder, L., Core, N., Alexandre, E., Vola, C., Jacq, B., Kerridge, S., 1991. The gene teashirt is required for the development of Drosophila embryonic trunk segments and encodes a protein with widely spaced zinc finger motifs. Cell. 64**,** 63-79.

Ferretti, E., Villaescusa, J. C., Di Rosa, P., Fernandez-Diaz, L. C., Longobardi, E., Mazzieri, R., Miccio, A., Micali, N., Selleri, L., Ferrari, G., Blasi, F., 2006. Hypomorphic mutation of the TALE gene Prep1 (pKnox1) causes a major reduction of Pbx and Meis proteins and a pleiotropic embryonic phenotype. Mol Cell Biol. 26**,** 5650-62.

French, C. R., Erickson, T., Callander, D., Berry, K. M., Koss, R., Hagey, D. W., Stout, J., Wuennenberg-Stapleton, K., Ngai, J., Moens, C. B., Waskiewicz, A. J., 2007. Pbx homeodomain proteins pattern both the zebrafish retina and tectum. BMC Dev Biol. 7**,** 85.

French, C. R., Erickson, T., French, D. V., Pilgrim, D. B., Waskiewicz, A. J., 2009. Gdf6a is required for the initiation of dorsal-ventral retinal patterning and lens development. Dev Biol. 333**,** 37-47.

Friedman, G. C., O'Leary, D. D., 1996. Retroviral misexpression of engrailed genes in the chick optic tectum perturbs the topographic targeting of retinal axons. J Neurosci. 16**,** 5498-509.

Gallet, A., Angelats, C., Erkner, A., Charroux, B., Fasano, L., Kerridge, S., 1999. The C-terminal domain of armadillo binds to hypophosphorylated teashirt to modulate wingless signalling in Drosophila. Embo J. 18**,** 2208-17.

Gallet, A., Erkner, A., Charroux, B., Fasano, L., Kerridge, S., 1998. Trunk-specific modulation of wingless signalling in Drosophila by teashirt binding to armadillo. Curr Biol. 8**,** 893-902.

Geerts, D., Revet, I., Jorritsma, G., Schilderink, N., Versteeg, R., 2005. MEIS homeobox genes in neuroblastoma. Cancer Lett. 228**,** 43-50.

Gosse, N. J., Baier, H., 2009. An essential role for Radar (Gdf6a) in inducing dorsal fate in the zebrafish retina. Proc Natl Acad Sci U S A. 106**,** 2236-41.

Goudet, G., Delhalle, S., Biemar, F., Martial, J. A., Peers, B., 1999. Functional and cooperative interactions between the homeodomain PDX1, Pbx, and Prep1 factors on the somatostatin promoter. J Biol Chem. 274**,** 4067-73.

Heine, P., Dohle, E., Bumsted-O'Brien, K., Engelkamp, D., Schulte, D., 2008. Evidence for an evolutionary conserved role of homothorax/Meis1/2 during vertebrate retina development. Development. 135**,** 805-11.

Hisa, T., Spence, S. E., Rachel, R. A., Fujita, M., Nakamura, T., Ward, J. M., Devor-Henneman, D. E., Saiki, Y., Kutsuna, H., Tessarollo, L., Jenkins, N. A., Copeland, N. G., 2004. Hematopoietic, angiogenic and eye defects in Meis1 mutant animals. EMBO J. 23**,** 450-9.

Huang, H., Rastegar, M., Bodner, C., Goh, S. L., Rambaldi, I., Featherstone, M., 2005. MEIS C termini harbor transcriptional activation domains that respond to cell signaling. J Biol Chem. 280**,** 10119-27.

In der Rieden, P. M., Mainguy, G., Woltering, J. M., Durston, A. J., 2004. Homeodomain to hexapeptide or PBC-interaction-domain distance: size apparently matters. Trends Genet. 20**,** 76-9.

Ingber, D. E., 2005. Mechanical control of tissue growth: function follows form. Proc Natl Acad Sci U S A. 102**,** 11571-2.

Itasaki, N., Ichijo, H., Hama, C., Matsuno, T., Nakamura, H., 1991. Establishment of rostrocaudal polarity in tectal primordium: engrailed expression and subsequent tectal polarity. Development. 113**,** 1133-44.

Kemp, H. A., Cooke, J. E., Moens, C. B., 2009. EphA4 and EfnB2a maintain rhombomere coherence by independently regulating intercalation of progenitor cells in the zebrafish neural keel. Dev Biol. 327**,** 313-26.

Kiecker, C., Lumsden, A., 2005. Compartments and their boundaries in vertebrate brain development. Nat Rev Neurosci. 6**,** 553-64.

Kobayashi, M., Fujioka, M., Tolkunova, E. N., Deka, D., Abu-Shaar, M., Mann, R. S., Jaynes, J. B., 2003. Engrailed cooperates with extradenticle and homothorax to repress target genes in Drosophila. Development. 130**,** 741-51.

Logan, C., Wizenmann, A., Drescher, U., Monschau, B., Bonhoeffer, F., Lumsden, A., 1996. Rostral optic tectum acquires caudal characteristics following ectopic engrailed expression. Curr Biol. 6**,** 1006-14.

Macdonald, R., Barth, K. A., Xu, Q., Holder, N., Mikkola, I., Wilson, S. W., 1995. Midline signalling is required for Pax gene regulation and patterning of the eyes. Development. 121**,** 3267-78.

Manfroid, I., Caubit, X., Kerridge, S., Fasano, L., 2004. Three putative murine Teashirt orthologues specify trunk structures in Drosophila in the same way as the Drosophila teashirt gene. Development. 131**,** 1065-73.

Mann, R. S., Lelli, K. M., Joshi, R., 2009. Hox specificity unique roles for cofactors and collaborators. Curr Top Dev Biol. 88**,** 63-101.

Moens, C. B., Prince, V. E., 2002. Constructing the hindbrain: insights from the zebrafish. Dev Dyn. 224**,** 1-17.

Moens, C. B., Selleri, L., 2006. Hox cofactors in vertebrate development. Dev Biol. 291**,** 193-206.

Mui, S. H., Hindges, R., O'Leary, D. D., Lemke, G., Bertuzzi, S., 2002. The homeodomain protein Vax2 patterns the dorsoventral and nasotemporal axes of the eye. Development. 129**,** 797-804.

Nelson, C. M., Jean, R. P., Tan, J. L., Liu, W. F., Sniadecki, N. J., Spector, A. A., Chen, C. S., 2005. Emergent patterns of growth controlled by multicellular form and mechanics. Proc Natl Acad Sci U S A. 102**,** 11594-9.

Onai, T., Matsuo-Takasaki, M., Inomata, H., Aramaki, T., Matsumura, M., Yakura, R., Sasai, N., Sasai, Y., 2007. XTsh3 is an essential enhancing factor of canonical Wnt signaling in Xenopus axial determination. EMBO J. 26**,** 2350-60.

Peters, M. A., Cepko, C. L., 2002. The dorsal-ventral axis of the neural retina is divided into multiple domains of restricted gene expression which exhibit features of lineage compartments. Dev Biol. 251**,** 59-73.

Picker, A., Brand, M., 2005. Fgf signals from a novel signaling center determine axial patterning of the prospective neural retina. Development. 132**,** 4951-62.

Picker, A., Cavodeassi, F., Machate, A., Bernauer, S., Hans, S., Abe, G., Kawakami, K., Wilson, S. W., Brand, M., 2009. Dynamic coupling of pattern formation and morphogenesis in the developing vertebrate retina. PLoS Biol. 7**,** e1000214.

Roder, L., Vola, C., Kerridge, S., 1992. The role of the teashirt gene in trunk segmental identity in Drosophila. Development. 115**,** 1017-33.

Saller, E., Kelley, A., Bienz, M., 2002. The transcriptional repressor Brinker antagonizes Wingless signaling. Genes Dev. 16**,** 1828-38.

Santos, J. S., Fonseca, N. A., Vieira, C. P., Vieira, J., Casares, F., 2010. Phylogeny of the teashirt-related zinc finger (tshz) gene family and analysis of the developmental expression of tshz2 and tshz3b in the zebrafish. Dev Dyn. 239**,** 1010-8.

Scholpp, S., Foucher, I., Staudt, N., Peukert, D., Lumsden, A., Houart, C., 2007. Otx1l, Otx2 and Irx1b establish and position the ZLI in the diencephalon. Development. 134**,** 3167-76.

Scholpp, S., Lohs, C., Brand, M., 2003. Engrailed and Fgf8 act synergistically to maintain the boundary between diencephalon and mesencephalon. Development. 130**,** 4881-93.

Shigetani, Y., Funahashi, J. I., Nakamura, H., 1997. En-2 regulates the expression of the ligands for Eph type tyrosine kinases in chick embryonic tectum. Neurosci Res. 27**,** 211-7.

Shim, S., Kim, Y., Shin, J., Kim, J., Park, S., 2007. Regulation of EphA8 gene expression by TALE homeobox transcription factors during development of the mesencephalon. Mol Cell Biol. 27**,** 1614-30.

Taghli-Lamallem, O., Gallet, A., Leroy, F., Malapert, P., Vola, C., Kerridge, S., Fasano, L., 2007. Direct interaction between Teashirt and Sex combs reduced proteins, via Tsh's acidic domain, is essential for specifying the identity of the prothorax in Drosophila. Dev Biol. 307**,** 142-51.

Taneja, R., Thisse, B., Rijli, F. M., Thisse, C., Bouillet, P., Dolle, P., Chambon, P., 1996. The expression pattern of the mouse receptor tyrosine kinase gene MDK1 is conserved through evolution and requires Hoxa-2 for rhombomere-specific expression in mouse embryos. Dev Biol. 177**,** 397-412.

Thisse, B., Thisse, C., 2004. Fast Release Clones: A High Throughput Expression Analysis. . ZFIN Direct Data Submission.

Thisse, B., Thisse, C., 2005. High Throughput Expression Analysis of ZF-Models Consortium Clones. ZFIN Direct Data Submission.

Wurst, W., Auerbach, A. B., Joyner, A. L., 1994. Multiple developmental defects in Engrailed-1 mutant mice: an early mid-hindbrain deletion and patterning defects in forelimbs and sternum. Development. 120**,** 2065-75.

Xu, Q., Mellitzer, G., Robinson, V., Wilkinson, D. G., 1999. In vivo cell sorting in complementary segmental domains mediated by Eph receptors and ephrins. Nature. 399**,** 267-71.

Appendix

Supplemental Figures

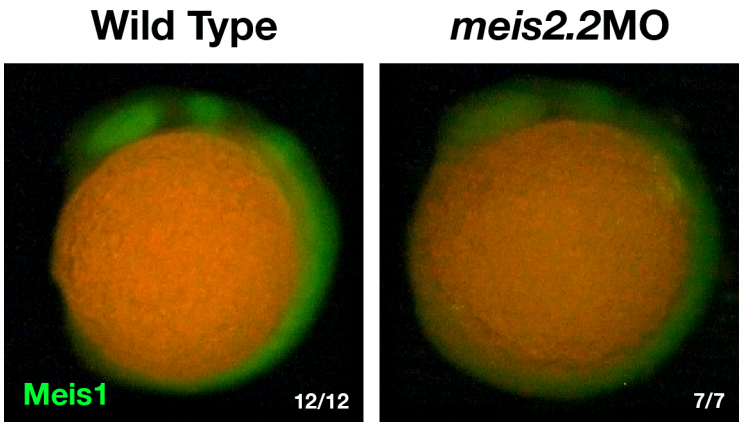

Figure S3-1. Immunostain for Meis1 protein in wild type and *meis2.2* morphant embryos at 13 hpf. Embryos are shown in lateral view is anterior at the top left.

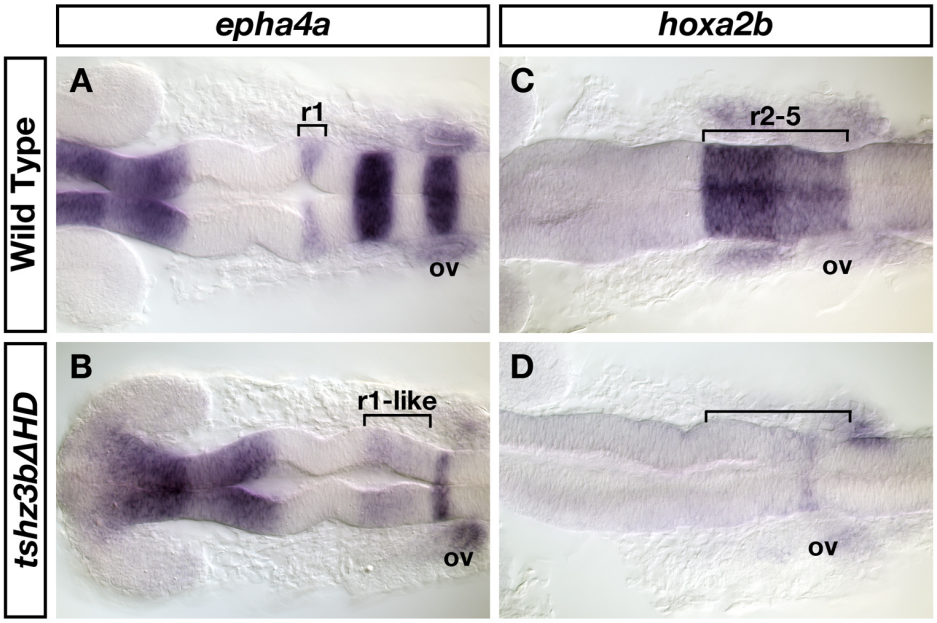

Figure S4-1. Tshz3bΔHD perturbs Hox-dependent hindbrain patterning. mRNA in situ hybridizations for *epha4a* (A, B) and *hoxa2b* (C, D) in wild type and *tshz3bΔHD*-injected embryos at 20 hpf. Ectopic *tshz3bΔHD* causes similar phenotypes as full-length *tshz3b* overexpression (see Figure 4-6E, G). Note: The wild type embryos in (A) and (C) are the same as those shown in Figure 4-6D, F.

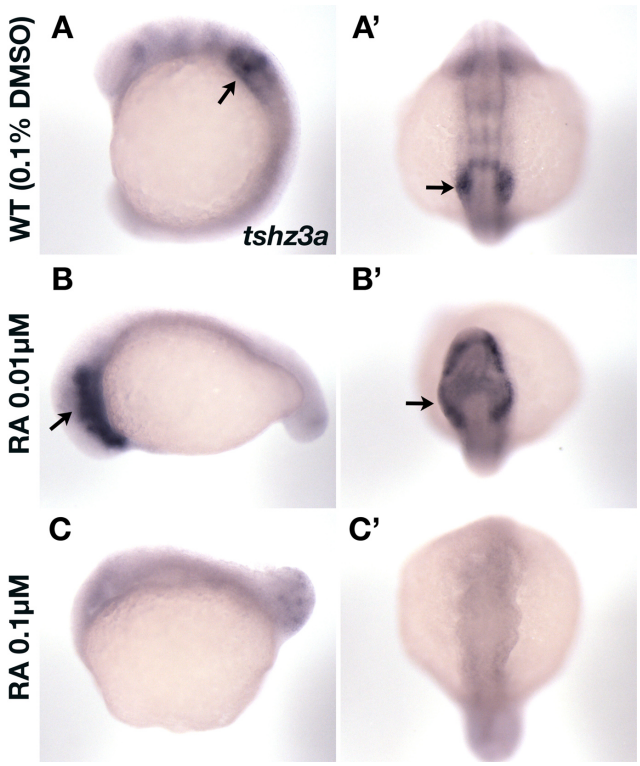

Figure S4-2. Expression of *tshz3a* in retinoic acid-treated embryos at 15 hpf. Views in A-C are lateral with anterior to the left, while views in A'-C' are dorsal with anterior at the top. Black arrows indicate *tshz3a*-expressing tissue adjacent to the hindbrain that is expanded upon RA treatment.

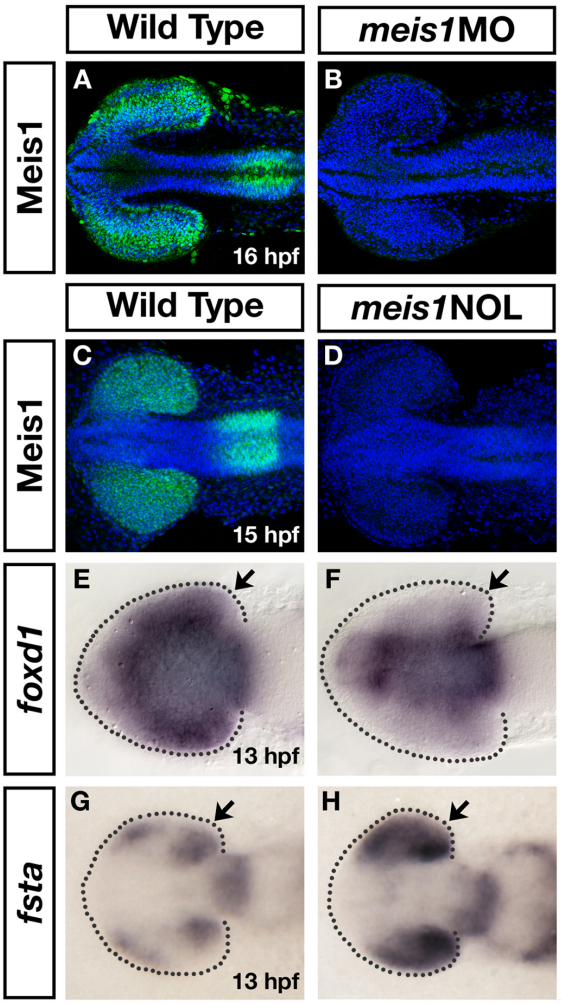

Figure S6-1. Two independent *meis1* morpholinos (MOs) result in similar phenotypes. **(A-D)** Two independent *meis1* translation blocking MOs effectively knockdown Meis1 protein, as shown by whole mount immunostain using a Meis1 monoclonal antibody. Hoechst 33258 stain marks the nuclei. **(E-H)** The *meis1* non-overlapping (NOL) MO gives similar phenotypes as the ATG-MO. *meis1*NOL morphants exhibit reduced *foxd1* expression in the presumptive temporal retina (*n*=27/29) (E, F), and upregulated *fsta* expression in the eye at 13 hpf (*n*=19/19). Dotted lines outline the optic vesicle. Views are dorsal with anterior to the left.

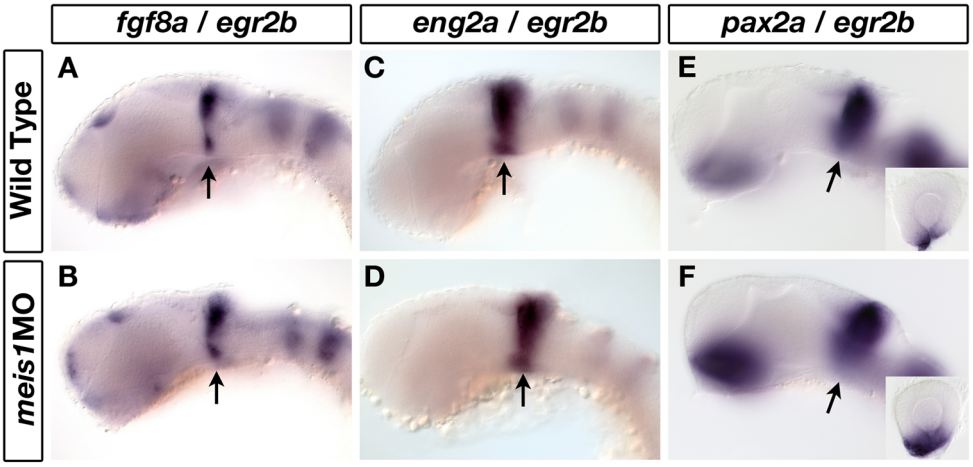

Figure S6-2. Meis1-knockdown does not affect patterning of the midbrain-hindbrain boundary. **(A-D)** mRNA in situ hybridization for midbrain-hindbrain boundary (MHB) markers *fgf8a* (A, B), *eng2a* (C, D) and *pax2a* (E, F) in 32 hpf wild type and *meis1* morphant embryos. Arrows indicate the relevant gene expression domain at the MHB. The insets in E and F are representative dissected eyes showing an upregulation of *pax2a* staining in the optic stalk of *meis1* morphants (*n*=18/18). Embryos are co-stained with the hindbrain r3 and r5 marker *egr2b*. Embryos are shown in lateral view with dorsal up and anterior to the left, and the dissected retinas are oriented with dorsal up and nasal to the left.

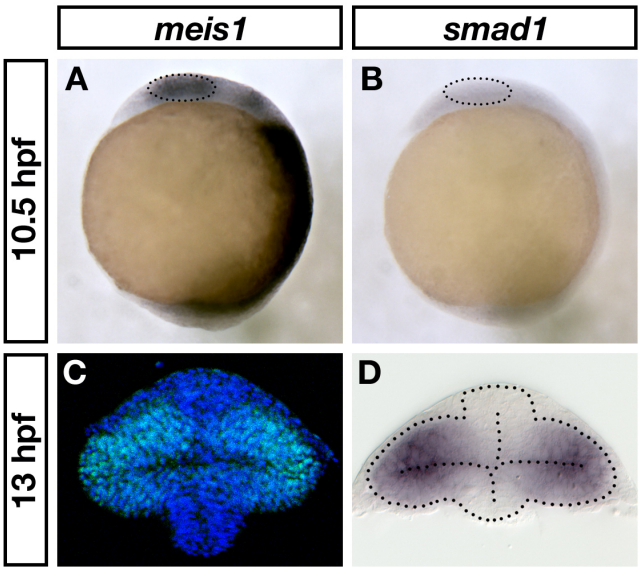

Figure S6-3. *meis1* and *smad1* expression in the early optic vesicle. **(A, B)** mRNA in situ hybridizations for *meis1* (A) and *smad1* (B) in 10.5 hpf embryos. The dotted circles indicate the eye fields. Views are lateral with anterior on the top. **(C, D)** Transverse sections of 13 hpf optic vesicles stained for Meis1 protein (C) and *smad1* mRNA (D). The Meis1 immunostain in panel C is the same as that shown in Figure 6-1. Dotted lines outline the optic vesicle and neural tube. Sections are oriented with dorsal at the top.

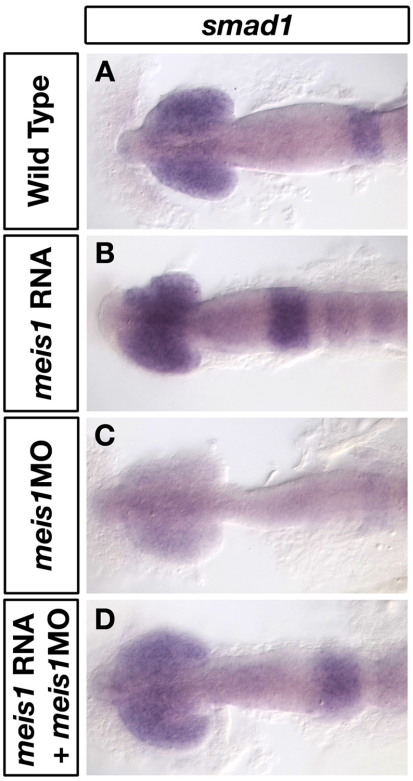

Figure S6-4. Morpholino-insensitive *myc-meis1* RNA can rescue the *smad1* expression defects in *meis1* morphants. mRNA in situ hybridizations for *smad1* in wild type (A), *myc-meis1* RNA (B), *meis1* morphant (C) and *myc-meis1* RNA/*meis1* morphant (D) embryos at 14 hpf. All embryos are shown in dorsal view with anterior to the left.

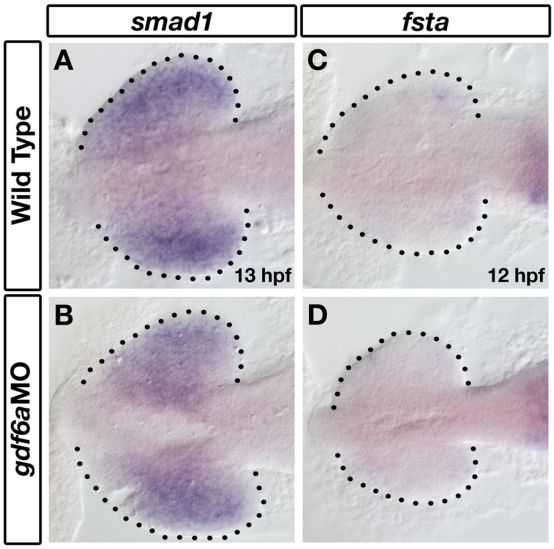

Figure S6-5. *gdf6a* morphants have normal *smad1* and *fsta* expression at 13 hpf. mRNA in situ hybridizations for *smad1* (A, B) and *fsta* (C, D) in wild type (A, C) and *gdf6a* morphants (B, D) at 13 hpf. Dotted lines outline the optic vesicle. Views are dorsal with anterior to the left.

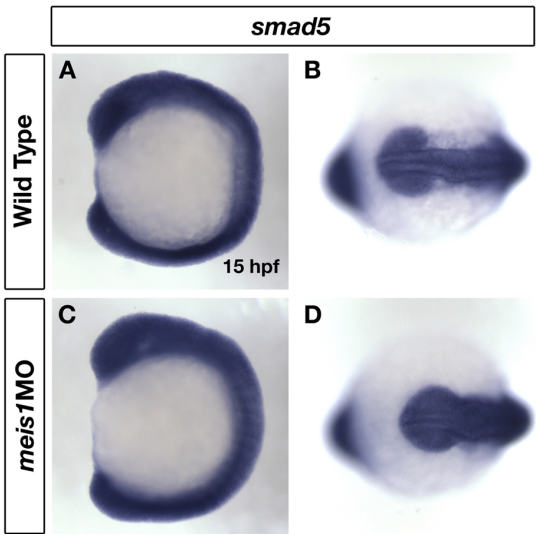

Figure S6-6. *smad5* expression is normal in *meis1* morphants. mRNA in situ hybridizations for *smad5* on wild type (A, B) and *meis1* morphant (C, D) embryos at 15 hpf. A and C are lateral views with anterior up, B and D are dorsal views with anterior to the left.

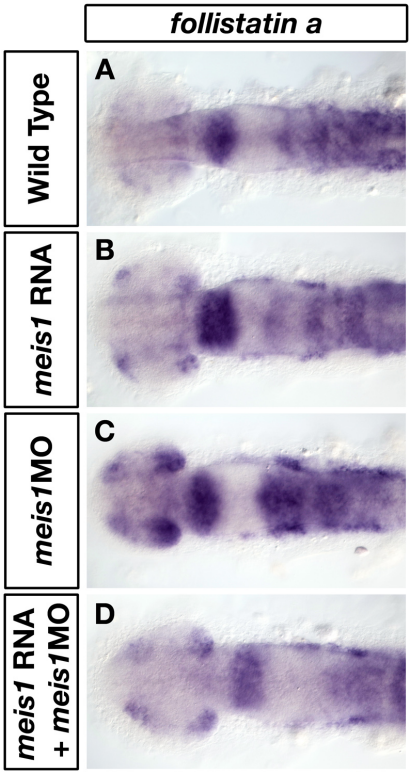

Figure S6-7. Morpholino-insensitive *myc-meis1* RNA can rescue the *fsta* expression defects in *meis1* morphants. mRNA in situ hybridizations for *fsta* in wild type (A), *myc-meis1* RNA (B), *meis1* morphant (C) and *myc-meis1* RNA/*meis1* morphant embryos (D) at 14 hpf. All embryos are shown in dorsal view with anterior to the left.

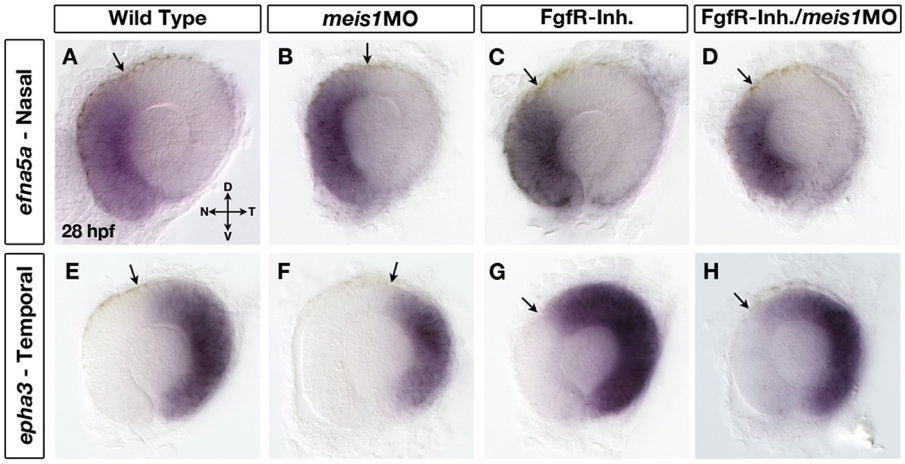

Figure S6-8. Interaction between Meis1-knockdown and reduced Fgf signaling using the Fgf receptor inhibitor SU5402. mRNA ISH for *efna5a* (A-D) and *epha3* (E-H) in wild type (A, E), Meis1-depleted (B, F), Fgf receptor-inhibitor (SU5402) treated (C, G), and FgfR-inhibited/Meis1-depleted retinas (D, H). Arrows indicate the dorsal-most extent of the gene expression domain. Representative dissected eyes are shown. Legend for retinal axial position: D - dorsal, V- ventral, N – nasal, T- temporal.

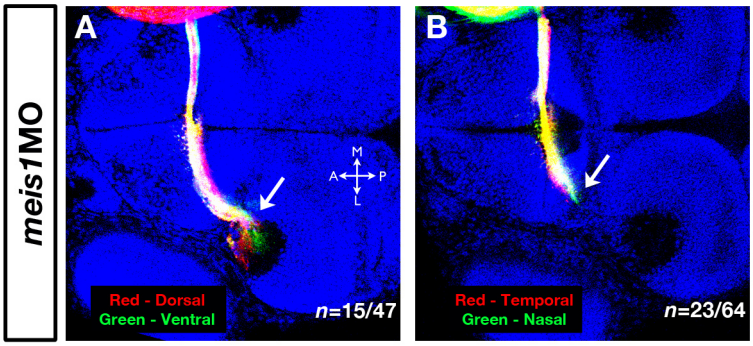

Figure S6-9. The RGC axon stalling phenotype in *meis1* morphants. **(A)** Dorsal-ventral and **(B)** nasal-temporal RGC axon stalling phenotypes in *meis1* morphants. Arrows indicate the stalled RGC axons. All views are dorsal with anterior to the left. Legend for axial position in the tectum: M – medial, L – lateral, A – anterior, P – posterior. Note: this experiment was performed by Curtis French.

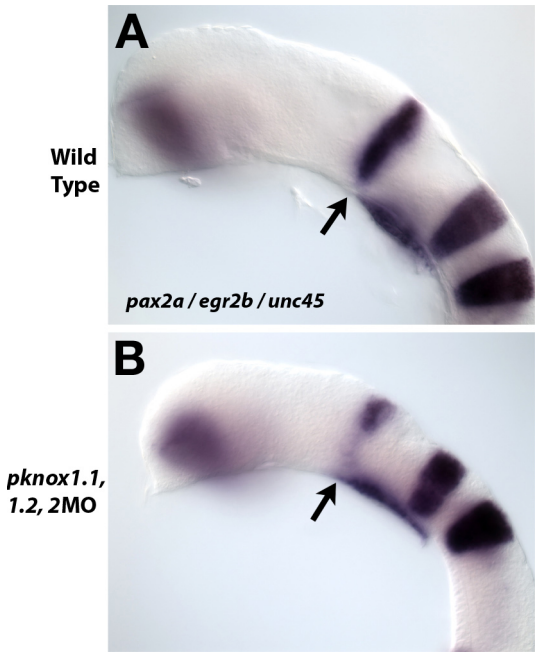

Figure S7-1. The expression of *pax2a* at the midbrain-hindbrain boundary (black arrows) in wild type (A) and *pknox1.1, 1.2, 2* triple-morphant (B) embryos at 20 hpf. Embryos are shown in lateral view with anterior to the left.